A study of yeast stress responses and conserved eukaryotic homeostatic mechanisms

Daniel D. Waller

Department of Biochemistry

McGill University

Montreal, Quebec, Canada

February 2011

A thesis submitted to McGill University in partial fulfillment of the requirements for the degree of Doctor of Philosophy

ABSTRACT

The ability to sense and respond to fluctuating environmental conditions is a conserved and essential feature of all living organisms. Cellular stress responses sense and transmit the demands of specific stressors to appropriate homeostatic effectors, which can then implement appropriate cellular adaptation mechanisms. This study examines two distinct and highly conserved eukaryotic signaling responses that are implemented in response to unfolded protein in the endoplasmic reticulum, a situation known as ER stress. We find that *Schizosaccharomyces pombe* calnexin (Cnx1p) is regulated by phosphorylation at a conserved serine residue in its cytoplasmic tail. Our analysis of Cnx1p-S553 phosphomutants suggests that this post-translational modification regulates the association of calnexin with ER membrane-bound ribosomes. We also find that this regulation of Cnx1p is important for cell size control and ER stress tolerance. Next, we identify and characterize a number of novel small-molecule inhibitors of the Ire1-dependent ER homeostatic mechanisms in *Saccharomyces cerevisiae*. We extend these findings beyond this yeast model by showing that one of these small-molecules also inhibits Ire1 signaling in mammalian cells. This compound, designated UPRM8, was used as a chemical probe to study the importance of Ire1-dependent ER homeostatic responses in constitutively ER-stressed multiple myeloma cells. UPRM8 elicited an apoptotic cell death in RPMI-8226 multiple myeloma cells due to its impairment of cytoprotective, Ire1-dependent ER homeostatic mechanisms. Lastly, this study also examines the roles of a cell polarity scaffold protein, called Bem1p, in the responses to pheromone and cell

wall stressors in *Saccharomyces cerevisiae.* A novel separation of function mutant of Bem1, called Bem1-*s3*, was identified and it revealed that the tandem SH3 domains of Bem1p are required for efficient pheromone signaling. Furthermore, we used mass spectrometry to identify novel Bem1p-interacting proteins and post-translational modifications. These novel physical interactions, as well as the phenotypes of Bem1 null and phosphomutants, suggested a novel role for Bem1p in the adaptive response to cell wall stressors. In summary, this thesis describes stress signaling mechanisms and some methods of manipulating them in order to exert control over cell fate.

ABRÉGÉ

La capacité à percevoir et à répondre aux fluctuations des conditions de l'environnement est une caractéristique essentielle et conservée chez tous les organismes vivants. Les réponses aux stress cellulaires sont sensibles aux exigences de facteurs de stress spécifiques qu'elles transmettent à des effecteurs homéostatiques appropriés, et qui à leur tour induisent des mécanismes cellulaires d'adaptation. Cette étude examine deux réponses distinctes et hautement conservées qui sont mises en oeuvre en réaction à la présence de protéines incorrectement repliées dans le Réticulum Endoplasmique (RE), une situation appelée "stress réticulo-endoplasmique". Nous avons démontré que la calnexin (Cnx1p) de *Schizosaccharomyces pombe* est régulée par la phosphorylation d'un résidu sérine conservé et localisé à l'extrémité cytoplasmique de la protéine. Notre analyse du phospho-mutant Cnx1p-S553 suggère que cette modification post-traductionnelle régule l'association de la calnexine aux ribosomes liés à la membrane du RE. Nous avons également constaté que la régulation de la phosphorylation de la calnexine est importante pour le contrôle de la dimension cellulaire et la tolérance au stress réticulo-endoplasmique. Ensuite, nous avons identifié et caractérisé un certains nombre de nouvelles petites molécules qui sont des inhibiteurs des mécanismes d'homéostasie du RE dépendant d'Ire-1 chez *Saccharomyces cerevisiae.* Ces résultats ont été étendu au-delà du modèle de la levure, en montrant que l'une de ces petites molécules inhibe également la voie de signalisation d'Ire-1 chez des cellules de mammifères. Ce composé, désigné par UPRM8, a été utilisé comme test chimique pour étudier l'importance de la réponse homéostatique au stress réticulo-endoplasmique constitutivement présent chez les

cellules de myélomes multiples. UPRM8 induit une apoptose chez les cellules de myélomes multiples RPMI-8226 en empêchant les mécanismes cyto-protectifs dépendants d'Ire-1. Finalement, cette étude a également examiné les rôles d'une protéine impliquée dans la polarité cellulaire, appelée Bem1p, dans la réponse à une phéromone et à un facteur de stress de la paroi cellulaire chez *Saccharomyces cerevisiae.* Un nouveau mutant de Bem1, nommé Bem1-s3, a été identifié et a révélé que les domaines SH3 en tandem de Bem1p sont requis pour une signalisation efficace des phéromones. De plus, nous avons utilisé la spectrométrie de masse pour identifier de nouvelles protéines qui interagissent avec Bem1p ainsi que des modifications post-traductionnelles. Ces nouvelles interactions ainsi que les phénotypes des mutants Bem1 et Bem1p ont suggéré un nouveau rôle pour Bem1p dans la réponse adaptative à des facteurs de stress de la paroi cellulaire. En résumé, cette thèse décrit des mécanismes de signalisation du stress et des moyens mises en œuvre par la cellule afin de composer avec les facteurs de stress et d'exercer un contrôle sur son devenir.

TABLE OF CONTENTS

LIST OF FIGURES AND TABLES

List of abbreviations

AD	activation domain (two-hybrid fusions)
ASK1	apoptosis signal-regulating kinase 1
Asn	Asparagine
ATF4	activating transcription factor 4
ATF6	activating transcription factor 6
BBDs	Bem1p-binding domains
Bem1	Bud emergence 1
BiP	binding immunoglobulin protein
BZ	bortezomib (also known as velcade or PS-341)
CDK	cyclin-dependent kinase
C/EBP-β	CCAAT/enhancer-binding protein-β
CHOP	C/EBP homologous protein
CI	Cdc42p-interacting (domain)
CK2	casein kinase II
CRIB	Cdc42/Rac interactive binding domain
DAPI	4',6-diamidino-2-phenylindole
DBD	DNA-binding domain (2-hybrid fusion)
2-DG	2-deoxy-D-glucose
DTT	dithiothreitol
EMM	Edinburgh minimal media
ER	endoplasmic reticulum
ERAD	ER-associated degradation
ERAF	ER-assisted folding
ERK1	extracellular signal-regulated kinase 1
ESR	environmental stress response
GAP	GTPase activating protein
GAS	general adaptation syndrome
GDI	guanine nucleotide dissociation inhibitor
GEF	guanine nucleotide exchange factor
GI	glucosidase I
GII	glucosidase II
Glc	glucose
GlcNac	N-acetylglucosamine
GPCRs	G-protein coupled receptors
GS	β1,3-glucan synthase
HSP	heat shock protein
HSR	heat shock response
Ig	immunoglobulin
Ire1	Inositol requiring enzyme 1 or Inositol-REquiring 1
$Ire1^{CYTO}$	cytoplasmic (kinase +RNase) domains of Ire1
ISR	integrated stress response
JNK	c-JUN NH_2-terminal kinase
KDa	kilodaltons
Man	mannose
MAPK	mitogen-activated protein kinase

List of abbreviations (continued)

MCM	mini-chromosome maintenance complex
MEFs	mouse embroyonic fibroblasts
MM	multiple myeloma
ORFs	open reading frames
OST	oligosaccharyl transferase
PAKs	p21-activated protein kinase
PB1	phox and Bem1 domain
PCs	plasma cells
PDK	proline-directed kinase
PERK	PKR-like endoplasmic reticulum kinase
phox	phagocyte oxidase
P_i	inorganic phosphate
PKC	protein kinase C
PtdIns(4)P	phosphatidylinositol 4-phosphate
PX	phox homology domain
RIDD	regulated Ire1-dependent decay
RNC	ribosome-nascent chain complex
SDS-PAGE	sodium dodecyl sulphate polyacrylamide gel electrophoresis
SR	SRP receptor
SRP	signal recognition particle
Ser	serine
SS	signal sequence
TG	thapsigargin
Thr	threonine
TM	tunicamycin
UGGT	(UDP)-glucose:glycoprotein glucosyltransferase
UPR	unfolded protein response
UPRM	unfolded protein response modulator (small-molecule)
UPRM8	5-{[1-(4-bromophenyl)-1H-pyrrol-2-yl]methylene}-2-thioxodihydro-4,6(1H,5H)-pyrimidinedione
VST	versipelostatin
X	denotes any amino acid in a given consensus sequence
Xbp1	X-box binding protein 1
Xbp1s	spliced form of Xbp1 (active)
Xbp1u	unspliced form of Xbp1 (inactive)

Acknowledgements

This thesis would not have been possible without the assistance and support of people too numerous to mention. I would like to start by expressing my deepest thanks to my supervisor, Dr. David Thomas, for his unwavering support and encouragement. The patience that Dr. Thomas has shown me, along with his unwavering dedication to my training, are testaments to his great capacity for scientific mentorship. Also, I am grateful to Dr. Malcolm Whiteway for his supervision and for the opportunities that he afforded me during the years I spent in his lab at the Biotechnology Research Institute. I consider myself truly fortunate for the combined supervision that I received from Drs. Thomas and Whiteway. Their scientific vision and enthusiasm, along with their willingness to let me explore research paths of my own choosing, have made for an amazing learning experience.

I would also like to thank Dr. Michel Tremblay for giving generously of his time and ideas as the third member of my advisory committee. Moreover, I'd like to thank the entire Department of Biochemistry for the wonderful advice and encouragement that I have received from faculty members too numerous to mention. The Department of Biochemistry has maintained the highest standards of scientific achievement throughout its storied history and it continues to provide a supportive and collaborative research environment for graduate students. I would also like to thank Christine Laberge and the rest of the departmental staff for their tireless efforts in support of biochemistry graduate students such as myself.

I would like to thank all members, both past and present, of the Thomas and Whiteway labs for making my daily life at McGill both memorable and enjoyable. In particular, I'd like to thank Drs. Robert Annan and Pekka Määttänen for their friendship during the course of our PhD studies and for their innumerable helpful discussions. I owe a deep debt of gratitude to Drs. Gregor Jansen, Kurt Dejgaard, Cunle Wu, Heidi Sampson, Suzana Anjos, Fabiana

Ciciriello, Graeme Carlile, and Dong Lei Zhang for sharing so freely of their time, knowledge, and expertise. I would also like to thank Laurent Bianchetti for sharing his knowledge of statistics and for helping with the French translation of my abstract. I'd also like to thank Katrina Teske, Amélie Fredette, and Carol Miyamoto for keeping the Thomas lab supplied, operating smoothly, and for making the workplace a fun and enjoyable environment. I have learned a great deal from each of my colleagues and I am extremely grateful for their help and encouragement. To all of my coworkers- thank you for your help, patience, support, sense of humour, and, most of all, for all of the wonderful memories.

I would be nothing without the love and support that I receive from my friends and family in New Brunswick. My brother, Shawn, and my parents, Linda and Wally, have provided me with every imaginable form of support and their unconditional love sustains me. I am thankful for the clarity of purpose and general appreciation for life that my many wonderful friends have afforded me. In particular, Steve, Craig, Charlotte, Shasta and the rest of my 'Lake George crew' have been, and will always be, an important part of the fabric of my life. I find myself at a loss for words when trying to adequately describe the positive influence and unwavering support that I have received from my girlfriend, Leslie Scarffe. Leslie - you entered my life at the most difficult of times and you single-handedly turned my world around and have restored my sense of purpose and passion for life. Thank you.

Original Contributions to Knowledge

1. A novel *in vivo* phosphorylation site was mapped to serine-553 in the cytoplasmic tail of *S. pombe* Cnx1p, thus establishing *S. pombe* as a viable genetic model to study calnexin phosphorylation.

2. Phosphomutants of *S. pombe* Cnx1p were used to demonstrate that this post-translational modification regulates the association of calnexin with ER membrane-bound ribosomes. This association had been previously demonstrated in mammalian cells but this interaction has never been demonstrated for *S. pombe* Cnx1p.

3. Phenotypic analysis of Cnx1p-S553 phosphomutants was used to demonstrate for the first time that phosphorylation of Cnx1p regulates cell size control and ER stress tolerance in *S. pombe*.

4. A high-throughput screen for small-molecule unfolded protein response modulators (UPRMs) is described. Subsequent characterization of these novel small-molecules revealed that one particular pyrimidinedione-based compound, which was named UPRM8, can impair Ire1 signaling in both yeast and mammalian cells.

5. The mechanism of action of UPRM8 was determined to be inhibition of the ribonuclease activity of Ire1. Both *in vitro* and *in vivo* data are used to support this claim and this is the first demonstration that a pyrimidinedione-based small molecule can inhibit the non-conventional splicing of Xbp1/Hac1 by Ire1.

6. UPRM8 was demonstrated to have anti-multiple myeloma properties *in vitro*. I discovered that UPRM8 elicits an apoptotic cell death response in RPMI-8226 multiple myeloma cells. This study demonstrates that chemical ablation of Ire1/Xbp1 signaling is a potential target for developing anti-multiple myeloma therapies or as adjuncts for current therapies. During the course of writing of this thesis, a study was published that supports the use of Ire1 inhibitors as anti-multiple myeloma agents.

7. UPRM8 was demonstrated to improve the *in vitro* anti-MM activities of bortezomib, an FDA-approved multiple myeloma chemotherapeutic agent. Furthermore, significant additive anti-MM properties were also demonstrated for UPRM8 and an eIF2α-phosphatase inhibiting compound called Salubrinal. These novel findings strongly argue for future *in vivo* validation of the anti-MM properties of the above drug combinations.

8. A structure-activity-relationship screen was used to identify important structural features for the anti-MM activity of UPRM8. This screen also identified UPRM8-like compounds that have even more potent anti-MM properties, in particular compound 17 warrants future study.

9. A novel separation of function mutant of *S. cerevisiae* Bem1p was identified and characterized. This Bem1-*s3* mutant was used to demonstrate that both SH3 domains of Bem1p are required for efficient MAPK signaling during the yeast mating response. Furthermore, this was the first demonstration that an F166L mutation in SH3-2 disrupts the PXXP-mediated binding to Ste20p and Boi1/2p.

10. Mass spectrometry analysis of Bem1p complexes identified novel Bem1p-interacting proteins and novel Bem1p phosphorylation sites. These physical interactions and phosphorylation sites of Bem1p allowed me to suggest a novel role for this scaffold protein in the response to cell wall stressors.

Contributions of Authors

Chapter 2, 3, and 4 of this thesis are manuscripts that have, or are currently, being prepared for submission for publication. As instructed by the guidelines for thesis preparation, the following section details the explicit contributions of all authors involved in these studies:

Chapter 2

The contents of this chapter have been submitted for publication as the following:

Daniel D Waller, Hetty N Wong, Eric Chevet, Stephanie Pollock, John JM Bergeron, and David Y Thomas. **Endoplasmic reticulum stress tolerance is mediated by a calnexin phosphorylation-dependent mechanism in *Schizosaccharomyces pombe*.**

Dr. Hetty Wong performed the *in vivo* metabolic labeling experiments required to map the site of calnexin phosphorylation (Figure 2.1A-D and Figure 2.2). Stephanie Pollock provided assistance by taking some of the OD measurements that are used for the growth curves presented in Figure 2.4. Dr. Eric Chevet provided assistance with the ribosomal pull-down assay. Drs. Chevet, Bergeron and Thomas provided helpful suggestions and reviewed numerous drafts of this manuscript. All other experiments and analysis were performed by me.

Chapter 3.

A manuscript for the contents of this chapter has been written and it will soon be submitted for publication:

Daniel D. Waller, Chloe Martel-Lorion, Kurt Dejgaard, Gregor Jansen, David Y. Thomas. **A high-throughput screen for small molecule modulators of the unfolded protein response identifies UPRM8, an inducer of apoptosis in multiple myeloma cells.**

The high-throughput screen was performed by Chloe Martel-Lorion. Dr. Kurt Dejgaard provided assistance with the HeLa cell cultures used to generate Figure 2.2. Drs. Dejgaard, Jansen and Thomas provided helpful suggestions and critical editing of this manuscript. Non-author collaborators for this manuscript include Dr. David Ron and Benedict Cross from Cambridge University, who tested our compounds in their Ire1 RNase assay (Figure 3.3B-D). All other experiments and analysis were performed by me.

Chapter 4

This thesis chapter represents ongoing work. A draft manuscript for the Bem1-*s3* separation of function mutant has been written and is being prepared for submission:

Daniel D. Waller, Robert B. Annan, Cunle Wu, Kurt Dejgaard, Malcolm Whiteway, and David Y Thomas. **Bem1-*s3* reveals that SH3 domain-mediated interactions are required for mating morphogenesis in *Saccharomyces cerevisiae.***

Dr. Dejgaard performed the in-gel digestions and mass spec analysis of Bem1p tryptic peptides. Drs. Annan, Wu, Dejgaard, Whiteway, and Thomas all provided invaluable guidance and suggestions for this project. All other experiments and analysis were performed by me.

CHAPTER ONE

General Introduction

1.1 The concept of biological stress

It is not surprising, given the collaborative nature of most scientific endeavours, that we are rarely able to attribute a given concept or idea to any one scientist. Moreover, the pursuit of science rarely provides large singular advances in our understanding of the natural world and so it is not surprising that scientists quickly develop a sort of self-effacing modesty when it comes to their achievements. This modesty could not be better evidenced than by these famous words, issued by Isaac Newton in a personal letter to his competitor Robert Hooke, "What Descartes did was a good step. You have added much several ways, ... If I have seen a little further it is by standing on the shoulders of giants." The greater meaning of these words has never been more apparent to me than they are now, as I attempt to communicate my research in this thesis and as I try to place my work into the broader context of stress research as a whole.

The biological concept of stress can be defined, at its most basic, as the response that results from placing a demand on any biological system. Given that biological stress is an abstraction, the word is often misused and it is easy to see how it can be confused with stressor, which is (are) the condition(s) that give rise to the biological demand in question. Also, given that stress is an unavoidable and ever-present consequence of life itself, it is not surprising that much has been written on the subject. It is also important to note that biological responses to the demands of stressors can be observed at almost every level of biology, from cellular stress responses right up to the emotional and physiological responses that manifest themselves in complex multicellular organisms like humans.

The subject of this thesis comprises an examination of several distinct cellular stress responses and, more specifically, I have investigated the signaling mechanisms that allow cells to communicate this demand in order to mediate an appropriate biological response. Wherever possible, I will highlight how these cellular stress responses can be impeded or supplemented in order to exert some degree of control over cellular fate. I choose to do this because the ability to exert control over life and death decision-making processes at the cellular level has widespread disease implications, particularly for cancer where dysregulated cell growth and evasion of cell death responses are frequently observed.

1.1.1 Historical context

For the same reasons discussed above, it has proven difficult to attribute our modern biological stress concept to any one scientist, even though a healthy amount of literature has examined this subject matter [1-4]. Hans Selye (1907-1982), a former McGill biochemistry professor, is widely accepted as one of the founding fathers of the modern concept of biological stress. Selye's work, although controversial to many, placed him at the forefront of stress research for more than four decades. In a landmark 1936 paper Selye described a 'general adaptation syndrome' (GAS) [5], when he observed what appeared to be a non-specific response in rats following exposure to a variety of 'nocuous agents'. This research stimulated important discussions on the concept of a generalized stress response but it was not until after the second world war that the concept of

biological stress became widely accepted. Selye freely admitted that his thoughts on the biological stress concept had borrowed heavily from pre-existing ideas put forth by Walter Cannon (1871-1945) and Claude Bernard (1813-1878).

Walter Cannon, a former professor of physiology at Harvard medical school, coined the terms "flight-or-fight response" and "homeostasis", although the latter was a concept based heavily upon Claude Bernard's description of what he described as the "Milieu intérieur". The central concept behind homeostasis or Milieu intérieur is that whole organisms, and the individual cells of which they are composed, all tend to maintain a constant internal environment. Importantly, the maintenance of this internal equilibrium requires the implementation of sophisticated feedback mechanisms in an open biological system that is subject to fluctuation. I will make liberal use of this homeostasis concept throughout this thesis because it is a concept that remains central to our understanding of cellular stress responses. I think Claude Bernard's words, issued more than a century ago, nicely summarize just how fundamental and important this concept of homeostasis is: "La fixité du milieu intérieur est la condition d'une vie libre et indépendante."

1.1.2 Cellular Stress

The study of biological stress has undergone a sort of natural evolution from the early works of Bernard, Cannon and Selye. Not surprisingly, stress research has expanded to include investigations of stress responses at the cellular level and examination of these responses has uncovered a large number of the

homeostatic mechanisms that are at work in order to maintain Bernard's observed milieu intérieur. I have chosen to borrow Dietmar Kültz's definition of cellular stress responses, which he defines as "a reaction to the threat of macromolecular damage" [6]. This definition of cellular stress is necessarily broad in order to be as inclusive as possible, given both the frequency and diversity of the stress responses that are employed by cells in their attempt to maintain homeostasis. Not surprisingly, the sources of cellular stress (stressors) are staggering in both number and diversity; however, cells have evolved diverse and sophisticated homeostatic responses to protect themselves in this constant struggle for internal balance. Here are but a few examples of the many cellular stressors that are known to exist: a lack or excess of nutrients, hypoxia, temperature extremes, high or low external osmolarity, and DNA damaging agents.

The heat shock response (HSR) provides a classic example of how cells attempt to maintain homeostasis in the face of a significant threat of macromolecular damage, in this case heat is the stressor (reviewed in [7, 8]). A primary requirement for the implementation of homeostatic responses is that cells must have sufficiently sensitive mechanisms to detect the biological demand being placed on them. In the case of heat shock this detection appears to be somewhat indirect. Cells do not have a thermostat per se, but instead they can monitor the structural fidelity of their protein machineries which can inform them of a multitude of threats, including heat shock.

Once detected, cellular stress responses require the implementation of mechanisms that are either rectifying or protective and in some cases are both. The HSR involves the transcription of a conserved set of genes that encode for a

class of proteins that became known as heat shock proteins (HSPs). Categorization of HSPs based on their biological function suggests that at least seven distinct classes of HSPs exist [8] and one very important class of HSPs are the molecular chaperones, like Hsp70 and Hsp90. Molecular chaperones assist protein folding by preventing proteins from adopting inappropriate conformations and by preventing aggregation during the folding process. The activities of these heat-induced chaperones illustrates the sort of protective mechanisms that cells employ to raise their tolerance thresholds for a variety of stressors by allowing them to protect the integrity of their macromolecular structures. Given the frequency with which cells encounter temperature fluctuations, it is not surprising to learn that many of these HSPs are evolutionarily conserved.

1.1.3 Conservation of cellular stress responses and the use of model organisms

The conservation of cellular stress response proteins extends beyond the aforementioned HSPs; in fact, stress response proteins represent some of the most evolutionarily conserved proteins [6, 9] and this reinforces the idea that a cellular capacity to respond to threats of macromolecular damage is a universality of life. For example, it has been shown that the stress response genes in humans account for 18% of the phylogenetically most highly conserved proteins [6].

Whenever such high degrees of conservation exist, it opens up opportunities to use model organisms to study these conserved biological processes. For example, cytological observation of the chromosomal puffs that appeared in the salivary glands of *Drosophila* species led to the eventual

discovery of the HSR (reviewed in [7]). Both budding yeast, *Saccharomyces cerevisiae*, and fission yeast, *Schizosaccharomyces pombe*, have long served as model eukaryotes for the study of conserved biological processes that operate at the cellular level.

The advantages of using yeast as model system for studying conserved eukaryotic processes are numerous and have been reviewed elsewhere [10, 11]. However, I would like to highlight a few of the most pertinent reasons why I have chosen to study cellular stress responses using yeast. Foremost is the high degree of conservation of cellular stress responses that I have mentioned above. Several of my findings, particularly those found in chapter three, extend significantly to human cells and have a direct relevance to disease processes. Furthermore, the powerful genetics of yeast and the accessibility of the yeast genomic knockout and over-expression collections provide many of the tools that are needed in order to dissect these cellular stress responses.

One final consideration is that yeast displays a minimalist set of conserved stress response mechanisms when compared to multicellular organisms. This minimalist set of yeast stress response mechanisms comes with both its advantages and disadvantages. The main disadvantage being that we cannot study the particulars of any stress response mechanisms that are not conserved between mammals and yeast. The added complexity of maintaining homeostasis in multicellular organisms seems to require an expanded repertoire of stress monitoring and response systems. The ER stress responses that I describe in chapter 3 of this thesis provide an excellent example of the added complexity of stress response mechanism found in higher eukaryotes. Yeast, such as *S.*

cerevisiae, contain only one ER-to-nucleus stress signaling pathway, whereas metazoan cells have at least three ER stress monitoring systems. This added complexity and/or redundancy in metazoan stress response systems can present significant investigational challenges that can be avoided by studying the most conserved stress responses in yeast.

1.2 The endoplasmic reticulum and protein folding stress

1.2.1 Protein synthesis and the endoplasmic reticulum

The endoplasmic reticulum (ER) is a membrane-enclosed organelle that is continuous with the outer nuclear envelope and is composed of an extensive network of cisternae. The rough ER is easily identified by its 'studded' appearance due to its decoration with ER-bound ribosomes. The ER is responsible for the production, post-translation modification, folding, and quality control monitoring of proteins destined for a variety of secretory compartments, including the plasma membrane and secretion into the extracellular milieu. The protein folding environment found within the interior of the ER, known as the ER lumen, is oxidizing [12] and contains high concentrations of calcium ions. These conditions closely mimic those found in the extracellular milieu and hence the ER allows for secretory protein maturation to occur under conditions that are relevant to those found at the final destination of these plasma membrane and secreted proteins (reviewed in [13]).

The presence of a short hydrophobic signal sequence (SS) at the NH_2-terminus is recognized and bound by the signal recognition particle (SRP), which

pauses protein translation. The SRP then targets the ribosome-nascent chain complex (RNC) to the ER by binding to its cognate membrane-bound receptor (SR) in a GTP-dependent fashion. The RNC is thus delivered to the ER translocon, the central core of which is composed of two Sec61αβγ heterotrimers. So only after SRP/SR-dependent delivery of the RNC to the translocon does chain elongation resume, thereby allowing cotranslational translocation of this newly synthesized polypeptide. Numerous excellent reviews on the targeting and translocation of nascent secretory proteins to the ER exist [14, 15]. The N-terminal signal sequences are usually removed from nascent proteins by the activity of the signal peptidase complex (SPC) during the process of cotranslational translocation (reviewed in [16]).

Secretory proteins are commonly subject to post-translational modification by the addition of asparagine-linked (N-linked) glycans. N-linked glycosylation occurs on the side chains of asparagine residues that typically fall within the canonical Asn-X-Ser/Thr consensus. A dolichol-linked fourteen-sugar core oligosaccharide unit ($Glc_3Man_9GlcNAc_2$) is transferred en bloc to asparagine side chains through the activity of the oligosaccharyl transferase (OST) complex (reviewed in [17]). N-linked glycosylation occurs co-translationally and is therefore not dependent on tertiary structure. N-linked glycosylation serves a multitude of biological functions and these have been discussed elsewhere in detail [18, 19]; however, the role of N-linked glycans in ER protein folding is particularly relevant to the work described in this thesis and so it is discussed briefly below (see section *1.2.2*).

1.2.2 ER-assisted folding and the calnexin cycle

Protein folding begins concomitantly with cotranslational translocation and continues until proteins reach their native conformations or until they are marked for destruction and extruded back out into the cytoplasm for degradation by the ubiquitin-proteasome system. A host of folding enzymes and chaperones reside within the ER and their concerted efforts, which are of course guided by the unique thermodynamic and kinetic properties of the protein fold in question, aid in the production and export of folded glycoproteins from the ER, in a process that has been referred to as ER-assisted folding (ERAF) [20, 21]. Classical ER-resident molecular chaperones include members of the Hsp70 (BiP/GRP78), Hsp90 (GRP94), and Hsp100 (Torsin A) families, amongst others [13]. These molecular chaperones, like their cytosolic counterparts, protect incompletely folded proteins from adopting irreversible non-native conformations. BiP has been proposed as a master regulator of ER function [22] and its role in protein folding, activation of ER stress sensors, and in ER-associated degradation are of particular relevance to this thesis.

In addition to the conventional members of the Hsp-family of molecular chaperones, the ER contains two lectin-like molecular chaperones, called calnexin and calreticulin. These molecular chaperones were isolated as Ca^{2+} binding proteins of the ER[23, 24] and were later shown to retain non-native glycoproteins in the ER via the carbohydrate binding properties of their lectin domains [25-30]. More specifically, this lectin-based chaperone system retains nascent glycoproteins by interacting with monoglucosylated oligosaccharide side chains

($Glc_1Man_9GlcNAc_2$). The role of this lectin-based chaperone system in ER-assisted folding has been discussed extensively in numerous excellent reviews ([13, 31-36]) and so I will only briefly cover this topic in the following paragraph.

Once the core oligosaccharide unit ($Glc_3Man_9GlcNAc_2$) has been transferred to asparagine side chains by the OST complex, trimming of this N-linked glycan can occur. The two outer-most glucose residues, called glucose 1 and glucose 2, are successively trimmed by the activities of glucosidase I (GI) and glucosidase II (GII), respectively. The resulting monoglucosylated nascent glycoprotein is then competent to bind to the lectin domains of calnexin and calreticulin. Not only do these lectins act as classical molecular chaperones in ERAF, but they also bring the oxidoreductase ERp57 into close association with these maturing glycoproteins[37-39]. The extended P-domains of calnexin or calreticulin allows binding to the B' domain of ERp57 and this physical interaction contributes to ERAF by directing the disulfide bond shuffling activities of ERp57 to the maturing glycoproteins that are bound to the lectin chaperone system.

After release of glycoprotein from the calnexin/ERp57 ERAF complex, the final glucose sugar can be trimmed, again by the enzymatic activity of GII, and this last glucose trimming event precludes further association with the lectin chaperone system. However, the final conformations of glycoproteins are assessed by the folding sensor function of UDP-glucose:glycoprotein glucosyltransferase (UGGT), which then reglucosylates partially- or mis-folded glycoproteins. This reglucosylation by UGGT returns non-native glycoproteins to the monoglucosylated form and hence permits re-entry into the lectin chaperone

system in what is often referred to as the calnexin cycle. In this way, rounds of glucose trimming and reglucosylation provides the means to both monitor the folding status of a protein, via UGGT, and retain, via calnexin/calreticulin, monoglucosylated non-native folding intermediates. If proteins become terminally misfolded or simply fail to achieve their native conformations after spending an extended amount of time in the calnexin cycle they are targeted for destruction in a process called ER-associated degradation (ERAD), which is discussed below (see 1.2.3).

1.2.3 ER-associated degradation

The efficiency of protein folding is variable and is highly dependent on the properties of the protein fold in question. As yet, no reliable sequence-based predictor of protein folding efficiency exists; regardless, such a predictor would likely have significant accuracy problems since the folding capacity of the ER depends on a number of environmental variables and is highly adaptive (see 1.2.4). The ERAF machinery, and in particular the glycan-dependent system outlined in section 1.2.2, continues folding attempts on non-native folding intermediates; however, cells must balance the investment of continued folding cycles with maintaining a sufficient throughput of ER protein folding and so it does this by removing off-pathway folding intermediates that have become terminally misfolded. Not surprisingly, cells have evolved sophisticated mechanisms for setting a timer on ERAF and have evolved equally sophisticated machineries to recognize, dislocate, and degrade terminally misfolded proteins.

Given that ERAD is crucial for maintaining the protein folding capacity of the ER and also given that ERAD mechanisms have been implicated in numerous diseases of protein misfolding [40, 41], excellent literature reviews on ERAD exist [42-44]. Of particular significance to this thesis is that disruption of ERAD clearance mechanisms via small-molecule proteasomal inhibitors, like bortezomib (BZ), can cause an accumulation of misfolded protein in the ER[45-49].

1.2.4 ER stress

The term ER stress is generally used to refer to stressors or demands that lead to an accumulation of unfolded protein in the ER. Such an accumulation of unfolded protein can result from normal differentiation cues, from pathological situations like viral infection, and from a variety of environmental conditions. In particular, nutrient deprivation, hypoxia, depletion of ER calcium, disruption of the oxidizing environment within the ER, disruption of N-linked glycosylation and, as mentioned in section 1.2.3, disruption of ERAD clearance mechanisms can all cause protein folding difficulties and are thus considered stressors of the ER.

The vast majority of ER stress research has centered on the study of acute ER stress responses that are produced by chemical stressors that strongly disrupt ER protein folding and hence lead to a dramatic and severe accumulation of unfolded protein. Classic examples of chemicals that act as ER stressors include the following: tunicamycin (TM), a selective and potent inhibitor of N-linked glycosylation; 2-deoxy-D-glucose (2-DG), a glucose analog that also causes N-

linked glycosylation defects; thapsigargin (TG), a SERCA pump inhibitor that causes depletion of ER Ca^{2+} stores; dithiothreitol (DTT), a strongly reducing reagent that disrupts the oxidative environment in the ER; and finally bortezomib or MG132, which are proteasomal inhibitors that disrupt ERAD.

These above chemical inducers of ER stress have proven to be invaluable tools for studying acute ER stress responses; however, a better understanding of *in vivo* ER stress responses will require the identification of more subtle, chronic, cellular responses to physiological sources of ER stress. A key requirement for identifying models of physiological ER stress is the development of robust and quantitative transcription-based reporters of ER stress, which can be used to monitor ER stress responses *in vivo*. Such *in vivo* reporters have proven instrumental in identifying the factors involved in the ER stress responses of yeast [50-52] and, more recently, reporters that allow the visualization of ER stress have been described for mammalian cell systems and transgenic mice have even been successfully generated [53, 54].

Transgenic mice that have disruptions in genes that have known functions in ER stress responses, like Xbox-binding protein 1 (Xbp1) or PKR-like endoplasmic reticulum kinase (PERK), have already proven useful in identifying developmental processes that rely on a robust ER homeostasis machinery. These developmental restriction points that rely on ER homeostatic mechanisms are, not surprisingly, frequently observed in tissues that carry a high secretory burden. For example, the transcription factor that is activated by mammalian Ire1, called Xbp1 (see 1.3.2), has been shown to be required for the differentiation of B lymphocytes into antibody-producing plasma cells [55, 56]. PERK knockout

mice, although viable, were found to develop diabetes mellitus following the loss of their insulin-secreting β-islet cells and had pathologies that closely resembled human Wolcott-Rallison syndrome [57]. Widespread use of these various transgenic animal models should allow us to greatly expand our current understanding of physiological ER stress responses and should highlight the importance of ER homeostatic mechanisms in a variety of developmental and pathological processes.

Given the importance of the ER in the synthesis, folding, and secretion of secretory proteins, it is not surprising that cells have evolved sophisticated mechanisms that allow them to monitor the protein folding within the ER and to adjust the folding capacity of the ER to match the secretory demands and to respond to various environmental insults. The study of these ER homeostatic processes forms an integral component of this thesis and I have devoted the next several subsections of this introduction (see 1.3) to expand on these concepts.

1.3 Cellular responses to ER stress

1.3.1 ER homeostasis and the unfolded protein response

Disturbances in the protein folding capacity of the ER can stimulate a number of homeostatic mechanisms that are collectively referred to as the unfolded protein response (UPR) [58]. A primary requirement for this adaptive response is the ability to sense an accumulation of unfolded protein within the ER lumen and to transmit this signal of unfolded protein across the ER membrane to the cytosol and ultimately to the nucleus, where appropriate biological counter

measures are implemented. In yeast, the sensing and transmission of unfolded protein relies on the activity of a type I ER-resident transmembrane protein originally termed the inositol requiring enzyme 1 (Ire1p). The Ire1 pathway is the most conserved UPR signaling system and Ire1 itself is highly conserved among eukaryotes; however, metazoan cells contain at least two additional ER transmembrane sensors of unfolded protein, called activating transcription factor 6 (ATF6)[59, 60] and PERK [61].

The aforementioned UPR sensor proteins each utilize distinct signaling mechanisms to transduce the signal for unfolded protein to cytoplasmic and nuclear factors (discussed in 1.3.2); however, a common theme for these UPR signaling pathways is that they each lead to the production of potent transcriptional activators. These various UPR-activated transcription factors translocate to the nucleus where they implement specific transcriptional programs that aim to resolve the protein folding stress in the ER. These transcriptional programs represent a central element of ER homeostatic mechanisms in eukaryotes as divergent as yeast and mammals. In fact, elucidation of the Ire1p and ATF6 UPR pathways was made easier by the identification of the relevant cis-acting elements upstream of ER stress-induced genes in yeast and human cells, respectively [52, 60]. ER stress-induced transcriptional programs serve to increase the protein folding capacity of the ER by increasing the expression of genes involved in protein folding, protein translocation, glycosylation, secretion, membrane biogenesis, ERAD, among others [62-64]. All three branches of the metazoan UPR result in the liberation or synthesis of distinct trans-acting factors and each of these transcription factors contributes to the overall transcriptional

response that results from exposure to ER stressors (Figure 1.1) (see 1.3.2 for more on these transcription factors).

In addition to these transcriptional responses, metazoan UPRs seek to alleviate the protein folding burden of the ER through the implementation of a global translational repression, which is the result of PERK-dependent phosphorylation of the translation initiation factor eIF2α [61]. This PERK-induced translational attenuation not only serves to reduce the amount of newly synthesized protein that enters the stressed ER, but it also paradoxically serves to increase the expression of a limited number of genes that act as effectors of the PERK-dependent UPR pathway and this includes the transcriptional activator ATF4 (see 1.3.2).

PERK-induced translational attenuation is now recognized to be the ER stress-activated component of the integrated stress response (ISR) [62]. The ISR was aptly named because it integrates stress signaling responses from numerous eIF2α kinases, which are activated by diverse stressors, such as amino-acid starvation, single stranded RNA, heme depletion, and ER stress (reviewed in [58]). The convergence of these diverse protein kinase-based stress responses on eIF2α underscores the importance of translational regulation to the successful implementation of numerous homeostatic stress responses.

1.3.2 Efferent signaling from the ER in response to unfolded protein

Saccharomyces cerevisiae relies solely on the Ire1p-dependent UPR pathway for sensing and responding to an accumulation of unfolded protein

within the ER (reviewed in [58, 65, 66]). The details of how Ire1 is activated by unfolded protein are discussed in section 1.4 and it culminates in the activation of Ire1p's C-terminal ribonuclease (RNase) domain. In response to ER stress the RNase domain of Ire1 is responsible for the removal of a 252-base pair intron from the mRNA of HAC1, a basic leucine zipper (bZIP) transcriptional activator [67]. The cleavage of full-length HAC1 mRNA ($Hac1^{u}$) by Ire1 is followed by ligation of the resulting 5' and 3' mRNA fragments, which requires the enzymatic activity of the tRNA ligase, Trl1p [68]. Trl1p-dependent ligation of these Hac1 mRNA fragments produces a spliced form of HAC1 mRNA ($Hac1^{i}$) that can be efficiently translated by ribosomes [67]. Hac1p, the protein product of $Hac1^{i}$ mRNA, binds directly to unfolded protein response elements (UPREs) and, together with another bZIP transcription factor Gcn4p [69], it induces the expression of yeast UPR target genes [64, 70, 71].

As mentioned previously, metazoan cells have an expanded repertoire of ER homeostatic mechanisms that involve at least three signaling pathways (Figure 1.1)(reviewed in [58, 65, 66]). The Ire1 pathway described above is extremely well conserved and two Ire1 homologs, Ire1α and Ire1β, have been identified in mammals [72, 73]. Ire1α is expressed ubiquitously, whereas Ire1β expression appears to be restricted predominantly to intestinal epithelial cells [72, 74].

XBP1, which is the metazoan ortholog of HAC1, produces an mRNA transcript (XBP1u) that is spliced by IRE1 in response to ER stress [75, 76]. Ire1-dependant removal of this 26-nucleotide intron from XBP1u mRNA produces a spliced XBP1 transcript (XBP1s) that contains an altered reading frame on the 3'

side of the splice-site junction [76]. Unlike HAC1 mRNA in yeast, both XBP1u and XBP1s mRNAs can be efficiently translated into protein; however, the protein encoded by XBP1u mRNA is rapidly degraded by the ubiquitin-proteasome system [76]. If the XBP1u protein is stabilized, either by proteasomal inhibition or by mutation of its ubiquitinated lysines, it behaves in a dominant negative fashion and suppresses XBP1s-dependent transcriptional activation [46, 76]. Since the above efferent Ire1-dependent signaling mechanisms ended up being the primary focus of my chemical biology investigations into UPR signaling (see Chapter 3), I have provided only a brief introduction to the other two metazoan UPR pathways in the following paragraphs.

In addition to IRE1, metazoan cells contain a second type I ER-resident transmembrane kinase, called PERK (Figure 1.1). PERK is also activated by dimerization in response to unfolded protein in the ER and its kinase activity leads to a global translational repression via phosphorylation of the translation initiation factor eIF2α [61]. PERK-dependant translational attenuation during ER stress is thought to reduce the burden on the ER chaperone system by reducing the amount of newly synthesized ER client protein. Somewhat paradoxically, this eIF2α-mediated translational repression leads to the increased translation of a small number of mRNAs, including the mRNA of activating transcription factor 4 (ATF4).

Increased expression of ATF4 occurs following PERK-mediated eIF2α-phosphorylation because delayed ribosome assembly causes several upstream open reading frames (uORFs) to be bypassed in favour of translational re-

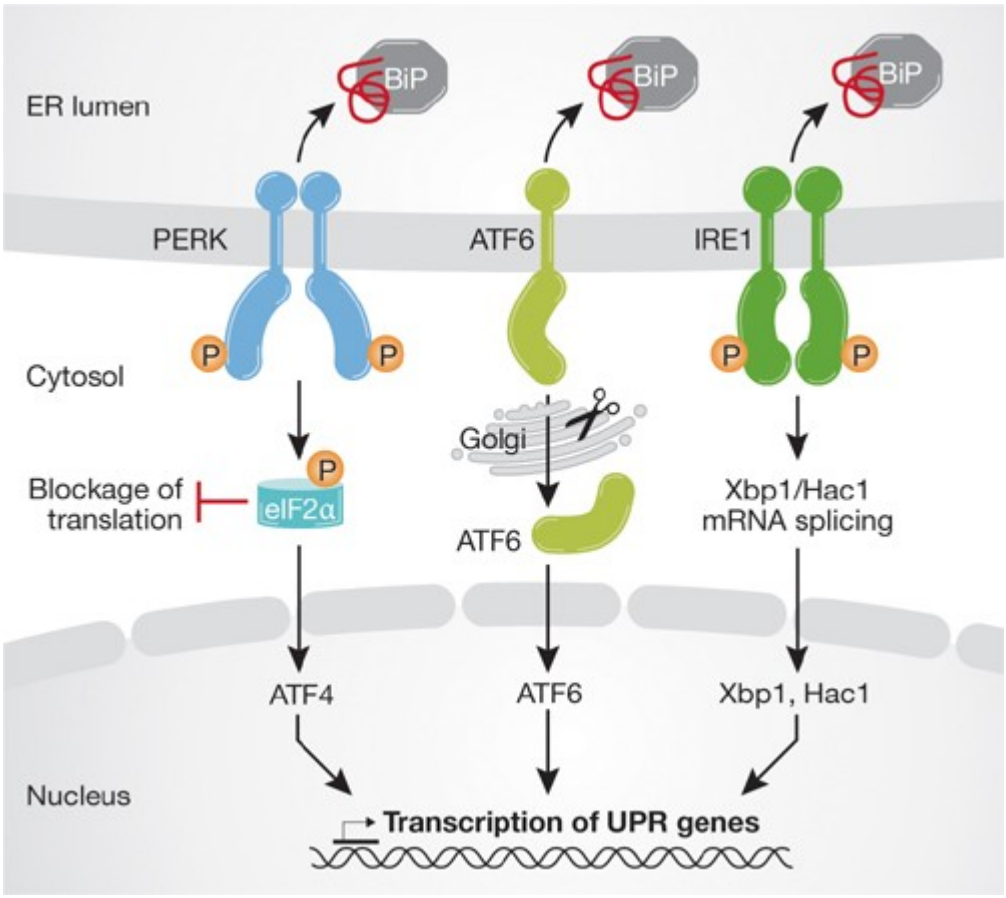

Figure 1.1. The unfolded protein response in metazoan cells. Three UPR signaling pathways culminate in the activation of distinct transcription factors that upregulate the expression of UPR target genes. PERK, ATF6, and IRE1 are ER transmembrane sensor proteins that detect unfolded protein and each of these sensors binds to BiP under resting (non-stressed) conditions. Unfolded protein in the ER causes these ER transmembrane sensor proteins to lose their association with BiP. PERK dimerizes in response to unfolded protein and this leads to the stimulation of its cytosolic kinase domain. PERK phosphorylates eIF2α and thereby instigates a global repression of translation. This translational attenuation paradoxically increases the expression of a transcription factor called ATF4. Ire1 activation involves its oligomerization in response to unfolded protein and this stimulates it cytosolic kinase activity. Ire1 trans-autophosphorylation leads to the activation of its C-terminal ribonuclease domain. The ER stress-regulated ribonuclease activity of Ire1 mediates the non-conventional splicing of a UPR transcription factor called Xbp1 (Hac1 in yeast). ATF6 is a membrane tethered bZIP transcription factor that is activated by proteolysis. Unfolded protein causes ATF6 to traffic to the golgi, where it is proteolytically cleaved and the liberated from the membrane. The liberated p50ATF6 fragment translocates to the nucleus and contributes to the induction of UPR genes. Adapted from [80].

initiation at the more downstream ATF4 start codon [77, 78]. This translational bypass mechanism of post-transcriptional gene regulation in response to stress is also conserved in yeast, where Gcn2p-dependent phosphorylation of eIF2α leads to increased translation of GCN4 mRNA in response to a variety of stressors, including amino acid limitation (reviewed in [79]).

ATF4 is potent transcriptional activator which upregulates a number of important ER stress responsive genes, including those involved in apoptosis, ER redox homeostasis, amino acid transport, amino acid metabolism, and recovery from eIF2α-mediated translational repression [62]. For example, ATF4 has been shown to heterodimerize with CCAAT/enhancer-binding protein-β (C/EBP-β) in order to upregulate the expression of C/EBP homologous protein (CHOP) [81, 82]. CHOP is itself a bZIP transcription factor whose activities contribute to ER stress-induced apoptosis and I will expand further on this important role of CHOP in section 1.3.3.

The third metazoan ER stress transducer, ATF6, was isolated in a yeast one-hybrid screen for its capacity to bind to mammalian ER stress response elements (ERSE) [60]. ATF6 encodes a bZIP transcription factor that is inactive under non-stressed conditions due to its tethering to the ER membrane via a transmembrane sequence. ER stress promotes the transport of full-length ATF6 (p90ATF6) from the ER to the Golgi, where it undergoes sequential cleavage by site 1 (S1P) and site 2 (S2P) proteases to produce a liberated ATF6 cytosolic fragment (p50ATF6 or ATF6f) [83]. This membrane-liberated p50ATF6 fragment can freely translocate to the nucleus, where it acts as potent

transcriptional activator by binding to ERSEs in the promoters of ER stress-regulated genes [59].

The complexity of this three-pathway ER homeostatic system that is found in metazoan cells remains the subject of current research efforts. These sophisticated ER homeostatic mechanisms aim to restore protein folding in the ER by increasing both the folding and ERAD capacities of the ER and by limiting new protein synthesis until the protein folding disturbances in the stressed ER can be resolved. Even after the successful implementation of these sophisticated countermeasures, the severity of some ER stress insults can exceed the protective capacity of these homeostatic mechanisms. In the face of this sort of irremediable ER stress the cells of multicellular organisms frequently execute a programmed cell death in order to safeguard the integrity of the organisms' secretory proteins.

1.3.3 Irremediable ER stress and apoptosis

The primary function of cellular stress responses is to protect from threats of macromolecular damage; however, if the encountered stressor is too severe for homeostatic mechanisms to overcome, programmed cell death is frequently employed as a protective measure in multicellular eukaryotes. This paradigm of programmed cell death in the face of irremediable stress holds true for severe ER stress. The mechanisms that contribute to ER stress-induced apoptosis are numerous and have been reviewed elsewhere [84-87]. The following paragraphs

provide a brief overview of some of the more pertinent signaling mechanisms that govern cell fate decisions in response to irremediable ER stress.

It has been shown that numerous ER stress-dependent mechanisms can promote apoptosis; the complexities of, and interplay between, these numerous ER stress-induced pro-apoptotic mechanisms remain the subject of current research efforts. It has been shown that activated Ire1 can recruit the adaptor protein tumour necrosis factor receptor-associated factor 2 (TRAF2), which ultimately results in the activation of the pro-apoptotic c-JUN NH_2-terminal kinase (JNK) [88]. It appears that TRAF2 activation of JNK occurs through apoptosis signal-regulating kinase 1 (ASK1), which forms part of the Ire1/TRAF2/ASK1 complex that was shown to be required for ER stress-induced JNK activation in mouse embryonic fibroblasts (MEFs) and primary neurons [89]. JNK activation promotes apoptosis in numerous ways, including the mitochondria/Apaf1-dependent (intrinsic) caspase activation pathway [88-90].

Murine caspase-12, an ER localized pro-apoptotic mediator, becomes activated specifically by ER stress and caspase-12 null mutant mice were found to be more resistant to ER stress-induced cell death [91]. Caspase-12 mediated cell death was found to occur through cytochrome c-independent activation of caspase-9, which then proceeds to activate its usual downstream effector caspase, which is caspase-3 [92]. It should be noted that the human version of the caspase-12 gene contains inactivating mutations [93] and so its role in ER stress-induced apoptosis remains unclear; however, a human caspase-4 is similar to murine caspase-12 and has been implicated in ER stress-induced apoptosis [94].

Another important pro-apoptotic mechanism that occurs in response to ER stress is the induction of CHOP mRNA. All three branches of the metazoan UPR converge on CHOP expression (reviewed in [95]); however, the PERK pathway appears to be the most important for CHOP induction since its upregulation is almost completely abolished in either PERK null mutants or in cells that contain a non-phosphorylatable version of eIF2α (eIF2α^{S51A}) [82, 96].

CHOP is a basic leucine zipper (bZIP) transcription factor that has numerous pro-apoptotic functions when ER stress conditions remain unresolved [95]. The pro-apoptotic functions of CHOP include some of the following: CHOP implements a negative feedback loop that alleviates the translational attenuation by increasing the expression of GADD34, a regulatory subunit of protein phosphatase 1 that targets its activity to mediate the dephosphorylation of eIF2α [97-99]; CHOP increases the expression of TRB3, a human homolog of the *Drosophila* tribbles protein [100]; and CHOP reduces the expression of the pro-survival apoptotic regulator, B-cell lymphoma 2 (Bcl2) [101]. The importance of the pro-apoptotic functions of CHOP are highlighted by the fact that CHOP knockout cells display increased resistances to a variety of ER stress-induced apoptotic stimuli [102].

The cytosolic ribonuclease domain of Ire1α has recently been found to be involved in the decay of a specific subset of ER-localized mRNAs in *Drosophila,* mice, and human cells [103-105]. This so-called "regulated Ire1-dependent decay" (RIDD) of mRNAs at ER translocons is expected to lessen the burden on the ER by limiting the amount of new protein synthesis that occurs at membrane-bound ribosomes. One study showed that divergent cell fates followed two

distinct artificial activation mechanisms for Ire1α; overexpression-induced phosphotransfer activation of Ire1 stimulated RIDD and led to significant apoptosis, whereas reduced cell death was observed following pseudokinase activation of Ire1[103]. Pseudokinase activation was induced by treating the analog-activatable Ire1(I641G) mutant [106] with 1NM-PP1 and this activation strategy resulted in Ire1-dependent cleavage of Xbp1 in the absence of RIDD [103]. These results suggest that divergent cell fates can be achieved by controlling the specific signaling outputs of the Ire1 pathway.

It also appears that differential activation of the three metazoan UPR pathways may also contribute to divergent cell fates. For example, prolonged exposure to ER stress led to attenuated Ire1 and ATF6 signaling responses, while PERK signaling, including CHOP induction, remained high [107]. These authors also observed increased cell survival if Ire1 signaling was maintained artificially, again via pseudokinase activation of the 1NM-PP1- activated Ire1(I641G) allele. These results imply that the ability to independently control the activity of multiple UPR signaling branches simultaneously in metazoan cells may afford the opportunity to control cell fate. In chapter 3 I took advantage of this knowledge by employing pathway-specific small molecules to artificially control both Ire1- and PERK-dependent signaling outputs and was able to promote apoptosis in cultured multiple myeloma cells.

When taken together, the literature suggests that individual UPR signaling pathways have both pro-survival and pro-apoptotic outputs. Furthermore, the differential timings of activation and subsequent attenuation of each these three canonical UPR pathways controls cell fate. I should mention that there are

numerous other pro-apoptotic mechanisms which, in the interest of brevity, I have elected not to describe here; however, they are described in the numerous excellent reviews of ER stress-induced cell death that I cited previously and will cite here again [84-87]. Given the importance of ER homeostatic mechanisms in controlling cell fate decisions in response to physiological, pathological, and environmental conditions that disturb protein folding in the ER, it is not surprising to learn that ER homeostatic mechanisms have been implicated in the pathogenesis of a multitude of human diseases.

1.3.4 ER homeostatic mechanisms in cancer

Given the importance of both secreted and plasma membrane proteins to eukaryotic biology, it is not surprising that ER homeostatic mechanisms have widespread disease implications [108-110]. Disease implications for ER stress and the UPR are varied, numerous, and include the following: viral infection [111], neurodegenerative disease [112], metabolic disease [113], renal disease [114], heart disease [115, 116], cerebral ischemia [117, 118], and cancer [119-122]. Such widespread disease implication underscores the need for a more complete understanding of ER homeostatic responses and for the identification of small-molecule modulators that can help dissect these important signaling pathways. Since the latter need was the objective of chapter 3 of this thesis and since I chose to apply our small-molecule UPR modulators (UPRMs) to the study of ER homeostatic mechanisms in cancer, I expand on this topic in the subsequent paragraphs of this subsection.

It is well established that the poor vascularization of many solid tumours can become growth limiting and, not surprisingly, much has been said on the importance of cancer cell adaptation to these harsh tumour microenvironments [123-128]. The adaptive mechanisms that are employed by cancer cells to survive in harsh tumour microenvironments are numerous and ER homeostatic mechanisms are now counted among them [119-121]. In particular, the hypoxic and glucose-limited conditions found in poorly vascularized tumours results in ER stress and so cancer cells frequently employ ER homeostatic mechanisms for their continued survival [54].

Activation of UPR mediators like Xbp1 and ATF6, or upregulation of their downstream pro-survival UPR target genes, like BiP or GRP94, has been observed in many different tumour types and cancer cell lines [129-133]. This evidence, although merely correlative, strongly supports a role for ER homeostatic mechanisms in cancer. Importantly, other studies have shown that impairment of ER stress-mediated BiP upregulation, whether achieved genetically [134] or through the activity of a small-molecule called versipelostatin (VST) [135], led to significant inhibition of tumour growth in two independent mouse xenograft models [134, 136].

Xbp1 and its downstream transcriptional targets, BiP and GRP94, have been shown to be induced in HT1080 human fibrosarcoma cells in response to hypoxia [137]. Similarly, over-expression of Xbp1 was found in primary breast cancers [138], as well as in colorectal adenomas and adenocarcinomas [139]. Xbp1-deficient mouse embryonic fibroblasts (MEFs) displayed severely compromised tumorigenicity in nude mice and the Xbp1-deficient tumours that

did develop showed significantly reduced growth rates in a mouse xenograft model [137]. The above studies clearly implicate ER homeostatic mechanisms, and more specifically the Ire1/Xbp1 UPR pathway, in the survival and proliferation of cancer cells in the frequently hypoxic/hypoglycemic microenvironment of solid tumours.

The relevance of the Ire1/Xbp1 pathway to cancer extends beyond the adaptations required for cancer cell survival in harsh tumour microenvironments; Ire1-mediated splicing of Xbp1 appears to be important not only for the differentiation of normal plasma cells (PCs)[55, 56] but also for the underlying pathogenesis of multiple myeloma (MM)[140]. When the activated (spliced) form of Xbp1, called Xbp1s, was expressed *in vivo* under the control of a B cell-specific immunoglobulin (Ig) promoter, transgenic mice developed disease symptoms that recapitulated many of the clinical features of human multiple myeloma, including: various skin and kidney pathologies, hypergammaglobulinemia, bone marrow plasmacytic infiltrates, and lytic bone lesions [140]. Furthermore, Xbp1s expression was observed in a significant number (50/70, 70%) of primary PCs isolated from human MM patients and not in PCs isolated from healthy donors[140]. The above evidence clearly supports a role for the Ire1/Xbp1 pathway in the pathogenesis of MM.

MM cells have also been found to be exquisitely sensitive to agents that cause ER stress, particularly proteasomal inhibitors, such as BZ or MG132 [46, 141, 142]. BZ, which is marketed as Velcade® by Millennium pharmaceuticals, has been clinically approved for treating both newly diagnosed and relapsed MM and is frequently administered to patients as part of a combination therapy with

other chemotherapeutics agents, such as melphalan (an alkylating drug) and dexamethasone (a glucocorticoid). Numerous studies have suggested that BZ-induced MM cell death is due in large part to ER stress-induced apoptosis, which results from impaired proteasome function in these Ig-producing secretory cells [46, 49, 141, 143].

The above literature suggest that MM cancer cells should provide an excellent model system to test novel small-molecule modulators of the UPR because these cells are exquisitely sensitive to ER stress and because they are reliant on their Ire1/Xbp1 ER homeostatic mechanisms. Given that the clinically-approved proteasomal inhibitors kill MM cells by inducing a terminal ER stress, I hypothesize that it should be possible to supplement or improve these proteasomal inhibitor therapies by simultaneously impairing cytoprotective ER homeostatic mechanisms. Since Ire1/Xbp1 UPR pathway has been directly implicated in tumorigenesis, in adaptation to harsh tumour microenvironments, and in MM pathogenesis, so the need to identify small-molecule modulators of this ER homeostatic response is apparent. Chapter 3 describes the identification and characterization of just such a small molecule modulator of the Ire1/Xbp1 UPR; implications for the use of this small molecule in killing multiple myeloma cells are also given.

1.4 Activation of Ire1 in response to ER stress: a multi-step process with features that lend themselves to chemical biology-based approaches for their study

The N-terminal lumenal domain of yeast Ire1p, mammalian Ire1, and PERK all sense unfolded protein in the ER because domain swapping experiments in yeast suggest that they are all functionally interchangeable [144, 145]. Structural insights from numerous groups have shed light on the activation requirements for both the lumenal sensing domain and cytosolic effector regions of Ire1 [146-150]. In response to unfolded protein the lumenal domain of Ire1 loses its association with BiP [144, 151], which was an event that was originally proposed to be an essential activation requirement; however, the identification of Ire1 mutants that failed to interact with BiP but that retained UPR function suggested that BiP servers as a negative regulator of Ire1 activity, rather than as an essential activation mechanism [152, 153].

The crystal structure of the yeast Ire1p lumenal domain revealed an extensive dimer interface; furthermore, the dimers formed by the lumenal domain created a major histocompatibility complex-like groove that has been proposed to bind directly to the unstructured hydrophobic regions of unfolded protein [146]. Direct binding of unfolded protein was predicted to result in the formation of higher-order Ire1 oligomers [146] and the formation of these higher-order oligomeric structures has been confirmed visually by immunofluorescence of Ire1p in stressed yeast cells [154]. Direct binding of yeast Ire1p to unfolded proteins was confirmed by showing that a recombinant Ire1p construct, containing the core stress sensing region (CSSR) of Ire1p, was able to inhibit the *in vitro* aggregation of guanidine-treated firefly luciferase or porcine citrate synthase enzymes [154]. However, the crystal structure of the lumenal domain of mammalian Ire1α suggests that direct binding to unfolded protein may not be as

important for activation of mammalian Ire1 [150]. The MHC-like grooves that were formed upon dimerization of the lumenal domains of Ire1α did not appear to be large enough to accommodate unfolded peptides and the lumenal domains spontaneously dimerize *in vitro* in the absence of unfolded protein [150].

Regardless of these differing capacities to bind unfolded protein directly, it is clear that dimer/oligomer formation is a critical activation event for both yeast and mammalian Ire1. For example, yeast Ire1p oligomerization has been shown to stimulate the inherent phospho-transfer activity of its cytosolic kinase domain, an activation step that results in trans-autophosphorylation of Ire1p [155, 156]. This oligomerization-induced autophosphorylation of Ire1p has been shown to activate its cytosolic RNase domain, which leads to the non-conventional splicing of $HAC1^{u}$ mRNA [67].

Interestingly, the identification Ire1-L745A and Ire1-L745G mutants, that were shown to bind to the ATP-competitive drug called 1NM-PP1, revealed that the kinase activity could be bypassed through the allosteric action of 1NM-PP1-binding to the nucleotide binding pocket [106]. This so-called pseudokinase activation of Ire1 actually served to shed some light on the previous observation that either ATP, ADP, or their non-hydrolysable analogs, all could potently stimulate the *in vitro* RNase activity of Ire1 [67]. Later crystallographic evidence suggested that nucleotide binding to the nucleotide-binding site of Ire1 results in a conformation change in Ire1 protomers that leads to back-to-back dimer formation of paired Ire1 RNase domains [148]. The formation of these back-to-back dimers of the RNase domains of Ire1 appears to be critical for its unconventional splicing activities, and more recently it has been shown that back-to-back dimer formation

can also be further stimulated by the binding of plant flavonols, like Quercetin, to a secondary ligand binding site (termed the 'Q-site') [149].

In theory, it should be possible to identify small molecules that can either stimulate or impair any of the numerous Ire1 activation steps discussed above. The following qualities of the Ire1-dependent UPR pathway make it an attractive candidate for chemical biology-based approaches: the activation of Ire1 involves a multi-step process with several steps that have already been bypassed by small molecules, its activation requires conformational changes, and its activation is regulated by at least two different ligand binding sites (nucleotide-binding and Q-site). Also, the aforementioned implications of the Ire1/Xbp1 pathway in controlling cell fate and in the pathogenesis of a variety of human diseases, such as cancer, only served to reinforce the need to identify small-molecule modulators of Ire1 function. These arguments coalesced into the central hypothesis that motivated the research contained in chapter 3 of my thesis, namely: that if small molecule modulators of Ire1 activity could be identified, we could employ these small molecules to exert artificial control over Ire1-dependent ER homeostatic responses and in so doing we should have the ability to exert some control over the fate of ER stressed cells, like multiple myeloma cancer cells.

1.5 Cytoplasm-to-ER signaling during ER stress via Calnexin phosphorylation

Calnexin was originally isolated as a Ca^{2+}-binding integral membrane protein of the ER and it was observed that it could be phosphorylated *in vitro* by

an ER-associated kinase activity [23]. This ER-associated kinase was later identified to be casein kinase II (CK2) and a purified version of CK2 was shown to phosphorylate calnexin that was obtained from heat-inactivated microsomes [26]. Numerous studies contributed to the elucidation of calnexin`s role as an important component of the lectin-based chaperone system, where it functions to retain monoglucosylated glycoprotein folding intermediates (see 1.2.2)[26, 30, 157-159]. The role of calnexin phosphorylation in regulating these important chaperone activities remained elusive; however, phosphorylated calnexin had been observed to bind to the null Hong Kong variant of α1-antitrypsin (NHK-AAT) [160] and to H-2L^{d} class I MHC molecules from mice [161]. These results demonstrated that phosphorylated calnexin can bind to glycoproteins that are terminally misfolded (NHK-AAT) or that are slow to fold and exit the ER (H-2L^{d}).

Eventually, mass spectrometry allowed for the identification of *in vivo* phosphorylation sites in mammalian calnexin [162]. All three of the identified *in vivo* phosphorylation sites were mapped to conserved serine residues within the cytosolic tail of calnexin. The serine-534 and serine-544 phosphoacceptor sites [162] were found to reside within canonical CK2 phosphorylation motifs [163] and this fits nicely with previously observed *in vitro* phosphorylation data [26]. The third phosphoacceptor site found in the cytosolic tail of mammalian calnexin, serine-563, was found to reside within a proline-directed kinase (PDK) motif [162] and such PDK motifs can be substrates of mitogen-activated protein kinases (MAPKs) [164] and cyclin-dependent kinases (CDKs) [165]. The serine-563 PDK site of mammalian calnexin was later found to be phosphorylated, both *in*

vitro and *in vivo*, by the extracellular signal-regulated kinase 1 (ERK1) MAPK [33, 166, 167].

Several studies have attempted to evaluate the functional significance of calnexin phosphorylation in mammalian cells. For example, phosphorylation of mammalian calnexin by ERK1 been shown to increase the association of calnexin with ER membrane-bound ribosomes and this regulated association was suggested to position the chaperone activities of calnexin near active translocons [167]. More recently, ERK1-dependent phosphorylation of mammalian calnexin was shown to occur in response to ER stress and this regulatory event increased the ER retention of partially misfolded AAT [166]. This was the first direct demonstration that phosphorylation of the cytosolic tail of calnexin could regulate its lumenal chaperone activities.

Phosphorylation of the CK2 sites found in calnexin has been shown to regulate its association with PACS-2, a cytosolic protein involved in protein sorting [168]. These authors suggest that this regulated interaction between calnexin and PACS-2 serves to control the retention and distribution of calnexin within the ER. This was evidenced by the fact that a double phospho-mimic mutant (SSDD) of its CK2 sites reduced the amount of calnexin that was localized to mitochondria-associated membranes (MAM) of the ER and increased calnexin leakage to the cell surface [168]. When taken together, it seems that phosphorylation of the cytosolic ERK1- and CK2- phosphoacceptor sites serves to control the distribution of calnexin between distinct regions of the ER.

Chapter 2 of this thesis comprises an examination of calnexin phosphorylation in the fission yeast *Schizosaccharomyces pombe*. We chose to

study *S. pombe* calnexin (Cnx1p) because this yeast contains all of the essential elements of the calnexin chaperone cycle, including functional homologs of calnexin [169, 170], UGGT [171], and GII [172]. We elected not to investigate calnexin phosphorylation in *Saccharomyces cerevisiae* because its calnexin homolog, Cne1p, does not have a cytoplasmic tail, does not appear to bind calcium, and is not essential for viability [170]. In contrast, *S. pombe* Cnx1p shares 38% sequence identity with its mammalian ortholog, was found to be essential for viability, and contains a short (48 amino acid) cytoplasmic domain[169, 170]. More detail on the important features of *S. pombe* Cnx1p are given in the introduction to chapter 2 (see 2.3) and so in the interest of conciseness I will avoid duplicating them here. The purpose of chapter 2 was to evaluate calnexin phosphorylation in *S. pombe* cells in order to determine if this regulatory event is evolutionarily conserved and to genetically evaluate its significance by assessing the phenotypes of Cnx1p phosphomutants.

1.6 Bem1p is a scaffold for polarized morphogenesis and MAPK responses in *S. cerevisiae*

1.6.1 The response to environmental stressors involves the actin cytoskeleton

Some of the earliest examinations of non-muscle cells in tissue culture by both light and electron microscopy revealed the presence of straight bundles of microfilaments [173-175]. These bundles of microfilaments were given the name ‘stress fibers’ because they were originally thought to result from the effects of mechanical tension on the protoplasm [175]. Many decades of subsequent

research have revealed that these actin stress fibers are themselves capable of generating contractile forces and they are implicated in cell motility, adhesion, and morphogenesis (reviewed in [176]).

Given that *S. cerevisiae* cells are non-motile and are protected by a rigid cell wall, consequently they have no need for the actin stress fibers mentioned above. However, the actin cytoskeleton in *S. cerevisiae*, which is composed of actin filaments and cortical actin patches, is a highly dynamic structure that polarizes towards sites of cell expansion [177-179].

Importantly, it has been observed that a variety of cellular stressors result in a transient depolarization of the yeast actin cytoskeleton [180-182]. This is also supported by the fact that mutational analysis of ACT1, *S. cerevisiae*'s only actin-encoding gene, identified numerous alleles that are sensitive to a variety of environmental stressors, including elevated temperature and osmolarity [180, 183]. This transient redistribution of the actin cytoskeleton in response to diverse stressors fits into the highly integrated environmental stress response (ESR). In yeast, this includes other generalized responses such as decreased translational initiation and an arrest of both the cell cycle and cell growth [184-187].

Given that dramatic redistributions of the actin cytoskeleton are involved in normal yeast morphogenic responses as well as in its response to stressors, I was keen to better understand how this highly dynamic actin cytoskeleton is regulated. Consequently, I evaluate the role of a scaffold protein called Bem1p because it is known to play an important role in regulating actin cytoskeleton dynamics in *S. cerevisiae*. My findings on Bem1p are presented in chapter 4 and

implications for the scaffolding activities of Bem1p during yeast morphogenesis and during responses to cell wall stress are discussed.

1.6.2 The morphogenesis programs of Saccharomyces cerevisiae

S. cerevisiae has proven to be an extremely valuable model to improve our understanding of the fundamental principles that underlie directed, or polarized, cell growth responses (reviewed in [188-190]). Polarized cell growth in *S. cerevisiae* can occur in response to a variety of cues and these can arise from both intracellular and extracellular sources. One essential polarized growth response in *S. cerevisiae* involves the formation of a bud and this morphogenic response arises from intracellular, cell cycle driven cues (reviewed in [179]). Bud formation is an essential morphogenesis program because this form of asymmetric cell division is how *S. cerevisiae* cells propagate during vegetative growth (Figure 1.2).

A second, non-essential, polarized growth response in yeast results in the formation of mating projections and this response arises from extracellular stimuli (reviewed in[191-193]). Mating projections are formed when yeast cells encounter peptide-based mating pheromones from cells of the opposite mating type. The extracellular pheromone gradient is sensed by cell surface G-protein coupled receptors (GPCRs) and yeast can reorient their cell growth when exposed to such a pheromone gradient. Only haploid yeast cells, specifically in the G1 phase of their cell cycle, are capable of responding to pheromone stimulation. This particular yeast morphogenesis program allows yeast to orient their cell

growth towards their nearest competent mating partner and ultimately leads to the fusion of two haploid cells to yield a single diploid zygote (see 1.6.5 for more).

A third morphogenesis program in *S. cerevisiae* results in a switch from yeast to filamentous growth and this occurs in response to nutrient limitation [194]. This switch to filamentous growth has been suggested to serve as a foraging mechanism, whereby non-motile yeast cells within a colony can seek out new nutrient sources by growing in this filamentous fashion [195]. Filamentous growth responses are orchestrated by multiple parallel signaling pathways and these pathways involve complex crosstalk and feedback mechanisms; however, it is well accepted that cyclic adenosine monophosphate (cAMP)-activated protein kinase A (PKA) and MAPK signaling pathways are involved in these filamentous growth response [194].

Chapter 4 details an examination of the requirement for Bem1p, an SH3 domain-containing scaffold protein, during both the budding and mating morphogenesis programs. I neglected to examine the function of Bem1p during the filamentous growth response primarily because morphological evaluation of filamentation phenotypes requires the use of specific *S. cerevisiae* strain backgrounds, such as Σ1278b [196].

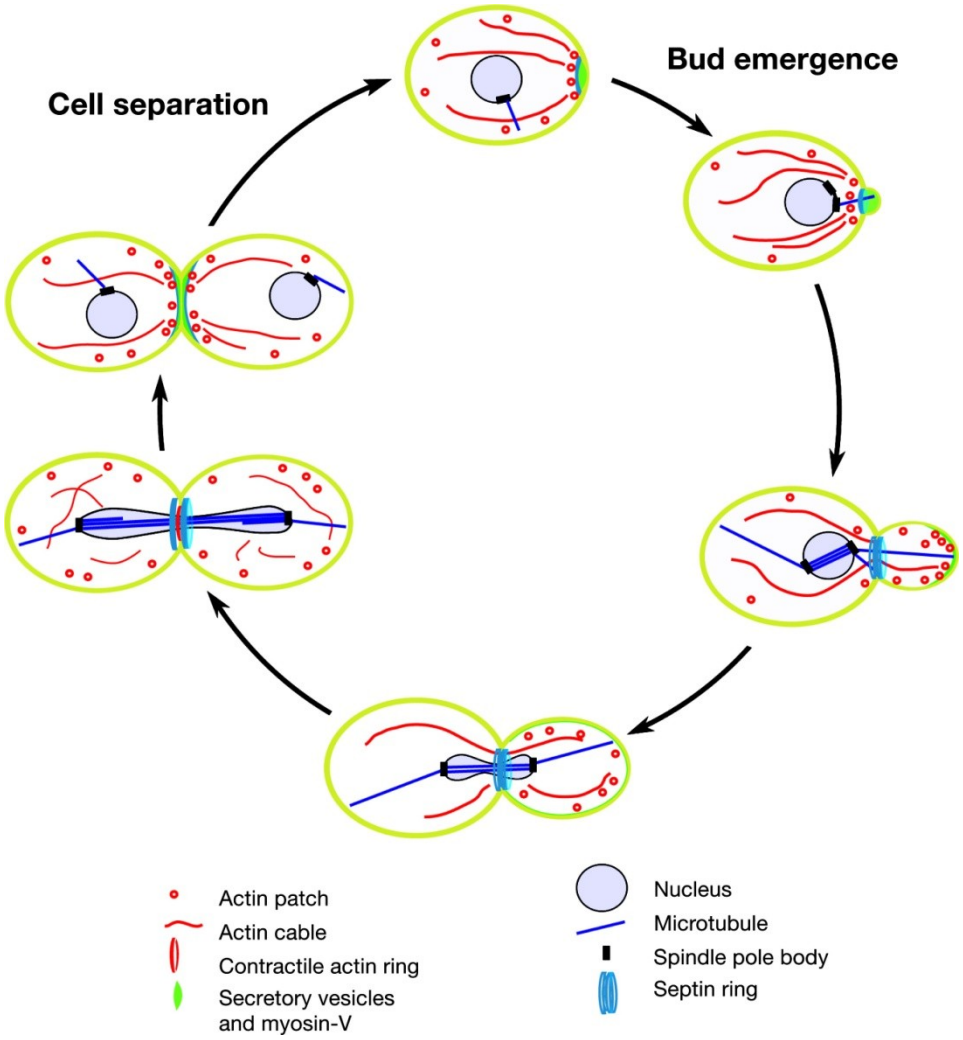

Figure 1.2. A dynamic actin cytoskeleton underlies *S. cerevisiae* morphogenesis. The above diagram depicts the cytoskeletal rearrangements that are required for a complete budding cycle. Adapted from [179].

1.6.3 Polarization of the actin cytoskeleton is required for directed growth in S. cerevisiae

The directed cell expansion that underlies each of the above morphogenesis programs requires the polarized delivery of proteins, particularly those involved in cell wall biosynthesis, and membrane components to a chosen

cortical growth site. This vectorial delivery of secretory vesicles to a designated growth site is guided by the actin cytoskeleton and is driven predominantly by the type-V myosin, Myo2p (reviewed in [189]). The actin cytoskeleton is a highly dynamic structure that is completely redistributed several times during a single cell division cycle (Figure 1.2) and can be similarly reoriented towards activated pheromone receptors during the yeast mating response (see 1.6.5).

This highly dynamic actin cytoskeleton requires intricate regulation of the actin polymerization machinery, often called the polarisome, and the small rho-type GTPase Cdc42 is central to controlling this actin polymerization machinery [179, 188, 190, 197]. Cdc42p, like other members of Ras superfamily, is regulated by the status of its bound guanine nucleotide and its ability to cycle between active (GTP-bound) and inactive (GDP-bound) states provides its characteristic 'switch-like' behaviour. The active GTP-bound conformation of Cdc42p binds to, and activates, a variety of cell polarity effectors, including: the p21-activated protein kinases (PAKs) Ste20p and Cla4p [198-201]; the formin protein Bni1p [202, 203]; the yeast IqGAP homolog Iqg1p [204]; and the adaptor proteins Gic1p and Gic2p [205]. Tight control of Cdc42p activation, through the status of its bound guanine nucleotide, at spatially constrained sites at the cells periphery directs the formation of a polarized actin cytoskeleton (reviewed in [188, 190]).

The intrinsic GTPase activity of Cdc42p results in the hydrolysis of GTP to GDP + P_i and this intrinsic rate of GTP hydrolysis can be further stimulated by GTPase activating proteins (GAP), which for Cdc42p includes Bem2p, Bem3p,

and Rga1p [206-208]. Furthermore, activation of Cdc42p requires the exchange of GDP for GTP and this is mediated by the activity of a guanine nucleotide exchange factor (GEF), Cdc24p [201, 209-211]. Also, Cdc42p binds to the guanine nucleotide dissociation inhibitor (GDI), Rdi1p [212, 213], and this GDI appears to be involved in the cell-cycle regulated detachment of Cdc42p from membranes [214]. Such plasma membrane anchorage of Cdc42p is facilitated by the geranylgeranyl transferase, Cdc43p, which adds a geranylgeranyl moiety to the C-terminal CAAX box of Cdc42p [215, 216].

The previous paragraph highlights some of the more important regulators of Cdc42p and their concerted activities allow for a strict spatiotemporal control of Cdc42p activity. Such strict regulation of Cdc42p is absolutely necessary for proper control of actin cytoskeleton reorganizations during yeast morphogenesis. Further regulation of Cdc42p is provided by Bem1p, which is a scaffold protein that is known to be important for Cdc42-dependent polarization of the actin cytoskeleton [217-219]. Chapter 4 comprises an examination of the scaffolding activities of Bem1p during the budding and mating morphogenesis programs and so I have chosen to expand on the various functions of Bem1p in the following sections (1.6.4 to 1.6).

1.6.4 Bem1p is a scaffold protein for the establishment of cell polarity

The BEM1 (bud emergence 1) gene was originally identified in a screen for synthetic lethal interactors of MSB1 [220], which is a gene that had been previously isolated as a multicopy suppressor of Cdc24 mutants [221]. Bem1 ts

mutants (bem1-1 and bem1-2) were later identified as synthetic lethal interactors of Bud5, which is a GEF that is involved in bud site selection [222]. The isolation and characterization of two mating-defective Bem1 mutants (Bem1-s1 and Bem1-s2) also provided an independent cloning of the full-length BEM1 gene [223].

Bem1Δ null mutants were generated and were found to be inviable at either 14°C or 37°C and they displayed heterogeneous morphologies at permissive temperatures (25°C or 30°C)[223]. Large, rounded, unbudded, multinucleate cells were well represented amongst the heterogeneous morphologies of Bem1Δ cells and these phenotypes became more pronounced upon shift to the restrictive temperature (37°C). Furthermore, rhodamine-phalloidin staining showed that the actin cytoskeleton was highly delocalized in Bem1Δ cells. The above phenotypic characterization of Bem1Δ mutants strongly supports its role as a regulator of the actin cytoskeleton.

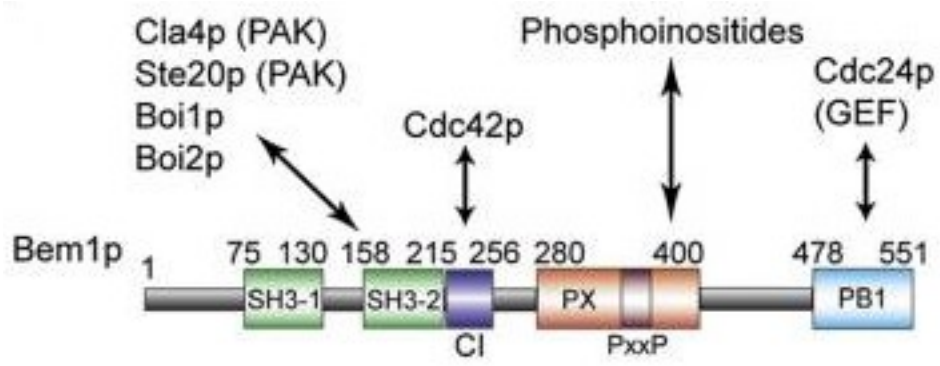

Figure 1.3. The domain architecture of Bem1p. The physical interactions mediated by each domain of Bem1p are represented by the arrows. The N- and C- terminal amino acid positions of each domain are indicated. SH3=src homology 3 domain; CI=Cdc42p-interacting domain; PX= phagocyte oxidase homology domain; PB1=Phox and Bem1 domain. Adapted from [224].

Bem1p contains 551 amino acids and it has an apparent molecular weight of 62 kilodaltons (KDa) upon separation by sodium dodecyl sulphate polyacrylamide gel electrophoresis (SDS-PAGE). As a scaffold protein, Bem1p contains no discernable enzymatic activities; however, it does contain numerous domains that are involved in mediating important protein-protein interactions (Figure 1.3). Bem1p contains two N-terminal src homology 3 (SH3) domains [223], which are referred to here as SH3-1 (aa 75-130) and SH3-2 (aa 158-215). The SH3-2 domain of Bem1p has been shown to mediate interactions with several polyproline (PxxP) motif-containing proteins, including Ste20p, Cla4p, Boi1p and Boi2p [217, 225-227]. A Cdc42p-interacting (CI) domain (aa 215-256) was found to flank SH3-2 and was shown to mediate the interaction of Bem1p with Cdc42p [228]. Bem1p also contains a phagocyte oxidase (phox) homology (PX) domain (aa 277-407) that has been shown to bind phosphatidylinositol-4-phosphate and this activity was proposed help target Bem1p to membranes [229, 230]. Lastly, Bem1p contains a type II Phox and Bem1 (PB1) domain at its C-terminus (aa 478-551) and this PB1 domain has been shown to mediate the interaction between Bem1p and Cdc24p [231-235].

Numerous studies have examined the scaffolding activities of Bem1p and have attempted to discern how they contribute to the establishment of cell polarity [217-219, 224, 227, 228, 231]. This body of literature has produced the following, perhaps slightly over-simplified, model for the role of Bem1p in cell polarity establishment: Bem1p binds to Cdc24p (via PB1), to the PAKs Ste20p and Cla4p (via SH3-2), and to Cdc42p (via CI). This capacity to simultaneously

bind to Cdc42p, its activating GEF, and its downstream effectors, allows Bem1p to positively reinforce Cdc42p signaling at cortical growth sites.

1.6.5 The contributions of Bem1p during the yeast mating response

Haploid *S. cerevisiae* can be one of two different mating types and these are designated as a and α mating types. As mentioned in 1.6.2, a and α cells secrete distinct peptide pheromones and these pheromones bind to specific cell surface GPCRs in order to instigate a mating response in cells of the opposite mating type. The yeast mating response involves activation of a canonical MAPK signaling cascade, subsequent transcriptional activation of mating response genes, and polarized morphogenesis (reviewed in [191-193]). I will provide a brief description of the mating response and a more detailed description of these events can be found in the above reviews.

Ste2p and Ste3p are pheromone-responsive GPCRs that are expressed on the surface of a and α cells, respectively. These GPCRs contain a canonical 7-transmembrane spanning architecture and their third intracellular loop is coupled to a heterotrimeric G-protein. Engagement of mating pheromone by the receptor results in the exchange of GDP for GTP on the Gα subunit (Gpa1p). This leads to the dissociation of Gβγ subunits (β=Ste4p, γ=Ste18p) from Gα and this event allows Ste4p to recruit and activate several downstream effectors. The PAK Ste20p and the MAPK scaffold protein Ste5p represent two of the primary effectors that are recruited by Ste4p.

Ste20p acts as a MAPKKKK by phosphorylating and activating the MAPKKK, Ste11p. The sequential activation of Ste11p (MAPKKK), Ste7p (MAPKK), and Fus3p (MAPK) exemplifies the prototypical MAPK signaling cascade (Figure 1.4). All three kinases of the MAPK cassette can bind directly to the scaffold protein, Ste5p, and the principle role of Ste5p appears to be the recruitment of these kinases to the plasma membrane. Once activated, Fus3p phosphorylates the transcriptional activator Ste12p, which upregulates the expression of mating response genes. Fus3p also stabilizes the G_1 CDK inhibitor Far1p, which is responsible for mediating the pheromone-induced G_1 cell cycle arrest [236-238]. In addition to its role as a CDK inhibitor, Far1p also appears to be important for the recruitment of numerous cell polarity establishment proteins, including Cdc24p and Bem1p, to activated pheromone receptors [231, 239, 240]. Far1p therefore serves to override the budding spatial cues by directing the Bem1p-dependent polarity establishment complex to activated pheromone receptors.

The role of Bem1p during the yeast mating response appears to be complex and extends beyond its well characterized role in cell polarity establishment. The ability of Bem1p over-expression to suppress a dominant negative Ste4p (Gβ) mutant [241] and the fus3-2 cell cycle arrest-defective mutant [242], suggests that Bem1p may have a more direct involvement in pheromone signaling.

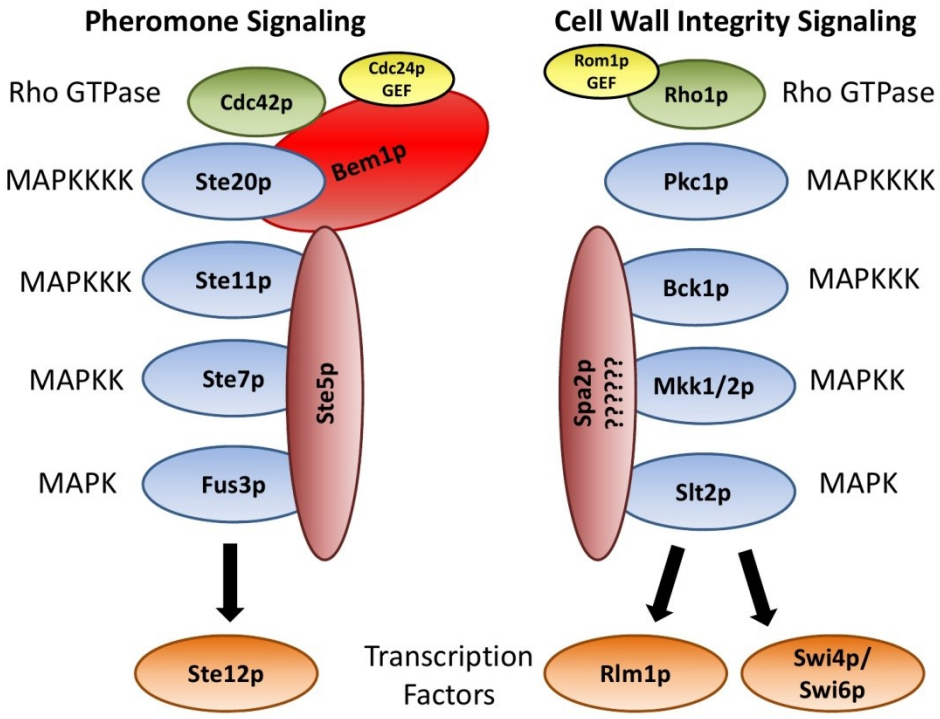

Figure 1.4. Schematic representation of the mating and cell wall integrity MAPK pathways in *S. cerevisiae.* Extracellular signals derived from either contact with mating pheromone or destabilization of the cell wall are sensed by cell surface receptors (not depicted) and are transmitted to the intracellular signaling pathways depicted above. The signal for pheromone and cell wall stress are transmitted through activation of the Rho-type GTPases Cdc42p and Rho1p, respectively. These GTPases contribute to the activation of the canonical MAPK signaling cascades shown above. These MAPK signaling pathways culminate in the phosphorylation and activation of pathway-specific transcription factors. These transcription factors induce the expression of genes involved in mating (Ste12p), cell wall metabolism (Rlm1p), and cell cycle control (Swi4/6p).

The ability of Bem1p to serve as a scaffold for Cdc42p-dependent activation of the MAPKKKK, Ste20p, would provide an obvious way for it to contribute to pheromone signaling (Figure 1.4); however, Ste20 mutants that have lost their Cdc42/Rac interactive binding (CRIB) domain still can elicit normal mating responses [199, 243]. This argues against the primary contribution of

Bem1p in pheromone-induced MAPK signaling being through Cdc42p-dependent activation of Ste20p. This is also supported by the fact that Bem1p overexpression can also stimulate MAPK signaling in certain Ste20Δ strains [241, 242]. However, examinations of specific Ste20p point mutants that are specifically disrupted in their ability to bind to SH3-2 of Bem1p have indicated that the Ste20p-Bem1p interaction does contribute to the pheromone response [227].

An interaction between Bem1p and the various kinases of the mating MAPK cascade (Ste11p-Ste7p-Fus3p) was shown to occur indirectly, via an interaction between Bem1p and the MAPK scaffold Ste5p (Figure 1.4) [242]. This Bem1p-Ste5p interaction tethers the polarity establishment machinery to components of the MAPK signaling cascade and this tethering might provide a possible mechanism for Bem1p to contribute to pheromone signaling. Identification of either Ste5p or Bem1p mutants that are specifically disrupted for the Ste5p-Bem1p interaction would be necessary to properly evaluate the importance of this interaction to MAPK signaling; however, the weakness of the Ste5p-Bem1p two-hybrid interaction has hampered the identification of such a mutant. Overall, it seems clear that the literature supports both Ste20p-dependent and Ste20p-independent roles for Bem1p during pheromone-induced MAPK signaling.

1.6.6 Phosphoregulation of Bem1p

Two independent large scale surveys that set out to identify substrates for *S. cerevisiae*'s primary CDK, called Cdc28p, found that Bem1p could be phosphorylated by Cdc28p [244, 245]. It was later found that Bem1p can be phosphorylated *in vivo* at serine-72 (S72) by Cdc28p when it is paired with its G_1 cyclin Cln3p [246]. This S72 phosphoacceptor site abuts the SH3-1 domain of Bem1p (aa 76-130) and these authors went on to characterize the phenotypes associated with Bem1p-S72A and Bem1p-S72D phosphomutants. It was suggested that Bem1p plays a role in vacuolar homotypic fusion events because Bem1Δ and Cln3Δ mutants both contain highly fragmented vacuoles. These authors went on to show that phosphoregulation of Bem1p at S72 impacts its function in vacuolar homeostasis. Bem1p-S72A displayed highly fragmented vacuoles whereas Bem1p-S72D displayed normal vacuolar morphologies. These authors concluded that Cdc28p-Cln3p phosphorylation regulates the function of Bem1p in vacuolar homotypic fusion events; however, the precise role of Bem1p in vacuolar homeostasis was not determined. Furthermore, some controversy exists on the role of S72 phosphorylation in vacuolar homeostasis because another group reported that there were no observable differences between Bem1p-S72A and Bem1p-S72D in an *in vitro* homotypic fusion assay [247].

Interestingly, it was noticed that Bem1p-S72D, unlike Bem1p-S72A, does not fully complement the bud emergence defect of Bem1Δ cells [246]. The bud emergence defect of Bem1p-S72D was evidenced by measuring the proportion of unbudded cells that contain mitotic spindles. This data clearly suggests that the

regulatory function that is imposed by phosphorylation of S72 of Bem1p extends beyond its role in vacuolar homeostasis. Identification of novel *in vivo* phosphorylation sites of Bem1p is of essential interest because they are likely to uncover new functions of Bem1p or new means of regulating its known functions in yeast morphogenesis and pheromone signaling. The mass spec analysis of affinity purified Bem1p-complexes that I describe in chapter 4 allowed me to identify Bem1p phosphorylation sites and mutants of one of these Bem1p-phosphoacceptor sites suggested a novel role for Bem1p in the cell wall integrity (CWI) stress response.

1.7 Cell wall stress and the Pkc1p-dependent cell wall integrity response in S. cerevisiae

The cell wall of *S. cerevisiae* consists of two layers: an inner load-bearing layer that is composed primarily of β1,3-glucan and an outer protective layer that is composed primarily of mannoproteins (reviewed in [248-250]). This relatively rigid cell wall structure serves numerous functions, such as stabilizing the internal osmotic conditions of the cell, providing a protective barrier against physical stresses, maintaining cell shape, and acting as a scaffold for proteins [248].

Cell wall biosynthesis is viewed as an attractive target for the development of anti-fungal agents and, owing to the increasing number life-threatening fungal infections found in immune-compromised patients, the need to identify novel and potent anti-fungal agents is unequivocal [251-253]. The conservation of the homeostatic responses that monitor the integrity of the fungal

cell wall allows for informative studies to be conducted in *S. cerevisiae* and the knowledge gleaned from such studies can be subsequently evaluated in opportunistic pathogens like *Candida albicans*. Consequently, it is important that we improve our understanding of fungal cell wall stressors and the homeostatic responses that fungal cell implement to counter cell wall lesions.

Given that my examination of the scaffolding activities of Bem1p (see chapter 4) led me to uncover a novel role for this cell polarity protein in the cell wall stress response, I briefly introduce *S. cerevisiae*'s cell wall integrity (CWI) response in the following section.

1.7.1 Overview of the cell wall integrity MAPK pathway in S. cerevisiae

S. cerevisiae requires the localized remodelling of its cell wall at sites of polarized cell growth and, consequently, CWI signaling mechanisms are intimately linked to morphogenic responses. The CWI response is also activated in response to cell wall lesions. Examples of stressors that can cause cell wall lesions include sudden decreases in external osmolarity, a rise in temperature, mechanical damage, and exposure to cell wall destabilizing agents. Cell wall destabilizing agents include: caffeine, although its mechanism of destabilization is unclear; congo red (CR), a β1,3-glucan-binding dye; calcofluor white, a chitin antagonist; and zymolase, a cell wall degrading enzyme. Detailed reviews on CWI signaling exist [254, 255] and so I will cover only the essential features of this important homeostatic response.

The Rho1p GTPase is the master regulator of CWI signaling and it has several key effectors that contribute to the CWI response. Rho1p activates Pkc1p, which is the sole yeast homolog of the mammalian protein kinase C (PKC) superfamily (reviewed in [256]). Activation of Pkc1p has numerous downstream effects, but the primary effect of Pkc1p is to stimulate the activation of a downstream CWI MAPK cascade that includes Bck1p (MAPKKK), redundant Mkk1p and Mkk2p (MAPKK), and Slt2p (MAPK) (Figure 1.4). Activation of Slt2p leads to activation of numerous downstream effectors, including the transcriptional activators Rlm1p and SBF, the latter of which is a dimeric TF that is composed of Swi4p and Swi6p. Rlm1p and SBF activate the transcription of genes involved in cell wall biosynthesis and cell cycle control, respectively.

Rho1p also contributes to the CWI response through its direct regulation of β1,3-glucan synthase (GS)[257, 258]. Furthermore, Rho1p signaling mediates direct effects on the actin cytoskeleton through its GTP-dependent interaction with two redundant formin proteins, Bni1p and Bnr1p [202, 259, 260]. Like Cdc42p, Rho1p is regulated by numerous enzymes that affect its GTP-GDP cycle. Rho1p is activated by a pair of functionally redundant GEFs, Rom1p and Rom2p [261]. The intrinsic rate of GTP hydrolysis by Rho1p can be stimulated by numerous yeast GAPs such as Bem2p, Sac7p, Bag7p and Lrg1p (reviewed in [255]). Like Cdc42p, Rho1p has been shown to interact with the RDI protein Rdi1p [212, 213]; however, the lack of any discernable CWI phenotype in Rdi1Δ cells [213] suggests that Rdi1p is not an important regulator of Rho1p function during the CWI response.

Five different cell surface receptors have been implicated in stimulating Rho1p, most likely through recruitment of Rom1/2p GEF activities and these cell surface receptors include, Wsc1p, Wsc2p, Wsc3p, Mid2p, and Mtl1p (reviewed in [255]). Wsc1p and Mid2p appear to be the more important of these five cell surface sensors [262]. Each of these receptors is a type I integral membrane protein and they all contain highly O-mannosylated extra-cellular domains, a single transmembrane domain, and a short cytoplasmic tail. These cell surface receptors have been proposed to act as mechanosensors but how they monitor and transmit the signal for cell wall stress remains largely undefined.

The above paragraphs provide only a brief survey of CWI signaling mechanisms and I will again direct the reader to an excellent and highly detailed review on the subject of CWI signaling [255]. Given that the CWI signaling is required for polarized morphogenesis, we should anticipate functional interplay between the polarity establishment machinery and the CWI signaling apparatus. In addition to dissecting the scaffolding activities of Bem1p during budding and mating morphogenesis, chapter 4 also uncovers a novel role for Bem1p in the CWI response.

1.7.2 High-throughput genetic data suggests that Bem1p may contribute to CWI signaling

Recent advances in high-throughput techniques have allowed for unprecedented global mapping of *S. cerevisiae*'s genetic, physical, and biochemical interactions [263-272]. This 'explosion' of high-throughput surveys

has produced a huge amount of data that serves as an invaluable resource and this data allows the generation of specific and testable hypotheses without ever having to set foot in a lab. A highly curated, searchable, repository of this yeast high-throughput datasets is made publically available at the "Saccharomyces genome database" (SGD) website (http://www.yeastgenome.org/).

Upon careful examination of the high-throughput datasets contained in the SGD, I noticed that BEM1 has been found to display genetic interactions with numerous genes that are implicated in CWI signaling. The following CWI-related genes have displayed some form of genetic interaction with BEM1 (these genetic data were from [263], unless otherwise referenced): BCK1 [265], BCK2, BEM2 [273], BEM4, PKC1, ROM2, SPA2, SWI4, and SWI6. An appreciation for the interconnectedness of CWI signaling responses and actin cytoskeletal reorganizations, during both CWI insults and normal morphogenesis, only serves to further highlight the significance of these particular high-throughput genetic interactions. These CWI-BEM1 genetic connections were foremost on my mind when I was analyzing the mass spectrometry data of Bem1p complexes in chapter four. Once I observed numerous CWI-related proteins physically interacting with Bem1p *in vivo*, I became very excited to follow up on these particular physical interactions. A functional assessment of the involvement of Bem1p in CWI responses was the next logical step given these observations.

1.8 Thesis overview

Cellular stress responses tend to be evolutionarily conserved and their study has uncovered many important adaptive mechanisms that are employed by cells in their constant struggle to maintain homeostasis. Studying cellular stress responses also frequently provides insight into the normal inner workings of eukaryotic cells. Consequently, for my thesis projects I chose to investigate three different stress signaling mechanisms. I employ yeast as a model for studying stress responses and I do so with the intention of extending some of my more important findings to stress responses in human cells.

In chapter two, I evaluate the fission yeast, *Schizosaccharomyces pombe,* as genetic model for studying calnexin phosphorylation. I found that this regulatory phosphorylation event is conserved in *S. pombe* Cnx1p and I map the phosphorylation site to serine-553 in the cytoplasmic tail of Cnx1p. Analysis of S553 phosphomutants allowed me to confirm previous findings from studies on phosphorylation of mammalian calnexin; namely, that this phosphorylation of the cytosolic tail of Cnx1p regulates its association with ER membrane-bound ribosomes. Importantly, I extend previous studies by demonstrating that phosphorylation of calnexin at this PDK site regulates both cell size control and ER stress tolerance in *S. pombe.*

In chapter three, I utilize a chemical biology approach to study Ire1-dependent ER homeostatic mechanisms. I describe and characterize novel small-molecule UPRMs that were isolated in a high-throughput chemical screen in *S. cerevisiae*. Significantly, I was able to extend these initial findings in yeast by

testing our identified UPRMs in human cell lines. One particular UPRM, designated UPRM8, was found to also block Ire1-dependent UPRs in HeLa cells. Importantly, I found that UPRM8 functions by inhibiting the ribonuclease activity of Ire1, both *in vitro* and *in vivo*.

Furthermore, I studied the activity of UPRM8 in multiple myeloma cells because these cancer cells are known to be reliant on ER homeostatic mechanisms due to the physiological ER stress that results from immunoglobulin production. I utilized UPRM8 to demonstrate that inhibition of cytoprotective UPR functions in constitutively stressed multiple myeloma results in an apoptotic cell death. I extend this important finding by showing that the ability of UPRM8 to kill MM cancer cells can be improved by concomitantly treating with ER stress-inducing agents or agents that block de-phosphorylation of eIF2α. Finally, I conducted a structure-activity-relationship screen to identify UPRM8-like compounds that also show this capacity to kill MM cancer cells. This SAR screen proved informative because it allowed me to identify even more potent UPRM8-like compounds and it highlighted some of the important features of the UPRM8 pharmacophore. I conclude chapter 3 by discussing the broader implications of UPRMs and speculate on their future potential use as chemotherapeutic agents.

In chapter 4 of this thesis I examine the functions and regulation of Bem1p, a protein that has been implicated in the establishment of cell polarity and MAPK signaling. I was interested in examining regulators of the actin cytoskeleton because previous studies in *S. cerevisiae* have shown that actin cytoskeleton reorganizations are intimately linked to a variety of different stress responses.

I first sought to investigate the parallel roles of Bem1p in budding and mating morphogenesis. By employing traditional genetic approaches, I was able to identify a novel separation of function mutant of Bem1p. This mutant, Bem1-*s3*, functions appropriately during bud morphogenesis but fails dramatically during mating morphogenesis. I further show that the separation of function seen in the Bem1-*s3* mutant results from its combined loss of SH3-1 and SH3-2 - mediated protein-protein interactions.

The Bem1-*s3* mutant clearly demonstrates the importance of Bem1p-mediated scaffolding activities during the yeast pheromone response, and so I wondered if similar scaffolding activities for Bem1p could exist in any of the other MAPK-dependent responses in *S. cerevisiae*. I hypothesized that the easiest way to address this would be to examine the physical interactions of Bem1p. My strategy to examine these physical interactions was to affinity purify Bem1p-complexes from a yeast cell lysate and to identify interacting proteins by mass spectrometry. This proteomics approach allowed me to identify both known and novel Bem1p-interacting proteins. Furthermore, I was also able to detect several novel phosphorylation sites in Bem1p and previous literature has established that Bem1p is a *bona fide* phosphoprotein.

Importantly, several of the Bem1p-interacting proteins that I identified have been previously implicated in the CWI MAPK response. This supported my previous assertion that Bem1p might be involved in other MAPK responses in yeast. To directly test the involvement of Bem1p in the CWI response, I examined the sensitivity of Bem1Δ and Bem1p phosphomutants to cell wall destabilizing agents. Bem1Δ mutants were exquisitely sensitive to cell wall

destabilizing agents, as was the Bem1p-S458E phosphomimc mutant. These findings support a novel role for Bem1p in the response to cell wall stress. Such a role for Bem1p in the CWI response furthers our appreciation of the inter-connectedness of cellular stress responses with regulators of actin cytoskeleton dynamics.

Overall, this thesis comprises and examination of cellular stress response mechanisms in yeast. Significantly, I was able to extend my findings on ER homeostatic mechanisms to human cells through the use of novel small-molecule UPRMs. This allowed me to demonstrate the importance of ER homeostatic mechanisms in the survival of multiple myeloma cancer cells. The ability to exert control over cellular fate by impeding or supplementing homeostatic mechanisms under conditions of stress has widespread disease implications and these are discussed in chapter five (general discussion). The studies of cellular stress responses contained in this thesis serves to further underscore the importance of these highly integrated and conserved adaptive mechanisms. These stress responses are essential for maintaining cellular homeostasis in the face of ever-fluctuating environmental conditions.

CHAPTER TWO

Endoplasmic reticulum stress tolerance is mediated by a calnexin phosphorylation-dependent mechanism in *Schizosaccharomyces pombe*.

2.1 Connecting text

The role of calnexin in ERAF has been studied extensively and the importance of this lectin chaperone to mammalian biology is evident by the postnatal lethality that has been observed in calnexin knockout mice [274]. Phosphorylation of mammalian calnexin has been reported previously [162, 167] and this post-translational modification has been shown to regulate its association with ER membrane bound ribosomes [167]. Also, ERK1-dependent phosphorylation of mammalian calnexin has been observed to regulate the retention of a partially misfolded glycoprotein substrate [166].

The above study clearly demonstrates that calnexin phosphorylation impacts the retention of misfolded glycoproteins. This result provides further impetus for studying this regulatory process because ER retention and degradation of misfolded glycoproteins is a paradigm for many protein trafficking diseases. Consequently, a more thorough understanding of how calnexin phosphorylation regulates the retention of misfolded glycoproteins is of essential interest. With this ultimate goal in mind, chapter two details my attempt to evaluate *Schizosaccharomyces pombe* as a model system to study calnexin phosphorylation. I found that phosphorylation of the cytosolic tail of calnexin is conserved in *S. pombe* Cnx1p, as is the capacity for this phosphorylation event to regulate the association of calnexin with ribosomes. Furthermore, I have provided an initial phenotypic characterization of Cnx1p phosphomutants.

2.2 Abstract

The fission yeast *Schizosaccharomyces pombe* contains the core elements of a conserved endoplasmic reticulum (ER) quality control apparatus. The lectin-like molecular chaperone calnexin is a type I ER-resident transmembrane protein that plays a central role in ER quality control processing. *S. pombe* calnexin (Cnx1p) contains a short cytosolically exposed domain that may be the target of Cnx1p regulatory actors *in vivo*. To gain an understanding of Cnx1p regulation, we first showed that this protein was phosphorylated *in vivo* on its cytosolic domain. The major *in vivo* phosphorylation site was then mapped to Serine 553. Phenotypic analysis of S553 mutants revealed that Cnx1p phosphorylation is connected to cell size control and the ability of cells to cope with ER stress. Furthermore, association of Cnx1p with ER membrane-bound ribosomes was also affected by Cnx1p phosphorylation. This work demonstrates that phosphorylation of calnexin represents an evolutionarily conserved mechanism to regulate its association with active translocons and that this intricate regulation of calnexin function impinges upon ER stress tolerance and cell size control in fission yeast.

2.3 Introduction

Membrane-anchored calnexin and its soluble paralog calreticulin are lectin-like components of the ER quality control in mammalian cells [26-28]. ER quality control processing of glycoproteins is achieved through cycles of glucose trimming and reglucosylation, which are mediated by glucosidase II (GII) and

UDP-glucose:glycoprotein glucosyl transferase (UGGT), respectively. The leguminous lectin domains of calnexin and calreticulin interact with monoglucosylated high-mannose-type oligosaccharide side chains present on nascent glycoproteins [29, 30, 275]. A prolonged association between calnexin and misfolded glycoproteins has been observed and supports its role as an important ER resident quality control protein [31, 33, 35].

Mammalian calnexin is a type I transmembrane protein and is phosphorylated within its cytosolic domain [23, 162] on three conserved serine residues *in vivo* [162]. Calnexin phosphorylation has been demonstrated to regulate the interaction between calnexin and ER membrane-bound ribosomes in mammalian cells [167]. It was proposed that calnexin phosphorylation might serve to increase calnexin concentrations near active translocons and this may be used to enhance the coupling of glycoprotein translocation and folding [167].

A more recent study in HepG2 cells has investigated the role of calnexin phosphorylation on the folding and secretion of improperly folded α1-antitrypsin (AAT) [166]. This study showed that treatment of HepG2 cells with L-azetidine 2-carboxylic acid (AZC), a proline analog, resulted in the misfolding of AAT and prolonged AAT-calnexin association. Furthermore, Cameron *et al.* found that AZC-induced protein misfolding enhanced the phosphorylation of calnexin's proposed ERK1 site at Ser^{563} and that either treatment with the MEK1 inhibitor PD98059 or expression of a dominant negative IRE1 could attenuate this enhanced phosphorylation. Importantly, it was shown that preventing AZC-induced calnexin phosphorylation with PD98059 led to increased dissociation of

calnexin from partially folded AAT and that this resulted in increased ER exit and secretion. This work by Cameron *et al.* was the first demonstration that calnexin phosphorylation provides a mechanism for cellular signaling cascades to regulate ER lumenal activities and hence fine tune the cells capacity to produce and secrete glycoproteins.

The fission yeast *Schizosaccharomyces pombe* contains the core components of the calnexin cycle needed for productive glycoprotein folding in the ER [169-172, 276]. *S. pombe* lacks a calreticulin homolog and it has been shown that calnexin (Cnx1p) is essential for viability [169, 170, 277]; however, the short cytosolic domain (48 amino acids) is dispensable for viability [169, 170, 277]. Overall, Cnx1p shares approximately 38% sequence identity with its mammalian ortholog and this level of conservation at both the sequence and functional level makes *S. pombe* a valuable genetic model to study calnexin biology [169, 170].

The highly conserved central domain (hcd), found in the lumenal portion of Cnx1p, allows both calcium- and ligand-binding [169, 170, 278]. Surprisingly, this hcd region, despite having been shown to be required for chaperone activity *in vitro*, was found to be dispensable for viability [279]. In addition to this conserved central domain, the Cnx1p lumenal domain contains a 52 amino acid juxtamembrane sequence that has been shown to interact with BiP, the ER lumenal Hsp70 homolog [278]. This juxtamembrane BiP-binding sequence is conserved in plant species but appears to be absent in mammalian calnexin [280]. It has been suggested that this Cnx1p-BiP interaction would coordinate BiP and

Cnx1p functions and serves to enhance glycoprotein folding efficiency in *S. pombe* [171, 172, 278, 281, 282].

In this study we tested whether *S. pombe* Cnx1p is regulated by phosphorylation and to uncover the biological consequence of this post-translational modification by genetically manipulating the phosphorylated residues. We have shown that *S. pombe* Cnx1p is phosphorylated *in vivo* at the proline-directed kinase (PDK) motif present at Serine 553. As has been demonstrated for mammalian calnexin [167], Cnx1p phosphorylation at this PDK site regulates its interaction with membrane-bound ribosomes. Genetic manipulation of this S553 phosphorylation site significantly affected cell size control and ER stress tolerance of *S. pombe* cells. Thus, we suggest that phosphorylation of Cnx1p is a highly conserved mechanism to control its ER functions and that this intricate regulation is required for normal cell cycle progression and ER stress tolerance in fission yeast.

2.4 Materials and Methods

Reagents

The production of rabbit polyclonal anti-Cnx1p antibodies was described previously [170]. ^{32}P-orthophosphoric acid (S.A. of 285 Ci/mg) and Tran^{35}S-label (S.A. of 1048-1504 Ci/mmol) were purchased from NEN-Mandel Scientific (Toronto, Ontario) and ICN Canada Ltd. (Montreal, Quebec), respectively.

Schizosaccharomyces pombe strains and medium

S. pombe strain Q358 (h^- ade6-M210 leu1-32 ura4-D18) was used as a wild-type control in these experiments. *S. pombe* Δ*cnx1* pCNX560, *S. pombe* Δ*cnx1* pCNX524, *S. pombe* Δ*cnx1* pCNX484 and *S. pombe* Δ*cnx1* pCNX474 were described previously [170]. Our strategy (Supplementary Figure 2.1) and primers (Supplementary Table 2.1) for replacing the endogenous chromosomal copy of $cnx1^+$ by integration of our $cnx1^+$ phosphorylation site mutants is detailed in the supplementary information. All strains were grown at 30°C or 37°C, as indicated, in Edinburg Minimal Medium (EMM) supplemented with the required nutrients and amino acids. All other growth media (EMMP, NSM) were prepared as described previously [282, 283]. Where indicated, tunicamycin (Sigma-Aldrich) was used at 0.5ug/ml to induce ER stress.

In vivo phosphorylation of S. pombe

S. pombe were cultured in EMM to log phase and resuspended to $2x10^8$ cells/ml in 1 ml volume. The cells were maintained in phosphate free medium (EMMP) supplemented with essential nutrients for 7 h. Cells were subsequently radiolabeled with 0.5 or 1 mCi/ml of ^{32}P-orthophosphate for 4h. At the end of the pulse, a final concentration of 0.1% NaN_3 was added to the cells and cells were collected by centrifugation before proceeding to lysis and immunoprecipitation.

SDS-PAGE autoradiography and Phosphoamino acid analysis

For Tran^{35}S-labeled samples, proteins were separated by SDS-PAGE and then processed by fluorography with EN^{3}Hance according to the manufacturer's instructions. For ^{32}P-labeled samples the proteins were separated by SDS-PAGE

and then gels were either dried for autoradiography or transferred onto PVDF membranes. Phosphoamino-acid analysis was performed as described previously [162].

Growth curves, microscopy, and cell size analysis

S. pombe Q358 wt and the genome-integrated Cnx1 phosphomutants (S553A and S553E) were grown in liquid EMM cultures. The cells were grown in a shaking incubator at either 30^{o}C or 37^{o}C and in the presence of 0.5 ug/ml tunicamycin where indicated. Growth curves are presented as the mean OD_{686} measurement of three independent growth experiments plotted versus time (in minutes). The growth of these *S. pombe* cultures was monitored for a minimum of 46 hours of post-treatment. Error bars represent one standard deviation from the plotted mean values. For the microscopy experiments 3 independent cultures of each strain under investigation was grown to mid-log phase in EMM at 30^{o}C with shaking. Mid-log phase cells were fixed for 10 minutes by the addition of formaldehyde (to a final concentration of 4%) to the media. Cells were then harvested by centrifugation and fixed for an additional 60 min in PBS + 4% formaldehyde at 4^{o}C. Cells were then washed twice in PBS, mounted on glass slides, and visualized at 400X magnification on a Zeiss Observer Z1 microscope. Cell size was determined by measuring the length of cells in the captured images for each culture of these three independent experiments. The total number of cells measured for each strains analyzed were as follows: Wild-type n=1012 cells, S553A n=1018 cells, S553E n= 436. Mean cell lengths were displayed graphically as % of the Q358 wild-type mean cell length. Error bars represent one

standard deviation from the calculated means. A one-sided wilcoxon rank-sum test was used to ensure that the mean Cnx1p-S553A cell length was significantly smaller than wild-type and, conversely, that the mean Cnx1p-S553E cell length was significantly larger than wild-type (p-value < 2.2e-16 for both tests).

Serial dilution growth assays

S. pombe cells were grown to mid-log phase in EMM media at 30^{o}C and diluted back to an OD686 of 0.1 in 100ul of sterile water. Four subsequent serial dilutions of this 0.1 OD686 suspension were made and all five of these dilutions were spotted on EMM plates and EMM plates that were supplemented with 4mM of dithiothreitol (DTT). Plates were incubated at 30^{o}C for 4 days and images were captured on a flat-bed scanner.

Analysis of ribosome-associated microsomal proteins

The association of membrane proteins with ribosomes was carried out as described previously [167, 284]. Briefly, 75 ul of microsomal membranes (approx. 750 ug proteins) were solubilized with 1.5% CHAPS (final concentration) for 30 min on ice. Solubilized rough microsomes were then centrifuged through a 100 ul cushion of 1.5 M sucrose in the same buffer containing only 0.1% CHAPS for 3h at 95000 rpm in a TLA-100.2 rotor (Beckman). Membrane proteins in the ribosomal pellet (i.e. Cnx1p) were detected by immunoblotting after separation by SDS-PAGE and transfer to nitrocellulose membranes.

2.5 Results

2.5.1 S. pombe Cnx1p is phosphorylated in vivo on cytosolic serine residues.

S. pombe Δcnx1 deletion strains that express from a plasmid either full length (p560) or carboxy-truncated (p524, p484, p474) Cnx1p were in vivo radiolabeled with ^{32}P-orthophosphate for 4h. Cnx1p was immunoprecipitated with anti-Cnx1p antibodies and immunoprecipitates were resolved by SDS-PAGE before visualization using autoradiography (Figure 2.1A), silver nitrate staining (Figure 2.1B), and immunoblotting (Figure 2.1C). Cnx1p immunoprecipitates from wild-type Q358 and the p560 plasmid-borne Cnx1p were highly phosphorylated, whereas the p524 Cnx1p mutant was only weakly phosphorylated (Figure 2.1A). The low level of phosphorylation of p524 was established by comparing it with p560, using the same exposure and by normalizing to the amounts of Cnx1p precipitated (Figure 2.1C). Cnx1p expressed by the p524 mutant retains both its transmembrane domain and 12 cytosolic amino acid residues (Figure 2.1E). The low level of phosphorylation observed for p524 is likely due to residual phosphorylation of the cytosolic serine residues that remain in the p524 mutant. From these data, we can conclude that the major region of Cnx1p phosphorylation, in vivo, is between amino acid positions 525 and 560.

A band corresponding to in vivo phosphorylated full-length Cnx1p was excised from the nitrocellulose membrane and was subjected to two-dimensional phospho-amino acid analysis. Autoradiograms of the two-dimensional TLC plate revealed that only ^{32}P-labeled serine co-migrated with the non-radiolabeled phosphoserine standard, which were detected by ninhydrin staining (Figure 2.1D).

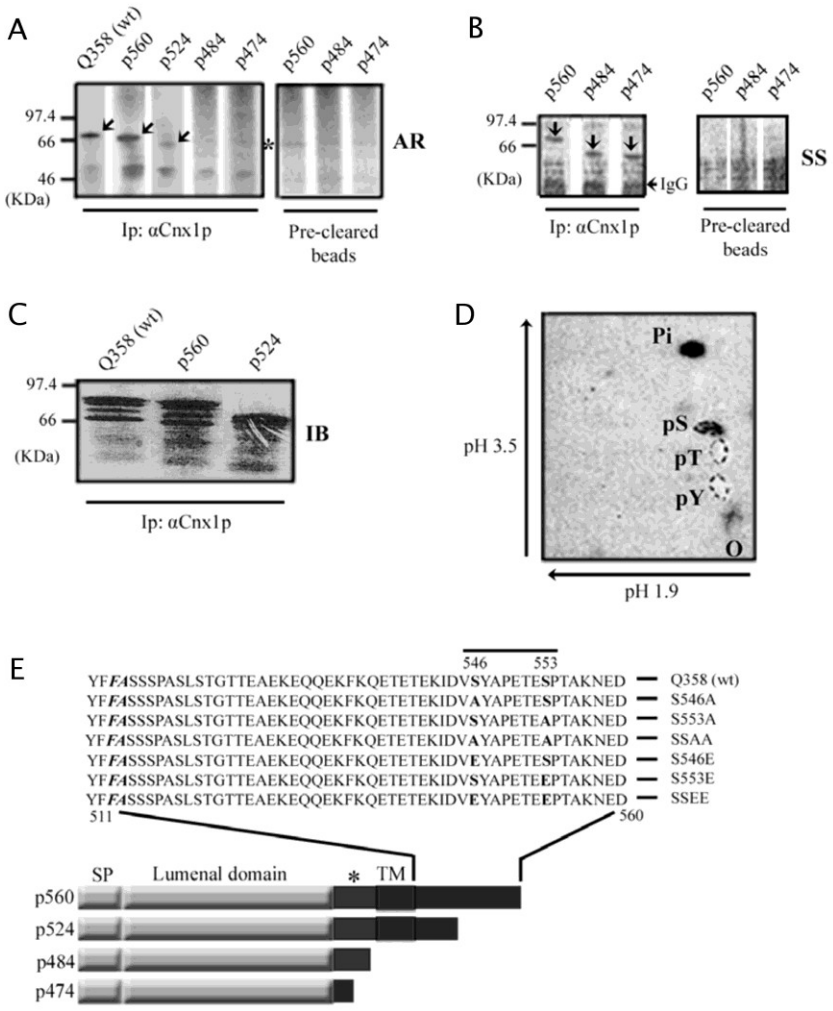

Figure 2.1. Analysis of S. pombe Cnx1p phosphorylation**. (A)** *S. pombe* Δ*cnx1* cells expressing pCNX560 (p560), pCNX484 (p484) and pCNX474 (p474) were *in vivo* labelled with ^{32}P-orthophosphate and Cnx1p immunoprecipitates were analysed by autoradiography. **(B)** Silver staining of samples from Fig 1A. **(C)** *S. pombe* WT (Q358), *S. pombe* Δ*cnx1* pCNX560 (p560), and pCNX524 (p524) were again ^{32}P-labeled and then Cnx1p immunoprecipitates were electroblotted onto nitrocellulose membranes and visualized by Western blotting. This was done to ensure equivalent amounts of Cnx1p are precipitated under the above conditions. **(D)** PVDF-bound Cnx1p (Q358 lane; Fig1C) was subjected to two-dimensional phosphoamino acid analysis. *Arrows* indicate the direction of migration and the dashed circles indicate the positions of the phosphoamino acid standards. Abbreviations are as follows: phospho-threonine (*pT*), phospho-tyrosine (*pY*), phospho-serine (*pS*), free phosphate (*Pi)* and origin (*o*). **(E)** Schematic diagram of the constructs expressed in *S. pombe* Δ*cnx1* strains. p560 encodes the entire precursor Cnx1p, p524, p484 and p474 encodes Cnx1p truncated at amino acid 524, 484 and 474, respectively. The lumenal (open), transmembrane (filled) and juxtamembrane domains (black) are depicted in rectangles. SP is the signal peptide and TM is the transmembrane domain. The sequence of the cytosolic domain of precursor *S. pombe* Cnx1p (amino acids 511-560) is provided. *FA* (in italic type) are predicted to be the last two residues of the transmembrane domain of *S. pombe* Cnx1p. Phosphorylated serine residues, or the corresponding point mutations made at that position, are in boldface type.

Hence, S. pombe Cnx1p is in vivo phosphorylated on serine residue(s), located between amino acid positions 525 and 560. Based on these observations, we investigated the role of Cnx1p phosphorylation by analyzing alanine- and glutamic acid- substituted mutants of the serine residues in this region (Figure 2.1E).

2.5.2 Cnx1p is phosphorylated in vivo at Serine 553.

There are two serine residues residing between amino acid positions 525 and 560 of precursor Cnx1p. We proceeded to identify the relevant *in vivo* sites of phosphorylation by the combined use of site-directed mutagenesis and *in vivo* ^{32}P-orthophosphate radiolabeling. Serine546 and Serine553 of Cnx1p were either singly or doubly mutated to alanine or glutamic acid (Figure 2.1E). A pMS plasmid that contains the coding sequence for *cnx1*$^{+}$, the *ura4*$^{+}$ cassette, its poly A tail, and the *nmt1* promoter, was used to create site-directed mutagenized Cnx1p mutants to replace the endogenous copy of Cnx1p in the Q358 wild-type strain (see Supplemental Figure 2.1). The expected point mutations were confirmed by sequencing genomic DNA that was isolated from the selected Ura+ transformants. The synthesis and stability of Cnx1p mutants was examined by metabolically radiolabeling cells with Tran^{35}S-label for 4 h. Cells were lysed with RIPA buffer and Cnx1p was immunoprecipitated, resolved by SDS-PAGE, and visualized by autoradiography (Figure 2.2A). A similar amount of newly synthesized Cnx1p was observed in each transformant when compared to the expression of Cnx1p in the wild-type Q358 strain. Cnx1p immunoprecipitates also contained two

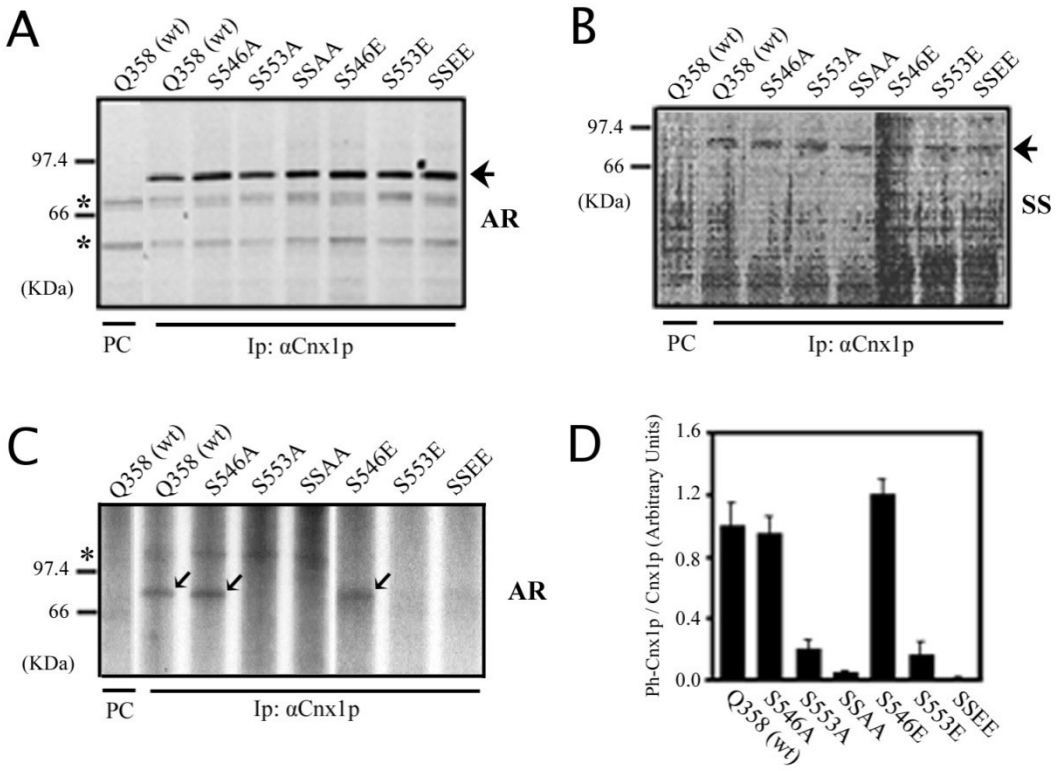

Figure 2.2. Metabolic labeling of *S. pombe* Cnx1p point mutants. **(A)** *S. pombe* wild-type (WT) and Cnx1p point mutants were metabolically labeled with trans-^{35}S label and immunoprecipitated with anti-Cnx1p antibodies, as described in Materials and Methods. Pre-cleared beads (*PC*) and Cnx1p immunoprecipitates were separated by SDS-PAGE and visualized by autoradiography. **(B and C)** Wild-type (WT) and Cnx1p mutants were *in vivo* ^{32}P-labeled and again immunoprecipitated with anti-Cnx1p antibodies. SDS-PAGE resolved immunoprecipates were visualized by (B) autoradiography for 7 days at -70^{o}C with intensifying screens or by (C) silver staining (SS). **(D)** Quantification of calnexin phosphorylation for each of the Cnx1p point mutants is presented here. Plotted values represent phosphorylated calnexin, defined as phosphorylated Cnx1p (^{32}P) over total Cnx1p (SS), and present as arbitrary units (A.U.) ±SD (n=3) relative to the wild-type Q358 control (A.U.= 1.0)

additional radiolabeled proteins, which showed a greater mobility than that expected for Cnx1p, but these proteins were also found to bind the protein A-Sepharose beads during the pre-clearing (PC) step and are therefore considered non-specific (Figure 2.2A; asterisks).

Next, wild-type and calnexin mutant *S. pombe* cells were *in vivo* radiolabeled with ^{32}P-orthophosphate. Cnx1p was immunoprecipitated, resolved by SDS-PAGE, and then visualized by autoradiography (Figure 2.2C) and silver staining (Figure 2.2B). Cnx1p-S546A remained highly phosphorylated, whereas Cnx1p-S553A was only weakly phosphorylated (Figure 2.2C). The Cnx1p-S546A,S553A double mutant displayed an undetectably low level of phosphorylation ('SSAA'; Figure 2.2C). Similar phosphorylation patterns were observed with the glutamic acid substituted versions of Cnx1p ('S546E', 'S553E', 'SSEE'; Figure 2.2C). The lack of detection by autoradiography in this experiment was not due to the absence of immunoprecipitated Cnx1p, as judged by the silver stain of the same polyacrylamide gel (Figure 2.2B). Quantification of Cnx1p phosphorylation in these point mutants revealed almost wild-type levels of phosphorylation in the S546A and S546E mutants, whereas the S553A or S553E mutants have approximately 10% of the Cnx1p wild-type phosphorylation (Figure 2.2D), and no phosphorylation was detected for SSAA or SSEE mutants. These results suggest that S553 is the major site of Cnx1p phosphorylation *in vivo*.

2.5.3 Phosphorylation of Cnx1p impacts cell size control and the association of Cnx1p with membrane-bound ribosomes.

As a first assessment of the biological consequence of genetically manipulating phosphorylation at S553 of Cnx1p, we examined the cellular morphologies of asynchronous cultures of wild-type, Cnx1-S553A, and Cnx1p-S553E cells (Figure 2.3A). Interestingly, Cnx1p-S553A cells appeared to be significantly shorter than

wild-type cells and, conversely, Cnx1p-S553E cells appeared to be significantly longer than wild-type cells. To better quantify this cell size phenotype, fixed cells from three-independent cultures of these strains were visualized by microscopy and captured images were used to determine mean cell lengths for each of these strains. The mean cell length of wild-type cells under the experimental conditions tested (EMM, 30^{o}C) was found to be 12.0 um, whereas the mean cell lengths of Cnx1p-S553A and Cnx1p-S553E cells were found to be 8.5 um and 17.0 um, respectively. These results are shown graphically by plotting the mean cell lengths as a % of the wild-type mean cell length, with error bars representing one standard deviation from the calculated means (Figure 2.3B). These results suggest that phospho-regulation of the S553 site of Cnx1p impinges on the ability of *S. pombe* cells to control their cell size.

Given that phosphorylation of mammalian calnexin at the PDK consensus site has been shown to regulate its interaction with ribosomes [167], we sought to investigate whether this aspect of calnexin regulation is conserved in fission yeast. Microsomal membranes were prepared and analyzed by ribosomal pull-down assays. Wild-type, S553A-, and S553E- Cnx1p was examined for the capacity to associate with membrane-bound ribosomes (Figure 2.3C). Ribosomal pull-downs were done using cells grown at both 30^{o}C and 37^{o}C, in both the presence and absence of 0.5ug/ml of tunicamycin, a glycosylation inhibitor and inducer of the unfolded protein response [52, 285]. Similar to mammalian calnexin, wild-type Cnx1p associated with ribosomes (Figure 2.3C) and increased temperature alone did not significantly affect this interaction; however, the ER stress induced

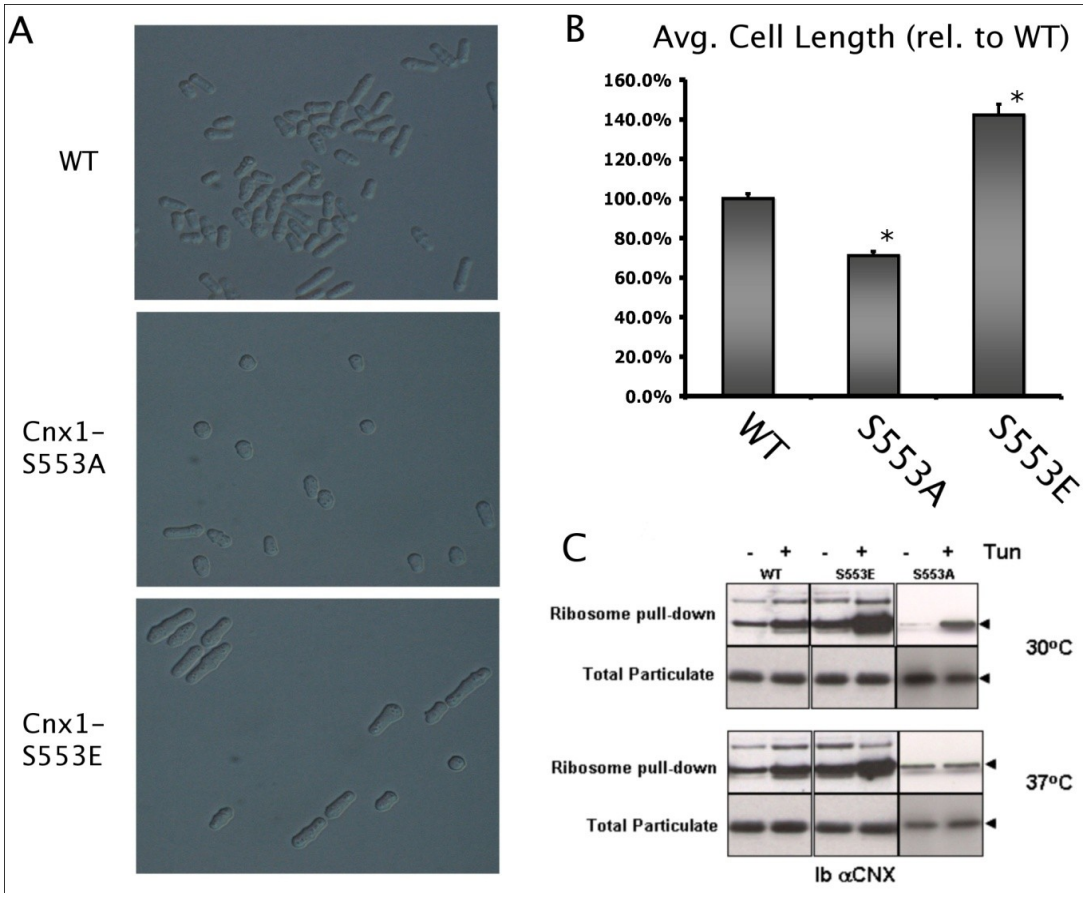

Figure 2.3. Cnx1p phosphorylation impacts cells size and Cnx1p's interaction with ribosomes. **(A)** Representative images of wild-type, Cnx1-S553A, and Cnx1-S553E cells are shown here at 1000X magnification to illustrate the cell size phenotype associated with these phosphomutants. **(B)** The average mean cell lengths were calculated for wild-type, Cnx1p-S553A, and Cnx1p-S553E from 3 independent experiments and are shown plotted here as % of the wild-type mean cell length. Error bars represent one standard deviation. Asterisks indicate that the calculated mean cell lengths were either significantly shorter (Cnx1p-S553A) or longer (Cnx1p-S553E) than the mean wild-type cell length (p-value of < 2.2e-16 for both using a one-sided wilcoxon rank-sum test). The number of cells counted for each strain was as follows: wild-type (n=1012), Cnx1p-S553A (n=1018) and Cnx1p-S553E (n=436). **(C)** *S. pombe* microsomes were prepared as described in the Material and Methods. The presence of Cnx1p (wild-type, S553E, or S553A) in both the total microsomal extract ("total particulate") and the ribosomal pellet ("Ribosome pull-down") was detected by immunoblotting in order to determine the abundance of ribosome-associated Cnx1p. Closed arrow heads are used indicate the position of the major Cnx1 species.

by 3 hours of tunicamycin treatment caused a significant increase in the amount of ribosome-associated Cnx1p (+ lanes; Figure 2.3C). Furthermore, when compared to wild-type Cnx1p under all conditions tested, more S553E Cnx1p is found to be associated with ribosomes and, conversely, less S553A Cnx1p is found to be associated with ribosomes (Figure 2.3C). This and previous results [52, 285] suggest that PDK-phosphorylation of the cytoplasmic tail of calnexin represents a highly conserved regulatory mechanism that increases the association between calnexin and ER membrane-bound ribosomes.

2.5.4 The Cnx1p-S553A phosphomutant displays an increased tolerance to ER stress

Next, we wished to investigate the biological consequence of Cnx1p phosphorylation by examining the growth phenotypes associated with our Cnx1p-S553 phosphomutants. The growth rates of both Cnx1p-S553A and Cnx1p-S553E mutants were comparable to that of wild-type *S. pombe* under normal growth conditions at 30^{o}C (Figure 2.4A). Given that calnexin is essential in *S. pombe* [169, 170], the viability of both Cnx1p-S553A and Cnx1p-S553E phosphomutant strains indicates that phospho-regulation of Cnx1p at S553 is not essential in standard growth conditions. Since some Cnx1p mutants, including those that lack most or all of the highly conserved central domain [278, 286], display cell wall defects so we also wished to examine whether our Cnx1p phosphomutants display similar sensitivities to cell wall destabilizing agents. To do this we used a

previously characterized SDS-sensitivity assay [286], where we induced halo formation in growing lawns of wild-type, Cnx1p-S553A and Cnx1p-S553E *S. pombe* cells by spotting 10-fold serial dilutions of a 10% SDS solution (Supplementary Figure 2.2). Interestingly, both Cnx1p-S553A and Cnx1p-S553E phosphomutant strains displayed SDS halo sizes comparable to that of wild-type cells, and so we conclude that neither of our Cnx1p-S553 phosphomutants displays prominent cell wall defects. This absence of obvious cell wall defects in our Cnx1p-S553 phosphomutants suggests that the lumenal substrate binding and chaperoning activities of Cnx1p remain largely unaffected in our mutant strains.

Cnx1p has previously been implicated in the tolerance of *S. pombe* cells to ER stress, including growth at elevated temperatures and growth in the presence of chemical stress agents like dithiothreitol (DTT) [278, 286, 287]. To ascertain whether our Cnx1p-S553 phosphomutants displayed any changes in their ER stress tolerance, we decided to measure the growth of our Cnx1p-S553 phosphomutants under conditions of ER stress. We first assessed cell growth at elevated temperature (37^{o}C; Figure 2.4B) and found that both Cnx1p-S553 mutants were able to cope with this mild temperature stress and grew much like the wild-type Q358 strain. We also monitored growth at 37^{o}C in the presence of tunicamycin (0.5ug/ml) and found that the Cnx1p=S553E phosphomutant and the wild-type control strain both showed a dramatically impaired growth capacity under these harsh ER stress conditions; however, the Cnx1p-S553A phosphomutant retained a significant growth capacity under these same harsh ER

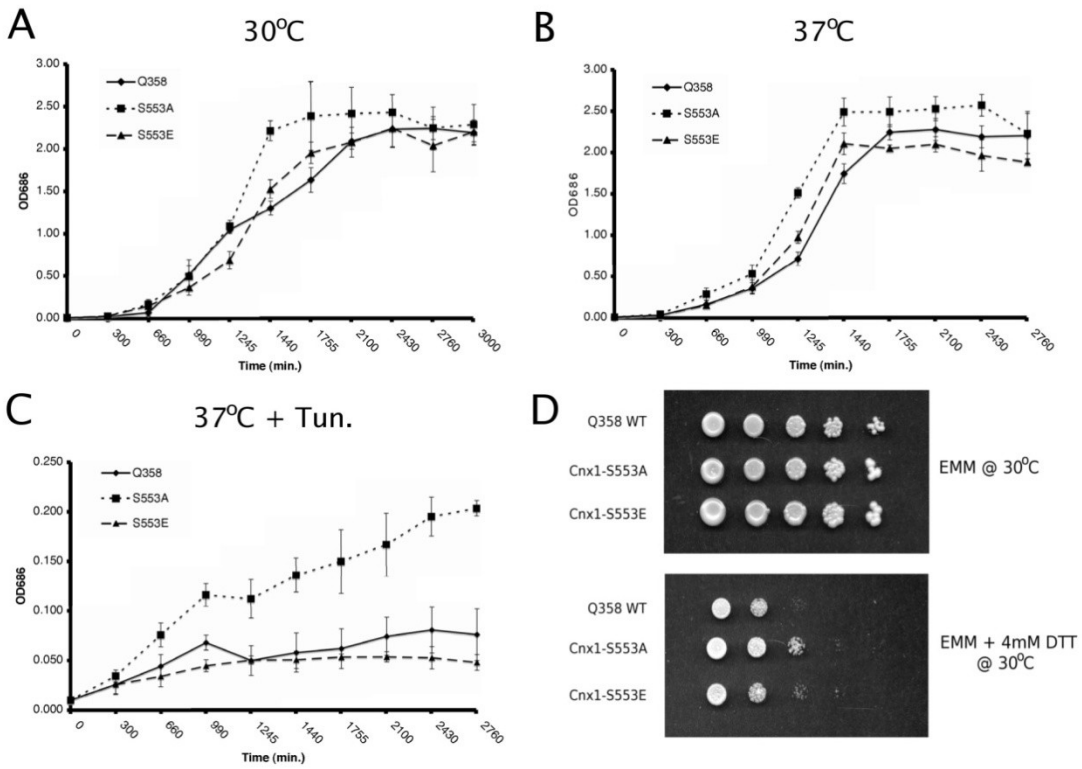

Figure 2.4. Cnx1p phosphorylation impacts ER stress tolerance. **(A-C)** Growth of wild-type, S553A and S553E Cnx1 strains was monitored via OD_{686} measurement under (A) standard growth conditions (30°C), (B) mild ER stress conditions by growth at elevated temperature (37°C), and (C) harsh ER stress conditions by growth at elevated temperature in the presence of 0.5 ug/ml of tunicamycin (37°C + Tun.). Plotted values represent the mean of 3 independent experiments and error bars represent one standard deviation from the plotted means. **(D)** 10-fold serial dilutions (3ul each) of wild-type, Cnx1p-S553A, and Cnx1p-S553E strains were spotted onto standard EMM agar plates (top panel) or standard EMM plates supplemented with 4 mM DTT (lower panel) and placed at 30°C for 4 days growth before images of these plates were taken on a flat-bed scanner.

stress conditions (Figure 2.4C). These results suggest that genetic ablation of phosphorylation at S553 by substituting this serine for alanine allows *S. pombe* cells to better cope with severe and protracted ER stress insults.

To ensure that the observed ER stress tolerance of the Cnx1p-S553A phosphomutant was not unique to tunicamycin-induced ER stress, we next wished to test the growth of our phosphomutants by conducting a serial dilution assay on

solid EMM media plates, both in the presence and absence of the oxidative stress agent DTT (Figure 2.4D). As expected, all three strains tested grew equally well on standard EMM plates at 30 ^{o}C; however, the Cnx1p-S553A cells showed an improved growth capacity on the EMM + 4 mM DTT plate when compared to the wild-type control and Cnx1p-S553E strains. This result agrees with our growth curve analysis and provides further evidence that Cnx1p-S553A cells are more resistant to ER stress. When taken together, the above results clearly indicate that preventing phosphorylation at S553 of Cnx1p allows *S. pombe* cells to better tolerate prolonged exposure to harsh ER stress insults.

2.6 Discussion

In this study we have used a genetically tractable fission yeast model to study calnexin phosphorylation and, more specifically, to investigate the biological consequences associated with genetic manipulation of the PDK site of Cnx1p. Importantly, phospho-regulation at this conserved PDK site appears to control the association of Cnx1p with membrane-bound ribosomes. Also, genetic manipulation of this S553 PDK phosphorylation site affects cell size control and ER stress tolerance and this suggests that calnexin function, and the post-translational mechanisms used to regulate this function, are involved in both of these biological processes in fission yeast.

By combining *in vivo* metabolic radiolabeling, deletion analyses, site-directed mutagenesis, and phosphoamino acid analysis, we have identified two potential *in vivo* phosphoacceptor sites within the cytosolic tail of Cnx1p. We

found what appears to be the major site of phosphorylation at serine 553, and a more minor site at serine 546 (Figure 2.2C). Interestingly, S553 is found within a PDK phosphorylation motif, which is a conserved phosphorylation site that was also found in mammalian calnexin [162]. In light of the above results, it appears that phosphorylation of this PDK site in the cytosolic domain of calnexin has been highly conserved and we hypothesized that the regulatory function imparted by this phosphorylation was also highly conserved.

Phosphorylation of mammalian calnexin at its Ser^{563} PDK site has been shown to regulate its interaction with ER-bound ribosomes and ERK1 has been suggested as the candidate kinase for this phosphoacceptor site [166, 167]. It has been demonstrated that phosphorylation of calnexin serves to locally increase the concentration of calnexin at active translocons and that this association may enhance co-translocational protein folding [33, 167]. In accordance with these data on mammalian calnexin, we have shown here that *S. pombe* Cnx1p that contains a phosphomimic glutamic acid substitution at its conserved (S553) PDK motif interacts more readily with membrane-bound ribosomes, under both normal and ER stress conditions (Figure 2.3C). Given that both yeast and mammalian calnexin behave similarly in this regard, we feel that these data strongly argue that phosphorylation of the cytosolic PDK site of calnexin is an evolutionarily conserved mechanism that is used to regulate the interaction between calnexin and ER membrane-bound ribosomes.

Morphological examination of our Cnx1p phosphomutants revealed that phosphorylation at S553 impacts cell size control in *S. pombe*. Both the ease of measuring rod-shaped *S. pombe* cells and their facile genetics have allowed this

fission yeast to long serve as a powerful model for studying the relationship between cell size control and cell cycle progression [288-291]. A large body of research has provided an understanding of how cyclin dependant kinases (specifically Cdc2 in *S. pombe*), along with their associated cyclins, can promote entry into mitosis (reviewed in [292, 293]). The protein encoded by the Wee1 gene in *S. pombe* is a Cdc2-inactivating protein kinase and mutations in Wee1, as the gene name aptly implies, provides an excellent illustration of how cell size control requires a precise coordination between cell cycle progression and cell growth [290, 294, 295].

Although we wish to avoid speculating too heavily on the precise cause of the cell size phenotypes that we observed with our Cnx1p-S553 phosphomutants, we do feel that a regulatory link between the cell cycle machinery and this important, rate-limiting [286], ER chaperone would not be entirely surprising. This is particularly true given that mammalian calnexin appears to be phosphorylated by ERK1 [166, 167], a mitogen activated protein kinase that is activated in response to extracellular growth stimuli [296, 297]. Given that increased protein production is expected to follow mitogenic stimuli, we find it tempting to speculate that calnexin phosphorylation may provide a means to coordinate cell growth with the cells capacity to productively fold proteins within the ER.

Here we have investigated the growth phenotypes of our Cnx1p phosphomutants under both normal and ER stress conditions. All of our Cnx1p mutants tolerated the mild ER stress that we induced by elevating the growth temperature from 30^{o}C to 37^{o}C (Figure 2.4A and B). Importantly, the Cnx1p-

S553A phosphomutant showed an improved tolerance to growth under conditions of prolonged ER stress, which we induced in liquid cultures by growth at 37^{o}C in the presence of tunicamycin (Figure 2.4C) and in solid EMM agar by the addition of 4mM DTT (Figure 2.4D). The implication of these results are that a non-phosphorylatable Cnx1p (S553A) is better suited than either wild-type Cnx1p or phospho-mimic Cnx1p (S553E) to provide the chaperone activities that are necessary to cope with either of these two insults to protein folding. This result is consistent with a previous study that showed that preventing AZC-induced phosphorylation of calnexin in HepG2 cells, by the addition of a MEK1 kinase inhibitor (PD98059), led to the release and secretion of partially misfolded AAT [166]. When taken together with the results we presented here, it seems that preventing phosphorylation of the cytosolic PDK site of calnexin, whether by genetic manipulation or by treatment with the appropriate kinase inhibitor, can reduce its retention of partially misfolded glycoproteins that normally occurs under ER stress conditions.

These studies on calnexin phosphorylation leave us with one counterintuitive observation that we feel we must address at this time: Why do cells phosphorylate calnexin in response to chemical insults that produce ER stress, as was observed in the AZC-treated HepG2 cells [166], given that we have demonstrated that non-phosphorylatable calnexin (Cnx1p-S553A) allows cells to better tolerate harsh ER stress insults? We feel that this contradiction could very likely stem from the inability of these harsh chemical insults to ER protein folding to faithfully recapitulate the milder physiological ER stresses that cells normally encounter and have evolved regulatory mechanisms to cope with. The study by

Cameron and colleagues showed that preventing AZC-induced calnexin phosphorylation by PD98059 allowed for the ER exit and secretion of partially misfolded AAT, following its release from calnexin. We suggest that tunicamycin- or DTT- stressed *S. pombe* cells may similarly benefit from a slackened fidelity of the ER retention capacity of Cnx1p and that this is the case for non-phosphorylatable Cnx1p-S553A; however, we might expect that the decreased retention capacity of Cnx1p-S553A might lower the fidelity of the ER quality control system and that this would not be beneficial outside of the context of these overly-harsh artificial ER stress conditions. We feel this could explain why cells, which don't normally encounter such harsh ER stress conditions, have evolved calnexin phosphorylation as a means to cope with milder physiological ER stresses by increasing the association of Cnx1p with ribosomes and to increase the fidelity of its glycoprotein retention capacity.

In summary, we have identified S553 as the major *in vivo* site of phosphorylation within *S. pombe* Cnx1p. We further show that Cnx1p interacts with ER-membrane bound ribosomes and that this important physical interaction increases upon phosphorylation of S553. Furthermore, Cnx1p phosphorylation at S553 impacts the ability of *S. pombe* cells to maintain an appropriate cell size and to tolerate harsh ER stress conditions. Overall, regulation of the distribution and chaperone activities of Cnx1p within the ER allows *S. pombe* cells to intricately coordinate its protein folding machinery to the protein folding demands present and thereby maximize the quality and efficiency of glycoprotein production.

2.7 Acknowledgements

We would like to thank Dr. Miho Shida for kindly providing the pMS vector. This work was funded by grants from the Canadian Institutes for Health Research to Dr. David Thomas, Dr. John Bergeron and Dr. Eric Chevet. Dr. Hetty Wong and Dr. Eric Chevet were supported by the Fond de la Recherche en Santé du Québec. Daniel Waller was supported by a CIHR STIHR Chemical Biology scholarship.

2.8 Supplementary Information

Supplementary Table 2.1 Oligonucleotide Primers used to generate cnx1 phosphomutants

Mutant	Oligonucleotide sequence
S546A	CUP-1: 5'-ctccattattctttcgattaagcttgctgatccatctcatcg-3' (109 -78) 5'-attttagcaggatcctagtcttcattcttcgcagttggtgattcagtttcgggagcgta**agc**aacgtctat-3'(1627-1708)
S553A	CUP-1: 5'-ctccattattctttcgattaagcttgctgatccatctcatcg-3' (109 -78) 5'-attttagcaggatcc ttagtcttcattcttcgcagttgg**tgc**ttcagtttcggg -3' (1645-1708)
S546E	CUP-1: 5'-ctccattattctttcgattaagcttgctgatccatctcatcg-3' (109 -78) 5'-attttagcaggatccttagtcttcattcttcgcagttggtgattcagtttcgggagcgta**ctc**aacgtctat-3 (1627-1708)
S553E	CUP-1: 5'-ctccattattctttcgattaagcttgctgatccatctcatcg-3' (109 -78) 5'-attttagcaggatccttagtcttcattcttcgcagttgg**ctc**ttcagtttcggg -3' (nt 1645-1708)
SSAA	CUP-1: 5'-ctccattattctttcgattaagcttgctgatccatctcatcg-3' (109 -78) 5'-attttagcaggatccttagtcttcattcttcgcagttgg**tgc**ttcagtttcgggagcgta**agc**aacgtctat-3 (1627-1708)
SSEE	CUP-1: 5'-ctccattattctttcgattaagcttgctgatccatctcatcg-3' (109 -78) 5'-attttagcaggatccttagtcttcattcttcgcagttgg**ctc**ttcagtttcgggagcgta**ctc**aacgtctat-3 (1627-1708)

The Hind III restriction site is underlined, the BamHI site is double underlined, the corresponding nucleotide sequence for the mutagenized amino acid residue is in boldface characters.

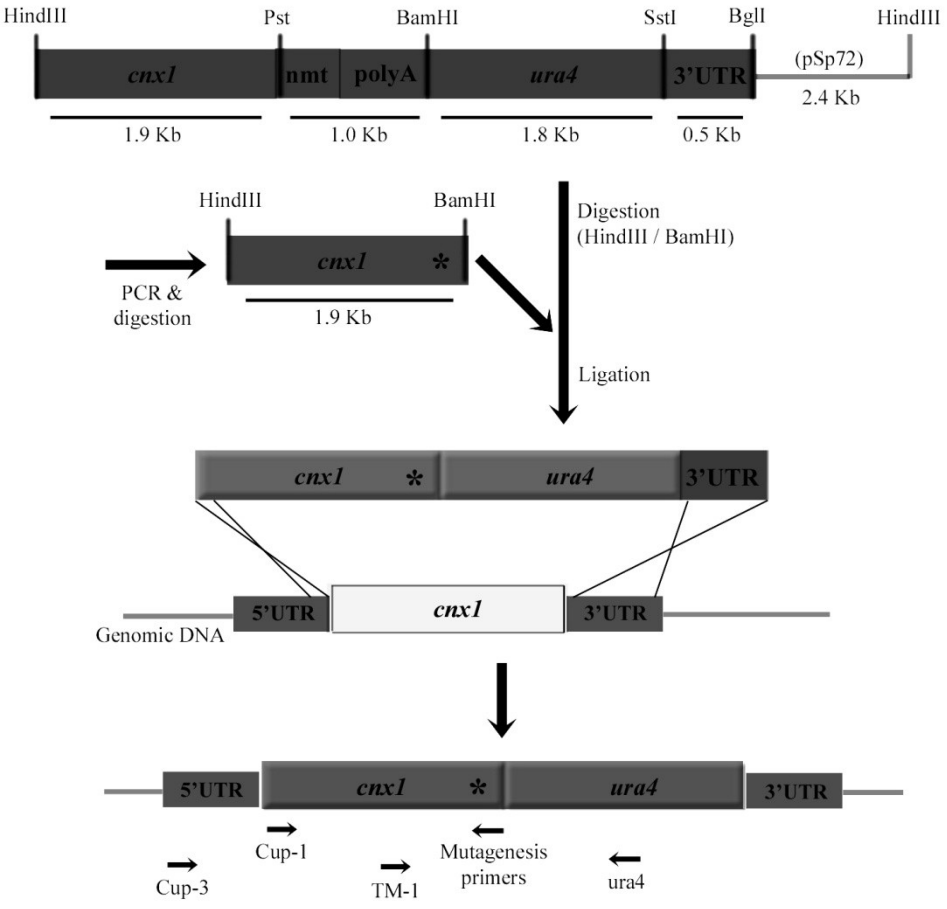

Supplementary Figure 2.1. A schematic diagram of our homologous recombination strategy to replace the endogenous cnx1^{+} with cnx1 phosphomutants. A linearized pMS vector modified from the pSp72 vector is shown at the top of this figure. Restriction sites of interest are indicated. The pMS vector contains the coding region of *cnx1*$^{+}$ (nt -360 to 1683) nmt1 promoter (*nmt*), poly A, *ura4*$^{+}$ cassette (*ura4*$^{+}$), and the 3' untranslated region of *cnx1*$^{+}$ (*3′ UTR*). A PCR fragment containing the relevant mutated phosphorylation site(s) (asterisk) was generated using the CUP-1 5' primer and a mutagenic 3' primer (see Table S1 for oligonucleotide sequences). Genomic DNA from wild-type *S. pombe* was used as the template for these mutagenic PCR reactions. Each 1.9kb Cnx1 PCR fragment was digested and ligated into the pMS vector. Ligation was confirmed by analyzing the vector size and by DNA sequencing (using primers TM-1 and ura4). These modified Cnx1 phosphomutant pMS vectors were amplified and used to transform the wildtype *S. pombe* Q358 and homology of the 5' and 3' UTRs was used to directed the recombination to the endogenous cnx1^{+} locus. Ura+ transformants were selected and PCR with primers CUP-3 and ura4 confirmed the homologous replacement of the endogenous *cnx1*$^{+}$. DNA sequencing was used (using TM-1 and ura4 primers) to confirm successful homologous recombination and generation of the appropriate cnx1 phosphomutants. Arrows at the bottom of this figure indicate the position of the relevant primers. The *asterisk* in the cnx1 sequence indicates the mutagenized amino acid residue.

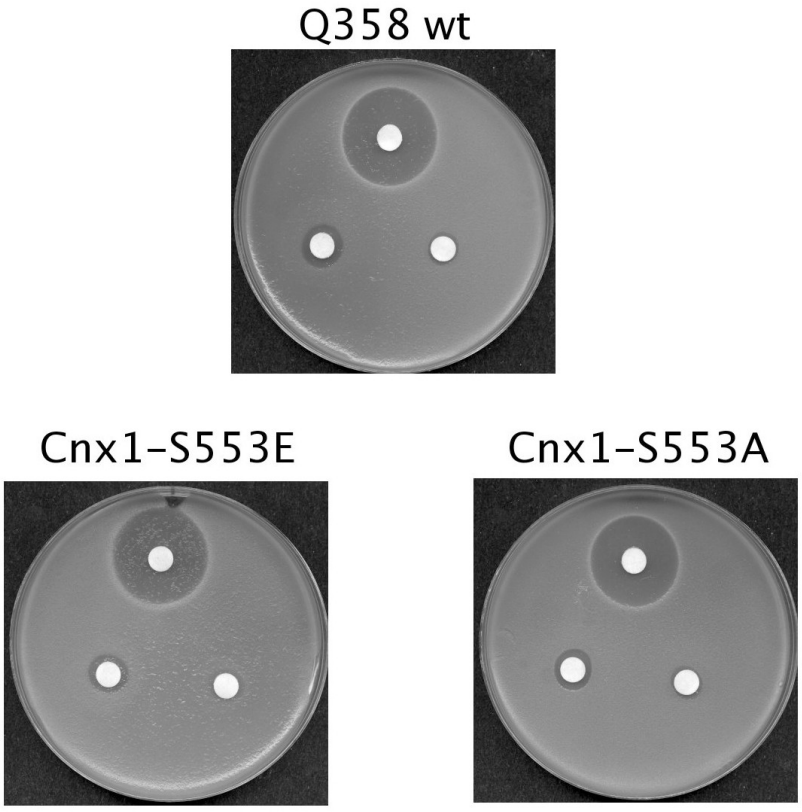

Supplementary Figure 2.2. Cnx1p phosphomutants do not have apparent cell wall phenotypes. SDS halos sizes indicate that wild-type Q358, Cnx1p-S553A, and Cnx1p-S553E cells all show similar sensitivities to cell wall destabilizing agents. Wild-type Q358, Cnx1p-S553A, and Cnx1p-S553E strains were grown overnight in 10 ml's of EMM media and 100 ul of 2.5 OD_{686} cells were used to inoculate molten (55^{o}C) top agar (0.7%). Innoculated top agars were vortexed and then carefully poured onto standard EMM plates. Three sterile whatman filter discs were placed on top of the cooled, solidified top agar in order to indicate the position of the spotted SDS solution. Next, 10 ul of a sterile SDS solution was spotted onto each filter disc to assess the sensitivity of these strains to cell wall destabilizing agents. The concentrations of the SDS solutions spotted were as follows: top middle disc = 10% SDS, lower left disc = 1%, and lower right disc = 0.1%.

CHAPTER 3

A high-throughput screen for small molecule modulators of the unfolded protein response identifies UPRM8, an inducer of apoptosis in multiple myeloma cells.

3.1 Connecting Text

ER-to-nucleus signal transduction pathways are activated in response to the accumulation of unfolded protein in the ER and the adaptive responses to this form of stress have been extensively studied over the past two decades. A significant and ever-increasing body of literature has implicated these ER homeostatic mechanisms in a wide assortment of human diseases, including cancer. Given this, our need for a better understanding of these important cellular stress responses is pressing. Furthermore, the identification of compounds that can either inhibit or supplement ER homeostatic mechanisms is of essential interest.

Given that the Ire1 pathway is the most conserved ER homeostatic response and that it has been widely implicated in tumorigenesis and cancer cell survival, I chose to study this pathway in *S. cerevisiae.* Chapter three details my efforts to identify and characterize novel small-molecule inhibitors of Ire1-dependent signaling. The findings presented in this chapter clearly demonstrate the value of an *S. cerevisiae* model for the identification of small-molecules that affect Ire1 signaling and which can later be used to evaluate the homologous pathway in higher eukaryotes. Significantly, I found one small-molecule UPRM that was able to block the cytoprotective functions of Ire1 in constitutively stressed multiple myeloma cells. The significance and implications of this finding are discussed.

3.2 Abstract

Oxidative protein folding of secretory and membrane proteins occurs within the endoplasmic reticulum (ER) and this protein folding environment is sensitive to insults that perturb N-linked glycosylation, ER calcium levels, and redox potential. Such perturbations in the ER can induce a set of homeostatic processes to restore productive protein folding; these are collectively referred to as the unfolded protein response (UPR). Given their constitutive demand for protein synthesis and the harsh nature of tumour microenvironments, cancer cells often co-opt the UPR to protect them from conditions that would otherwise cause cell death. Accordingly, the identification of UPR-modulating compounds is of essential interest. Here, we present the results of a screen for small-molecule UPR modulators (UPRMs). Our *in vivo* screening, conducted in *Saccharomyces cerevisiae*, identified three candidate UPRMs that prevent tunicamycin-induced activation of the Ire1 UPR pathway in yeast. One of these compounds, UPRM8, also exhibited this same UPRM activity in human cell lines. UPRM8 displayed an ability to specifically interfere with the ribonuclease activity of Ire1 *in vitro*, while leaving the kinase function of Ire1 intact. UPRM8 treatment induced an apoptotic cell death in RPMI-8226 multiple myeloma (MM) cells and this UPRM8-mediated cell death was enhanced when combined with agents that exacerbate ER stress levels. These results support a growing body of literature that suggests that multiple myeloma cancer cells are exquisitely sensitive to ER stress and that small-molecule disruption of ER homeostatic mechanisms in MM cells may one

day provide useful adjuncts to conventional therapies for treating this deadly hematological malignancy.

3.3 Introduction

Secretory proteins produced by eukaryotic cells are co-translationally translocated into the endoplasmic reticulum (ER), where they can be modified by N-linked glycosylation and are assisted in reaching their correct tertiary structure by a host of ER-resident folding enzymes. Protein folding in the ER is sensitive to changes in calcium levels, N-linked glycosylation capacity, and redox potential. Insults to these protein folding conditions or physiological demands that exceed the folding capacity of the ER can cause an accumulation of unfolded protein, a situation referred to as ER stress. Given the importance of secretory proteins to the biology of eukaryotic cells, it is not surprising that homeostatic mechanisms have evolved to cope with ER stress. These ER homeostatic mechanisms, collectively referred to as the unfolded protein response (UPR), provide stressed cells an opportunity to restore protein folding conditions before critical cell fate decisions must be made (reviewed in [58, 86]).

Saccharomyces cerevisiae possesses a single UPR pathway that aims to restore protein folding by increasing the transcription of an expansive set of genes, including those involved in protein folding, glycosylation, secretion, membrane biogenesis, and ER-associated degradation (ERAD) [64]. The discovery of a 22-base pair unfolded protein response element (UPRE) in the

promoter of KAR2 (yeast BiP, an ER-resident HSP70 family chaperone) helped uncover the yeast UPR transcriptional programme [70] and also allowed for the design of effective UPR reporters, such as a UPRE-regulated β-galactosidase (β-gal) reporter [52]. Employing UPRE reporters in a genetically tractable yeast model has helped define elements of the UPR; for instance, their use allowed for the identification of Ire1p, a novel type-I ER transmembrane kinase that senses unfolded protein in the ER [50, 51]. Two Ire1 orthologs have been identified in mammalian cells and Ire1α was found to be ubiquitously expressed, whereas Ire1β expression was found mostly in cells of gastrointestinal tract [72, 73].

Ire1 is activated by unfolded protein in the ER, which leads to its dimerization/oligomerization [146, 151, 156]. This event stimulates the cytosolic kinase domain of Ire1, which then leads to trans-autophosphorylation of Ire1 oligomers [147, 155, 156]. Trans-autophosphorylation of Ire1 increases access to its nucleotide-binding pocket and the binding of ATP or ADP to this pocket results in the formation of back-to-back dimers [148, 149]. The formation of this back-to-back dimer activates the C-terminal ribonuclease domain of Ire1, which results in the removal of an intron from mRNA that encodes a potent UPR transcriptional activator, called HAC1 (yeast) or XBP1 (metazoans) [67, 75, 76]. The basic leucine zipper transcription factors that are produced from this regulated Ire1-dependent mRNA splicing event are then able to translocate to the nucleus, where they can bind directly to UPREs (Hac1p) or ER stress response elements (ERSEs; Xbp1) and thereby induce the expression of UPR target genes [60, 64, 70, 71].

Metazoan cells also contain two additional proximal ER stress sensors, called PKR-like ER kinase (PERK) and activating transcription factor-6 (ATF6). PERK is an ER transmembrane kinase that induces the expression of the ATF4 by instigating a global translational repression through its phosphorylation of eIF2α [61, 62, 82]. ATF6 is an ER membrane-tethered transcription factor that is liberated in response to unfolded protein by proteolytic cleavage, after which it can freely translocate to the nucleus and contribute to the UPR transcriptional program [59, 60, 83]. The concerted activities of the Ire1/Xbp1, PERK, and ATF6 UPR pathways allows metazoan cells to adapt the protein folding and degradative capacities of their ER in order to cope with ER stressors or increased secretory demands.

The UPR is activated in numerous cancers (reviewed in [120]); consequently, a significant amount of research has been directed at uncovering the role of the UPR during tumorigenesis. Solid tumours often suffer hypoxic or nutrient-limited growth conditions due to poor vascularization and these are conditions known to cause ER stress. A growing body of literature suggests that the UPR contributes to cancer cell survival in such harsh tumour microenvironments (reviewed in [298, 299]). For instance, Xbp1-deficient cell lines have been used to show that the Ire1/Xbp1 pathway is directly involved in promoting cell survival under hypoxic conditions and is required for tumour growth [137]. Several studies have also shown that cancer cells employ the UPR to tolerate glucose deprivation and that suppressing the UPR under glucose-limiting conditions leads to cancer cell death [136, 300]. For these and other

reasons, ER homeostatic mechanisms have been receiving great attention as potentially powerful therapeutic targets that may open up a broad array of new anti-cancer strategies.

The involvement of UPR mechanisms in cancer is not limited to solid tumours, as evidenced by the high levels of Xbp1 expression found in multiple myeloma (MM) cell lines [301]. Multiple myeloma is a hematological malignancy characterized by uncontrolled proliferation of plasma cells in the bone marrow, resulting in bone lesions, hypercalcaemia, increased monoclonal immunoglobulin (Ig) in the blood, immunodeficiency, and renal failure (reviewed in [302, 303]). Several studies have highlighted the importance of the Ire1/Xbp1 UPR pathway during the differentiation of mature, activated B cells into antibody-producing plasma cells [56, 304]. Numerous studies have suggested that the FDA-approved proteasomal inhibitor Bortezomib, marketed as Velcade by Millenium Pharmaceuticals, induces apoptosis in MM cells following a sustained, lethal, ER stress response [49, 143, 305, 306]. Furthermore, siRNA-mediated knockdown of Xbp1 expression in MM cell lines has been shown to sensitize them to ER stress-induced apoptosis by compounds like tunicamycin or bortezomib [46, 143]. Given that MM cells appear to be reliant on ER homeostatic mechanisms for their continued survival and that they are so exquisitely sensitive to ER stress inducers like bortezomib, these cancer cells provide an ideal model to evaluate the anti-cancer potential of novel small-molecule UPR modulators (UPRMs)

The involvement of UPR mechanisms in both solid tumours and in hematological malignancies underscores the importance of identifying compounds that can modulate this important homeostatic response. Novel UPR modulators may represent candidates for therapeutic lead development and could be used to rationally design new therapeutic strategies for treating ER stress-sensitive cancers, such as multiple myeloma. Once identified, any such UPR modulating compounds could also be employed as chemical probes to investigate the importance of ER stress in a wide variety of human disease processes.

In this study, we report the results of a high-throughput screen for novel small-molecule UPRMs and we report one such UPRM that functions in both yeast and human cells. This lead UPRM molecule, designated UPRM8, inhibits the ribonuclease activity of Ire1 and hence blocks the Ire1/Xbp1 UPR pathway. This blockade of the Ire1/Xbp1 UPR pathway is able to induce apoptosis in cultured MM cells, presumably by preventing the cytoprotective measures that are normally implemented by this important ER homeostatic pathway. Furthermore, UPRM8 increases the MM cytotoxicity of ER stress inducing agents such as 2-deoxy-D-glucose (2-DG) and bortezomib (BZ). Our results suggest that ablating the cytoprotective functions of the Ire1/Xbp1 UPR pathway through the use of novel small-molecule UPRMs, particularly when combined with agents that exacerbate ER stress, may represent a viable therapeutic strategy for treating this deadly hematological malignancy.

3.4 Materials and methods

Materials

Standard PCR reactions were done using Expand High Fidelity PCR amplification system from Roche. Deoxyribonucleotides for PCR were purchased from either Stratagene or Fermentas. Lumi-light chemiluminescent reagents and Complete protease inhibitor tablets were purchased from Roche. HRP-conjugated secondary antibodies were purchased from Santa Cruz biotechnology. Hoechst 33342, ProLong Gold antifade reagent, and oligonucleotide primers, including the 5' AF647 and 3' BHQ- labelled synthetic RNA probes, were purchased from Invitrogen. Ortho-nitrophenyl-β-D-galactopyranoside (ONPG), Chlorophenol Red-β-D-galactopyranoside (CPRG), acid washed glass beads, myelin basic protein, tunicamycin, and 2-deoxy-D-glucose were all purchased from Sigma. Bortezomib was purchased from LC Laboratories and salubrinal was purchased from Santa Cruz Biotechnology. Glutathione Sepharose 4B resin was purchased from GE Healthcare. Radiolabeled [γ-32P]-Adenosine 5' triphosphate was purchased from Perkin Elmer.

Generation of the Cml8-1 UPR reporter yeast strain

Yeast media, growth conditions, manipulations, and lithium chloride transformation protocols were conducted as described previously [307]. The previously reported AD1-8 (*MATα, PDR1-3, ura3, his1, Δyor1::hisG, Δsnq2::hisG, Δpdr5::hisG, Δpdr10::hisG, Δpdr11::hisG, Δycf1::hisG, Δpdr3::hisG, Δpdr15::hisG*) drug sensitized yeast strain [308] was transformed

with a linearized pLGD178 UPRE-Y-355 plasmid [52]. Linearization of this plasmid by *StuI* digestion was used to direct the homologous recombination of this cassette into the URA3 locus of AD1-8. A single Ura+ transformant, designated Cml8-1, was selected and the stability of the URA3 marker was used to confirm that the UPRE::LacZ reporter cassette was stably maintained following genomic integration. When this Cml8-1 strain was exposed to 0.5 ug/ml of TM it gave a 6.5-fold induction of β-galactoside activity, confirming the successful creation of yeast UPR reporter strain for use in our high throughput chemical screen.

β-*galactoside Assays*

Assaying of β-galactoside activity from tunicamycin stressed (0.5 ug/ml or 2.0 ug/ml, as indicated) Cml8-1 reporter yeast was done using either the permeabilized cell method or the crude extract method as described previously [307].

A high-throughput screen for small-molecule UPRMs

40,000 small molecules from Chembridge's microformats synthetic compound library were tested for the ability to reduce TM-induced UPR reporter activation in Cml8-1 cells. The first and last columns of each 96-well plate were reserved for negative (no TM exposure) and positive (2.0 ug/ml TM-alone) controls. This meant that 80 test compounds per 96-well plate could assessed for their ability to impair UPR reporter activation following a 3-hour co-treatment of Cml8-1 with test compounds (at 1 uM) and TM stress (2.0 ug/ml). The presence of positive

and negative control wells on each individual screening plate allowed us to monitor Z' scores and we re-screened any plates that had Z' scores below an arbitrary threshold of 0.5. Preliminary hits were selected from this primary screen based on their ability to impair UPR reporter activation to less than 50% of the activation observed in TM alone-treated positive control wells. We counter screened our preliminary hits for potent fungicidal activity by doing standard growth curves with Cml8-1 yeast that were treated with 1 uM of each test compound. After removing compounds that were cytotoxic to yeast cells we subsequently retested their inhibition of UPR reporter assay on three independent days, each with 3 biological replicates (total n=9). After again selecting a p-value cut-off of 0.05 following these additional replicates, we were able to confidently select three lead UPRMs that were non-toxic to yeast cells and that were able to significantly and reproducibly impair TM-induced UPR reporter activation. Each of these three lead UPRM molecules were also counter-screened using a galactose-inducible β-galactoside reporter to ensure that their observed UPRM activity did not arise from a capacity to generally inhibition transcription, translation, or β-galactosidase enzyme function (see Fig. S1).

Semi-quantitative RT-PCR of HAC1 and XBP1 mRNA

Total RNA was isolated from treated Cml8-1 yeast using the Ribopure yeast kit (Ambion/Applied Biosystems). The Oligotex mRNA mini kit (Qiagen) was used to purify mRNA from yeast total RNA. Total RNA was extracted from treated HeLa cells using TRIzol reagent (Invitrogen) following the manufacturers protocol. First strand cDNA synthesis was done using either PowerScript (BD

Biosciences) or AffinityScript (Agilent/Stratagene) reverse transcriptase enzyme kits. HAC1- and XBP1-specific oligonucleotides were used to PCR amplify the HAC1 and XBP1 sequences from first strand cDNA. The PCR primers used were as follows (5' to 3'): HAC1 fwd-TAGACTGAATCTAGAATGGAAATGACTGATTTTGAACTAACTAGTAATT rev-AGAACGTCAGGATCCTCATGAAGTGATGAAGAAATCATTCAATTCAAATG (969 bp product; unspliced); XBP1 fwd-CCTTGTAGTTGAGAACCAGG, rev- GGGGCTTGGTATATATGTGG (442 bp product; unspliced); GAPDH fwd-CAAGAAGGTGGTGAAGCAGG, rev- TCCACCACCCTGTTGCTGTAG (300 bp product). The PCR products were separated by electrophoresis in 2% agarose gels followed by ethidium bromide staining for visualization. Densitometry of the spliced and unspliced XBP1 PCR products was done using the Quantity One analysis software (Bio-Rad).

Purification of GST-Ire1p from Yeast

An *S. cerevisiae* strain that contained a galactose-inducible GST-Ire1p expression plasmid was selected from a previously reported yeast GST-kinase fusion library [272]. An overnight culture of this strain was grown in SD -Ura + 3% raffinose and was diluted to an OD_{600} of 0.2 in 100 ml's of SD -Ura + 3% raffinose. Cells were grown to an OD_{600} of 0.6 before the addition of a sterile galactose solution (3% final concentration) was used to induce the expression of the GST-Ire1p fusion. After 4 hours of induction cells were harvested, washed in sterile dH_2O, and lysed by glass bead vortexing in lysis buffer (50 mM Tris-HCl pH7.5, 150

mM NaCl, 5 mM EDTA, 0.5% Triton X-100, Complete Protease inhibitor, 1 mM PMSF). The resulting supernatant was cleared by centrifugation and incubated with glutathione sepharose 4B resin. Bead-bound GST-Ire1p was washed extensively (5 times) in 10 column volumes of wash buffer (50 mM Tris-HCl pH7.5, 150mM NaCl). GST-Ire1p was eluted from glutathione beads by 30 minute incubation with glutathione elution buffer (50mM Tris-HCl pH8.0, 10 mg/ml reduced gluthathione). Eluted GST-Ire1p was simultaneously concentrated and buffer-exchanged into storage buffer (25 mM HEPES pH8, 50 mM KCl, 1 mM DTT, 0.1 mM EDTA, 10% glycerol) using an Amicon Ultra centrifugal filtration device (10,000 MW cut-off). The concentrated fusion protein was stored at -80^{o}C until further use.

In vitro protein kinase assay

Standard *in vitro* kinase assays were performed as described previously [309]. Approximately 1.0 μg of myelin basic protein was resuspended in kinase buffer supplemented with 1 μM ATP, 1 μl [γ-32P]ATP (4,500 Ci/mmol and 10 Ci/μl, respectively) and approximately 0.2 μg of purified GST-Ire1p. DMSO (0.2%) reaction mixtures were incubated for 30 min and then boiled for 5 minutes after the addition of SDS sample buffer. Samples were separated by SDS-PAGE, dried and visualized by autoradiography.

In vitro ribonuclease assay

The purification of *s.c.*Ire1^{CYTO} and its use in a fluorescence-based ribonuclease assay to monitor Ire1-dependent cleavage of a synthetic AlexaFluor 647-conjugated RNA substrate was carried out as described previously [149].

Cell culture and transfections

The RPMI-8226 multiple myeloma cell line was obtained from ATCC and was maintained at 37^{o}C, 5% CO_2 in standard RPMI-1640 media supplemented with 10% FBS. Transient transfection of RPMI-8226 cells with the pCAX-F-XBP1 ΔDBD-venus ERAI reporter construct was done using the FuGene transfection reagent at a 6:2 ratio of fugene reagent (ul) to plasmid DNA (ug).

Western Blotting

Treated RPMI-8226 cells were washed in ice cold PBS and lysed on ice for 20 minutes in a standard RIPA buffer (50 mM Tris-HCl pH7.5, 150 mM NaCl, 1% NP-40, 0.5% deoxycholic acid, 0.1% SDS) supplemented with Complete protease inhibitor tablets. The resulting cell lysates were cleared by centrifugation at 12,000 RPM and protein concentration was determined using the Bio-Rad protein assay. 50 ug of each lysate was separated by SDS-PAGE and transferred to nitrocellulose. Membranes were blocked in TBST containing 5% skim milk and probed with indicated primary antibodies overnight. Standard chemiluminescence reagents and techniques were used to visualize bound HRP-conjugated secondary antibodies. The following primary antibodies were used (at the indicated dilutions): anti-GFP (Roche, 1:1000 dilution of 0.4mg/ml), anti-

caspase-3 (Cell Signaling, 1:1000), anti-tubulin tyrosine (Sigma, 1:10,000), anti-PARP1 (F2) (Santa Cruz, 1:1000).

Microscopy

RPMI-8226 cells (3 mls of 5x10^5 cells/ml) were seeded into 6-well dishes and grown for 18 hours in standard RPMI-1640 media. Then UPRM8 (8 uM final) or DMSO (0.5% final) was added to individual wells and cells were grown for an additional 8 hours before harvesting. Harvested cells were fixed at -20^{o}C in ice cold methanol for 10 minutes, washed in phosphate buffered saline (PBS), and stained with 1 uM Hoechst 33342 for 15 minutes. Stained cells were washed 3 times in PBS, resuspended in ProLong Gold antifade mounting solution and spotted onto glass microscope slides. Mounted cells were visualized at 400X magnification on a Zeiss Observer Z1 microscope. The fluorescence signal was overlayed on top of brightfield images to allow simultaneous assessment of cellular and nuclear morphologies.

Viability Assays

The viability of RPMI-8226 cells was monitored by measuring ATP using the luminescence-based ATP Lite kit (Perkin Elmer) following the manufacturer's protocol. Briefly, 30,000 RPMI-8226 cells were seeded into individual wells of a 96-well plate and they received the indicated drug treatment for 24 hours, unless otherwise stated. Following the drug treatment period, 100 ul of the ATP Lite reagent was added to each well, plates were subsequently sealed with sealing film and vortexed for 3 minutes. The luminescence produced in each well was then

measured using an Analyst HT microplate reader (Molecular Devices). Individual chemical treatments were done at least in quadruplicate (up to 8 times) and the viability of cells receiving a given treatment was expressed as a percentage of the values obtained for the relevant DMSO negative control treatment.

3.5 Results

3.5.1 An in vivo screen for small molecule modulators of the unfolded protein response

To identify small molecules that modulate the cellular response to ER stress, we performed a cell-based reporter screen in *Saccharomyces cerevisiae,* employing yeast's endogenous UPR machinery to screen for small molecules that modulate the cells response to ER-stressing chemicals (Figure 3.1A). We employed a robust, well-characterized β-galactosidase reporter [52] to monitor UPR activation following exposure of cells to tunicamycin (TM), a highly specific inhibitor of N-linked glycosylation [52]. This UPRE-CYC1-LacZ reporter (hereafter referred to as UPRE::LacZ) was integrated at the URA3 locus of AD1-8, a drug sensitized yeast strain that lacks much of the cellular detoxification machinery [308]. We chose this drug sensitized strain background to minimize false negatives due to active clearance of test compounds by the yeast drug efflux machinery. The resultant screening strain (CML8-1) therefore has a greatly reduced drug efflux capacity and contains a sensitive β-galactosidase reporter under the control of UPRE, allowing a quantitative measure of the

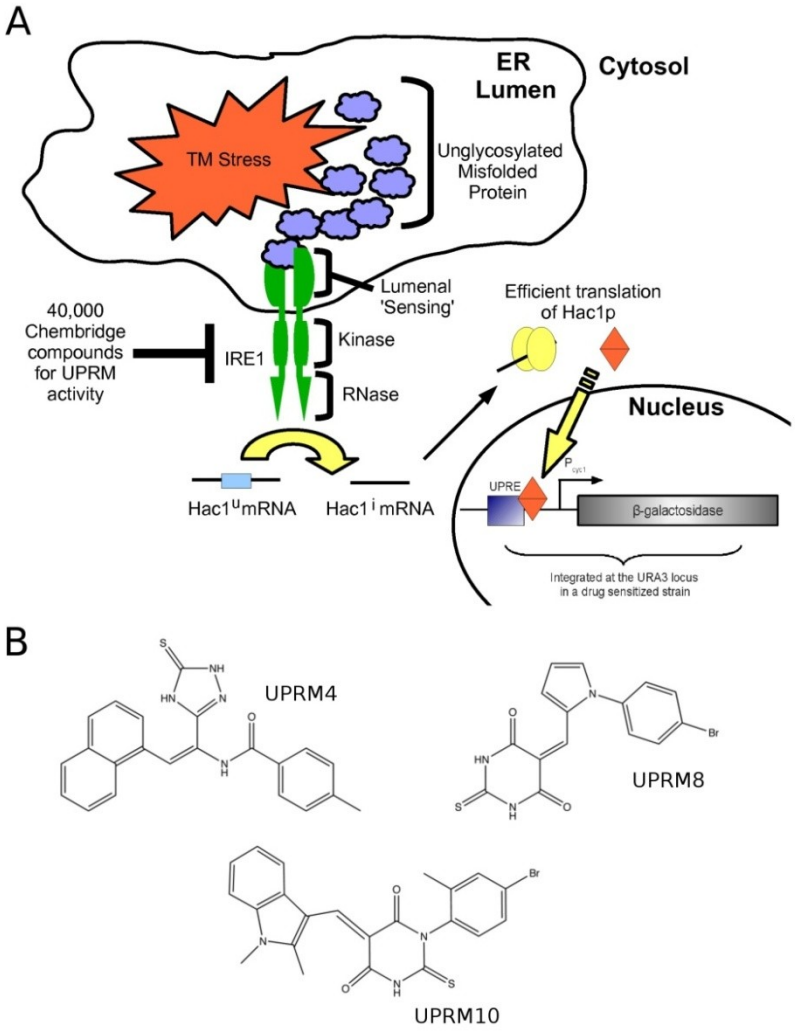

Figure 3.1. A screen to identify small-molecule UPR modulators in *S. cerevisiae*. **(A)** A schematic overview of the highly conserved core UPR found in *S. cerevisiae* and our screening methodology for identifying small-molecule UPRMs. Our CML8-1 yeast strain, which contains an integrated UPRE-regulated β-galactosidase reporter, was exposed to TM stress and UPR activation was monitored following exposure to one of 40,000 compounds from a Chembridge microformats library. β-galactosidase activity in treated CML8-1 cells served as an indirect measure of UPR activation and we selected compounds that impaired UPR reporter activation to less than 50% of the activation found in TM-only treated control cells. Counter screens were employed to remove compounds that were cytotoxic to non-stressed yeast cells and also compounds that were general inhibitors of transcription, translation, and enzymatic activity of the β-galactosidase reporter were also removed. **(B)** The chemical structures the of three lead UPRMs that we selected after employing counter-screening strategies to remove false positives. The IUPAC naming conventions for these UPRMs are as follows: UPRM4 is 4-methyl-N-[2-(1-naphthyl)-1-(5-thioxo-4,5-dihydro-1H-1,2,4-triazol-3-yl) vinyl]benzamide; UPRM8 is 5-([1-(4-bromophenyl)-1H-pyrrol-2-yl]methylene)-2-thioxodihydro-4,6(1H,5H)-pyrimidinedione; UPRM10 is 1-(4-bromo-2-methylphenyl)-5-[(1,2-dimethyl-1H-indol-3-yl)methylene]-2-thioxodihydro-4,6(1H,5H)-pyrimidinedione.

cellular response to ER stress.

The CML8-1 strain was used to screen 40,000 compounds from the Chembridge (San Diego, CA) combinatorial small molecule library for the ability to impair UPR reporter activation following a TM-derived ER stress insult. We anticipated that true positives could result by either inhibiting UPR signaling events or by alleviating the TM-derived stress insult (i.e. improved ERAD efficiency, forward transport of misfolded protein, etc). Given that ER stress impinges on diverse cellular processes and UPR mechanisms have been implicated in tumorigenesis, we surmised that small molecules that fall into either of these two categories would be worth investigating.

From the 40,000 compounds tested, we identified 422 compounds (1.06%) as preliminary hits, based on their ability to diminish UPR reporter activation to less than 50% of the maximal signal we observed in TM-alone positive control wells. We subsequently employed counter-screening strategies to remove compounds that were cytotoxic to yeast cells and then subjected the remaining non-toxic compounds to duplicate retesting in our screen assay. After these counter-screening strategies were employed we selected three compounds, designated UPRM4 (UPR modulator 4), UPRM8 and UPRM10, as modulators of TM-induced UPR in *S. cerevisiae*. Next, we confirmed that these UPRMs are not general inhibitors of transcription or translation and that they are not directly impairing β-galactosidase enzyme function by testing their effect on a galactose-inducible β-gal reporter (Supplementary Figure 3.1). Given the observed specificity of these UPRMs for impairing UPRE::LacZ reporter induction and not

Gal1::LacZ induction, we concluded that these compounds can modulate yeasts response to TM-induced ER stress. The chemical structures of our three candidate UPRMs are presented in Figure 3.1B, and it is interesting to note that both UPRM8 and UPRM10 share a central pyrimidinedione ring structure.

3.5.2 UPRMs 4, 8 and 10 prevent tunicamycin-induced splicing of Hac1 mRNA in vivo

We sought to confirm the results of our UPR reporter assay by investigating the ER stress-dependent splicing of Hac1 mRNA *in vivo,* a more direct measure of UPR activation. We treated cells with TM (2 ug/ml) to induce a robust UPR, both in the presence and absence of UPRMs 4, 8 and 10. Following a 6-hour co-treatment period, cells were harvested and total RNA was extracted, mRNA was purified and used as a template for RT-PCR amplification of Hac1. As expected, TM treatment resulted in a shift of the unspliced Hac1 RT-PCR product ($Hac1^{u}$) found in untreated control cells to a faster-migrating RT-PCR product that represents spliced Hac1 ($Hac1^{i}$) in the TM-stressed cells (Figure 3.2A). A dose-dependent decrease in Hac1 splicing was observed when UPRMs were present during the TM exposure (Figure 3.2A). UPRM8 and UPRM10 appeared to be more potent inhibitors of Hac1 mRNA splicing than UPRM4, and the former two compounds showed nearly complete inhibition of splicing at the highest tested dosage of these UPRMs (50 uM). These Hac1 splicing results are consistent with the results of the UPR reporter assay and confirm that UPRMs 4,

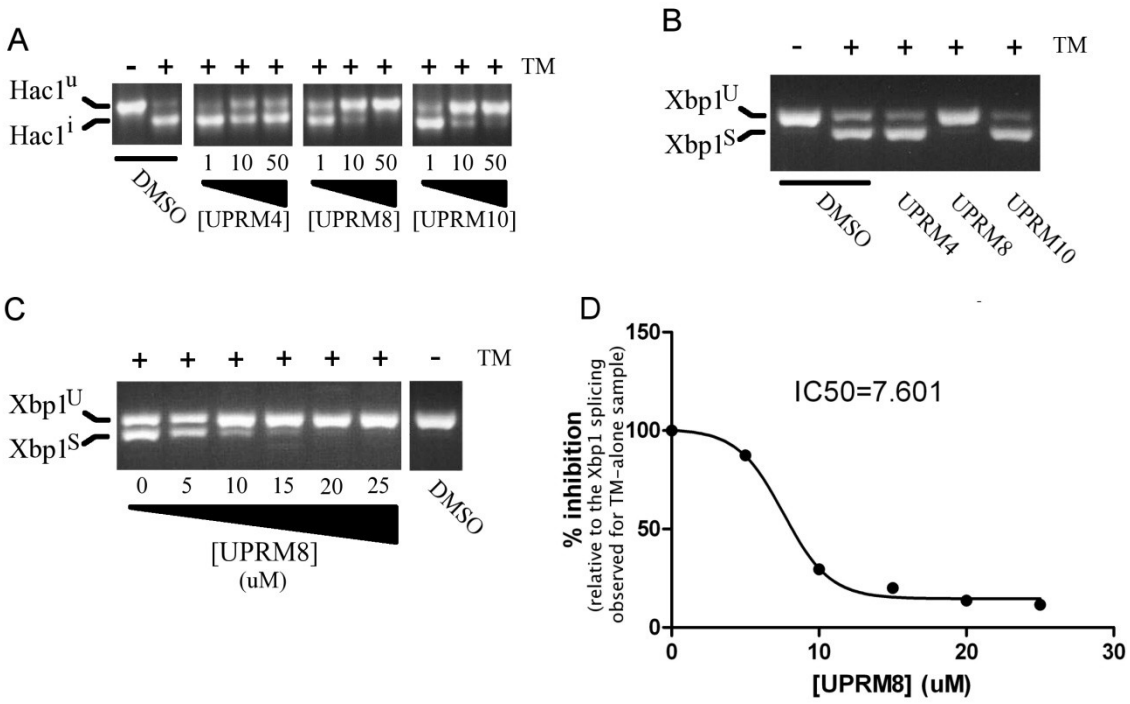

Figure 3.2. UPRM8 inhibits Hac1 and Xbp1 splicing *in vivo.* **(A)** The effect of our candidate UPRMs on Ire1p-dependent Hac1 mRNA splicing was monitored by RT-PCR. The left-most panel contains both negative (no TM exposure) and positive (TM alone treatment) controls to show the expected sizes of the $Hac1^{u}$ and $Hac1^{i}$, respectively. Three concentrations (1, 10, and 50 uM) of each UPRM were tested here for the ability to impair this TM-induced splicing event. **(B)** Semi-quantitative RT-PCR of Xbp1 mRNA was used to monitor the effects of UPRMs in TM-stressed HeLa cells. DMSO vehicle control treated cells were tested in both the absence and presence of TM stress (5 ug/ml) to indicate the expected sizes of $Xbp1^{U}$ and $Xbp1^{S}$ RT-PCR products, respectively. We chose to test a high dose (50 uM) of each of our lead UPRMs in this assay to increase the chance to observing an effect on Xbp1 splicing. **(C)** A dose response of UPRM8-mediated inhibition of Xbp1 splicing as monitored by RT-PCR amplification of Xbp1 mRNA from treated HeLa cells. Doses ranging from 0 to 25 uM of UPRM8 were tested for the ability to impair Xbp1 splicing in response to TM stress (5 ug/ml). The right panel indicates the size of $Xbp1^{U}$ (no TM exposure) and the left-most lane was from cells receiving no UPRM8 (0 uM), which indicates the amount of $Xbp1^{S}$ that was produced by an unmitigated TM insult. **(D)** Densitometry analysis of the Xbp1 splicing RT-PCR products from C allowed us to plot the dose response of the inhibtion of Xbp1 splicing by UPRM8 in TM-stressed HeLa cells.

8, and 10 display a significant capacity to alter the cells response to TM-derived ER stress.

3.5.3 UPRM8 also inhibits TM-induced splicing of Xbp1 in mammalian cells

To determine whether these UPRMs retained their UPR modulating activities in human cells, we used RT-PCR to monitor the Ire1-dependant splicing of Xbp1 mRNA in TM-stressed HeLa cells (Figure 3.2B). As expected, the DMSO treated vehicle control samples show unspliced Xbp1 mRNA in unstressed HeLa cells and TM exposure (5ug/ml) of these DMSO control treated cells produced a shift to the spliced $Xbp1^{s}$ mRNA species. Importantly, cotreatment of TM-stressed HeLa cells with each of our three lead UPRMs clearly indicated that UPRM8, but not UPRMs 4 or 10, is capable of impairing TM-induced Xbp1 splicing. This result implies that the biological activity of UPRM8, specifically the impairment Ire1-dependant UPR signaling events, is conserved from yeast to mammalian cells.

To evaluate the potency of UPRM8 in HeLa cells we conducted a dose response experiment in cells that had been cotreated with a constant amount of TM (5 ug/ml) and increasing doses of UPRM8. After this cotreatment period we again monitored the amount of spliced Xbp1 mRNA by RT-PCR (Figure 3.2C). The results clearly show reduced Xbp1 splicing with increasing doses of UPRM8. Next we used densitometry analysis of these Xbp1 mRNA species to determine the % inhibition of TM-induced Xbp1 mRNA splicing and the results indicate that the IC_{50} of UPRM8 in TM-stressed HeLa cells is 7.6 uM (Figure 3.2D). The

observed IC_{50} for UPRM8 in these TM-stressed HeLa cells is quite similar to the IC_{50} of approximately 10 uM that we observed in TM-stressed CML8-1 yeast cells, as monitored by inhibition of the UPRE::LacZ transcriptional reporter (Supplementary Figure 3.2). When taken together these results indicate that UPRM8 is a low micromolar inhibitor of Ire1-dependent UPRs in both yeast and mammalian cells.

Given that the activity of UPRM8 seems to be conserved in higher eukaryotes, we chose to focus our subsequent investigative efforts on this compound. Despite narrowing the focus of this study to UPRM8, we expect that UPRMs 4 and 10 may still serve as useful chemical probes for studying ER homeostatic responses in yeast. Furthermore, elucidation of the mechanism of action of these two yeast-specific UPRMs may uncover heretofore unappreciated differences between the Ire1 pathways of yeast and mammalian cells.

3.5.4 UPRM8 interferes with the ribonuclease activity of Ire1 but leaves its kinase activity intact

Given the pyrimidinedione-based structure of UPRM8, we wondered if this small molecule might interfere with Ire1-dependent splicing of either Hac1 or Xbp1 by interfering with the kinase activity of Ire1p. To test this possibility, we employed a full length GST-Ire1p clone from a previously characterized galactose-inducible yeast GST-kinase fusion library [272]. We purified this GST-Ire1p fusion from yeast under galactose-inducing conditions, an over-expression that is known to produce artificial activation of Ire1p in the absence of exogenous

ER stress [147, 155]. This yeast GST-Ire1p fusion displayed robust phosphorylation of a myelin basic protein (MBP) test substrate in a standard

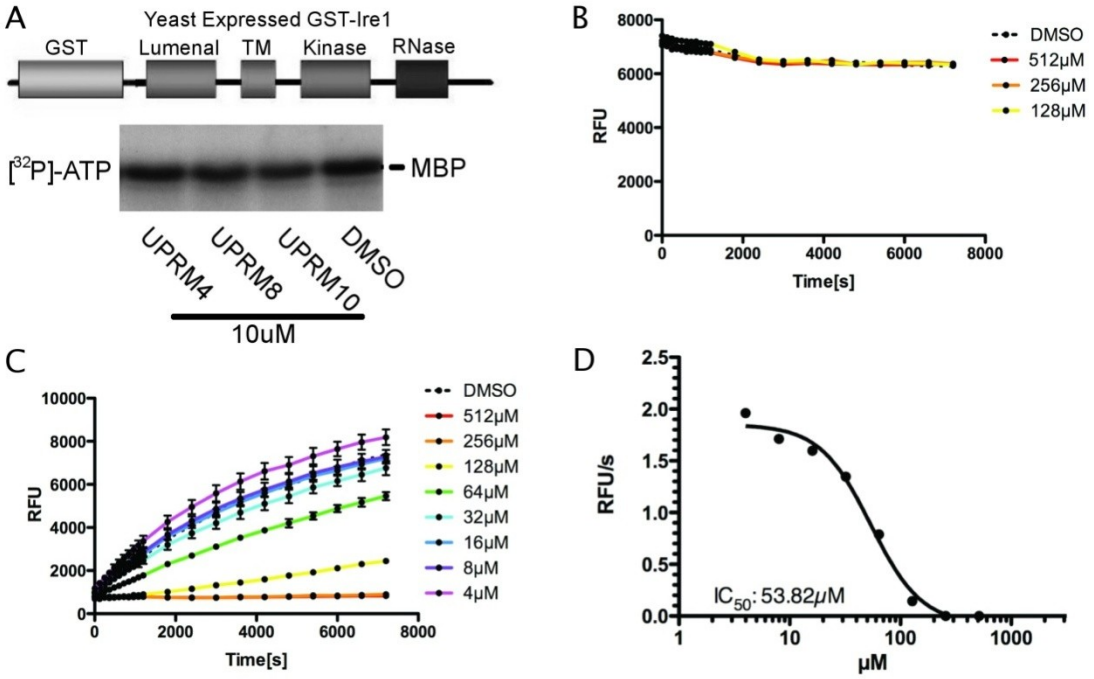

Figure 3.3. UPRM8 inhibits the *in vitro* RNase activity of Ire1. **(A)** A full-length GST-Ire1p fusion protein was purified from *S. cerevisiae* and tested in an *in vitro* [γ-^{32}P] ATP kinase assay with myelin basic protein (MBP) serving as the phosphoacceptor substrate. The presence of 10 uM of UPRMs 4, 8, or 10 had no apparent effect on the kinase activity of this purified GST-Ire1p, when compared to the DMSO-treated (0.2%) control reaction. **(B)** We monitored the effect of UPRM8 on the fluorescence produced by the 5' AF647 in our synthetic RNA probe following its liberation from the 3'BHQ by pre-incubation with RNaseA. Relative fluorescence units (RFU) were plotted as a function of time following the addition of the indicated doses of UPRM8 or a DMSO vehicle control. **(C)** Increasing doses of UPRM8 were used to inhibit the *in vitro* ribonuclease activity of a purified *s.c.*Ire1^{CYTO} construct. A DMSO-treated sample served as a negative vehicle control for ribonuclease inhibition in this assay. Error bars represent one standard deviation from the plotted means. **(D)** A dose response curve for UPRM8-mediated inhibition of the *in vitro* ribonuclease activity of Ire1 was generated by plotting the initial rates (in RFU/second) of the reactions presented in (C) against the dose of UPRM8 tested. The IC_{50} for UPRM8-mediated inhibition of Ire1's *in vitro* ribonuclease activity was determined from this plot.

[γ-^{32}P]-ATP *in vitro* kinase assay (Figure 3.3A). Importantly, this robust phosphorylation of MBP was not affected by treatment with 10 uM of UPRMs 4, 8 or 10, when compared to the DMSO control treated sample (Figure 3.3A). Of note, this yeast-purified GST-Ire1 did not display strong autophosphorylation in this assay; however, this lack of autophosphorylation is likely attributable to prior occupancy of the autophosphorylation sites of Ire1, given that it was purified from yeast under activating conditions. We also tested our UPRMs for the ability to interfere with the autophosphorylation of a recombinant GST-Ire1 cytoplasmic domain fusion that was purified from *E. coli* and we obtained similar negative results (Supplementary Fig 3.3). Since none of our UPRMs appear to inhibit the kinase activity of Ire1p *in vitro,* we conclude that these small-molecules are not achieving their UPRM activities by impairing Ire1 kinase function.

Since UPRM8 had no observable effect on the kinase activity of Ire1, we next wished to see if UPRM8 could be preventing TM-induced splicing of either Hac1 or Xbp1 mRNA by directly impairing the ribonuclease function of Ire1. To test this hypothesis we chose a recently described *in vitro* ribonuclease assay that uses fluorescence to monitor the cleavage of a synthetic RNA stem-loop substrate by a recombinant yeast Ire1 cytoplasmic domain (*s.c.*Ire1^{CYTO}) [149]. This synthetic RNA stem-loop contains the Xbp1 recognition sequence in its loop region and its destabilized stem facilitates dissociation of the 5' AlexaFluor 647 (AF647) fluorophore from the 3' Black Hole Quencher 3 (BHQ) following ribonuclease cleavage. The use of this fluorescence-based RNase cleavage assay requires that we rule out any ability of UPRM8 to quench the fluorescence produced by the liberated AF647 fluorophore. Even at concentrations as high as

512 uM, UPRM8 showed no ability to quench the fluorescence produced by AF647 when this synthetic RNA substrate was cleaved by a pre-incubation with RNase A (Figure 3.3B). This result shows that UPRM8 is not able to quench the fluorescence produced by AF647 when it is liberated from the 3' BHQ by a ribonuclease activity. Therefore any effect we observe for UPRM8 on Ire1-mediated cleavage of this fluorescent probe must reflect a specific impairment of ribonuclease activity.

To examine the effect of UPRM8 on the ribonuclease activity of Ire1, increasing doses of UPRM8 were incubated with the purified $Ire1^{CYTO}$ protein in the presence of our synthetic RNase substrate (Figure 3.3C). A clear dose-dependent inhibition of the ribonuclease activity of *s.c.*$Ire1^{CYTO}$ was observed with UPRM8 treatment. This result suggests that UPRM8 impairs the ribonuclease activity of Ire1, which explains the inhibition of TM-induced splicing of both Hac1 and Xbp1 mRNAs that we observed in UPRM8-treated yeast and human cells, respectively.

When the initial rates (RFU/s) of the ribonuclease assay results from Figure 3.3C were plotted against the concentration of UPRM8 tested, the resultant dose response curve suggested that the IC_{50} of UPRM8 in this *in vitro* RNase assay was 53.82 uM (Figure 3.3D). This *in vitro* IC_{50} is significantly higher than the IC_{50} we observed for the inhibition of Xbp1 or Hac1 splicing *in vivo*. This difference may result from the propensity of UPRM8 to concentrate in the vicinity of Ire1 on the surface of ER membranes or perhaps cells are able to modify UPRM8 in a way that can improve its potency. Alternatively, the 1 mM dithiothreitol (DTT) that was required in the RNase assay to observe a robust

ribonuclease activity might cause some degree of UPRM8 inactivation. Our reason for believing that inactivation of UPRM8 occurs in the presence of DTT is because we observed a reduction in UPRM activity and the formation of chemical adducts when UPRM8 was exposed to 2-mercaptoethanol, another sulfhydryl-containing reducing reagent (data not shown). Regardless of the differences in these observed IC_{50} values, our *in vitro* and *in vivo* data suggests that UPRM8 can impair the ribonuclease activity of Ire1 and thereby prevent the splicing of Hac1 or Xbp1 mRNAs in yeast and human cells, respectively.

3.5.5 UPRM8 induces apoptosis in cultured multiple myeloma cells

Given its ability to inhibit the Ire1-dependent UPR pathway, we wanted to see whether UPRM8 could impact the growth of multiple myeloma (MM) cells because these cancer cells are reliant on ER homeostatic mechanisms for their continued survival. To determine whether UPRM8 treatment could impact MM cell growth *in vitro,* we cultured RPMI-8226 MM cells in standard growth medium and subjected them to increasing doses of UPRM8. After 24 hours of UPRM8 treatment, we estimated the number of viable cells remaining in each well by measuring the ATP content of wells and relating these values to those obtained in DMSO-treated negative control wells (% Viability relative to DMSO) (Figure 3.4A). The results clearly showed decreased MM cell viability with increasing doses of UPRM8. From this assay, we estimated the IC_{50} for UPRM8 to be approximately 5uM, which is quite similar to the IC_{50} of 7.6 uM that we observed for UPRM8's inhibition of Xbp1 splicing in TM stressed HeLa cells.

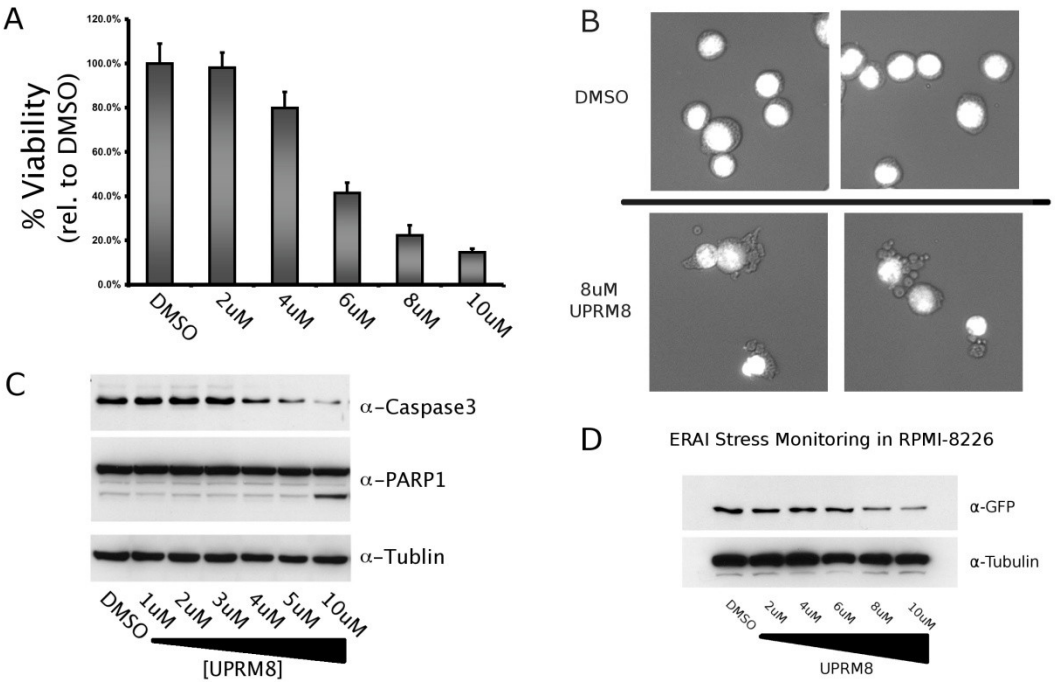

Figure 3.4. UPRM8 induces apoptosis in RPMI-8226 cells. **(A)** The viability of RPMI-8226 MM cells was monitored by measuring ATP following a 24-hour exposure to DMSO (0.5%) or the indicated doses of UPRM8. **(B)** RPMI-8226 cells were treated with DMSO (0.5%) or UPRM8 (8uM) for 8 hours, fixed, and then stained with Hoechst 33342. Shown here is are Hoeschst 3342 fluorescent signal (white) overlaid on brightfield images to allow simultaneous assessment of both nuclear and cellular morphologies. **(C)** Western blotting of lysates from RPMI-8226 cells that were treated for 6 hours with DMSO (0.5%) or the indicated doses of UPRM8. Cleavage of Caspase 3 (top panel) and poly [ADP-ribose] polymerase 1 (PARP1; middle panel) indicates that UPRM8-treated RPMI-8226 cells displayed hallmark proteolytic events associated with an apoptotic cell death. An anti-tubulin western blot (lowest panel) was used to ensure equal loading of cell lysates. **(D)** RPMI-8226 cells were transiently transfected with an Xbp1-venus reporter (F-Xbp1ΔDBD-venus) and cells were grown for 24-hours before being exposed for 4 hours to DMSO (0.5%) or the indicated dose of UPRM8. Following this treatment period we monitored the splicing of the Xbp1-venus reporter by western blotting with anti-GFP antibodies (upper panel). An anti-tubulin blot was used to ensure equal loading of these cell lysates (lower panel).

We next wondered if the observed decrease in cell viability in UPRM8-treated RPMI-8226 MM cells was due to apoptosis. We treated RPMI-8226 cells with either DMSO or 8 uM UPRM8 for 8 hours and stained the nuclei of cells using Hoechst 33342 following a short methanol fixation. UPRM8-treated cells displayed morphologies consistent with apoptotic cell death, including cellular blebbing, apoptotic bodies, and nuclear condensation (Figure 3.4B). This is in marked contrast to DMSO-treated control cells, which retained their normal cell and nuclear morphologies. This result suggests that UPRM8 reduces MM cell viability by inducing apoptosis in these cultured RPMI-8226 cells.

To confirm the apoptotic cell death phenotype induced by UPRM8, we employed western blotting to examine the cleavage of caspase 3 and poly [ADP-ribose] polymerase 1 (PARP1), hallmarks of apoptosis. After a short 6-hour treatment period, we observed increased cleavage of caspase 3 with increasing doses of UPRM8 (Figure 3.4C). Some cleavage of caspase 3 was evident with doses as low as 4 uM UPRM8 and nearly complete cleavage of caspase 3 is evident in the 10 uM UPRM8 treatment sample. Cleavage of PARP1 was observed in response to the highest (10 uM) UPRM8 treatment but was not observed in the DMSO control treated sample or with any of the lower doses of UPRM8. These results suggest that UPRM8 shows a significant capacity to induce apoptosis in cultured MM cells and does so at similar doses to those required to inhibit XBP1 splicing in TM-stressed HeLa cells. Importantly, we observed no significant UPRM8 cytotoxicity in unstressed HEK293 cells at these same low micromolar dosages (Supplementary Figure 3.4). This result suggests that the capacity of UPRM8 to induce apoptosis in cultured MM cells likely stems

from the reliance of these cancer cells on the Ire1 UPR pathway for survival. The capacity of UPRM8 to selectively kill ER stressed MM cancer cells, while leaving healthy non-stressed cells intact, begs for further evaluation of the therapeutic potential of novel UPRMs in treating cancers that rely on ER homeostatic mechanisms for their continued survival.

To confirm that the apoptotic cell death we initiated in UPRM8-treated MM cells was associated with impaired Ire1-dependent UPR activation, we monitored the splicing of an Xbp1-venus fusion construct that has been used previously to monitor ER stress both *in vitro* and *in vivo* [53]. This Xbp1-venus fusion can be detected in cells by GFP western blotting only after Ire1-dependent splicing of the 26-nucleotide Xbp1 intron places the C-terminal venus moiety in the correct translational reading frame. We transiently transfected RPMI-8226 MM cells with this Xbp1-venus reporter and then subjected these transfected cells to increasing doses of UPRM8 (Figure 3.4D). GFP western blotting confirmed that DMSO vehicle control treated RPMI-8226 MM cells displayed moderate levels of basal Ire1-dependent Xbp1 splicing. Increasing doses of UPRM8 resulted in reduced expression of this Xbp1-venus reporter, which suggests that UPRM8 is indeed impairing Xbp1 splicing in these constitutively stressed MM cells. Anti-tubulin western blotting was used to confirm equal loading of cell lysates (Figure 3.4D; lower panel). Also, since tubulin protein levels remained unchanged with UPRM8 exposure, we feel that this provides further evidence that indicates that UPRM8 is not generally impairing protein synthesis.

Importantly, the low micromolar doses of UPRM8 that was required to observe impaired Xbp1-venus reporter splicing after 4 hours of treatment were the

same doses that showed a strong apoptotic phenotype after 8 hours of UPRM8 exposure. When taken together, these results strongly suggest that UPRM8 causes a reduction in the output of the Ire1/Xbp1 UPR pathway in RPMI-8226 MM cells and that this impairment of UPR mechanisms ultimately leads to an apoptotic cell death phenotype in these MM cells.

3.5.6 Combining UPRM8 with ER stressors or salubrinal results in more potent anti-MM activities

Given that UPRM8 appears to selectively kill MM cells by impairing Ire1-dependent UPR signaling, we wondered if supplementing the constitutive ER stress found in these cancerous plasma cells would improve the MM cytotoxicity observed following UPRM8 treatment. We first tested this hypothesis by treating RPMI-8226 cells with 2-deoxy-D-glucose (2-DG), a glucose analog that produces ER stress by interfering with N-linked glycosylation [310, 311]. Not surprisingly, 2-DG reduced the viability of MM cells and did so presumably by increasing the amount of unfolded protein in the ER of these already constitutively stressed plasma cells (Figure 3.5A). When 2-DG exposure was combined with UPRM8 treatment, the viability of RPMI-8226 cells was reduced even further than the 2-DG alone or UPRM8 alone control treatments. This result reinforces the idea that MM cancer cells are sensitive to chemical insults that produce ER stress and that UPRM8 can be used to maximize the MM cell death that results from exposure to such ER stress agents.

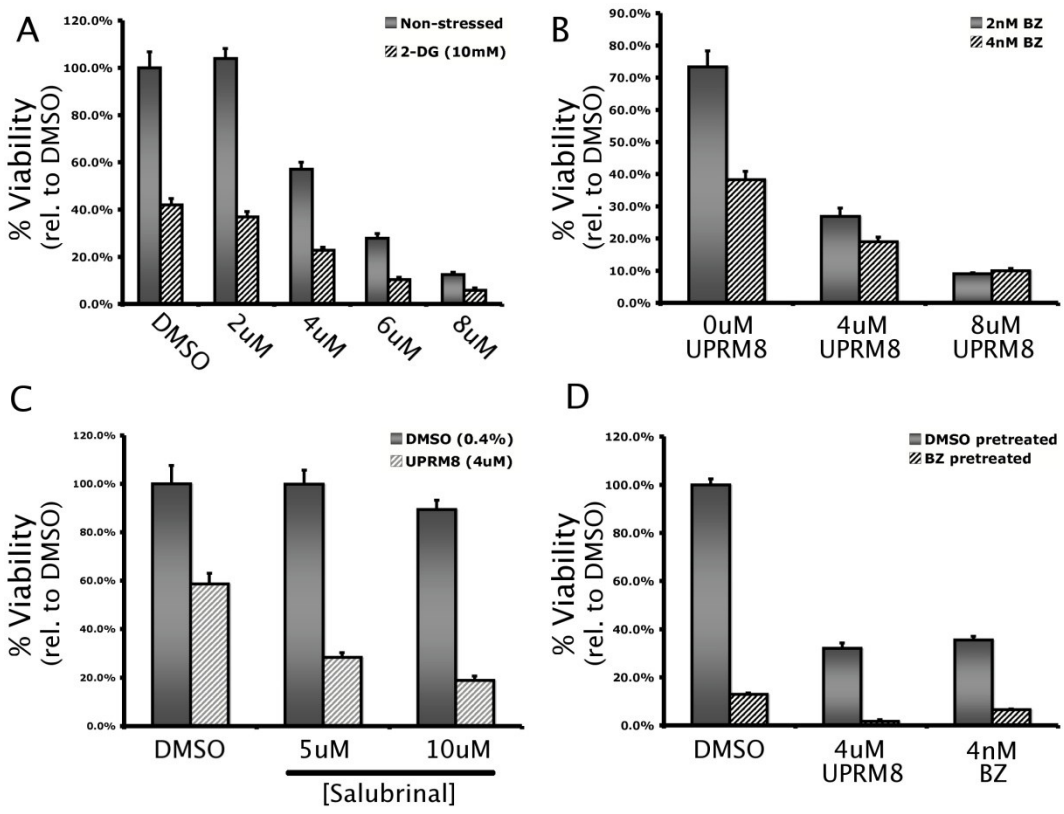

Figure 3.5. UPRM8 improves the MM cytotoxicity of ER stressors and salubrinal. **(A)** The viability of RPMI-8226 MM cells was monitored following a 24-hour treatment period with increasing doses of UPRM8 alone (unstressed; solid bars) or when combined with a 2-DG-induced ER stress insult (10 mM; hashed bars). **(B)** The effects of bortezomib-induced proteasomal inhibition (2 or 4 nM BZ), either alone or in combination with UPRM8 exposure (4 or 8 uM), on the viability of RPMI-8226 cells was examined after 24 hours of treatment. **(C)** The ability of salubrinal, an eIF2α-phosphatase inhibitor, to potentiate the cytotoxic effects of UPRM8 on RPMI-8226 MM cells was examined after a 24-hour treatment period. **(D)** The benefit of supplementing proteasomal inhibitor therapies with UPRM8 was assessed *in vitro* by monitoring the viability of RPMI-8226 cells following a sequential treatment regime. Cells were preconditioned for 48 hours in either DMSO or 4 nM bortezomib and then received one of three secondary treatments (DMSO, 4 uM UPRM8, 4 nM bortezomib) for 24 hours. Following the secondary treatments, viability was assessed by measuring ATP and plotted as a % of the viability observed for cells that received sequential DMSO negative control treatments.

To further reinforce our hypothesis that UPRM8 can be used to improve the potency and efficacy of anti-MM agents that cause ER stress-dependent apoptosis, we decided to test if UPRM8 could improve the MM cytotoxicity of bortezomib (Figure 3.5B). As anticipated, this clinically-approved, proteasomal inhibitor significantly reduced the viability of cultured RPMI-8226 MM cells at either 2 or 4 nM; however, when these same doses of bortezomib were combined with either 4 or 8 uM of UPRM8, we observed markedly improved MM cytotoxicity when compared to either single treatment alone. This result supports our 2-DG experimental results and confirms that UPRM8 can be used to maximize the cytotoxicity of chemical agents that exacerbate ER stress in cultured MM cells.

Salubrinal is a small molecule that was identified based on its ability to protect cells from ER stress-induced apoptosis by inhibiting eIF2α-phosphatases, including GADD34-PP1C, and this activity promotes survival by maintaining high levels of phosphorylated eIF2α [312]. More recently, salubrinal was shown to help eradicate the quiescent MM cells (G_0-G_1 arrested) that survive proteasomal inhibitor therapies [313]. The inhibition of eIF2α-phosphatases by salubrinal prevented the surviving quiescent cells from attenuating eIF2 phosphorylation, which appears to be how bortezomib-resistant cells evade the pro-apoptotic activities that ensue following CHOP induction [313]. We next wondered if cotreating cells with salubrinal could similarly potentiate UPRM8-mediated MM cytotoxicity by artificially maintaining high levels of

phosphorylated eIF2α. We again monitored the viability of RPMI-8226 cells by measuring ATP in wells of cells that were treated with DMSO or 4uM UPRM8 alone or in combination with either a 5uM or 10uM dose of salubrinal (Figure 3.5C). The addition of 5 uM salubrinal to DMSO vehicle control treated MM cells had no significant effect on MM cell viability and even the 10 uM dose of salubrinal produced only a 10% reduction in MM cell viability; however, a markedly more potent UPRM8-mediated MM cytotoxicity was observed when cells were cotreated with 4uM UPRM8 and either 5uM or 10uM salubrinal (Figure 3.5C). This result suggests that maintaining high levels eIF2α phosphorylation levels, achieved here by salubrinal exposure, can significantly potentiate the anti-MM activity of UPRM8. We feel this potentiation of the anti-MM activities of UPRM8 by salubrinal further supports our hypothesis that UPRM8 produces an ER stress-related apoptotic cell death in MM cells due to its impairment of the cytoprotective activities of the Ire1/Xbp1 UPR.

We wished to further investigate the value of using UPRM8 to maximize the anti-MM activities of bortezomib. We surmised that the value of such a combination treatment should be considered by comparing its anti-MM effects to a constitutive bortezomib-only treatment regime. To this end, we created two populations of preconditioned RPMI-8226 MM cells; one of these populations had been pretreated with DMSO (0.4%) to serve as naive control cells and the other population had been pretreated with bortezomib (4 nM). Following this 48-hour preconditioning treatment, the cells from both pretreatments were washed with fresh media and then subjected to secondary treatments of DMSO (0.4%), UPRM8 (4 uM), and bortezomib (4 nM) for 24 hours. After this secondary

treatment period we again monitored MM cell viability by measuring ATP in the various treatment wells (Figure 3.5D). The viability of MM cells for this experiment were plotted as a % of the viability observed for cells that received successive DMSO (0.4%) control treatments. Not surprisingly, cells that were preconditioned using the 4 nM bortezomib treatment showed markedly reduced viability compared to DMSO-preconditioned cells, regardless of the secondary treatment they received. Also as expected, the viability of naive DMSO-pretreated cells was reduced when secondary treatments included either UPRM8 (4 uM) or bortezomib (4 nM). Importantly, we observed the most pronounced reduction in MM cell viability when bortezomib pretreatment (4 nM) was followed by UPRM8 exposure (4uM) during the secondary treatment phase. The MM cytotoxicity produced by this sequential bortezomib + UPRM8 treatment was superior to that which we observed for sequential bortezomib (4 nM) treatments. These results suggest that UPRM8-mediated impairment of the Ire1/Xbp1 UPR that follows bortezomib exposure can be used to improve, at least *in vitro*, the efficacy of proteasomal inhibitor therapies for killing multiple myeloma cancer cells.

3.5.7 Structure-activity-relationship screening identifies UPRM8-like molecules with even more potent anti-MM activities

A search for molecules similar to UPRM8 using the National Center for Biotechnology Information (NCBI) Pubchem database (UPRM8 ID=1348638) revealed that 92 similar compounds have previously entered into this database.

We selected 20 of these 92 compounds based on their similarity to UPRM8 and on the availability to purchase pre-synthesized compounds from a commercial supplier. The chemical structures of these 20 UPRM8-like small molecules are presented (Figure 3.6A) and we gave these compounds a simple numerical designation, analogs 1 through 20. Each of these small molecules contains a pyrimidinedione- or pryrimidinetrione-based ring structure and several of these analogs are nearly identical to UPRM8. For example analogs 14 and 15 are identical to UPRM8 except that the 4-bromophenyl ring of UPRM8 is replaced by a 4-fluorophenyl ring and a 4-iodophenyl ring in 14 and 15, respectively.

We next tested which, if any, of these 20 small molecules shares the capacity of UPRM8 to induce apoptosis in cultured RPMI-8226 MM cells. As before, we used the ATP-based cell viability assay and again normalized the observed viabilities for each of these 4 uM treatments to that of the DMSO negative control treatment (Figure 3.6B). A 6 uM dose of UPRM8 served as the positive control treatment for the induction of apoptosis in these RPMI-8226 MM cells. Analogs 5, 7, 11, 13, 14, 15, 16, and 17 at this 4 uM dose showed a reduction in viability equal to, or greater than, that which we observed in the UPRM8-treated (6 uM) positive control. This result indicates that we have successfully identified numerous additional small molecules that are similar to UPRM8 in structure and that display *in vitro* anti-MM activities with potencies equal to or greater than that of UPRM8.

From this relatively small structure-activity-relationship screen we can already begin to identify some of the important features of the pharmacophore

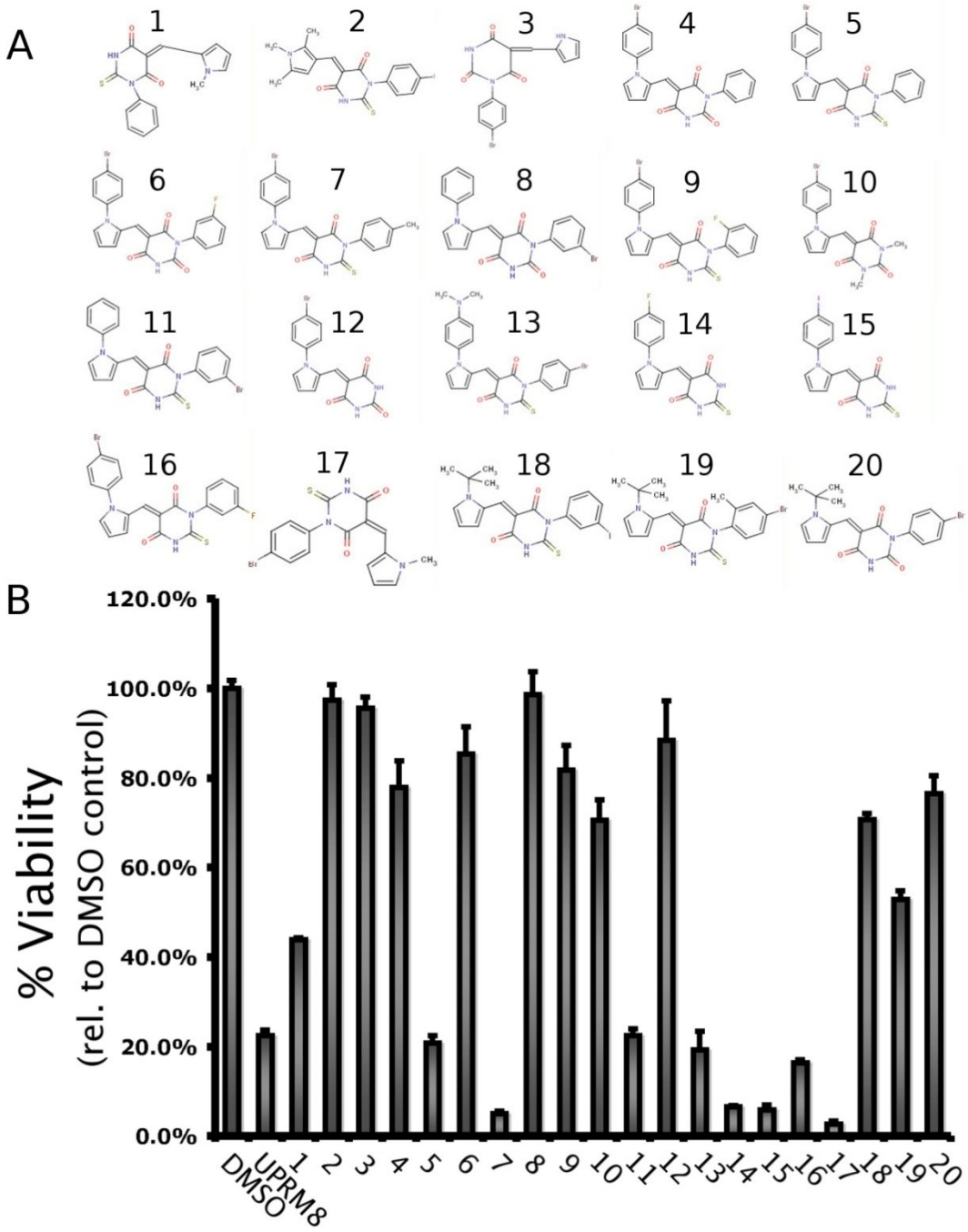

Figure 3.6. An evaluation of the anti-MM properties of UPRM8 analogs. **(A)** The chemical structures of 20 different UPRM8-like compounds are presented. (**B)** The viability of RPMI-8226 MM cells was monitored following a 24-hour treatment period 4 uM doses of each of the 20 UPRM8-like compounds that are represented in (A). Viabilities were normalized to the DMSO negative control and a 6 uM treatment with UPRM8 positive control treatment is shown for comparison purposes.

of UPRM8 by looking at the analogs that are severely compromised in their ability to reduce the viability of MM cells. For example, analogs 4 and 5 are identical except that the central ring of 4 is a pyrimidinetrione, whereas the central ring of 5 is a thioxodihydro-substituted pyrimidinedione, just like UPRM8. Given that analog 4 displayed a significantly reduced anti-MM activity compared to analog 5 and UPRM8, it seems that the 2-thioxodihydro-substitution of the pyrimidinedione ring is important for the anti-MM activities of UPRM8-like small molecules.

Analogs 5, 7, 11, 13, 16 and 17 all contain bulky phenyl substitutions at the same (1-nitrogen) position of their respective pyrimidinedione rings compared to UPRM8, which lacks a substitution at that position. Given that 5, 7, 11, 13, 16 and 17 all show anti-MM potencies equal to or greater than UPRM8, we can conclude that the pharmacophore can tolerate, and perhaps can even be improved by, bulky substitutions at the 1-N position of its pyrimidinedione ring. This structure-activity-relationship screen was informative and should be expanded upon in future studies in order to identify small molecules with even more potent anti-MM properties. Analog 17 displayed the most potent anti-MM activity and so we feel that this compound will provide a good starting point for future structure-activity-relationship screens to expand our current understanding of the important features of this UPRM8-like pharmacophore.

3.6 Discussion

We have reported here the discovery of UPRM8, a pyrimidinedione that impairs Ire1-dependent UPR signaling in both yeast and mammalian cells. We conducted a high-throughput screen for novel UPRMs in yeast because it contains a simplified, yet highly conserved, core UPR machinery. Given that the Ire1 pathway is the most ancient and conserved UPR pathway found in eukaryotes, we correctly anticipated that it would be possible to isolate UPRMs from a yeast screen that would retain their biological activity in other metazoan cell types. However, we did isolate two yeast-specific UPRMs (UPRM4, UPRM10) in our chemical screen and we hope that these compounds may provide useful tools in the future to study yeast ER homeostatic mechanisms.

The use of pyrimidinedione-based small molecules to modulate biological function is well established; for instance, 5-fluorouracil (5-FU) was synthesized more than 4 decades ago [314] and prodrugs of 5-FU are still employed as anticancer agents today [315, 316]. Various pyrimidinediones have also been reported to have the following biological activities: to inhibit viral entry and reverse transcription of the human immunodeficiency virus [317, 318]; to inhibit riboflavin biosynthesis [319-321]; and to antagonize certain subtypes of α1-adrenoceptors [322, 323]. The pyrimidinedione structure of UPRM8 is reminiscent of a nucleoside and so we wondered if it could possess some nucleoside-mimetic capacity that might explain its UPRM activity. Small-molecule inhibitors of other ribonucleases, such as pancreatic ribonuclease A, have been reported previously and these include the following nucleoside-based

inhibitors: vanadyl-ribonucleoside complexes (VRC) [324]; both 2'-5' and 3'-5'diribonucleoside monophosphates [325]; and 5'-diphosphoadenosine 3'-phosphate [326]. Therefore, we feel there is good scientific precedent to expect that a nucleoside-like pyrimidinedione may possess some capacity to impair the ribonuclease activity of Ire1.

We monitored Xbp1 and Hac1 splicing in TM-stressed human and yeast cells, respectively, to show that UPRM8 impairs Ire1-dependent signaling mechanisms *in vivo*. We furthered this claim by using a fluorescence-based *in vitro* ribonuclease assay to show that UPRM8 can directly inhibit Ire1-dependent splicing of a synthetic RNA substrate. This capacity to directly impair the ribonuclease activity of Ire1 would account for UPRM8-mediated impairment of Xbp1- and Hac1- splicing *in vivo*. Importantly, *in vitro* kinase assays were used to rule out modulation of the kinase function of Ire1 as a potential mechanism for the biological activities of UPRM8. We did not explicitly test to see if UPRM8 can inhibit other ribonucleases, like RNase A or RNase P; however, we felt that UPRM8's lack of cytotoxicity in yeast cells, even at very high doses (i.e. 200 uM), strongly suggests that the capacity of UPRM8 to impair ribonuclease function must be selective for Ire1 because other cellular RNase activities are essential for yeast viability. For example, the biochemical activities of numerous gene products that are common to both RNase P and RNase MRP complexes are essential for yeast viability [327-330]. A precise mechanistic understanding of how UPRM8 specifically impairs the ribonuclease activity of Ire1, while leaving other important cellular RNase activities intact, will require structural studies to ascertain how UPRM8 fits into the previously described catalytic structure of Ire1

[148]. If such a structure-based mechanism can be ascertained for UPRM8, we feel that this information could prove invaluable for guiding future medicinal chemistry efforts to identify new UPRMs that show improved potency and solubility.

The use of chemical agents to perturb oxidative protein folding within the ER is a frequently used and effective method to study acute ER stress responses; however, a more fundamental understanding of how UPR mechanisms serve to protect cells from physiological ER stress requires the use of tissue- or cell-specific models of chronic ER stress. To this end, we found that UPRM8 reduced the constitutive splicing of an Xbp1-venus reporter in RPMI-8226 MM cells. This constitutive splicing of Xbp1 in RPMI-8226 MM cells likely results from the physiological ER stress that is associated with the production of lambda light chain in these MM cancer cells [331]. UPRM8-mediated inhibition of the splicing of this Xbp1-venus reporter was observed after only 4 hours of UPRM8 exposure and an apoptotic cell death phenotype ensued in these same cells after 8 hours of UPRM8 treatment. These UPRM8 results support a previous study that employed both siRNA-mediated Xbp1 knockdown and the expression of a dominant negative Xbp1 construct to show that the Ire1/Xbp1 UPR pathway is critical for MM survival in ER stress conditions [46]. Our Xbp1-venus reporter suggests that RPMI-8226 cells constitutively splice Xbp1 and that this can be impaired by UPRM8 exposure. Chemical ablation of this chronic ER stress response by UPRM8 in these lambda light chain-expressing MM cancer cells is an important step towards evaluating the therapeutic potential of modulating ER homeostatic mechanisms.

While UPRM8 displayed clear cytotoxic effects on cultured MM cells, we observed little or no cytotoxicity when we applied these same doses of UPRM8 to human cells lines that have negligible basal ER stress levels, like HEK293 cells. This selective cytotoxicity for ER-stressed cancer cells should theoretically leave healthy surrounding tissues unharmed and this sort of selectivity is obviously an important consideration when designing safe and effective chemotherapies. Widespread use of new reporters for monitoring ER stress *in vivo* [53, 54] should provide the means to evaluate the importance of ER stress in a large number of human cancer models. Once a causal or contributive role for ER stress has been linked to a given cancer or disease model, researchers should be able to make use of any available UPRMs, to improve upon current disease therapies. UPRMs for use in such a rationally designed therapeutic strategy could be UPR antagonists, like UPRM8, when blocking the cytoprotective functions of UPRs could prove beneficial, like with MM cells. In cases where ER stress contributes to disease pathology by causing unwanted cell death, disease progression could be slowed or halted by UPRMs that stimulate cytoprotective UPRs. Therefore, we feel that the need to identify small molecules with potent UPRM activities is apparent and that the isolation and characterization of UPRM8 is an important step towards this end.

We reported here the discovery of UPRM8, a novel pyrimidinedione UPRM that impairs Ire1-dependent UPRs. We feel that small molecules like UPRM8 will serve as useful chemical probes for studying UPRs *in vivo* and their widespread use may uncover new roles for ER homeostatic mechanisms in human disease. Future therapeutic strategies for treating ER stress-related diseases,

including cancers like multiple myeloma, will no doubt benefit from availability of small-molecule UPRMs, like UPRM8, that can modulate the activities of these important ER homeostatic mechanisms. The ability to perturb homeostatic mechanisms in ER-stressed cancer cells with small molecules may well lead to the development of powerful adjuncts to conventional chemotherapies and we predict that UPRMs will be used in future therapies to improve treatment outcomes for a host of ER stress-related diseases.

3.7 Acknowledgments

We would like to thank Dr. Masayuki Miura for kindly providing the Xbp1-venus splicing reporter construct. This work was funded by grants from the Canadian Institutes for Health Research to Dr. David Y Thomas. Daniel Waller and Chloe Martel-Lorion were supported by CIHR STIHR Chemical Biology scholarships.

3.8 Supplementary Information

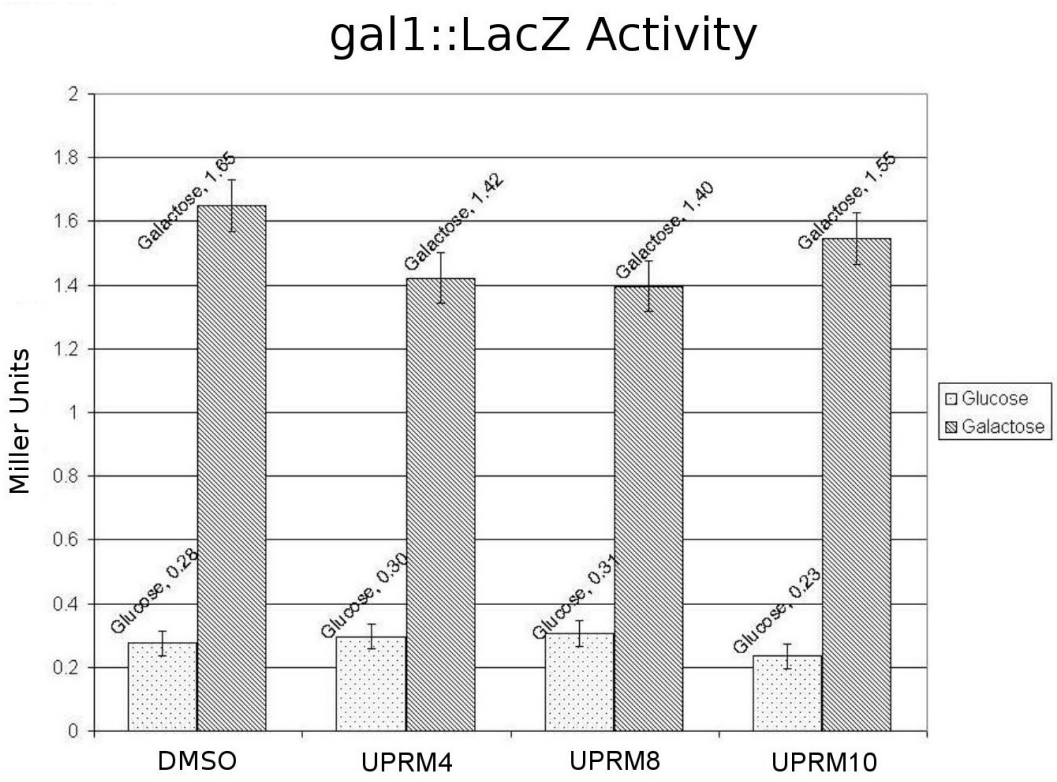

Supplementary Figure 3.1. UPRMs do not affect the transcription, translation, or enzymatic activity of a Galactose-driven β-gal reporter. Yeast cells harboring a Gal1::LacZ reporter were grown overnight in YPD. Cells were harvested the following day, split, washed in fresh media and then given either 4-hour induction in YP+Galactose media (hashed bars) or YP+Dextrose media (spotted bars). The presence of DMSO (0.5%) or 1uM of each of our UPRMs was included during the entire 4-hour induction period and the effects on gal1p::lacZ induction were observed by quantifying the β-galactosidase activity of permeabilized cells by the miller method. β-galactosidase activities were plotted as 1/100 of a Miller Unit (i.e. 1.0 = 100 Miller Units). Error bars represent one standard deviation from the calculated means.

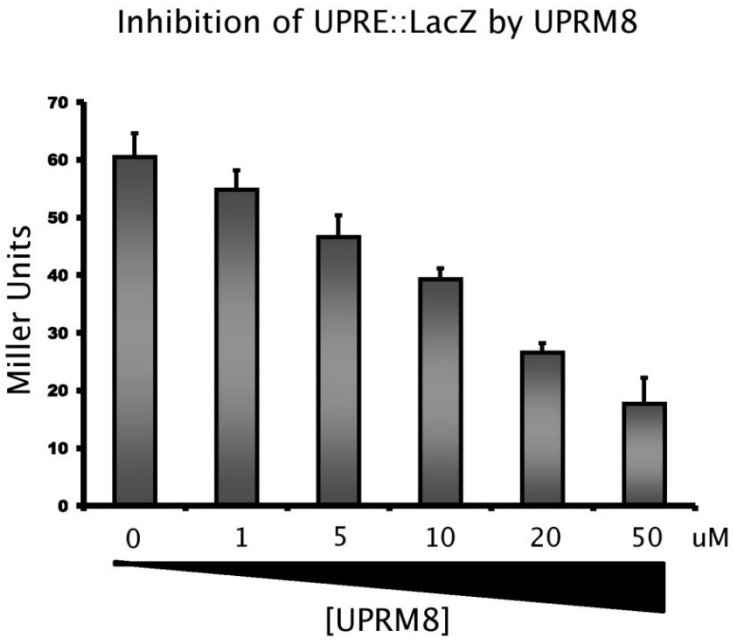

Supplementary Figure 3.2. A dose response of UPRM8 in TM-stressed CML8-1. Reporter yeast were cotreated with 2 ug/ml of tunicamycin and the indicated dose of UPRM8. UPRE::LacZ reporter induction was monitored by measuring β-galactosidase activity after the 4-hour cotreatment period. Maximal UPRE::LacZ inhibition was seen at 50 uM UPRM8 and from this assay we estimate the IC50 of UPRM8 to be approximately 10 uM in TM-stressed Cml8-1 cells.

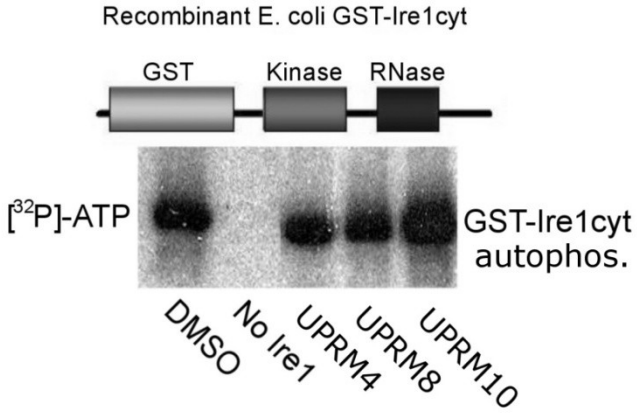

Supplementary Figure 3.3. UPRM8 does not inhibit the *in* vitro kinase activity of the recombinant GST-Ire1^{CYTO} fusion protein. An *in vitro* kinase assay was used to monitor the autophosphorylation of a recombinant GST-Ire1 fusion that was expressed in, and purified from, BL21 *E. coli* cells. This GST-Ire1^{CYTO} construct contains the cytosolic portion of yeast Ire1p fused to GST. The autoradiograph shown here indicates the level of autophosphorylation of this GST-fusion in a standard [γ-^{32}P]-ATP *in vitro* kinase assay, which was conducted in the presence of DMSO (0.1%) or UPRMs 4, 8 and 10 (1uM each).

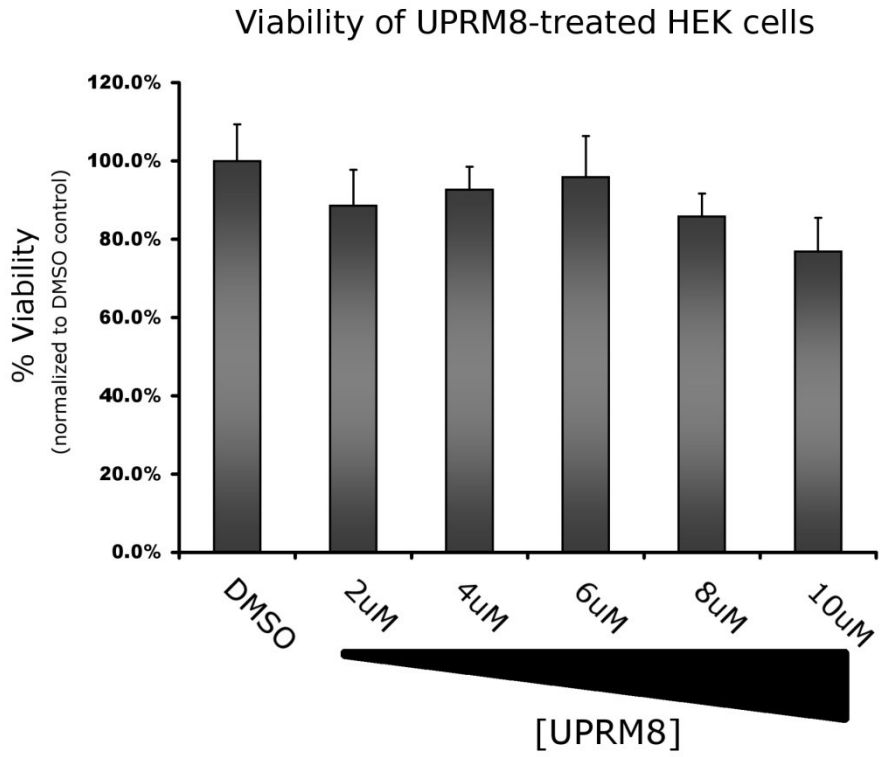

Supplementary Figure 3.4. UPRM8 is not cytotoxic to HEK293 cells. The viability of HEK293 cells was assessed by the ATPlite assay following a 24-hour treatment with DMSO (0.5%) or the indicated doses of UPRM8. The viability of these treated HEK293 cells was normalized to the DMSO negative control wells (100% viability), just as was done for viability of RPMI-8226 MM cells in Figure 4A.

CHAPTER 4

Genetic and proteomic analysis of Bem1p-dependent scaffolding activities in *Saccharomyces cerevisiae* reveals their requirement for efficient mating and for cell wall stress tolerance.

4.1 Connecting Text

The construction of a rigid cell wall is essential to *S. cerevisiae* because this structure provides a protective barrier and is critical for maintaining cell integrity. Remodelling of the cell wall occurs at sites of polarized cell growth and also in response to cell wall stressors. Furthermore, dramatic redistributions of the actin cytoskeleton are known to result from exposure to cell wall stressors [181], as well as a variety of other cellular stressors [180, 182]. Given these observations, it appears that intimate connections exist between the machineries that regulate the actin cytoskeleton and those that signal CWI responses. *S. cerevisiae* is a proven model for studying both of these machineries and so it was an obvious choice for examining the connectedness of these two cellular processes.

In chapter four I examined the scaffolding activities of the cell polarity scaffold protein, Bem1p. My reasons for choosing to study Bem1p were numerous and principal among these reasons was the fact that a role for Bem1p in regulating actin cytoskeleton dynamics during yeast morphogenesis was already well-established. Secondly, literature suggests that Bem1p sits at the interface between actin cytoskeleton regulation and pheromone-induced MAPK signaling. Consequently, I hypothesized that Bem1p might serve an analogous, parallel function in connecting CWI MAPK responses to the machinery that controls actin cytoskeleton dynamics.

The identification of a novel separation of function allele of bem1 (Bem1-*s3*) revealed the importance of its tandem SH3 domains in executing a proper mating response. Subsequent examination of the physical associations of Bem1p revealed numerous CWI signaling components. The sensitivity of numerous Bem1 mutants to a variety of cell wall destabilizing agents confirmed my above-stated hypothesis.

4.2 Abstract

Actin cytoskeleton rearrangements and cell wall remodeling processes are essential for polarized morphogenesis in *Saccharomyces cerevisiae*. Bem1p is a multi-domain scaffold protein that has well established roles in polarized morphogenesis and in pheromone-induced MAPK signaling. Given its role in connecting critical regulators of actin cytoskeleton dynamics to mating MAPK signaling components, we hypothesize that Bem1p may similarly be involved in linking cell wall integrity (CWI) MAPK signaling to the regulatory machinery of the actin cytoskeleton. We first examined the parallel requirements for Bem1p-mediated scaffolding during both budding and mating morphogenesis, and we did this by isolating a novel separation of function mutant, Bem1-*s3*. Bem1-*s3* cells displayed dramatically reduced shmooing efficiencies, decreased activation of a mating transcriptional reporter, and decreased sensitivity to pheromone-induced cell cycle arrest. We found that the Bem1-*s3* mating defect resulted from the combined loss of protein-protein interactions that are mediated by its tandem SH3

domains. Proteomic analysis of affinity-purified Bem1p complexes allowed us to identify both known and novel physical interactors of, and phosphorylation sites within, Bem1p. The identities of these novel physical interactors, along with our phenotypic analysis of Bem1Δ and serine-458 phosphomutants, strongly supported a role for Bem1p in the cell wall integrity stress response. These findings further our understanding of the scaffolding activities of Bem1p during yeast morphogenesis and also suggest that Bem1p may serve as an important link between the actin cytoskeleton machinery and components of the cell wall integrity response.

4.3 Introduction

Yeast cells are protected from their external environment by a rigid cell wall that is principally composed of mannoproteins, β-glucan polymers, and chitin [248]. This protective barrier constitutes up to 30% of the dry weight of yeast cells and is required for their ability to maintain cell shape and integrity [250, 255]. Given these essential functions of the cell wall, and also given the fact that mammalian cells do not construct cell walls, drugs that target the synthesis or integrity of the cell wall constitute a large segment of our current spectrum of anti-fungal agents [252, 332]. The need to develop new, more potent, anti-fungal agents is apparent and is made more pressing by recent increases in the observed frequency of systemic fungal infections, which has been attributed to the increasing demographic of immune-compromised individuals [252, 253, 333].

Saccharomyces cerevisiae has proven to be an invaluable model for studying yeast cell wall integrity (CWI) signaling and polarized cell growth [179, 190, 255]. The CWI pathway monitors and regulates the cell wall remodeling processes that occur at sites of polarized cell growth and in response to a variety of cell wall stressors, such as growth at elevated temperatures, hypo-osmotic shock, and exposure to a number of cell wall destabilizing agents like caffeine, congo red, or calcofluor white [255, 334]. The strength of the *S. cerevisiae* model for studying CWI responses is reinforced by the high degree of conservation of its CWI monitoring system to the homologous systems found in opportunistic fungal pathogens, such as *Candida albicans* [254].

The small GTPase Rho1p acts as the master regulator of the CWI pathway in *S. cerevisiae* and it instigates CWI signaling through its GTP-dependent activation of numerous downstream effectors (reviewed in [255, 334]). Examples of downstream GTP-Rho1p effectors include, the β1,3-glucan synthase complex[257, 258], protein kinase C (Pkc1p) [335, 336], the related formin proteins Bni1p and Bnr1p [202, 259, 260] and a component of the exocytic machinery called Sec3p [337].

Pkc1p is known to activate a prototypical MAPK cascade that is composed of the MAPKKK Bck1, the redundant MAPKKs Mkk1p/Mkk2p, and the MAPK Slt2p (reviewed in [255]). Activation of Slt2p leads to its phosphorylation of two transcriptional activators, called Rlm1p and SBF. Once activated, Rlm1p and SBF lead to the up-regulation of genes involved in cell wall metabolism and cell cycle regulation, respectively [338, 339]. This Pkc1p-dependent signaling

response is a conserved feature of CWI responses in *C. albicans* and it has been shown that agents that inhibit Pkc1 function in *C. albicans* can potently synergize with β1,3-glucan synthase-inhibiting (echinocandin) anti-fungal agents [253]. This strategy of combining anti-fungal agents to concomitantly target cell wall synthesis/structure and CWI homeostatic responses appears to be a therapy that holds much promise for treating azole-resistant fungal infections.

Given that CWI signaling components are required for cell wall remodeling at polarized growth sites and also given that Rho1p is directly involved in the polarization of the actin cytoskeleton [202, 259, 260], it seems clear that there is significant functional interplay between CWI signaling and the highly dynamic actin cytoskeleton. This connection is further supported by the transient depolarization of the actin cytoskeleton that has been observed in response to CWI stressors [181]. This transient actin depolarization was reported by Delley et al. to be Pck1p- and Rho1p- dependent but completely independent of downstream components of the CWI MAPK pathway. We wished to further evaluate this functional interplay between regulation of the actin cytoskeleton and CWI signaling proteins.

S. cerevisiae has three distinct morphogenesis programs, the foremost of which derives from internal cell cycle-dependent cues that direct the formation of a bud. A second morphogenesis program occurs in response to contact with mating pheromone from cells of the opposite mating type and results in the formation of mating projections. The third morphogenesis program in *S. cerevisiae* occurs in response to nutrient limitation and results in a transition from

budding to filamentous growth. The polarized cell growth that underlies these morphogenesis programs requires the formation of a highly polarized actin cytoskeleton and the regulatory machinery that controls the dynamic actin cytoskeleton in yeast have been well-studied (reviewed in [188, 190]).

Two master regulators of the actin cytoskeleton are yet another Rho-type GTPase, Cdc42p, and its activating guanine nucleotide exchange factor (GEF), called Cdc24p. Once activated, Cdc42p results in the formation of a polarized actin cytoskeleton by locally activating the actin polymerization machinery, or polarisome, through a variety of downstream effectors like Ste20p, Cla4p, Gic1/2p and Bni1p [188, 190]. The activation of Cdc42p by Cdc24p-mediated GEF activity is facilitated by the scaffolding activities of Bem1p, which binds to both of these proteins [217, 218, 228, 232]. Furthermore, Bem1p also contributes to the formation of a polarized actin cytoskeleton by bringing GTP-bound Cdc42p into close association with several of its effectors, such as the p21-activated kinases (PAKs) Ste20p and Cla4p [217, 218, 227]. In addition to these scaffolding activities during symmetry breaking, Bem1p has also been shown to contribute, in both Ste20p-dependant and Ste20p-independant ways, to the MAPK signaling that occurs in response to mating pheromone [242]. This, combined with the fact that Bem1p has been shown to bind the mating MAPK scaffold protein Ste5p [242], illustrates how Bem1p sits at the interface between MAPK signaling and the cell polarity establishment machinery.

Bem1p is a multi-domain protein that contains two tandem N-terminal SH3 domains, which have been shown to mediate interactions with a variety of

proteins, such as Sec15p, Ste20p, Cla4p, Boi1p, and Boi2p [217, 226, 227, 231]. A Cdc42p-interacting (CI) domain has been identified and it was found to flank the C-terminal end of the SH3-2 domain of Bem1p [228]. Bem1p also contains a PX domain that has been shown to bind to phosphatidylinositol-4-phosphate [229] and this interaction is believed to contribute to the association of Bem1p with PtdIns(4)P-containing membranes [230]. Finally, the C-terminus of Bem1p contains a PB1 domain that has been shown to bind to the C-terminal PB1 domain of Cdc24p [231-235].

Here we show that while the N-terminal SH3 domain of Bem1p makes a minor contribution to mating morphogenesis, we could identify point mutants in conserved residues in the SH3-2 domain that render an SH3-1 truncated Bem1p truly pheromone-insensitive. This new Bem1p mutant was designated Bem1-*s3,* following the nomenclature of the original -*s1* and -*s2* mating-defective mutants [223]. In contrast with these original -*s* mutants, our Bem1-*s3* allele displays no obvious defects during the bud morphogenesis program. Furthermore, we find that it is the combined loss of SH3-1 and the PXXP-binding capacity of SH3-2 that gives rise to the separation of function observed in Bem1-*s3* cells. Furthermore, we employed a proteomics approach to examine novel Bem1p-complexes *in vivo* and we identified numerous components of the CWI response, as well as novel Bem1p phosphorylation sites. Analysis of the cell wall stress sensitivity of Bem1 null and phosphomutants strongly argues that Bem1p contributes to CWI responses. Consequently, we suggest that Bem1p may serve as an important link between the CWI signaling proteins and regulators of the

actin cytoskeleton.

4.4 Materials and Methods

Materials

All restriction enzymes used in our cloning experiments were from New England Biolabs. All constructs, except for the low fidelity mutagenesis reaction, were amplified with Expand High Fidelity PCR amplification system from Roche. Low fidelity PCR mutagenesis was performed with recombinant Taq polymerase from Invitrogen. All other DNA modifying enzymes were from either New England Biolabs or GE Healthcare. Nucleotides were purchased from Stratagene, as was the Quick Change site-directed mutagenesis kit. Lumi-light chemiluminescent reagents along with the Complete protease inhibitor tablets were purchased from Roche. Anti-His_6 antibodies and HRP-conjugated secondary antibodies were purchased from Santa Cruz biotechnology. Rhodamine phalloidin, ProLong anti-fade solution, and oligonucleotide primers were all purchased from Invitrogen. Ortho-nitrophenyl-b-D-galactopyranoside (ONPG), yeast alpha mating pheromone, and acid washed glass beads were purchased from Sigma. Glutathione-Sepharose 4B beads and the PreScission protease were purchased from GE Healthcare.

Construction of plasmids.

Bem1 (nucleotides 1-1656), ΔSH3 (nucleotides 394-1656) and ΔPB1

(nucleotides 1-1260) fragments were amplified from a previously published Bem1-AD two-hybrid plasmid [340]. The C-terminal His_6 tag, along with a three amino acid linker (Arg-Gly-Ser), was included in the 3' oligonucleotide primer. These fragments were cloned into the copper-inducible pCu413 centromeric plasmid [341] using EcoRI and EcoRV restriction sites. The Bem1-*s3* allele was created by employing a simple low-fidelity PCR amplification of ΔSH3-His_6. This protocol is similar to the one used by Nishiya et al. [342] except that we used standard Taq polymerase and lowered the final concentration of dTTP to 40uM. The GFP-tagged version of the Bem1-*s3* construct was created by recombining the His_6 constructs with a C-terminally tagged Bem1-GFP construct that was inserted into pRS316. For the expression of recombinant protein, ΔSH3 Bem1 (nucleotides 394-1656) was amplified from genomic DNA and cloned into the pGEX6P-1 vector using the EcoRI and XhoI restriction sites. The F166L, W192K, S252D mutations were introduced into the ΔSH3 pGEX6P-1 and the ΔSH3-His_6 plasmids by using the Quick Change mutagenesis kit. The Bem1-binding domains of Ste20p (nucleotides 1260-1410) and Boi1p (nucleotides 1026-1362) were cloned into the EcoRI and XhoI sites of pGEX6P-1. The Bem1-AD two-hybrid construct was described previously [340], as was the Boi2-DBD construct [264]. The ΔSH3-AD and Bem1*s3*-AD constructs were created by amplifying the coding sequences of the respective His_6–tagged construct and cloning these PCR products into the EcoRI and XhoI sites of pGAD424. The Ste20 BBD construct was created by amplifying nucleotides 1300-1490 of Ste20 and cloning this fragment into the SalI/PstI sites of pBTM116. The Ste20 BBD+CRIB construct was constructed similarly, except that nucleotides 892-

1490 were amplified and this fragment was cloned into the BamHI/PstI sites of pBTM116. The Bem1p-4xFLAG::LEU2 plasmid was generated by PCR amplifying the Bem1 coding sequence plus 800 bp of upstream promoter sequence and the codons for the c-terminal 4x FLAG epitope were introduced by including them in the 3' primer. The Bem1-4xFLAG PCR product was inserted into the pGREG505 vector by homologous recombination.

Yeast strains and manipulations

Yeast media, culture conditions, and manipulations were described previously [307]. Yeast transformation and plasmid isolation was performed using standard techniques [307]. The Bem1 deletion strain and the BY4741 wild-type control strain were purchased from ATCC as part of the haploid deletion collection. To elicit the mating response in MATa cells, cells were treated with 5uM of alpha-factor for the indicated time period. Yeast viability was assessed by spotting 10-fold serial dilutions of mid-logarithmic phase cultures onto selective media plates and incubating these plates for 2 days at the indicated temperature. Halo assays were performed as described previously [243]. Mating was done on solid YPD media for the indicated time period before selecting for diploids on the appropriate selectable media. SD -lys -met selection was used to select for the diploids from the crosses of our Bem1p mutants with themselves (transformed into Bem1Δ from BY4741 and BY4742 backgrounds).

Shmooing Efficiency

Shmooing efficiency was determined by visually counting cells that had adopted mating projections following exposure (75 min.) to 5uM α-factor. Shmooing efficiency was plotted as a percentage of the total number of cells counted for each individual strain (# of shmoos / total # of cells). The minimum total number of cells counted for each strain was 400, divided between three independent experiments. Error bars represent one standard deviation from the calculated means.

Microscopy

Cells were grown under the indicated conditions and viewed with a microscope (Nikon Eclipse E800) equipped with Nomarski optics. Microscopic photographs were acquired with a 100x objective and a Nikon DXM1200 camera and ACT-1 version 2.10 software (Nikon). Visualization of actin by rhodamine phalloidin staining of formaldehyde fixed cells and visualization of GFP-tagged Bem1 in live cells was performed as described previously [307].

β-galactosidase Assay

Yeast containing our mutant plasmids and the *URA3*-marked Fus1::LacZ plasmid were grown overnight at 30^{o}C. The next day cells were diluted to an OD_{600} of 0.2 and allowed to grow to an OD_{600} of 0.8, at which time they were treated with 5uM α-factor for 75 minutes. Cells were harvested by centrifugation and the β-

galactosidase assay was performed as described previously [307]. The plotted values are expressed in Miller units**.**

Western Blotting

The preparation of yeast cell extracts was performed as described previously [343]. Protein samples were resolved in standard 10% SDS-PAGE gels and transferred to nitrocellulose membranes. Membranes were blocked with 5% (w/v) skim milk for 1 hour and probed overnight with a 1:1000 dilution of either rabbit polyclonal anti-His_6 antibody (Santa Cruz, sc-803) or mouse monoclonal anti-FLAG M2 antibody (Sigma, F1804) . Standard washing, secondary antibody incubation, and chemiluminescent techniques were used.

Preparation of Recombinant GST proteins

The pGEX6P-1 plasmids expressing the GST-fusion proteins were expressed in BL21 *E. coli* cells (Invitrogen). Protein expression, extraction, and glutathione Sepharose purifications were performed as described previously [309]. Ste20p and Boi1p fusions were left bound to the glutathione beads. All Bem1 constructs were eluted from the beads by cleavage with Prescission protease, following the manufacturer's instructions (GE Healthcare). The buffer was exchanged to storage buffer (25mM HEPES 50mM KCl, 1mM DTT, 0.1mM EDTA, 10% Glycerol) and proteins were concentrated with Amicon Ultra 5,000 MW cut-off centrifugal filters before storage at -80^{o}C.

In vitro binding assay

Ste20 and Boi1 Bem1-binding domain (BBD)-containing beads were aliquoted into Eppendorf tubes, each with 15ul bed volume (~5ug protein). Naked glutathione beads served as a negative control for non-selective binding (not shown). Beads were then diluted with 750 ul of wash buffer (50 mM Tris-HCl pH 7.5, 150mM NaCl, 5mM EDTA) and 5ug of untagged ΔSH3 Bem1 protein, or mutants, were then added. These mixtures were incubated for 1 hour at 4^{o}C with rotation to allow the untagged Bem1 proteins to bind to bead-bound Ste20p- and Boi1p- BBD fragments. The slurry was then transferred to Micro Bio-Spin chromatography columns (Bio-Rad) and gravity flow-throughs were collected. The beads were then washed 5 times with 1ml of wash buffer and bead-bound proteins were eluted by the addition of 35ul of 1X SDS sample loading buffer. A quick spin (2 min. at 12,000 RPM) was used to collect the SDS-eluates. SDS-eluates were then analyzed by running them in 10% SDS-PAGE gels and subsequent visualization by Coomassie staining. A 10% loading control (~0.5ug) lane for each untagged Bem1 construct was also included in the SDS-PAGE analysis to ensure equivalent amounts were incubated with BBD-containing beads.

Two-Hybrid analysis

Ste20 LexA DBD fusions (BBD+CRIB and BBD) and the pBTM116 vector control were transformed into the L40α two-hybrid strain. Similarly, Bem1-AD

fusions were transformed into the L40a two-hybrid strain. These strains were then mated in a pairwise fashion on YPD plates and diploids were selected on SD -Trp-Leu plates. Small streaks of these diploids were patched to fresh SD -Trp -Leu plates and positive interactions were then scored by replicating these streaks onto selective SD -Trp -Leu -His plates. These selection plates also contained 5mM of 3-amino-1,2,4-triazole (3AT) to increase the stringency for detecting interactions. The same basic protocol was used for detecting interactions between full length Boi2-DBD and our Bem1-AD fusions, except that these constructs were transformed into PJ694α and PJ694a two-hybrid strains, respectively. The PJ694 strain background was used for this second set of experiments because the Boi2-DBD construct was in the pODB2 vector, which contains the Gal4 DNA binding domain rather than the LexA DNA binding domain that is present in the pBTM116-based Ste20-DBD plasmids.

Affinity purification of Bem1p complexes from yeast

Bem1Δ cells were transformed with a GST-Bem1p plasmid that was picked from a yeast genomic GST-fusion library [344]. Two liters of this GST-Bem1p strain were grown in SD –Ura media to an OD_{600} 1.0. No exogenous copper source was added because significant expression GST-Bem1p was observed without $CuSO_4$ induction and we wished to avoid massive over-expression of this fusion protein. After the culture reached OD_{600} of 1.0, cells were harvested by centrifugation at 3,500 RPM for 10 minutes. The preparation of crude cell extracts and the subsequent isolation of GST-Bem1p by standard GST affinity purification

procedures were performed as described previously [343]. Proteins were eluted from glutathione Sepharose by two subsequent washes with 0.5 ml of glutathione elution buffer (10 mg/ml reduced glutathione in 50 mM Tris-HCl, pH 8.0). Eluted proteins were concentrated and stored as described above for our recombinant GST-fusion proteins.

Mass spectrometry analysis of Bem1p complexes

Purified GST-Bem1p complexes (described above) were resuspended in 4X SDS sample buffer and loaded onto a polyacrylamide stacking gel (no resolving gel). Samples were electrophoresed for 75 min. at 150 volts in this stacking gel to concentrate the proteins into a single coomassie stained band. This band was excised from the gel and subjected to standard trypsinization procedures [345]. The resulting tryptic digests were analyzed by reverse phase separation, followed by MS/MS on a Brucker HCT Ultra ion trap mass spectrometer. Data files were formatted and searched as described previously [346], except that the *S. cerevisiae* NCBI database was used (version NCBInr 20080410, or later).

mORF fusion pull-downs to confirm Bem1p-interactors

A genome-wide *S. cerevisiae* moveable ORF (mORF) plasmid collection has been described previously [347]. These are sequence-verified plasmids that express *S. cerevisiae* ORFs as C-terminal fusions with a triple affinity tag, which is composed of His_6, HA epitope, and the ZZ domain of protein A (from N- to C-

terminus). Expression of these ORFs is driven by the GAL1 promoter. Bem1Δ cells that had been previously transformed with a Bem1-4Flag plasmid were retransformed with one of a number of mORF plasmids that encode for known components of the CWI signaling pathway. CWI proteins that were not present in the mORF plasmid library were not tested. Co-transformed cells were cultured overnight in 25 ml's of SD –Ura –Leu + 3% raffinose media. Cells were harvested by centrifugation and resuspended in 25 ml's of fresh SD –Ura –Leu + 3% raffinose. When cultures reached an OD_{600} of 0.8, a concentrated galactose solution was added to a final concentration of 3% in order to fully induce the expression of these mORF fusions. After 4 hours of induction cells were harvested and extracts were prepared as described previously [343]. mORF fusion proteins were affinity purified from cleared extracts using IgG Sepharose beads. Beads were washed 4 times with >10 column volumes of wash buffer (50mM Tris-HCl pH 7.5, 150 mM NaCl). Bound proteins were eluted by boiling for 5 min. in 1x SDS sample loading buffer. Eluted proteins were resolved on 10% SDS-PAGE gels and transferred to nitrocellulose. Standard western blotting procedures were used to visualize the pulled-down proteins. Anti-FLAG and Anti-His_6 antibodies were used to visualize the Bem1-4Flag and CWI mORF fusions, respectively.

Cell wall stress sensitivity assay

A previously described serial dilution spotting assay [348] was used to assess the sensitivity of the indicated Bem1 mutants on plates containing the indicated

concentrations of calcofluor white, congo red, or caffeine.

4.5 Results

4.5.1 SH3-1 is largely dispensable for the morphogenesis functions of Bem1p

The first SH3 domain of Bem1 (SH3-1) contains one confirmed cyclin-dependent kinase (CDK) phosphorylation site at serine-72 (S72) and it was proposed that this phosphorylation may regulate vacuolar fusion events [246]; however, Xu H. et al. have provided conflicting evidence that suggests that S72 phosphorylation is not required for the lipid mixing step of vacuolar fusion [247]. Furthermore, the only confirmed direct protein-protein interaction mediated by SH3-1 is with Sec15p, a component of the exocyst complex [349]. Since SH3-1 of Bem1p is regulated by CDK phosphorylation and the molecular function of this domain has not been clearly established, we first asked whether this region of Bem1p is required for its role in budding and mating morphogenesis.

We created Bem1p constructs that contain 6 histidine residues at their C-terminus to allow for easy detection. These Bem1-his_6 constructs were placed under the control of the Cup1 copper-inducible promoter by cloning them into pCu413 vector [341]. We constructed mutants that were deleted for SH3-1 (ΔSH3, aa 132-551) and for the PB1 domain (ΔPB1, aa 1-420) (Figure 4.1A). This latter mutant was constructed to serve as a negative control because this PB1 domain is responsible for binding to Cdc24p and this binding has been shown to be important for both budding and mating [231]. These two mutants, along with

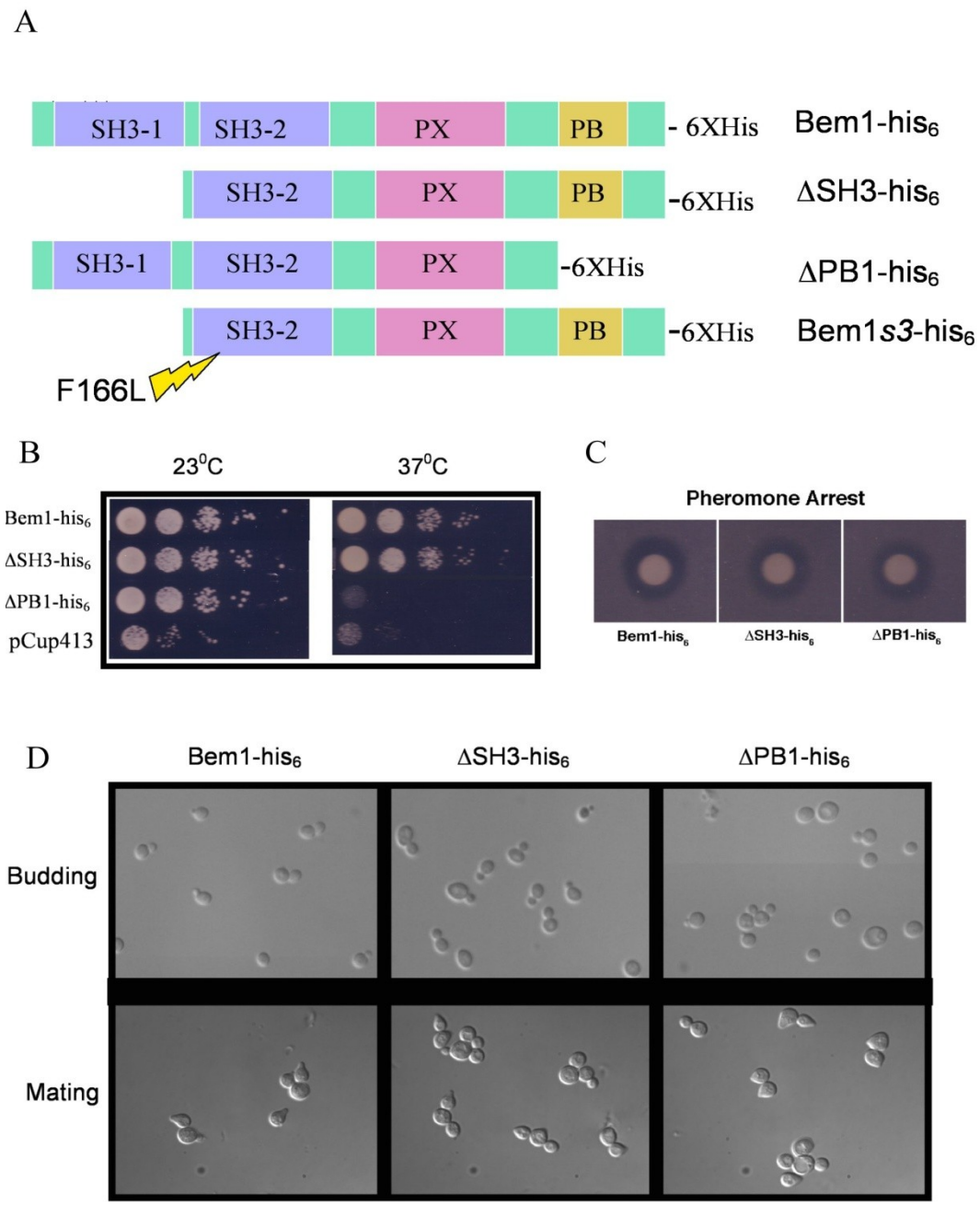

Figure 4.1. SH3-1 of Bem1 is largely dispensable. **(A)** Schematic diagram of the domain architecture of the Bem1p constructs used in this study. SH3= Src homology 3 domain, PX= phox homology domain, PB1= phox and Bem1 domain **(B)** Bem1Δ cells were transformed with the indicated Bem1p constructs and tested for growth complementation at 23°C and 37°C by spotting serial dilutions onto solid agar plates. **(C)** The indicated strains were tested for pheromone arrest by using a standard halo assay. 10ul of 5mM alpha-factor was spotted onto the filter disks and plates were incubated at 30 °C. **(D)** Photomicroscopy was used to examine the morphology of the indicated strains under asynchronous budding (top panel) or mating (lower panel) conditions.

the wild-type Bem1-his$_6$ and the vector control, were transformed into Bem1Δ cells and we investigated their ability to complement Bem1 function in both the mating and budding morphogenesis programs.

Since Bem1Δ cells are temperature sensitive for growth due to failed bud emergence at elevated temperatures [223], we spotted serial dilutions of the above strains and monitored their growth at 37^0C (Figure 4.1B). All four strains were viable at 23^0C but when placed at the restrictive temperature (37^0C), the Bem1-his$_6$ and ΔSH3-his$_6$ strains remained viable, whereas ΔPB1-his$_6$ and vector control strains did not. We also looked at the morphologies of cells from asynchronous cultures of these strains and found that ΔSH3-his$_6$ cells are indistinguishable from Bem1-his$_6$ cells, whereas ΔPB1-his$_6$ cells often appear larger and more rounded (Figure 4.1D, Budding panel). These results suggest that Bem1-his$_6$ and ΔSH3-his$_6$ complement Bem1p function during the bud morphogenesis program, whereas ΔPB1-his$_6$ does not.

The ability of these deletion mutants to complement the function of Bem1p in pheromone-induced cell cycle arrest was determined by using a standard halo assay, which involves spotting mating pheromone on a lawn of growing cells (Figure 4.1C). Halo sizes for Bem1-his$_6$, ΔSH3-his$_6$, and ΔPB1-his$_6$ cells were similar, which suggests that mating-dependent cell cycle arrest remains largely intact in these mutants. Microscopic examination of pheromone treated cells reveals that Bem1-his$_6$ and ΔSH3-his$_6$ cells are able to form shmoos correctly, whereas ΔPB1-his$_6$ cells form broader, shorter shmoos (Figure 4.1D; lower panels). It should be noted that, despite the ability of ΔSH3-his$_6$ cells to

form morphologically sound shmoos, we did notice that the number of shmoos formed is reduced when compared to wild-type cells and this will be discussed further (Figure 4.2B). The ability to form morphologically correct shmoos and buds indicates that SH3-1 plays only a minor role during the budding and mating morphogenesis programs. This is in contrast to the loss of the PB1 domain, which results in more dramatic bud emergence and shmoo-formation defects. This latter result is supported by the work of others who have clearly shown that the Cdc24-binding capability of the PB1 domain is important for the role of Bem1p in bud emergence and mating projection formation [231, 232].

4.5.2 Identification of a shmooing-deficient Bem1-s3 mutant

Since removal of SH3-1 failed to reveal any dramatic morphogenesis phenotypes during the mating and budding morphogenesis programs, we sought to identify Bem1 separation of function mutants. The original Bem1-s mutants [223] and the Bem1-m mutants [231] result in disruption of its PB1 domain and thereby abolishes the Bem1p-Cdc24p interaction, which has been shown to be required for proper bud emergence and shmoo formation [231]. Given that these previously identified Bem1p mutants have problems during both budding and mating we decided to identify new separation of function alleles of Bem1. We have chosen a low fidelity PCR-based mutagenesis strategy, using the ΔSH3-his_6 as our template for mutagenesis. Our reasons for choosing to mutagenize ΔSH3-his_6 were two-fold. Firstly, we were concerned that any redundancy in function amongst the two SH3 domains might decrease the probability of finding single

point mutations that confer interesting phenotypes. Secondly, we have shown above that SH3-1 provides only a minor contribution to the morphogenesis functions of Bem1p during either shmoo formation or bud emergence.

Our approach to identify Bem1 separation of function alleles was based on a simple visual screen, where we transformed the mutagenized ΔSH3-his$_6$ plasmid into the MATa Bem1Δ strain and screened for mutants that failed to form shmoos when treated with mating pheromone. The C-terminal His$_6$ tag allowed us to remove nonsense mutants that were identified, all of which lacked discernible Bem1 function; one particularly interesting missense mutation was identified in this screen. This missense mutant, hereafter referred to as Bem1-*s3,* appears to be a true separation of function allele and its characterization is described below.

Bem1-*s3* mutant cells fail to achieve the characteristic shmoo morphology under conditions where we were able to detect mating projections in the Cdc24-binding mutant, ΔPB1-his$_6$ (Figure 4.2A). This suggests that the mating deficiencies in this new mutant are stronger than the mating defects seen with C-terminal PB1 domain mutants [223, 231].

To further quantify and compare the decreased shmooing capacity of Bem1-*s3* cells, we determined the shmooing efficiency of the above strains by counting the percentage of cells that had adopted a shmoo morphology after a 75 minute treatment with alpha-factor (5uM) (Figure 4.2B). At 75 minutes 43.2% of Bem1-his$_6$ cells had formed discernible mating projections, while removal of SH3-1 resulted in a modest but detectable decrease in shmooing efficiency to 30.4%. An even greater reduction in shmooing efficiency was observed in

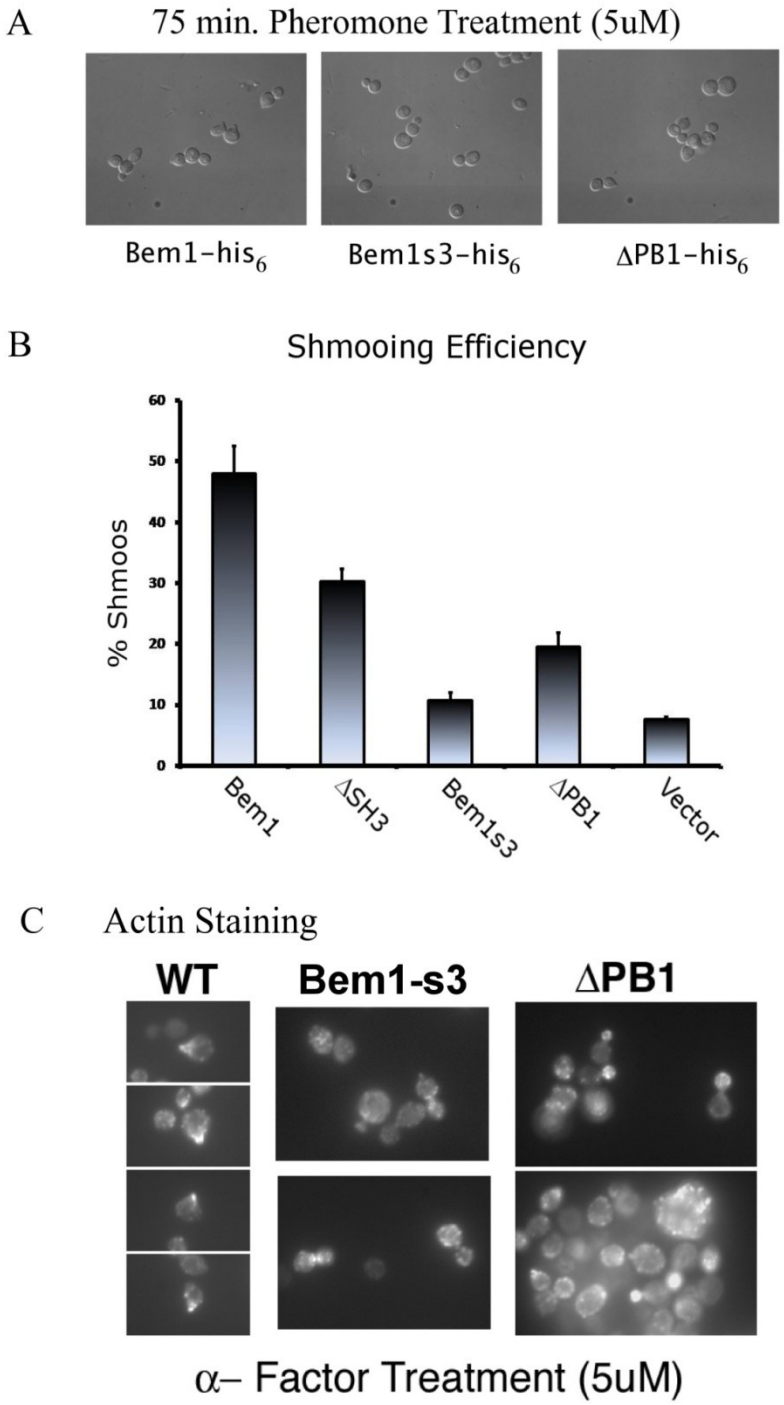

Figure 4.2. Identification of a shmooing-defective Bem1*s3* mutant. **(A)** The morphologies of the indicated strains were examined under mating conditions. **(B)** The shmooing efficiency of the indicated strains is presented here. Percentages indicate the number of shmoos formed out of the total population of cells counted. **(C)** Rhodamine phalloidin staining of the actin cytoskeleton of the indicated strains under mating conditions (5uM alpha-factor for 75 minutes). WT corresponds to Bem1-his_6, S3 to Bem1s3-his_6, and ΔPB1 to ΔPB1-his_6 cells.

pheromone-treated ΔPB1-his$_6$ cells (21.2%), but this is not surprising given that it is known that failure to bind Cdc24 disrupts proper mating morphogenesis. Finally, Bem1-*s3* cells had an even more pronounced shmooing defect with only 10.4% of cells achieving the shmoo morphology and this is only slightly above the empty vector-containing negative control strain (7.4%).

To further investigate the failure of Bem1-*s3* cells to form shmoos, we visualized the actin cytoskeleton in pheromone treated cells by rhodamine phalloidin staining. We found that Bem1*s3*-his$_6$ and ΔPB1-his$_6$ cells failed to properly polarize their actin cytoskeleton under mating conditions, whereas Bem1-his$_6$ cells displayed a tightly polarized actin distribution at their shmoo tips (Figure 4.2C). Taken together, these results suggest that the Bem1-*s3* mutant is strongly compromised for mating morphogenesis and this failure stems from the inability of Bem1-*s3* cells to properly polarize their actin cytoskeleton following exposure to mating pheromone.

4.5.3 Bem1-s3 contains an F166L mutation and results in mating defects

Next we sought to identify the mutation(s) contained in the Bem1-*s3* mutant, so we isolated the plasmid from yeast, amplified it in *E. coli*, and sequenced the Bem1 open reading frame. Bem1-*s3* was found to contain a single nucleotide change that resulted in a phenylalanine to leucine substitution mutation at amino acid 166 (F166L). This residue falls within SH3-2 of Bem1p and it is highly conserved in the 5 most similar fungal SH3 domains (Figure 4.3A).

Furthermore, this phenylalanine-166 residue of Bem1p is conserved in many other SH3 domains, including those found in human proteins, such as c-Crk, SH3D19, and c-abl (Figure 4.3A). This particular residue was also predicted by the NCBI conserved domain database (CDD) to be important for binding to polyproline (PXXP) motifs [350]. This CDD prediction was made based on structural data that was provided by the crystal structure of c-Crk SH3-N complexed to a polyproline peptide [351].

It has been shown that complete disruption of Bem1 function reduces mating efficiency when crosses are done with other shmooing defective strains [231, 232]. This sort of bilateral mating defect was also observed when we performed mating experiments with our Bem1 mutant strains; shmooing deficient Bem1*s3*-his$_6$ and ΔPB1-his$_6$ cells readily formed diploids only when mated against wild-type Bem1-his$_6$ and not when mated against themselves or each other (Figure 4.3B). This result confirmed our hypothesis that the failure of Bem1*s3* cells to form shmoos leads to bilateral mating defects.

Next we assessed the cell cycle arrest capacity of Bem1-*s3* cells, again by performing standard halo assays. All four strains examined produced similar sized halos in response to the 5 mM concentration of spotted pheromone; however, the halos for ΔSH3-his$_6$, Bem1*s3*-his$_6$, and ΔPB1-his$_6$ were appreciably smaller than wild-type at the 0.5 mM dose of spotted pheromone (Figure 4.3C). Furthermore, both ΔSH3-his$_6$ and Bem1*s3*-his$_6$ strains produced halos that were noticeably less clear than the other strains. These 'fuzzy' halos could result from either a proportion of cells failing to arrest their cell cycle within the pheromone

A

```
Bem1 SH3-2 (Sc)      159   YAIVLYDFKAEKADELTTYVGENLFICAHHNCEWFIAKPIGRLGGPGLVPVGFVSI  214
Bem1 (Cg)            149   ..........S...D.F..........Y.....................  204
AEL241Wp (Eg)        148   ..........S...SAFA.........F.....................  203
KLLA0E23441g (Kl)    59    ........Q........A.A.........DF.....................T.  114
DEHA0E22924g (Dh)    136   ..VT..E....RE...DIIP....I.....AF.....N.........LY.K.  191
Bem1 (Ca)            151   ..VT..E....RD...DIMPN...I.....DY.....N.........SY.K.  206

c-Crk (Hs)           136   .VRA.F..NGNDEED.PFKK.DI.R.RDKPEEQWN.E--DSE.KR.MI..PY.EK  189
SH3D19 (Hs)          437   H.V..H..P..QV.D.NLTS..IVYLLEKIDTDYRGNCRNQI.IFPANY.KVIID  492
c-abl (Hs)           38    LFVA....V.SGDNT.SITK..K.RVLGY..G..E.QTKNGQ.WVPSNYITP.NS  493
```

B

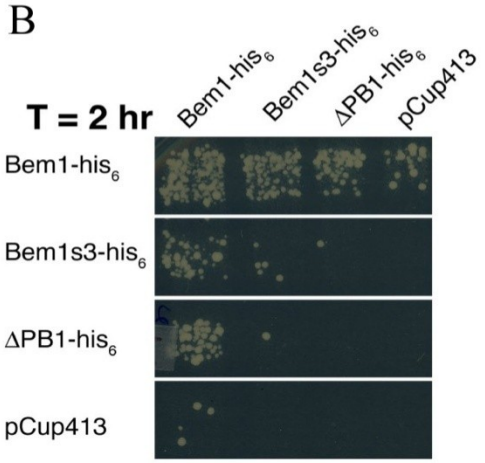

C

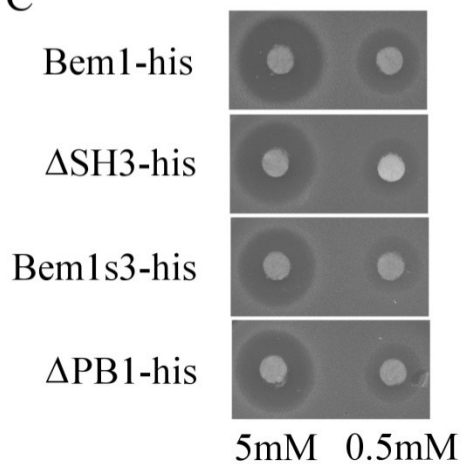

D

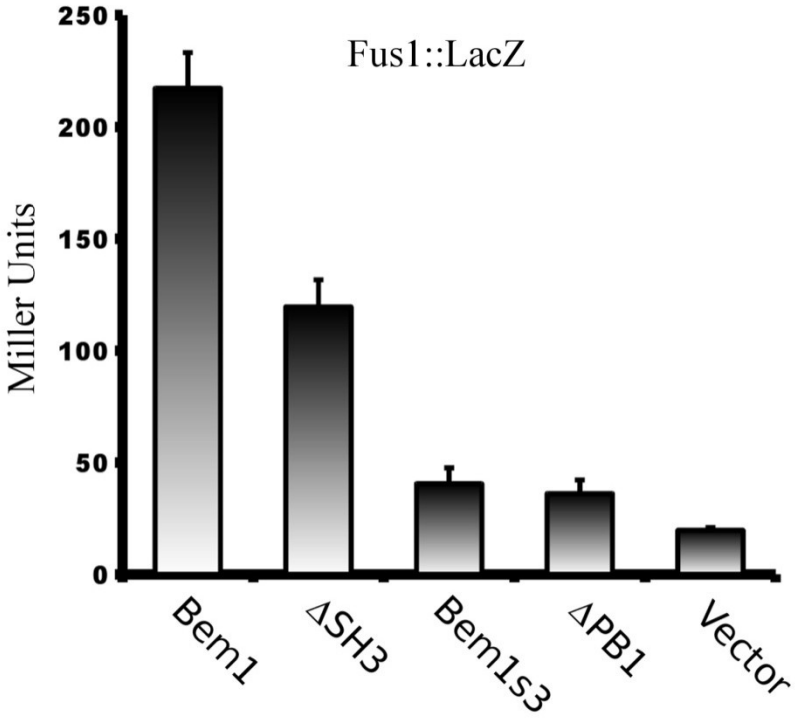

Figure 4.3. Bem1s3 contains an F166L mutation and results in compromised mating. **(A)** Alignment of the SH3-2 domain of Bem1p with 5 similar SH3 domains from fungi and 3 from human sequences. Highlighted in yellow is the conserved phenylalanine, in purple is the conserved tryptophan and in blue is the conserved proline. These three residues are predicted to be important for mediating PXXP interactions. **(B)** The results of a mating experiment where crosses of the indicated constructs (in Bem1Δ a-strains on Y-axis and in Bem1Δ α-strains across X-axis at the top) were mated for 2 hours before replica plating to the diploid selection plate shown here. **(C)** Pheromone-induced cell cycle arrest of Bem1-his$_6$, ΔSH3-his$_6$, ΔPB1-his$_6$, and vector control strains was monitored by a standard halo assay, where 10ul of the indicated α-factor concentration was spotted onto sterile filter disks. **(D)** Mating-dependant transcriptional activation was monitored after pheromone treatment by co-transforming a Fus1::LacZ reporter plasmid with the indicated Bem1p-his$_6$ constructs into Bem1Δ cells. **(E)** Rhodamine phalloidin staining was used to visualize the actin cytoskeleton in pheromone-treated Bem1Δ cells that were transformed with the indicated Bem1 plasmids.

halo or they could be due to a faster recovery of cells from the pheromone-induced cell cycle arrest. Regardless, this result clearly indicates that ΔSH3-his$_6$, Bem1*s3*-his$_6$, and ΔPB1-his$_6$ cells display decreased sensitivity to pheromone induced cell cycle arrest.

To test for the induction of the mating-dependent transcriptional program we transformed our mutants with a plasmid containing a FUS1 promoter-driven β-galactosidase reporter (Fus1::LacZ). Bem1*s3* and ΔPB1 mutants both showed greatly reduced transcriptional induction in response to pheromone treatment and, interestingly, the ΔSH3 mutation alone caused a moderate decrease in reporter activation (Figure 4.3D). This latter result, along with the mating experiments, implies that the loss of SH3-1 and the impairment of SH3-2 by the F166L mutation are the major contributing factors to the severe mating phenotype seen in Bem1-*s3* mutant cells.

Taken together, the above experiments clearly indicate that Bem1-*s3* cells

are less sensitive to pheromone-induced cell cycle arrest, they fail to induce a proper transcriptional response during yeast mating, and they fail dramatically in their execution of the mating morphogenesis program. Not surprisingly, these failures lead to mating defects when Bem1-*s3* cells are mated to other shmooing-compromised strains.

4.5.4 Bem1-s3 cells properly execute the budding morphogenesis program

In order to verify that Bem1-*s3* is a true separation of function allele, we assessed its ability to complement the function of Bem1 during bud emergence. The viability of Bem1-his$_6$, Bem1*s3*-his$_6$, ΔPB1-his$_6$ and vector control strains was assessed at permissive (30^0C) and restrictive (37^0C) temperatures by spotting 10-fold serial dilutions of cells onto solid media plates (Figure 4.4A). All strains tested were viable at 30^0C; however, Bem1-his$_6$ and Bem1*s3*-his$_6$ strains remained viable at 37^OC, whereas viability was poor for ΔPB1-his$_6$ and vector control strains under these restrictive conditions. This result suggests that, in contrast to the ΔPB1 allele, the Bem1-*s3* allele is capable of complementing Bem1 function during bud emergence, even when cells are grown at elevated temperatures.

To further this claim that Bem1-*s3* can fully complement Bem1p function during bud morphogenesis, we examined the cellular morphologies of each of the above Bem1 mutant strains when they are grown at permissive (30^oC) temperatures. We found that asynchronous cultures of Bem1-his$_6$ and Bem1*s3*-his$_6$ strains gave indistinguishable wild-type cell sizes and budding patterns

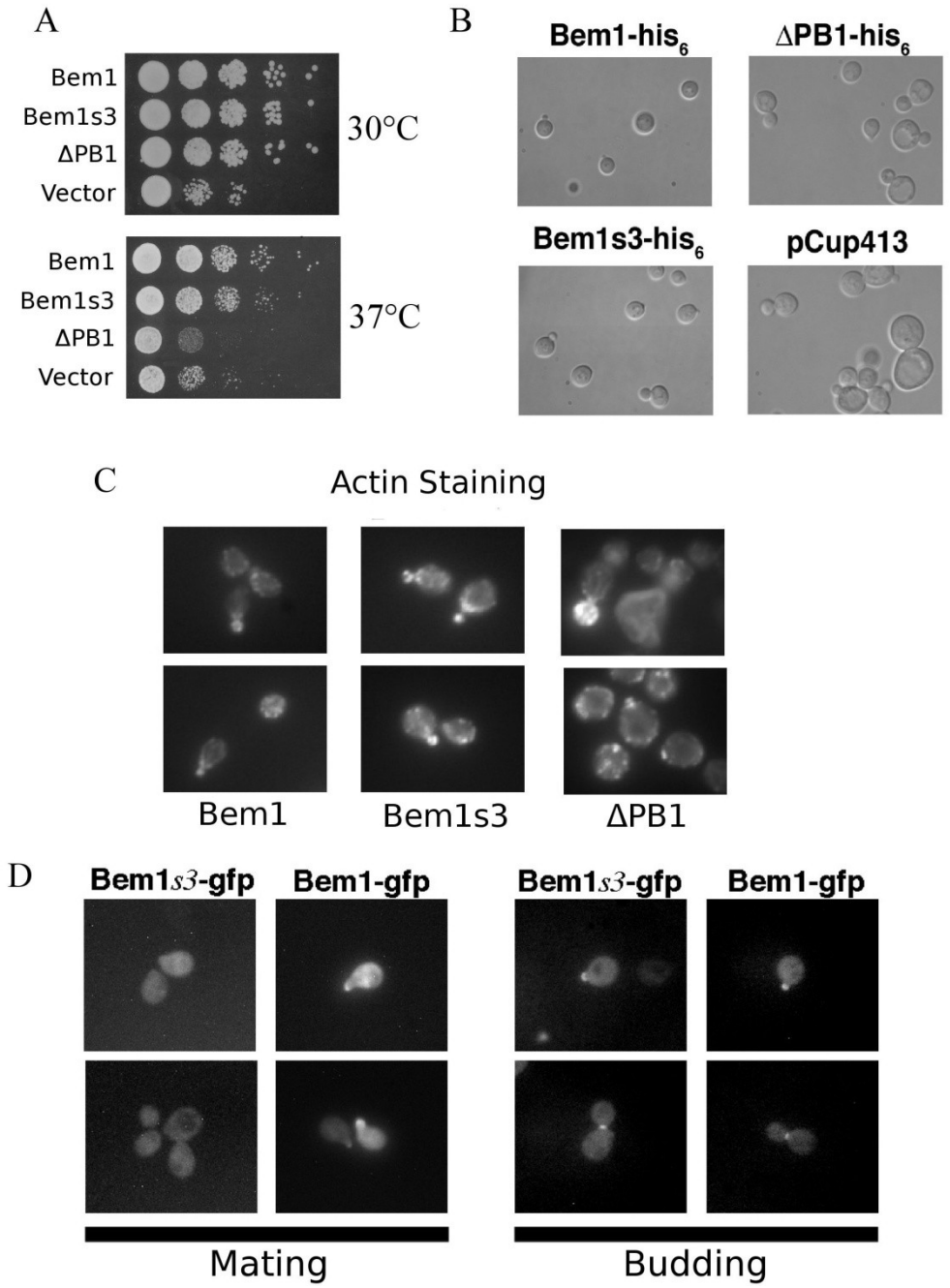

Figure 4.4. Bem1s3 appears to allow for a normal budding morphogenesis program. (A) Viability assay of the indicated Bem1 strains at 30°C and 37°C. (B) Photomicroscopy of asynchronous liquid cultures of the indicated Bem1 strains grown at 30°C under normal budding conditions. (C) Rhodamine phalloidin staining of the actin cytoskeletons of the indicated Bem1 strains under the same budding conditions as in B. (D) Fluorescence microscopy of Bem1-gfp and Bem1s3-gfp cells, as indicated, under mating (leftmost 4 panels) and budding (rightmost 4 panels).

(Figure 4.4B). This is in contrast to the ΔPB1-his$_6$ and vector negative control strains, which both showed a predominance of large unbudded cells and this fits with their inability to complement Bem1p function during bud emergence.

Since the actin cytoskeleton failed to polarize during the mating morphogenesis program for Bem1*s3*-his$_6$ cells, we investigated whether the normal budding morphologies seen in these cells contained the expected polarized actin distribution. Rhodamine phalloidin staining revealed that, like wild-type Bem1-his$_6$ cells, Bem1*s3*-his$_6$ cells exhibited normal actin polarization to incipient bud sites and to growing buds (Figure 4.4C). This was again in contrast to ΔPB1-his$_6$ cells, which displayed a high proportion of large unbudded cells with depolarized actin distributions or, alternatively, misshapen cells with inappropriately polarized actin cytoskeletons (Figure 4.4C). The above results indicate that, in contrast to ΔPB1-his$_6$, the Bem1-his$_6$ and Bem1*s3*-his$_6$ alleles are able to provide the required scaffolding activities of Bem1p for the execution of a normal bud morphogenesis program.

A possible explanation for the clear separation of function provided by the Bem1-*s3* mutant might be that the Bem1*s3* protein is properly targeted to incipient bud sites in budding cells, whereas shmoo-tip targeting fails in mating cells. To address this possibility, we used a recombination-based strategy to replace the C-terminal 6XHis tag with GFP to allow us to visualize these proteins in live cells. The Bem1-GFP and Bem1*s3*-GFP constructs were tested and found to complement Bem1 function exactly like their respective parent Bem1-his$_6$ or Bem1*s3*-his$_6$ plasmids (data not shown). We compared these two GFP-tagged

proteins in their abilities to localize to polarized growth sites in shmooing and budding cells (Figure 4.4D). Both Bem1-GFP and Bem1*s3*-GFP polarized correctly to emerging buds and both of these proteins properly redistributed to bud necks prior to cytokinesis (Figure 4.4D; budding panels). During mating morphogenesis Bem1-GFP localized to the tips of emerging mating projection; however, Bem1*s3*-GFP predominantly failed to polarize in this expected fashion, even in the ~10% of cells that are able to form shmoo-like structures (Figure 4.4D, mating panels). This result suggests that the failure of Bem1-*s3* to complement Bem1p function during mating morphogenesis likely stems from the inability of the Bem1*s3* mutant protein to localize properly to emerging shmoo tips. This failure to localize to shmoo tips would prevent Bem1p-mediated scaffolding activities from positively reinforcing Cdc42p activation by the Cdc24p GEF at the chosen polarized growth site.

4.5.5 The F166L mutation disrupts the binding of PXXP motif-containing proteins to SH3-2

To address the failure of the Bem1-*s3* protein to provide the required scaffolding activities during shmoo formation, we next wished to test whether PXXP-binding of SH3-2 is disrupted by the F166L mutation, as predicted by the CDD alignment with other SH3 domains. Thus, we investigated several well-characterized PXXP-binding partners of SH3-2, namely Ste20p and Boi1/2p [226, 227].

To test binding of SH3-2 to PXXP-containing Bem1p interactors, we

purified recombinant ΔSH3, Bem1*s3* (F166L), W192K, and S252D proteins from *E. coli*. We tested these SH3-2 point mutations in the context of the ΔSH3-1 version of Bem1 because the presence of the SH3-1 domain lessens or blocks the binding of SH3-2 to its PXXP-containing substrates (data not shown). We chose to include the W192K mutation because it has been shown previously that mutation of this conserved SH3 residue in SH3-2 disrupts binding to Ste20p [228]. Our reasons for including the S252D Bem1p mutant in this *in vitro* binding assay were two-fold: firstly, we have identified serine-252 as an in vivo Bem1p phosphorylation site by mass spectrometry (see 4.5.6); secondly, the adjacent

Figure 4.5. F166L in Bem1s3 disrupts the PXXP-binding activities of SH3-2. **(A)** *In vitro* binding experiment where recombinant, untagged ΔSH3-1 Bem1 constructs (as indicated) were run through columns containing glutathione sepharose beads preloaded with equivalent amounts of GST-tagged Ste20p Bem1p-binding domains (BBDs). After extensive washing, any retained protein was eluted with SDS-sample buffer and run on a standard SDS-PAGE gel and visualized by coomassie staining. The position of the eluted Bem1p material as well as the GST-tagged Ste20p BBD is indicated on the right. The lower panel is the loading control gel showing 10% of the amount of each Bem1p construct loaded onto the columns. **(B)** A similar *in vitro* binding experiment done exactly as described in A, except that columns contained GST-tagged Boi1p BBDs. **(C)** The results of a two-hybrid experiment are shown here. Strains containing Bem1-AD fusions, as indicated, were crossed with either strains containing Ste20p-DBD fusions (BBD with or without the CRIB domain, as indicated) (left panels) or a full length Bio2-DBD fusion (right panels). For each experiment the interaction selection plate (-Trp-Leu-His + 5mM 3AT) and the diploid selection plate (-Trp-Leu) is shown. **(D)** Viability assays of the indicated Bem1 constructs at 30^{o}C and 39^{o}C. W192K and P208L mutations are made in the ΔSH3-his$_6$ plasmid, just like the F166L in Bem1s3. The lower half of this panel shows an anti-his$_6$ western blot to determine the expression of the above Bem1p constructs. **(E)** The shmooing efficiency of the indicated strains is displayed here and was calculated the same as in FIG.2B. **(F)** Transcription activation of the Fus1::LacZ in the indicated Bem1 strains after a 60 minute incubation with 5uM α-factor.

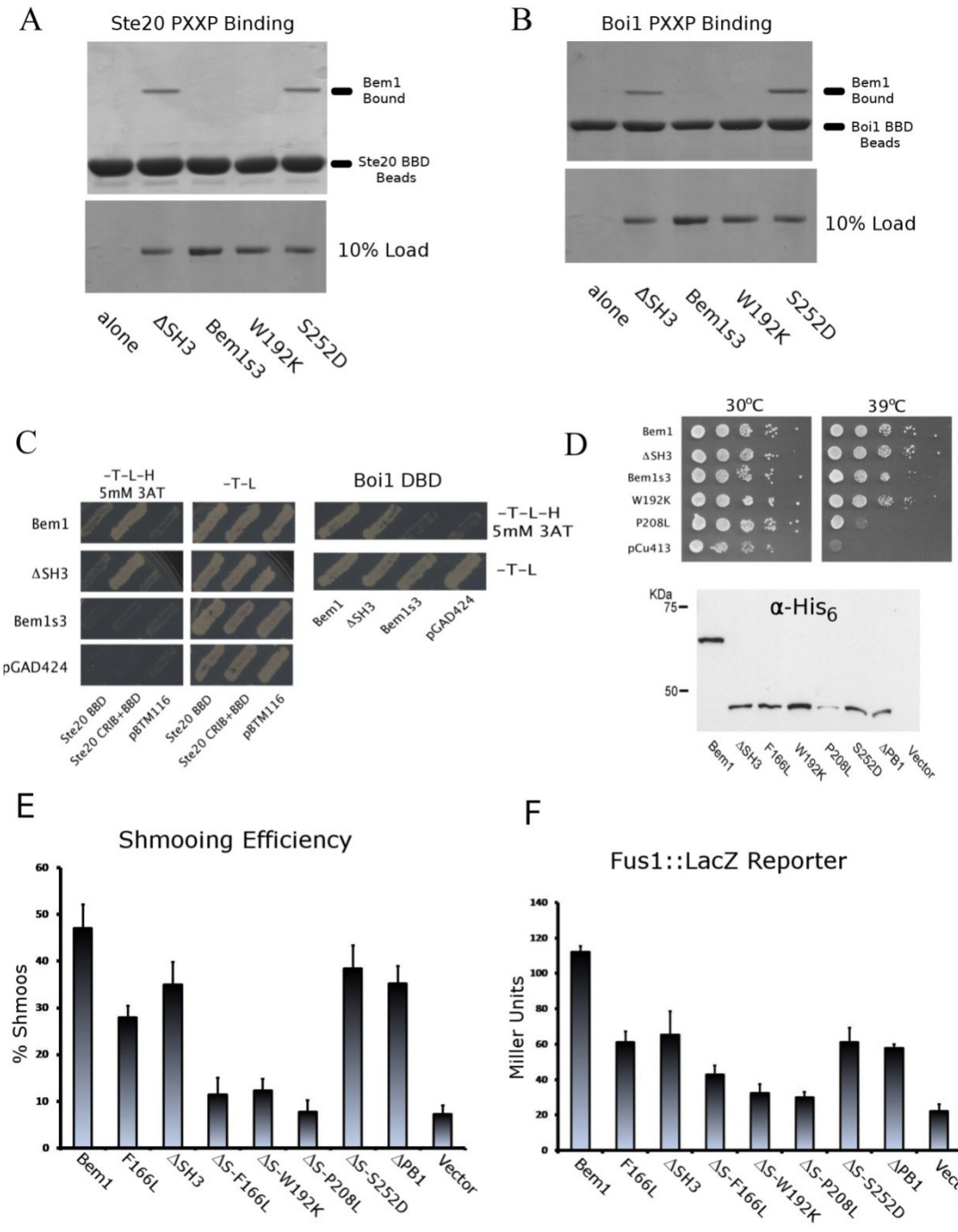
A
Ste20 PXXP Binding
Bem1 Bound
Ste20 BBD Beads
10% Load
alone
ΔSH3
Bem1s3
W192K
S252D
B
Boi1 PXXP Binding
Bem1 Bound
Boi1 BBD Beads
10% Load
alone
ΔSH3
Bem1s3
W192K
S252D
C
-T-L-H 5mM 3AT
-T-L
Boi1 DBD
Bem1
ΔSH3
Bem1s3
pGAD424
-T-L-H 5mM 3AT
-T-L
Bem1
ΔSH3
Bem1s3
pGAD424
Ste20 BBD
Ste20 CRIB+BBD
pBTM116
Ste20 BBD
Ste20 CRIB+BBD
pBTM116
D
30°C
39°C
Bem1
ΔSH3
Bem1s3
W192K
P208L
pCu413
KDa
75
50
α-His6
Bem1
ΔSH3
F166L
W192K
P208L
S252D
ΔPB1
Vector
E
Shmooing Efficiency
% Shmoos
0
10
20
30
40
50
60
Bem1
F166L
ΔSH3
ΔS-F166L
ΔS-W192K
ΔS-P208L
ΔS-S252D
ΔPB1
Vector
F
Fus1::LacZ Reporter
Miller Units
0
20
40
60
80
100
120
140
Bem1
F166L
ΔSH3
ΔS-F166L
ΔS-W192K
ΔS-P208L
ΔS-S252D
ΔPB1
Vector

asparagine 253 residue has been shown to be critical for the binding of the CI domain of Bem1p to Cdc42p and this residue was shown to be unimportant for binding to Ste20p [228].

GST-tagged fragments of Ste20p and Boi1p that contain their expected polyproline-containing Bem1p binding domains (BBDs), were also purified and left bound to the glutathione beads (Ste20 BBD beads and Boi1 BBD beads). We incubated these BBD-containing beads with equivalent amounts of the various untagged ΔSH3-1 constructs described above to allow binding to occur and then washed these BBD beads extensively. SDS-PAGE analysis confirmed, as expected, that ΔSH3 and S252D retained the ability to bind to both Ste20p- and Boi1p- BBD beads (Figure 4.5A, B; ΔSH3 and S252D lanes). In contrast, both Bem1*s3* (F166L) and W192K failed to bind to either Ste20p- or Boi1p- BBD beads (Figure 4.5A,B; Bem1*s3* and W192K lanes). This latter result suggests that the F166L mutation in Bem1*s3* abrogates binding to the PXXP-motifs found within Ste20p and Boi1p, as does the W192K SH3-2 mutant. The unaltered PXXP-binding of S252D fits with the results of others who found that an N253D mutant failed to bind to Cdc42p but retained significant Ste20p-binding [228].

To further support the above *in vitro* binding data, we used a standard yeast two-hybrid assay to detect interactions between our Bem1p mutants and the PXXP-containing binding proteins Ste20p and Boi2p. Full length Bem1p and ΔSH3 behaved similarly in that they both interacted with a BBD+CRIB fragment of Ste20p and full length Boi2p, whereas Bem1*s3* failed to interact with either Ste20p or Boi2p in this two-hybrid assay (Figure 4.5C). It should be noted that

the interaction of these Bem1 constructs with the Ste20 BBD two-hybrid construct was very weak when compared to the CRIB+BBD fragment. This weaker two-hybrid interaction for the minimal Ste20p BBD fragment is very likely due to the loss of residues that are important for a robust interaction with SH3-2 of Bem1p. Regardless, the failure of Bem1*s3* to interact with Ste20p or Boi1/2p using both *in vitro* binding and two-hybrid analysis strongly supports our hypothesis that the F166L mutation in Bem1-*s3* abrogates binding of SH3-2 to PXXP-containing binding partners.

If Bem1*s3* is truly disrupted in its PXXP-binding activities as our above results clearly suggest, then the mating deficiencies seen in Bem1*s3* cells should be recapitulated when other SH3-2 mutations are made in the context of ΔSH3-1. To investigate this we created W192K, P208L and S252D mutations in the context of ΔSH3-his$_6$ in order to compare them to the mating defects we have observed for Bem1*s3*-his$_6$. The W192K and S252D mutants complemented Bem1 function when grown at elevated temperature, whereas P208L did not (Figure 4.5D; top panel). Western blotting with an anti-His$_6$ antibody showed that the failure of P208L to complement Bem1 function is likely attributable to its markedly decreased expression levels (Figure 4.5D; lower panel). It should be noted that the P208L SH3-2 mutation has been shown previously to result in reduced protein expression (or stability) *in vivo* [219].

We next compared the shmooing efficiencies of each of these SH3-2 mutants and we also assessed the shmooing efficiency of the F166L mutation when made in the context of full length Bem1p. In this assay we found that

W192K and P208L, when placed in the context of a ΔSH3-1 Bem1p, recapitulated the severity of the shmoo formation defect that we observed for Bem1*s3* (Figure 4.5E). The full-length Bem1p-F166L mutant also showed decreased shmooing efficiencies when compared to full-length wild-type Bem1p (Figure 4.5E; F166L bar). Interestingly, the shmooing defect of Bem1-*s3* appears to be of the same magnitude of the additive defects of the F166L mutant and the ΔSH3 mutant. Also of note, the S252D mutation formed shmoos as efficiently as its ΔSH3 control so we conclude that the S252D mutation has no significant impact on mating morphogenesis when made in the context of ΔSH3.

We next examined the ability of these various SH3-2 mutants to activate the pheromone-induced transcriptional program, again by the employing the Fus1::lacZ reporter (Figure 4.5F). The W192K and P208L mutations in the context of ΔSH3, like the F166L mutation in Bem1*s3*, dramatically reduced the transcriptional activation of the Fus1::lacZ reporter, whereas the S252D mutant retained the same transcriptional activation that was seen with the ΔSH3 parent construct. The F166L mutation when made in the context of full-length Bem1p caused a defect in pheromone-induced transcription (Figure 4.5F; F166L bar) that was intermediate between wild-type full-length Bem1p and Bem1*s3*.

When taken all together, the above results support our hypothesis that the F166L mutation found in Bem1*s3* disrupts the PXXP-binding activity of SH3-2, much like the canonical W192K and P208L SH3 mutations. Furthermore, comparison of full-length Bem1p-F166L and ΔSH3-F166L suggests that the severe mating defect observed in Bem1*s3* cells results from the combined

disruption of SH3-2 and loss of SH3-1. Our results therefore imply that SH3-1 and SH3-2 make separate and additive contributions to mating morphogenesis and the separation-of-function displayed by the Bem1-*s3* mutant further suggests that these SH3-mediated interactions are largely dispensable for proper bud morphogenesis. For bud morphogenesis, it appears the primary scaffolding activity of Bem1p is mediated through its binding to Cdc24p and Cdc42p, hence the strong bud formation defects observed for ΔPB1 Bem1p mutants.

4.5.6 Mass spectrometry analysis of purified Bem1p-complexes identifies novel protein-protein interactors and phosphorylation sites of Bem1p.

In order to extend our understanding of the protein scaffolding activities of Bem1p, we decided to employ a proteomic approach to identify proteins found in Bem1p-complexes, which we isolated by affinity purification of Bem1p from actively growing yeast cells. We transformed Bem1Δ cells with a plasmid that expresses an N-terminal GST-tagged Bem1p fusion (GST-Bem1p) and an unrelated GST fusion (GST-Gin4p) plasmid, which served as a negative control to identify non-specific binding to the GSH resin or the GST affinity tag. These plasmids were obtained from a previously published yeast GST-fusion library [344]. Importantly, N-terminally tagged GST-Bem1p has been previously shown to complement the Bem1Δ mutant and was used to identify Bem1p-interacting proteins involved in mating MAPK signaling by western blotting GST-Bem1p pull-downs [242]. We wished to extend this previous western blotting-based examination of Bem1p-complexes by examining the proteins present in GST-

Bem1p complexes in an unbiased mass spectrometry-based approach. Our goal was to identify novel Bem1p-interacting proteins that might indicate new roles for Bem1 and thereby extend our understanding of its scaffolding activities.

Table 4.1. Known Bem1p-interacting proteins identified by mass spectrometry

Protein	Peptides	Mascot Score	Biological Process
Cla4p	2	66	Establishment of cell polarity
Boi1p	12	72	Establishment of cell polarity
Boi2p	3	47	Establishment of cell polarity
Sec8p	2	40	Bud site selection, exocytosis
Sec3p	2	39	Bud site selection, exocytosis

Importantly, our mass spectrometry-based analysis of GST-Bem1p complexes identified five previously characterized Bem1p-interacting proteins and the identities, peptide counts, mascot scores, and previously annotated biological functions of these known Bem1p-interactors are presented in Table 4.1. The absence of other known Bem1p-interactors like Cdc24p, Cdc42p, and Ste20p may relate to their low abundance or to limitations in our ability to detect their corresponding tryptic peptides using this tandem reverse phase HPLC-MS/MS approach. Regardless, the identification of multiple known physical interactors of Bem1p suggests that we have isolated biologically relevant Bem1p complexes. Further support of this comes from our ability to detect a previously reported physical association between GST-Gin4p and Nap1p [352] in our negative control sample (data not shown). Analysis of proteins that were common to both GST-Bem1p and GST-Gin4p negative control pull-downs yielded a number of non-

specific physical interactions (Supplementary Table 4.1). Most of these non-specific physical interactors are proteins with known functions in protein folding or high-abundance metabolic proteins that have been previously reported as non-specific physical interactors in proteomic studies [266, 353].

Table 4.2. Novel Bem1p-interacting proteins detected by mass spectrometry

Protein	Peptides	Mascot Score	Biological Process
Gic1p	3	40	establishment of cell polarity
Pkc1p	**3**	**46**	**actin polarization, CWI signaling**
Pkh2p	**4**	**40**	**Sphingolipid signaling, CWI signaling**
Bem4p	**4**	**56**	**actin polarization, Rho1p-binding**
Zeo1p	**2**	**67**	**cell wall organization, stress response**
Sph1p	**3**	**39**	**actin polarization, Rho1p signaling**
Ssk1p	5	57	Osmolarity stress signaling
Cyr1p	11	69	G-protein signaling, cAMP signaling
Ase1p	4	47	cytokinesis, mitotic spindle stability
Nud1p	5	46	Mitotic exit, chromosome segregation
Hsl1p	7	44	Cell cycle regulation, G_2-M
She3p	5	41	mRNA localization
Mlp1p	8	44	mRNA export, nuclear import
Mlp2p	9	57	mRNA export, nuclear import
Ubi4p	2	76	protein ubiquitination
Mec1p	5	40	DNA damage response
Tel1p	8	60	DNA damage response
Mrc1p	4	71	DNA replication checkpoint
Dbf4p	3	37	DNA replication initiation
Mcm5p	7	40	DNA replication, MCM complex,
Mcm4p	2	38	DNA replication, MCM complex
Mcm3p	2	37	DNA replication, MCM complex
Mcm6p	1	36	DNA replication, MCM complex
Kap95p	3	86	protein import into nucleus
Kap123p	2	58	protein import into nucleus

BOLD= CWI-related proteins

Our mass spectrometry analysis of affinity purified GST-Bem1p

complexes identified peptides from 25 unique proteins that have not been previously reported to physically interact with Bem1p (Table 4.2). These novel Bem1p physical interactors include proteins involved in numerous biological processes and amongst these novel interactors were five different proteins with known connections to CWI signaling, namely Pkc1p, Pkh2p, Bem4p, Zeo1p, and Sph1p. Given that actin cytoskeleton rearrangements are known to occur in response to cell wall stressors [181], and also given that high-throughput studies have shown that BEM1 displays genetic interactors with numerous components of CWI signaling [263, 270], we felt that further examination of the physical associations of CWI signaling proteins with Bem1p was warranted.

4.5.7 Physical interactions of Bem1p and the phenotype of Bem1Δ cells implicate Bem1p in cell wall stress tolerance

To assess the potential involvement of Bem1p in CWI signaling, we first wished to confirm that Bem1p physically interacts with proteins that are implicated in the CWI signaling. We used standard pull-down procedures with subsequent western blotting visualization to confirm the interaction of Bem1p with CWI proteins because this approach proved successful in identifying the role of Bem1p in pheromone-induced MAPK signaling [242]. We co-transformed Bem1Δ cells with a Bem1-4FLAG plasmid and with plasmids encoding CWI-related proteins from a previously described *S. cerevisiae* mORF plasmid library [347]. The fusion proteins expressed from these mORF plasmids contain a C-terminal triple-affinity tag that is composed of His_6-HA-ZZdomain. We

employed a single-step pull-down approach by allowing mORF-tagged CWI proteins to bind to IgG Sepharose via their C-terminal protein A (ZZ) domain. These IgG pull-downs of CWI-related mORF fusions were done in the presence of Bem1-4FLAG and so the amount of coprecipitated Bem1-4FLAG that came down with the IgG-purified mORF fusion proteins was evaluated by anti-FLAG western (Figure 4.6A; top panel). Reprobing of the membrane with anti-His_6 primary antibodies allowed for visualization of the amount of each mORF fusion protein that was affinity purified by the IgG Sepharose beads (Figure 4.6A: middle panel). Total cell extracts were also probed with anti-FLAG antibodies to ensure that equal amounts of the Bem1-4FLAG protein was expressed in the mORF fusion lysates prior to IgG-purification (Figure 4.6A; bottom panel).

In this assay both the Cdc24p- and Boi2p- mORF fusion proteins were able to successfully coprecipitate Bem1-4FLAG, which suggested that our assay is capable of detecting known Bem1p-interacting proteins. Since we tested numerous CWI proteins that were not observed as Bem1p-interactors by mass spectrometry, we assumed some of these mORF fusions would fail to coprecipitate Bem1-4FLAG and hence serve as our negative controls for this assay. We tested all of the CWI signaling proteins that were present in the mORF fusion collection and found that Bem1-4FLAG was able to interact with many of these mORF fusions (Figure 4.6A). Strong Bem1-interactors included: Rho1p, Pkh2p, Pkh3p, and each of the components of the CWI MAPK pathway

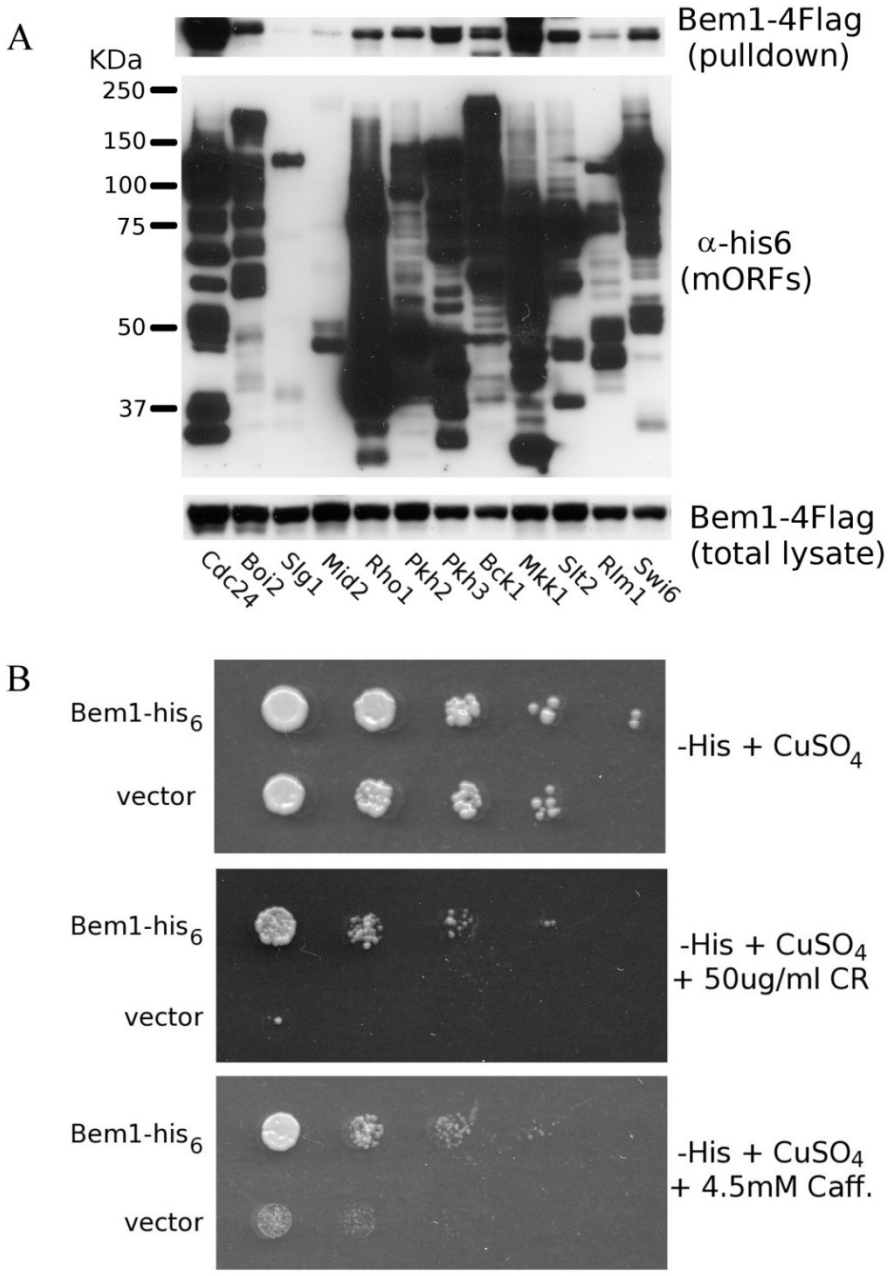

Figure 4.6. Bem1p is involved in the CWI stress response. **(A)** Physical interactions between Bem1p and CWI proteins were assessed by IgG pull-downs of various CWI mORF proteins and subsequent visualization of the amount of coprecipitated Bem1p-4FLAG by western blotting (upper-most panel). The amount of each pulled-down CWI mORF fusion protein was assessed by reprobing the membrane with α-His_6 antibodies (middle panel). The amount of Bem1-4FLAG present in each of CWI mORF lysates prior to IgG purification is also shown (lowest panel). **(B)** Serial diluation growth assay of Bem1-his_6- and vector- transformed Bem1Δ cells on standard (top panel), congo red (CR; middle panel) and caffeine (Caff; bottom panel) –His solid media plates. Copper sulphate ($CuSO_4$) (50 uM) was included to induce the expression of Bem1p.

Bck1p (MAPKKK), Mkk1p (MAPKK) and Slt2p (MAPK). We were initially surprised at the number of CWI proteins that appear to be interacting with Bem1p but these results are reminiscent of the binding of Bem1p to multiple proteins in the mating MAPK pathway. Since Bem1p binds to the mating MAPK scaffold protein Ste5p, it was found in complexes that contained all of the protein kinases of the mating MAPK pathway [242]. From our physical interaction data and from the known role of Bem1p in pheromone MAPK signaling, it seems likely that an analogous role for Bem1p in CWI signaling, whereby it interacts with multiple CWI proteins through an as yet unidentified CWI scaffold protein.

Given the novel physical associations that we have detected for Bem1p with CWI signaling proteins, we next wished to examine if Bem1p is required for *S. cerevisiae* cells to tolerate exposure to cell wall destabilizing agents. To do this we used a previously reported [348] serial dilution growth assay to see if Bem1-his_6 and vector transformed Bem1Δ cells were able to grow on congo red- and caffeine- containing media plates (Figure 4.6B). The results of this growth assay clearly indicated that Bem1-his_6 cells can grow normally on plates that contained 50 ug/ml of congo red (CR) or 4.5 mM caffeine (Caff.), whereas vector-transformed Bem1Δ cells showed significantly impaired growth under these same cell wall destabilizing conditions. This result indicates that Bem1p is required for an appropriate response to cell wall destabilizing agents.

4.5.8 Phosphorylation of Bem1p at S458 regulates cell wall stress tolerance.

In addition to identifying suspected novel Bem1p physical interactions, our mass spectrometry analysis of affinity-purified Bem1p complexes also allowed us to identify *in vivo* post-translational modifications of Bem1p. In order to identify post-translational modifications of Bem1p, we used the mascot search engine to identify tryptic peptides in our GST-Bem1p mass spec data (see 4.5.6) that have masses that correspond to phosphorylated or ubiquitinated Bem1p peptide species. The results of this search for post-translationally modified Bem1p tryptic peptides is presented in Table 4.3 and these results strongly suggest that Bem1p can be phosphorylated or ubiquitinated *in vivo* at numerous different residues. Importantly, Bem1p has previously been reported to be a phosphoprotein *in vivo* [246] and was found to be a substrate of Cdc28p [244-246], which is the primary CDK in *S. cerevisiae*. Despite detecting numerous novel phosphoacceptor sites in Bem1p, we were not able to detect phosphorylation of serine-72, which is the previously published Cdc28p-dependent phosphorylation site [246]. Our lack of detection of serine-72 phosphorylation is most likely due to the low occupancy of this phosphoacceptor site in the asynchronously growing cells that we used to purify our GST-Bem1p samples.

Serine-458 (S458) was the highest scoring Bem1p phosphorylation site that we identified and this phosphopeptide was detected in numerous subsequent biological replicates of this GST-Bem1p mass spectrometry experiment (data not shown). This S458 phosphorylation site lies in the linker region between the PX and PB1 domains of Bem1p and so it is difficult to predict the possible function of

Table 4.3. Bem1p peptides modified by phosphorylation or ubiquitination

Peptide	Modification	Mascot Score	Modified Residue
L(**pS)**DLSLSGSK	Phosphorylation	82.4	S458
A(**pS)**NISLGSVEQQQQQSITK	Phosphorylation	37.1	S252
TD(**pS)**QVSNIIQAK	Phosphorylation	46.0	S534
GDTTY(**ggK)**ELR	Ubiquitination	54.6	K501
TDSQVSNIIQA(**ggK)**LK	Ubiquitination	46.2	K543
SA(**ggK)**LVDGELLVK	Ubiquitination	45.1	K276
YLSSSSTPV(**ggK)**SQR	Ubiquitination	25.5	K54

(pS)- phosphorylated serine
(ggK)- lysine that contained a double-glycine ubiquitin remnant

this post-translation modification based on its location in the primary sequence of Bem1p. As mentioned in section 4.5.5, we detected S252 as a putative Bem1p phosphorylation site and this site is of particular interest because it lies within the CI domain of Bem1p. This S252 phosphoacceptor site sits adjacent to an asparagine residue (N253) that has been shown to be critical for the Bem1p-Cdc42p interaction [228]. The S534 phosphorylation site that we detected lies within the PB1 domain of Bem1p and the C-terminal lysine of this peptide was also detected as the second highest scoring ubiquitination site. Given its location in the PB1 domain it is plausible that either phosphorylation of S534 or ubiquitination of K543 might provide a means to regulate the Bem1p-Cdc24p interaction or, alternatively, these modifications could regulate the protein stability of Bem1p.

Given that we identified numerous putative phosphorylation sites in Bem1p and also given that Bem1p is a known phosphoprotein *in vivo*, we next wished to identify phenotypes associated with one or more of these

phosphorylation sites. We generated non-phosphorylatable (S-to-A) and phospho-mimic (S-to-D or -E) mutants of the S252, S458, and S534 phosphorylation sites and we chose to construct these mutants in our Bem1-his_6 plasmid. We transformed these phosphomutant plasmids into Bem1Δ cells and visualized their protein expression levels in total yeast cell extracts by anti-Bem1p western blotting (Figure 4.7A). All of these Bem1p-phosphomutants gave similar expression levels except for Bem1p-S534E, which was not detectable in steady state western blotting experiments. This failure to detect Bem1p-S534E was also consistent in anti-His_6 western blots (data not shown), so it is very unlikely that this mutation has simply disrupted epitopes that are required for detection by our polyclonal anti-Bem1p antibodies. Interestingly, the non-phosphorylatable Bem1p-S458A mutant protein displayed an increased mobility in SDS-PAGE gels and this suggests that S458 of Bem1p is a bona fide *in vivo* phosphorylation site.

We next wished to examine phenotypes of our Bem1p phosphomutants and so we started by examining their ability to complement Bem1p function during bud emergence at elevated growth temperatures and during growth in the presence of cell wall destabilizing agents. The results of this serial dilution growth assay clearly indicated that each of our tested phosphomutants, unlike vector-transformed negative control cells, was able to complement a Bem1Δ function at elevated growth temperatures (37^{o}C) (Figure 4.7B; middle panel). This suggests that none of our Bem1p phosphomutants are dramatically impaired in their ability to provide the required scaffolding activities of Bem1p during bud emergence. This was a particularly surprising observation for the Bem1p-S534E

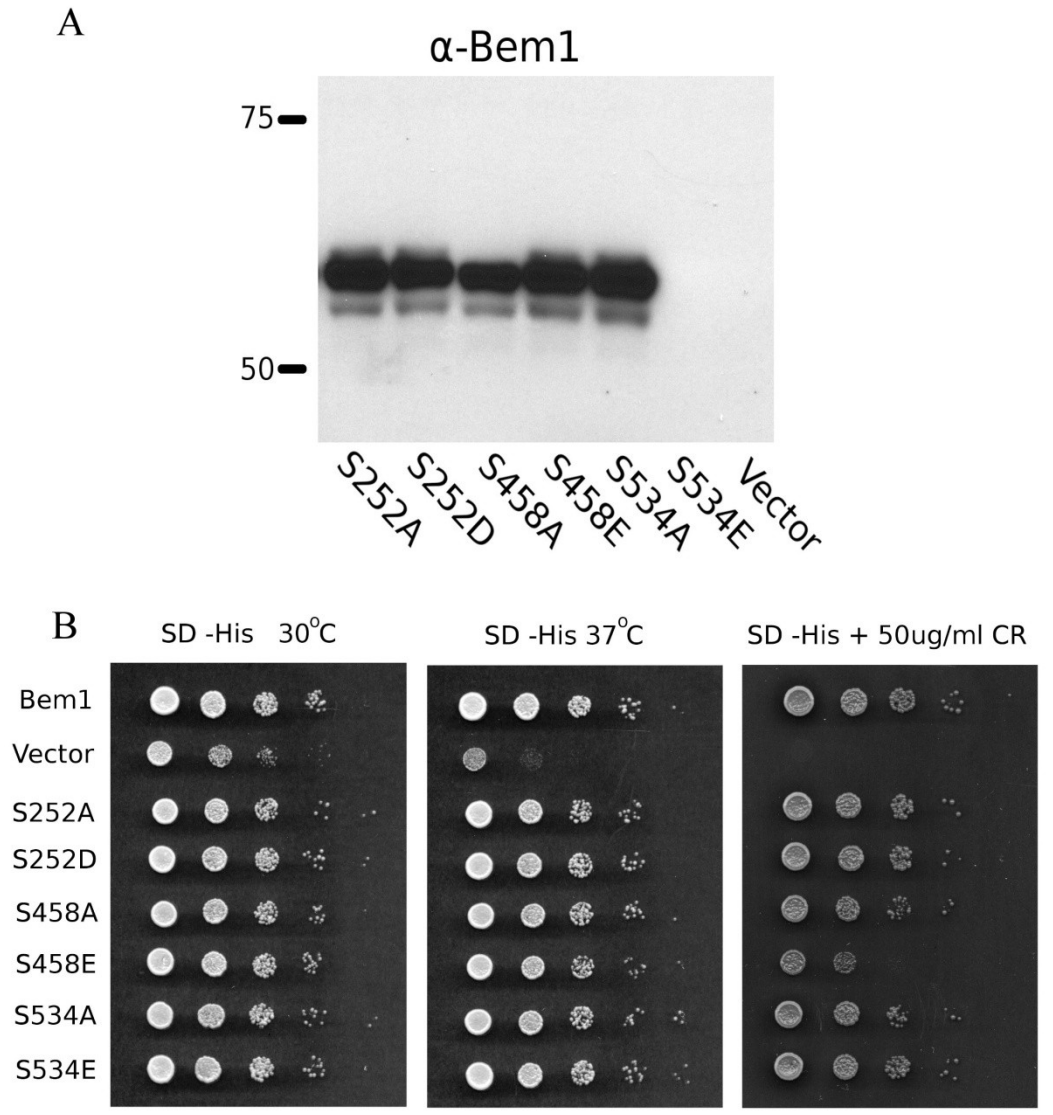

Figure 4.7. Bem1p is phosphorylated at S458 to regulate CWI stress tolerance. **(A)** Western blotting (α-Bem1p) of total cell extracts of the indicated Bem1p phosphomutant strains suggests that S458A is a relevant *in vivo* phosphoacceptor site due to the observed increase in electrophoretic mobility for Bem1p-S458A. Bem1p-S534E was not detected in this steady state western blotting experiment for unknown reasons. **(B)** Growth of Bem1p phosphomutant strains on standard –His media (left panel; 30°C), at elevated temperature (middle panel; 37°C), and in the presence of the cell wall destabilizing agent, congo red (left panel; CR, 30°C).

phosphomutant because it was reproducibly not detected in western blotting experiments of yeast total cell extracts.

When we tested the growth of our Bem1p phosphomutants on solid media plates that contained 50 ug/ml of congo red dye (Figure 4.7B; right panel) we noticed that Bem1p-S458E, unlike the rest of our Bem1p phosphomutants, showed an increased sensitivity to this cell wall destabilizing agent (Figure 4.7B; right panel). When taken together, these results suggest that S458 is a biologically relevant *in vivo* phosphorylation site and that phosphorylation of S458 impacts the ability of Bem1p to provide its required function in response to cell wall destabilizing agents. Future studies of the Bem1p-S458 phosphomutants that we have generated here should provide valuable insight into the novel role we have described here for Bem1p in mediating *S. cerevisiae*`s response to cell wall stressors.

4.6 Discussion

In this study we have isolated a novel separation of function mutant, called Bem1-*s3,* which fails dramatically at mating morphogenesis but is capable of normal bud morphogenesis. We found that Bem1-*s3* contained a phenylalanine to leucine substitution mutation that disrupted the PXXP-binding capacity of SH3-2 and when this was combined with the truncation of SH3-1, it resulted in the severe mating phenotypes that we observed in Bem1-*s3* cells. These results

provide direct evidence that efficient mating morphogenesis requires the protein-protein interactions mediated by both SH3 domains of Bem1p. Furthermore, our mass spectrometry analysis of Bem1p-complexes and post-translational modifications of Bem1p allowed us to propose a novel role for this scaffold protein in the CWI response to cell wall stressors.

Previous work has shown that two adjacent PXXP motifs in Ste20p are important for mediating its interaction with the SH3-2 domain of Bem1p and that this interaction contributes to the yeast mating response [227, 228]. Our results support these previous findings because we showed that the F166L mutation of Bem1-*s3* impaired the binding of the SH3-2 to the polyproline-containing BBD region of Ste20p (Figure 4.5). We have also extended previous findings by showing that loss of SH3-1 also contributes to the dramatic mating defects seen in our Bem1-*s3* separation-of-function mutant. The contribution of SH3-1 to the scaffolding activities of Bem1p during the yeast mating response remains an unanswered question that we feel should be addressed in future studies.

The SH3-1 domain of Bem1p has been shown to be regulated by CDK phosphorylation [246] and SH3-1 has been shown to mediate the interaction of Bem1p with the exocyst complex, through its direct interaction with the C-terminal region of Sec15p [349]. Intriguingly, loss of SH3-1 has been shown to improve the two-hybrid interaction between Bem1p and Ste20p [340] and reduces its two-hybrid interaction with GTP-Cdc42p [217] and Ste5p [242]. Given these previous implications for SH3-1 in Bem1p function, we were somewhat surprised to find that loss of SH3-1 did not result in more apparent morphological

phenotypes. Nevertheless, this finding is supported by the work of others who have shown that deletion of SH3-1 had no effect on growth rate or the ability to complement Bem1Δ at elevated temperature [349]. So it now seems clear that loss of SH3-1 of Bem1p does not dramatically impair the cells ability to complete a productive budding cycle. This is also supported by a recent study on the *Aspergillus nidulans* ortholog of Bem1p, called BemA, where these authors showed that SH3-1 of BemA is dispensable for normal cell morphology and conidiation in *A. nidulans* [354].

Although loss of SH3-1 did not impair the cells ability to form morphologically correct shmoos, truncation of SH3-1 did modestly reduce both shmooing efficiency (Figure 4.2B and 4.5E) and induction of the mating transcriptional response (Figure 4.3D and 4.5F). These phenotypes suggest that loss of SH3-1 reduces the signaling capacity of the mating MAPK pathway. This reduction in MAPK signaling in ΔSH3-1 cells is particularly intriguing given that the predicted PXXP-binding consensus of the SH3-1 domain of Bem1p has been shown to be PPxVxPY (where X is any amino acid) [355] and a close match of this consensus motif can be found in the N-terminus of Ste5p (153-PPKVAPF-159). Furthermore it has been shown that Ste5p can interact with Bem1p and that N-terminal truncation of Bem1p leads to reduced Ste5p-binding [242]. From these data we find it tempting to speculate that the contribution of SH3-1 of Bem1p to the mating MAPK signaling response may be its involvement in mediating the physical interaction between Bem1p and Ste5p; however, this hypothesis has proven difficult to confirm because the Bem1p-Ste5p two-hybrid

interaction that has been previously reported [242] is an extremely weak interaction using our two-hybrid reagents (data not shown).

The failure of Bem1*s3*-GFP to localize to shmoo tips indicates that SH3-mediated interactions are required for the proper localization of Bem1p during shmoo formation. Given the above implications that SH3-1 contributes to the interaction of Ste5p with Bem1p, it is tempting to speculate that Ste5p may help to recruit Bem1p to activated Gβ subunits (Ste4p). Once recruited to Ste4p, Bem1p is expected to contribute to Cdc42p signaling by bringing it into close association with its upstream activator (Cdc24p) and downstream effector (Ste20p).

The fact that Bem1s3-GFP retains a normal localization pattern in budding cells reveals that non-SH3 mediated interactions allow for the proper targeting of Bem1p to incipient bud sites, bud tips, and to bud necks just prior to cytokinesis. It has been shown that the targeting of Bem1p to incipient bud sites is dependent on GTP-bound Cdc42p [231] and this interaction with GTP-Cdc42p has been shown to be mediated by CI domain of Bem1p [228]. On the basis of these data it seems likely that Bem1*s3*-GFP is properly localized in budding cells in an SH3-independent manner via the interaction of its CI domain with GTP-Cdc42p.

Our data shows that the F166L mutation that we identified in SH3-2 abolishes the interaction of Bem1p with the PXXP-containing regions of Ste20p and Boi1/2p (Figure 4.5). Alignments of the SH3-2 domain of Bem1p with other fungal and human SH3 domains (Figure 4.3A) suggested that phenylalanine-166

has been evolutionarily conserved and this conservation almost certainly stems from its importance in mediating contacts with target PXXP motifs. Given the conservation and significance of this phenylalanine in mediating SH3-PXXP contacts, we suggest that this mutation could be employed as a canonical PXXP-binding mutation and this hypothesis should be tested in future studies on other, functionally diverse, SH3 domains. This phenylalanine to leucine substitution is a modest change compared to the proline to leucine substitution mutations that are frequently used to disrupt PXXP-binding of SH3 domains. Furthermore, substituting a leucine for a phenylalanine does not add an extra basic charge or trypsin cleavage site, like the commonly employed tryptophan-to-lysine SH3 domain mutation does. These features should make the phenylalanine to leucine substitution mutation that we have identified here an ideal mutation to make precise changes to the PXXP-binding capacity of SH3 domains.

Given that the SH3 domain-mediated interactions of Bem1p are absent in Bem1*s3* cells, and yet these cells remain viable, it is clear that the previously reported shared essential function of the yeast PAKs, Ste20p and Cla4p [356], must not have a strict requirement for Bem1p-mediated scaffolding. The CRIB domains present in these two PAKs, which can bind directly to GTP-Cdc42, must therefore be sufficient to allow for the proper targeting and execution of their shared essential kinase function during vegetative growth.

The requirement for SH3-mediated scaffolding activities during yeast mating and budding, most notably when positional landmarks are absent, provides the foundation for a general mechanism that underlies eukaryotic morphogenesis.

Recently it has even been suggested that tethering of a Cdc42p-GEF-PAK complex, which is mediated by Bem1p in *S. cerevisiae*, is a conserved requirement for eukaryotic symmetry breaking [224]. Future studies should provide additional insight into how these important protein-protein interactions are regulated to provide control of the redistribution of the Cdc42p-dependent cell polarity machinery that is required during the reorientation of cell growth.

Our mass spectrometry analysis of Bem1p-complexes allowed us to identify numerous CWI-related proteins, which directed us to evaluate the role of Bem1p in the response to cell wall stressors. We decided to examine the interaction of Bem1p with known CWI proteins, but we were unable to follow up on all of our detected mass spectrometry interactions and so confirming these remaining putative Bem1p-interacting proteins should be a priority of future studies. Of particular interest are the two karyopherin proteins that we detected because they suggest that Bem1p may have an unappreciated nuclear localization and perhaps also specific nuclear functions. A nuclear role for *S. cerevisiae* Bem1p is supported by the fact that *Ustilago maydis* Bem1 was shown recently to contain a nuclear export sequence and was found to localize to the nucleus when its nuclear export was disrupted [357].

Several of our mass spectrometry Bem1p-interactions point towards possible nuclear functions for Bem1p. We detected four of the six proteins of the mini-chromosome maintenance (MCM) complex, which is found at chromosomal origins of replication, and Bem1 has been previously shown to be one of only 28 genes that are transcriptionally co-regulated with these MCM genes [358]. Also

given that we found numerous proteins involved in DNA damage checkpoints (Mec1p, Tel1p) and DNA replication (Dbf4, Mrc1p), it would seem that our mass spectrometry data strongly encourages future studies to evaluate possible nuclear roles for Bem1p.

In this study we were able to show that numerous CWI-related proteins physically associate with Bem1p-complexes by doing conventional pull-down/coprecipitation experiments (Figure 4.6A). These physical associations, combined with previously reported high-throughput genetic interaction data [263], suggested to us that Bem1p may play a role in CWI signaling responses (see 1.7.2). The sensitivity of Bem1Δ and Bem1p-S458E phosphomutants to cell wall stressors strongly supports our hypothesis that Bem1p contributes to the homeostatic responses that allow yeast to tolerate cell wall stressors. Future studies will also be required to confirm and evaluate the significance of the other phosphorylation and ubiquitination sites we identified.

The precise role of Bem1p in mediating appropriate responses to cell wall stressors remains unclear; however, we find it tempting to speculate that Bem1p may contribute to CWI responses in an analogous fashion to its role in the mating response. We hypothesize that Bem1p may contribute to CWI MAPK signaling and provide a physical link between these CWI signaling proteins and regulators of the actin cytoskeleton. This putative role in linking CWI signaling and the actin cytoskeleton-regulating machinery suggests that Bem1p may be important for proper execution of the actin cytoskeleton redistributions that have been previously shown to accompany cell wall stress insults [181].

The novel CWI function of Bem1p that we have detailed in this study strongly suggests that future studies should closely evaluate the precise role of Bem1p in this important cellular homeostatic response. More generally, future research should aim to better our understanding of the interconnectedness of actin cytoskeleton dynamics and cellular stress response mechanisms. Such research will undoubtedly improve our understanding of the homeostatic mechanisms that yeast cells employ to adapt to their extracellular environments and this improved understanding may be invaluable in designing new anti-fungal therapies.

4.7 Acknowledgments

This work was funded by grants from the Canadian Institutes for Health Research to Dr. David Y. Thomas and Dr. Malcolm Whiteway. Daniel Waller was supported by the CIHR STIHR chemical biology training program.

CHAPTER 5

General Discussion

5.1 Summary

This thesis describes the examination of multiple cellular stress signaling mechanisms in yeast. Chapter two describes the identification of the primary phosphorylation site within the cytosolic tail of *S. pombe* calnexin. This finding suggests that phosphorylation of the cytosolic tail of calnexin represents an evolutionarily conserved mechanism to regulate its association with ER membrane-bound ribosomes. The examination of Cnx1p-S553 phosphomutants implicated this signaling event in the regulation of ER stress tolerance and cell size control in *S. pombe.* This thesis also describes the identification and characterization of novel small-molecule inhibitors of Ire1p signaling in *S. cerevisiae*. One such small molecule, UPRM8, was also found to impair Ire1-dependent ER homeostatic mechanisms in human cell lines. In addition, this study revealed that chemical disruption of Ire1-dependent signaling by UPRM8 in constitutively stressed multiple myeloma cells resulted in an apoptotic cell death. The final study detailed in this thesis describes a combined genetic and proteomic approach to study the scaffolding activities of Bem1p in *S. cerevisiae*. The identification of Bem1-*s3*, a novel separation of function mutant, provided evidence that the SH3-1 and SH3-2 domains of Bem1p make distinct contributions to mating morphogenesis and are dispensable for bud morphogenesis. Proteomic analysis of Bem1p-complexes identified novel post-translational modifications and physical interactions of Bem1p. This analysis led to the characterization of a novel role for Bem1p in cell wall stress tolerance.

5.2 Cytoplasm-to-ER signaling via calnexin phosphorylation

One of the more obvious, yet significant findings presented in chapter two was that phosphorylation of calnexin represents a highly conserved signaling mechanism that is found in very divergent eukaryotes, like fission yeast and humans. The identification of a conserved PDK phosphorylation site in the cytosolic tail of *S. pombe* Cnx1p clearly indicates that this genetically tractable fission yeast is a viable model for studying calnexin phosphorylation. The usefulness of this *S. pombe* model for studying calnexin phosphorylation was also evidenced by the fact that S553 phosphorylation increases the association of Cnx1p with ER membrane-bound ribosomes. This regulatory function has also been previously ascribed to phosphorylation of the PDK site in mammalian calnexin [167]. This provides an excellent illustration of the value of model organisms for examining conserved post-translational modifications since the regulatory functions imparted by these conserved modifications clearly also tend to be conserved.

The *S. pombe* kinase that phosphorylates S553 of Cnx1p remains to be identified. However, given that ERK1 has been shown to be the kinase that phosphorylates the analogous PDK site (S563) in mammalian calnexin, it would seem logical to test *S. pombe* MAPKs for their ability to phosphorylate Cnx1p at S553. *S. pombe* has three known MAPKs, named Spk1, Sty1, and Pmk1. These *S. pombe* MAPKs have 54.8% (Spk1), 49.1% (Sty1) and 47.7% (Pmk1) overall sequence identity shared with human ERK1. Given that Sty1 (also called Spc1)

has been shown to be activated by numerous cellular stressors [359, 360] and has also been shown to be involved in cell cycle control [361], this *S. pombe* MAPK is a particularly attractive candidate kinase for Cnx1p. Given that affinity- tagged expression plasmids for the entire *S. pombe* ORFeome are available [362], future studies using immunopurified-kinases should now allow for quick identification of the relevant Cnx1p-phosphorylating kinase in *S. pombe* cells. In addition, a genome-wide collection of *S. pombe* deletion mutants is now commercially available from Bioneer Inc. (Alameda, CA), and so testing of *S. pombe* kinase deletion mutants (e.g. Ire1Δ, Sty1Δ, etc.) should help to identify the relevant signaling mechanisms that lead to Cnx1p phosphorylation.

Mammalian ERK1 has been previously shown to be activated in response to ER stress in a manner that is dependent on both Ire1α and MEK1 activities [166, 363]. The precise mechanism of how ERK1 becomes activated downstream of Ire1α during ER stress adaptation remains unclear. It is clear that expression of a dominant negative Ire1α or treatment with the MEK1-inhibitor PD98059 prevents ERK1 activation, and hence Ser^{563} phosphorylation of calnexin, in response to ER stress [166]. The role of Ire1α in ERK1activation probably involves a mechanism that is analogous to the previously reported TRAF2-dependent activation of JNK by Ire1α [88, 89]. An adaptor protein-mediated activation mechanism for ERK1 is supported by a previous study that reported the involvement of an SH3 domain-containing scaffold protein, called Nck, in ER stress-dependent activation of ERK1 [363]. Although it was not tested in this thesis, it would also be interesting to see if inhibition of Ire1-dependent Xbp1/Hac1 splicing by UPRM8 has any impact on the downstream signaling

events that lead to calnexin phosphorylation. Future studies are required to elucidate the precise signaling mechanisms that occur downstream of Ire1 that ultimately result in calnexin phosphorylation.

The functional significance of the association of calnexin with ER-bound ribosomes is still not entirely understood. This thesis (chapter 2) and a recent study done in mammalian HepG2 cells [166] have both implicated PDK phosphorylation of calnexin in cellular responses to protein misfolding in the ER; however, the study by Cameron and colleagues further suggested that ERK1 phosphorylation of Ser^{563} directly impacts the retention of partially misfolded AAT by calnexin. It is still not known whether the increased calnexin-ribosome association that occurs in response to calnexin (Ser^{563}) phosphorylation is necessary or sufficient for the concomitant increased retention of misfolded glycoprotein.

Following this validation of *S. pombe* Cnx1p as a viable model to study calnexin phosphorylation, it should be possible to employ genetic approaches in this model eukaryote to improve our understanding of how calnexin function is regulated by phosphorylation. For example, identification of Cnx1p separation of function mutants would be useful in addressing whether ribosomal-association, increased glycoprotein retention, and altered ER stress tolerance represent separable biological functions of Cnx1p.

The generation of phospho-Ser^{563}-specific antibodies, which allow for the detection of ERK1-phosphorylated mammalian calnexin, have been reported [166] and this antibody should prove to be an invaluable reagent to monitor calnexin phosphorylation over the duration of a complete adaptive response to a

transient ER stress insult. Future studies should attempt to simultaneously monitor Ser^{563} phosphorylation, Ire1 activation, and the association of calnexin with ribosomes and misfolded glycoproteins (i.e. AAT) over the course of a complete ER homeostatic response to a transient ER stress insult. This sort of holistic time-course experiment should provide meaningful insight into the timing of numerous molecular events that have been previously associated with ER stress adaptation.

Given that previous studies have suggested that phosphorylation of calnexin regulates its subcellular localization [168, 364], immunofluorescence- or immunogold- visualization of calnexin phosphomutants throughout a complete time-course adaptation to acute ER stress insults should provide valuable insight into the functional significance of phosphorylation-mediated redistribution of calnexin during ER stress responses. Another intriguing, but admittedly risky, approach to evaluate the importance of the ER associations of calnexin would be to attempt to directly exert control over the sub-ER distribution of calnexin by translationally fusing it to translocon-associated proteins, like TRAPα for example. An even more sophisticated approach to control the distribution of calnexin by its physical associations within the ER would be to utilize a previously reported [365-367] rapamycin-induced heterodimerization system to exert chemical control over the association of calnexin with various ER proteins of the researchers choosing, such as translocon or ER-exit site proteins.

Previous studies have reported ER sub-compartmentalization [168, 368-370] and there is increasing evidence that such ER microdomains can have specialized functions, as was observed for protein quality control [369] and

ERAD [368]. It will be important for future studies to address if phosphorylation-mediated control of the distribution of calnexin to various ER microdomains affects glycoprotein retention and ER stress tolerance. The findings presented in chapter two of this thesis suggest such a regulatory role for calnexin phosphorylation, but future studies are required to tease out the details of how calnexin function is regulated by its distribution within the ER.

5.3 Inhibition of Ire1-dependent UPR signaling by UPRMs and the relevance of these small molecules to multiple myeloma

The chemical biology study presented in chapter 3 detailed the identification of novel small-molecule inhibitors of Ire1 signaling and this was done by conducting a high-throughput chemical screen in TM-stressed *S. cerevisiae* cells. This research provides yet another example of how studying highly conserved cellular stress signaling mechanisms can lead to the identification of genes or, as is the case here, chemical reagents that can prove to be informative for studying the orthologous signaling mechanisms in higher eukaryotes. Given that *S. cerevisiae* Ire1p only shares 28.3% overall sequence identity with human Ire1α, at first glance it would seem unwise to expect that small-molecule modulators of yeast Ire1p would retain their activities on mammalian Ire1α. However, domain swapping experiments in *S. cerevisiae* have previously shown that the lumenal domains of Ire1p and Ire1α are functionally interchangeable [145] and a human Ire1α was shown to cleave yeast HAC1 mRNA *in vitro* [72]. Furthermore, a hybrid Ire1 protein that is composed of the

lumenal region of Ire1α and the cytoplasmic effector domains of yeast Ire1p was able to cleave Xbp1 mRNA in transfected Ire1$^{-/-}$ MEF cells, following treatment with the Ire1-RNase agonist quercetin [149]. The above literature clearly indicates that a high degree of functional conservation exists between yeast and mammalian Ire1 signaling mechanisms, and so it was not surprising that UPRM8 was found to inhibit Ire1 function in both yeast and mammalian cells.

Even though UPRM8 was clearly shown to inhibit the ribonuclease activity of Ire1 *in vitro*, there are numerous possibilities of how it might act on Ire1 to achieve this effect. It was clearly demonstrated that UPRM8 does not affect the kinase activity of Ire1 *in vitro,* so this can be ruled out as a possible mechanism; however, trans-autophosphorylation of Ire1 has been proposed to result in structural changes that increases the accessibility of nucleotides to the nucleotide binding pocket [148], so it is possible that UPRM8 could inhibit ribonuclease activation by restricting access of nucleotides to the nucleotide binding pocket of Ire1 following its autophosphorylation. Restricting access of nucleotides to the autophosphorylated ('open') conformation of the nucleotide binding pocket would prevent the formation of back-to-back dimers and this has been shown to be critical for RNase activity [148, 149]. Other possibilities for the mechanism of RNase inhibition by UPRM8 include: the potential to physically prevent or disrupt back-to-back dimer formation (independent of nucleotide-binding), binding to the catalytic surface that is formed by back-to-back paired RNase domains, and by binding to the RNA substrate in a manner that makes it an inviable Ire1 substrate. Generating a co-crystal of Ire1 bound to UPRM8 would

be the best and most irrefutable way of gaining a precise mechanistic insight into how UPRM8 inhibits the RNase activity of Ire1.

The identification of numerous UPRM8-like small molecules that display varying anti-MM potencies compared to the parent UPRM8 molecule suggests that an optimal pharmacophore can be elucidated if future studies are implemented to expand the structure-activity-relationship screen that was described in chapter 3. Chemical biology approaches for studying biological activities are improved and simplified by the identification of the most specific and potent small molecules that are available for the biological activity under investigation. This is even more so the case in the pharmaceutical industry, where off-target effects of a given drug can significantly lower its maximum tolerated dose (MTD) or in some cases can severely compromise patient safety by causing serious unwanted side effects. Given that the next logical step for the UPRM8 project is to test its activity in an *in vivo* mouse model of MM, investing current research efforts into identifying the most potent and specific UPRM8-like compounds possible should improve the likelihood of a successful preclinical evaluation of UPRMs in a mouse model of MM.

Bortezomib, the peptide boronic acid proteasome inhibitor, is now clinically approved for treating MM patients and it has been successfully incorporated into numerous promising MM combination therapies (reviewed in [302]); however, in the clinical setting, the response to bortezomib is frequently short-lived and the molecular mechanisms that underlie bortezomib resistance remains the subject of ongoing research [371, 372]. Numerous studies have specifically implicated mutations in, or increased expression of, the proteasome

subunit PSMB5 as means of aquiring bortezomib resistance [373-376]. Given that the combination of UPRM8 and salubrinal displayed *in vitro* anti-MM activities that nearly matched the combination of UPRM8 and bortezomib, it is both exciting and tempting to speculate that the former combination might prove effective at killing bortezomib resistant MM cells since neither of these drugs targets or requires proteasomal function. Future studies are needed to examine this possibility and primary MM cells that are derived from the bone marrow of patients who have developed bortezomib resistance would make an excellent preliminary model to test the effectiveness of a UPRM8+salubrinal combination treatment.

One previously described mouse model of MM pathogenesis involved the generation of transgenic animals that expressed constitutively spliced Xbp1 under the control of a B-cell specific promoter [140]. Obviously this mouse MM model would be of limited value for testing UPRM8-like inhibitors of Ire1-dependent Xbp1 splicing because it is the constitutively spliced form of Xbp1 that is driving MM pathogenesis in this model. A more appropriate mouse MM model for testing UPRM8-like compounds would be the previously described Vk*myc transgenic mice [377]. This transgenic mouse model relies on the B cell-specific expression of a V-kappa exon that has been translationally fused (in frame) to exons 2 and 3 of human MYC; however, this vector has an engineered stop codon at third codon of the V-kappa exon which normally prevents translation of the full-length Vk-MYC fusion protein. This MM model relies on somatic hypermutations, which occur in activated germinal center B cells, to revert the engineered stop codon and thereby allow expression of the full-length Vk-MYC

fusion protein. This sporadic oncogene activation in germinal center B cells causes VK*MYC mice to develop a monoclonal plasma cell expansion that underlies the progression to MM in these transgenic mice. Importantly, these mice display many of the clinical features of human MM and they respond in the expected fashion to chemotherapeutic agents that are used in treating human MM patients. Similar to what is observed in human MM patients, the response to bortezomib therapy is only transient in these Vk*MYC mice [377]. This widely accepted mouse model of MM would provide an excellent model to evaluate UPRM8-like compounds, dosed either alone or in combination with salubrinal or bortezomib, for reducing MM disease burden in these Vk*mice.

A prerequisite for testing UPRMs in a sophisticated transgenic mouse MM model like the one described above is a careful evaluation of the maximum tolerated dose of these compounds in healthy mice of the same genetic background (C57/BL6 for Vk*MYC mice). Particularly close attention should be paid to tissues that carry heavy secretory burdens, such as the pancreas, because any toxic effects of UPRM8-like compounds are most likely to occur in tissues that are reliant on ER homeostatic mechanisms. Given that Xbp1 knockout mice can survive to adulthood if their embryonic lethality is rescued by the expression of XBP1s in the developing liver [56, 378], this suggests that transient inhibition of Ire1-dependent Xbp1 splicing by UPRMs in adult animals should be reasonably well tolerated.

During the preparation of this thesis, a study was published that described the identification of a chemical agent called STF-083010, which inhibits the RNase activity of Ire1 *in vitro* and *in vivo* [379]. Of note, this compound is

structurally dissimilar to UPRM8, so it remains unknown whether this compound inhibits RNase activity through a mechanism similar to UPRM8. These authors also tested the anti-MM potential of this compound in a mouse xenograft model and found that it significantly inhibited tumour growth. Importantly, they also examined the effect of STF-083010 in healthy mice and found that it was well-tolerated and caused no observable cytotoxicity in healthy tissues and organs.

The activities that have been reported for STF-083010 [379] only serve to provide further support and motivation for the immediate *in vivo* validation of the anti-MM activities of the structurally distinct UPRMs that are described in chapter 3. The results presented in this thesis further suggest that *in vivo* testing of UPRMs in a mouse model of MM should certainly include an evaluation of combination therapies, such as UPRM8 and salubrinal or UPRM8 and bortezomib.

Future studies should also be done to evaluate the effects of UPRM8-like compounds on the growth of solid tumours, since it has been well established that tumour cells are protected from their hypoxic and hypoglycaemic microenvironments by their activation of ER stress homeostatic mechanisms (reviewed in [120, 121]). A recent study directly confirmed the activation of the Ire1/Xbp1 pathway in primary breast tumours by crossing transgenic mice that express an Xbp1-luciferase splicing reporter with transgenic mice that develop breast tumours due to their expression of middle T antigen under the control of the mouse mammary tumour virus promoter [54]. The ability to monitor, in real time, the activation of the Ire1/Xbp1 UPR pathway in these genetically predisposed tumour-forming mice would provide an ideal mouse model to

evaluate the effects of UPRM8-like compounds on the growth of solid tumours. Furthermore, a recent study found significant Xbp1 expression in 90% of the 395 human breast tumours examined and they also showed that UPR activation increased chemoresistance to both doxorubicin and 5-fluorouracil [380]. The need for future studies to evaluate UPR inhibitors in the growth and chemoresistance of solid tumours is both apparent and pressing.

From the above evidence, it seems likely that future chemotherapies for treating both solid tumours and haematological malignancies, like MM, should employ UPRMs to block the cytoprotective ER homeostatic mechanisms that are co-opted by cancer cells in their continued struggle for survival. Combining current chemotherapeutic agents that cause increased ER stress, like bortezomib, with UPRMs that block cytoprotective UPR signaling mechanisms shows real promise for improving chemotherapeutic outcomes.

5.4 Bem1p-mediated scaffolding in mating and cell wall stress responses

The identification of the Bem1-*s3* separation of function mutant revealed that both SH3 domains of Bem1p are required to mediate a proper mating response in *S. cerevisiae*. The role of Bem1p in scaffolding important regulators of the actin cytoskeleton, like Cdc42p and Cdc24p, is well established; however, the role of Bem1p in reinforcing MAPK signaling during the response to mating pheromone is still not well understood. The findings presented here suggest that SH3-1 of Bem1p is not essential for the morphogenesis functions of Bem1p, since

ΔSH3-his$_6$ cells form morphologically correct shmoos and buds. On the other hand,, the decreased shmooing efficiency and decreased induction of the Fus1::lacZ transcriptional reporter suggests that SH3-1 contributes to efficient mating pheromone signal transduction. The precise contribution of SH3-1 to pheromone signaling remains unclear at this time, but there is good evidence that it may contribute by mediating the Bem1p-Ste5p physical interaction. Future studies should examine the direct binding of SH3-1 to the PXXP-motif in Ste5p by doing *in vitro* binding experiments similar to those described here for the analysis of the interaction between SH3-2 and Ste20p (or Boi1/2p). Another approach would be to disrupt the PXXP of Ste5p by site directed mutagenesis because a Ste5p-PXXP mutant should closely mimic the mating phenotype observed in ΔSH3-his$_6$ and these two mutants should be epistatic with each other.

The novel protein-protein interactions that we detected between Bem1p and CWI-related proteins led us to uncover a novel role for Bem1p in mediating an appropriate response to cell wall stressors. Given its previously characterized role in pheromone MAPK signaling [227, 242], it is tempting to speculate that Bem1p may be acting similarly in the CWI MAPK response; however, an immediate priority for future studies would be to examine the fidelity of CWI signaling in various Bem1 mutants (e.g. Bem1Δ, Bem1p-S458E) and this could be easily evaluated by transforming these mutant strains with plasmids that contain previously described CWI transcriptional reporters [254]. It will also be important to identify the kinase(s) responsible for phosphorylation of S458 of Bem1p, since phosphorylation of Bem1p at this residue clearly affects cell wall stress tolerance.

Further studies on the Bem1p phosphomutants described in this thesis should help to uncover the functional significance of Bem1p phosphorylation. Given their location in the primary sequence of Bem1p, it is tempting to speculate that S252 and S534 phosphorylation may regulate the interaction of Bem1p with Cdc42p and Cdc24p, respectively. Phospho-regulation of the protein-binding activities of scaffold proteins is not uncommon in eukaryotes. For example, phosphorylation of the SH3 domain-containing scaffold protein $p47^{phox}$ has been shown to regulate the plasma membrane recruitment and activation of the superoxide-producing NADPH oxidase complex (reviewed in [381, 382]). A closer examination of the protein-binding activities of the various phosphomutants of Bem1p should provide a better understanding of how phosphorylation serves to control the scaffolding activities of Bem1p.

Future studies should also ascertain whether the double-glycine remnants that we detected at multiple lysines represent *bona fide* ubiquitination sites in Bem1p. Given that western blotting of endogenous Bem1p reproducibly detects two Bem1p bands that are not compressed by phosphatase treatment (our unpublished data), it seems plausible that ubiquitination could represent a possible means of regulating the scaffolding activities of Bem1p. The pre1-1 pre2-2 double mutant strain [383] accumulates ubiquitinated species when shifted to the restrictive temperature ($37^{o}C$) and so western blotting of Bem1p in this strain, when grown at the restrictive temperature, may confirm the *in vivo* ubiquitination of Bem1p. Phenotypic characterization of point mutants (K to A substitutions) of the ubiquitinated lysines that we detected may help to uncover the functional significance of Bem1p ubiquitination.

Given that many of our current anti-fungal agents ultimately disrupt the structural fidelity or synthesis of the fungal cell wall, identifying novel agents that can be used to concomitantly inhibit CWI homeostatic mechanisms could improve the cytotoxicity and potencies of cell wall destabilizing anti-fungal agents. Support for the above hypothesis was provided by the anti-fungal synergy that was observed when *C. albicans* were cotreated with cercosporamide, an inhibitor of Pkc1, and a cell wall destabilizing echinocandin analog [253]. Given that loss of Bem1p, or constitutive phosphorylation of its S458 residue, resulted in dramatically increased sensitivity to cell wall stressors suggests a novel mechanism to sensitize yeast cells to cell wall destabilization. Given that Bem1 homologs have been identified in *Candida* and *Aspergillus* species [354, 384], and also given that humans do not have an identifiable Bem1 homolog, it is tempting to speculate that chemical reagents that disrupt the function of Bem1 in CWI homeostatic responses would make safe adjuncts to improve anti-fungal therapies that target the fungal cell wall. Given that precise role of Bem1p in CWI responses currently remains unknown, this should be a priority of future investigations.

5.5 General perspectives on cellular stress responses and homeostasis

The conservation of eukaryotic stress responses strongly argues that the ability to sense and adapt to specific demands is an inherent feature of all eukaryotic cells. Given the vast number of fluctuating conditions that are

encountered by cells in their struggle to maintain homeostasis, it is not surprising that eukaryotic cells devote significant resources to maintaining a multitude of stress monitoring and response systems. Importantly, the study of homeostatic responses to stressors frequently expands our general understanding of eukaryotic cell biology. This thesis describes the study of three distinct stress signaling mechanisms in yeast and two of these responses are known to be conserved from yeast to man. Furthermore, these investigations provide further support for the value of model organisms in studying conserved homeostatic mechanisms.

An important central theme of this thesis is that artificial manipulation of homeostatic responses, whether achieved chemically or genetically, allows for control of cell fate in response to specific stress insults. Consequently, discovering new means of controlling cellular homeostatic mechanisms tends to have significant and widespread implications. Pharmaceutical agents that act at the cellular level tend to achieve their desired effect by causing a specific stress (or demand) to be placed on a cell. Therefore, the ability to identify and exert control over the cellular homeostatic mechanisms that respond to a given drug treatment is of essential interest. For example, the ability of UPRM8 to modify the cellular response to bortezomib treatment is of significant interest since this combination shows significantly improved MM cytotoxicity. Generally speaking, it is important to identify not only the specific target of any given drug, but also the cellular homeostatic mechanisms that cope with the loss (or gain) of function of the specific drug target.

Yet another fundamental observation arises from studies of cellular stress responses: distinct cellular homeostatic mechanisms tend to converge on essential

cellular processes. For example, diverse cellular stressors are known to converge on eIF2α phosphorylation to transiently reduce protein synthesis (reviewed in [58]). Similarly, homeostatic mechanisms that are instigated by diverse stressors in *S. cerevisiae* can converge on regulators of the actin cytoskeleton and lead to the transient depolarization of cell growth [180-182]. The identification of stress response elements (STRE) in the promoters of genes that are induced by diverse environmental stressors [385-387] led to the elucidation of a general environmental stress response (ESR) in *S. cerevisiae* (reviewed in [388]). This convergence of diverse cellular stressors on a common set of ESR genes in *S. cerevisiae* underscores the highly integrative nature of homeostatic responses and it also serves to highlight the importance of a number of essential cellular processes in stress adaptation, and these include protein translation, cell cycle control, and cytoskeleton dynamics.

After years of championing the cause of studying biological stress responses, Hans Selye eventually came to recognize that, although stress is an inevitable consequence of life itself, not all stresses lead to negative outcomes. In 1975, Selye coined the term 'eustress', which can be loosely defined as stress that produces positive or beneficial outcomes to an organism [389]. Not only can stresses at the level of whole organisms be viewed as beneficial, since a significant body of literature suggests that encountering one type of cellular stressor can lead to cross-protection from other cellular stressors. This type of cellular stress preconditioning has been frequently observed in *S. cerevisiae* cells, where numerous studies have demonstrated that exposure to a mild 'dose' of one stress can raise cellular tolerance to other types of stressors [185, 390-392].

Therefore, the general concept of eustress functions even at the level of cellular stress and it is clear that stress is inevitable at all levels of biology, but that encountered stressors can have beneficial or 'hardening' effects on an organism. Numerous studies have even suggested that cellular stress responses are important for lifespan and it seems reasonable to expect that a breakdown of cellular stress responses could be an important underlying cause of ageing [393-395].

5.6 Conclusions

This study expands our current understanding of cellular stress responses and it describes two distinct ER stress signaling mechanisms that operate in eukaryotes as divergent as yeast and humans. In addition, it also describes a novel connection between an important regulator of the actin cytoskeleton and the yeast response to cell wall stress. Studying these stress response mechanisms that are of central importance to maintaining cellular homeostasis often provides fundamental insights into eukaryotic cell biology. A more detailed understanding of cellular stress responses is certain to highlight new opportunities to exert control over cellular homeostasis and this knowledge is sure to have widespread disease implications.

References

1. Appley, M.H. and R. Trumbull, *Psychological stress, issues in research; [papers] Edited by Mortimer H. Appley [and] Richard Trumbull*. The Century psychology series, ed. M.H.e. Appley, R.e. Trumbull, and P. York University . Dept. of. 1967, New York: Appleton-Century-Crofts.
2. Bartlett, D., *Stress: Perspectives and processes*. 1998: Open University Press.
3. Mason, J.W., *A historical view of the stress field.* J Human Stress, 1975. **1**(2): p. 22-36 concl.
4. Mason, J.W., *A historical view of the stress field.* J Human Stress, 1975. **1**(1): p. 6-12 contd.
5. Selye, H., *A syndrome produced by diverse nocuous agents.* Nature, 1936. **138**(July 4): p. 32.
6. Kultz, D., *Evolution of the cellular stress proteome: from monophyletic origin to ubiquitous function.* J Exp Biol, 2003. **206**(Pt 18): p. 3119-24.
7. Lindquist, S., *The heat-shock response.* Annu Rev Biochem, 1986. **55**: p. 1151-91.
8. Richter, K., M. Haslbeck, and J. Buchner, *The heat shock response: life on the verge of death.* Mol Cell, 2010. **40**(2): p. 253-66.
9. Kultz, D., *Molecular and evolutionary basis of the cellular stress response.* Annu Rev Physiol, 2005. **67**: p. 225-57.
10. Botstein, D., S.A. Chervitz, and J.M. Cherry, *Yeast as a model organism.* Science, 1997. **277**(5330): p. 1259-60.
11. Botstein, D. and G.R. Fink, *Yeast: an experimental organism for modern biology.* Science, 1988. **240**(4858): p. 1439-43.
12. Hwang, C., A.J. Sinskey, and H.F. Lodish, *Oxidized redox state of glutathione in the endoplasmic reticulum.* Science, 1992. **257**(5076): p. 1496-502.
13. Hebert, D.N. and M. Molinari, *In and out of the ER: protein folding, quality control, degradation, and related human diseases.* Physiol Rev, 2007. **87**(4): p. 1377-408.
14. Egea, P.F., R.M. Stroud, and P. Walter, *Targeting proteins to membranes: structure of the signal recognition particle.* Curr Opin Struct Biol, 2005. **15**(2): p. 213-20.
15. Zimmermann, R., et al., *Protein translocation across the ER membrane.* Biochim Biophys Acta, 2010.
16. Paetzel, M., et al., *Signal peptidases.* Chem Rev, 2002. **102**(12): p. 4549-80.
17. Weerapana, E. and B. Imperiali, *Asparagine-linked protein glycosylation: from eukaryotic to prokaryotic systems.* Glycobiology, 2006. **16**(6): p. 91R-101R.
18. Woods, R.J., C.J. Edge, and R.A. Dwek, *Protein surface oligosaccharides and protein function.* Nat Struct Biol, 1994. **1**(8): p. 499-501.
19. Varki, A., et al., *Essentials of Glycobiology*. Vol. 2. 2009, Cold Spring Harbor (NY): Cold Spring Harbor Laboratory Press.

20. Sekijima, Y., et al., *The biological and chemical basis for tissue-selective amyloid disease.* Cell, 2005. **121**(1): p. 73-85.
21. Wiseman, R.L. and W.E. Balch, *A new pharmacology--drugging stressed folding pathways.* Trends Mol Med, 2005. **11**(8): p. 347-50.
22. Hendershot, L.M., *The ER function BiP is a master regulator of ER function.* Mt Sinai J Med, 2004. **71**(5): p. 289-97.
23. Wada, I., et al., *SSR alpha and associated calnexin are major calcium binding proteins of the endoplasmic reticulum membrane.* J Biol Chem, 1991. **266**(29): p. 19599-610.
24. Waisman, D.M., B.P. Salimath, and M.J. Anderson, *Isolation and characterization of CAB-63, a novel calcium-binding protein.* J Biol Chem, 1985. **260**(3): p. 1652-60.
25. David, V., et al., *Interaction with newly synthesized and retained proteins in the endoplasmic reticulum suggests a chaperone function for human integral membrane protein IP90 (calnexin).* J Biol Chem, 1993. **268**(13): p. 9585-92.
26. Ou, W.J., et al., *Association of folding intermediates of glycoproteins with calnexin during protein maturation.* Nature, 1993. **364**(6440): p. 771-6.
27. Peterson, J.R., et al., *Transient, lectin-like association of calreticulin with folding intermediates of cellular and viral glycoproteins.* Mol Biol Cell, 1995. **6**(9): p. 1173-84.
28. Schrag, J.D., et al., *The Structure of calnexin, an ER chaperone involved in quality control of protein folding.* Mol Cell, 2001. **8**(3): p. 633-44.
29. Vassilakos, A., et al., *Oligosaccharide binding characteristics of the molecular chaperones calnexin and calreticulin.* Biochemistry, 1998. **37**(10): p. 3480-90.
30. Zapun, A., et al., *Conformation-independent binding of monoglucosylated ribonuclease B to calnexin.* Cell, 1997. **88**(1): p. 29-38.
31. Bergeron, J.J., et al., *Calnexin: a membrane-bound chaperone of the endoplasmic reticulum.* Trends Biochem Sci, 1994. **19**(3): p. 124-8.
32. Chevet, E., et al., *The endoplasmic reticulum: integration of protein folding, quality control, signaling and degradation.* Curr Opin Struct Biol, 2001. **11**(1): p. 120-4.
33. Chevet, E., et al., *Calnexin family members as modulators of genetic diseases.* Semin Cell Dev Biol, 1999. **10**(5): p. 473-80.
34. Chevet, E., et al., *Calnexin phosphorylation: linking cytoplasmic signalling to endoplasmic reticulum lumenal functions.* Semin Cell Dev Biol, 2010. **21**(5): p. 486-90.
35. Ellgaard, L., M. Molinari, and A. Helenius, *Setting the standards: quality control in the secretory pathway.* Science, 1999. **286**(5446): p. 1882-8.
36. Hammond, C. and A. Helenius, *Quality control in the secretory pathway.* Curr Opin Cell Biol, 1995. **7**(4): p. 523-9.
37. Frickel, E.M., et al., *TROSY-NMR reveals interaction between ERp57 and the tip of the calreticulin P-domain.* Proc Natl Acad Sci U S A, 2002. **99**(4): p. 1954-9.
38. Kozlov, G., et al., *Crystal structure of the bb' domains of the protein disulfide isomerase ERp57.* Structure, 2006. **14**(8): p. 1331-9.

39. Pollock, S., et al., *Specific interaction of ERp57 and calnexin determined by NMR spectroscopy and an ER two-hybrid system.* Embo J, 2004. **23**(5): p. 1020-9.
40. Hutt, D.M., E.T. Powers, and W.E. Balch, *The proteostasis boundary in misfolding diseases of membrane traffic.* FEBS Lett, 2009. **583**(16): p. 2639-46.
41. Powers, E.T., et al., *Biological and chemical approaches to diseases of proteostasis deficiency.* Annu Rev Biochem, 2009. **78**: p. 959-91.
42. Hebert, D.N., R. Bernasconi, and M. Molinari, *ERAD substrates: which way out?* Semin Cell Dev Biol, 2010. **21**(5): p. 526-32.
43. Nakatsukasa, K. and J.L. Brodsky, *The recognition and retrotranslocation of misfolded proteins from the endoplasmic reticulum.* Traffic, 2008. **9**(6): p. 861-70.
44. Vembar, S.S. and J.L. Brodsky, *One step at a time: endoplasmic reticulum-associated degradation.* Nat Rev Mol Cell Biol, 2008. **9**(12): p. 944-57.
45. Fribley, A., Q. Zeng, and C.Y. Wang, *Proteasome inhibitor PS-341 induces apoptosis through induction of endoplasmic reticulum stress-reactive oxygen species in head and neck squamous cell carcinoma cells.* Mol Cell Biol, 2004. **24**(22): p. 9695-704.
46. Lee, A.H., et al., *Proteasome inhibitors disrupt the unfolded protein response in myeloma cells.* Proc Natl Acad Sci U S A, 2003. **100**(17): p. 9946-51.
47. Nawrocki, S.T., et al., *Bortezomib inhibits PKR-like endoplasmic reticulum (ER) kinase and induces apoptosis via ER stress in human pancreatic cancer cells.* Cancer Res, 2005. **65**(24): p. 11510-9.
48. Nawrocki, S.T., et al., *Bortezomib sensitizes pancreatic cancer cells to endoplasmic reticulum stress-mediated apoptosis.* Cancer Res, 2005. **65**(24): p. 11658-66.
49. Obeng, E.A., et al., *Proteasome inhibitors induce a terminal unfolded protein response in multiple myeloma cells.* Blood, 2006. **107**(12): p. 4907-16.
50. Cox, J.S., C.E. Shamu, and P. Walter, *Transcriptional induction of genes encoding endoplasmic reticulum resident proteins requires a transmembrane protein kinase.* Cell, 1993. **73**(6): p. 1197-206.
51. Mori, K., et al., *A transmembrane protein with a cdc2+/CDC28-related kinase activity is required for signaling from the ER to the nucleus.* Cell, 1993. **74**(4): p. 743-56.
52. Mori, K., et al., *A 22 bp cis-acting element is necessary and sufficient for the induction of the yeast KAR2 (BiP) gene by unfolded proteins.* Embo J, 1992. **11**(7): p. 2583-93.
53. Iwawaki, T., et al., *A transgenic mouse model for monitoring endoplasmic reticulum stress.* Nat Med, 2004. **10**(1): p. 98-102.
54. Spiotto, M.T., et al., *Imaging the unfolded protein response in primary tumors reveals microenvironments with metabolic variations that predict tumor growth.* Cancer Res, 2010. **70**(1): p. 78-88.

55. Iwakoshi, N.N., et al., *Plasma cell differentiation and the unfolded protein response intersect at the transcription factor XBP-1.* Nat Immunol, 2003. **4**(4): p. 321-9.
56. Reimold, A.M., et al., *Plasma cell differentiation requires the transcription factor XBP-1.* Nature, 2001. **412**(6844): p. 300-7.
57. Zhang, P., et al., *The PERK eukaryotic initiation factor 2 alpha kinase is required for the development of the skeletal system, postnatal growth, and the function and viability of the pancreas.* Mol Cell Biol, 2002. **22**(11): p. 3864-74.
58. Ron, D. and P. Walter, *Signal integration in the endoplasmic reticulum unfolded protein response.* Nat Rev Mol Cell Biol, 2007. **8**(7): p. 519-29.
59. Haze, K., et al., *Mammalian transcription factor ATF6 is synthesized as a transmembrane protein and activated by proteolysis in response to endoplasmic reticulum stress.* Mol Biol Cell, 1999. **10**(11): p. 3787-99.
60. Yoshida, H., et al., *Identification of the cis-acting endoplasmic reticulum stress response element responsible for transcriptional induction of mammalian glucose-regulated proteins. Involvement of basic leucine zipper transcription factors.* J Biol Chem, 1998. **273**(50): p. 33741-9.
61. Harding, H.P., Y. Zhang, and D. Ron, *Protein translation and folding are coupled by an endoplasmic-reticulum-resident kinase.* Nature, 1999. **397**(6716): p. 271-4.
62. Harding, H.P., et al., *An integrated stress response regulates amino acid metabolism and resistance to oxidative stress.* Mol Cell, 2003. **11**(3): p. 619-33.
63. Reimertz, C., et al., *Gene expression during ER stress-induced apoptosis in neurons: induction of the BH3-only protein Bbc3/PUMA and activation of the mitochondrial apoptosis pathway.* J Cell Biol, 2003. **162**(4): p. 587-97.
64. Travers, K.J., et al., *Functional and genomic analyses reveal an essential coordination between the unfolded protein response and ER-associated degradation.* Cell, 2000. **101**(3): p. 249-58.
65. Kohno, K., *Stress-sensing mechanisms in the unfolded protein response: similarities and differences between yeast and mammals.* J Biochem, 2010. **147**(1): p. 27-33.
66. Malhotra, J.D. and R.J. Kaufman, *The endoplasmic reticulum and the unfolded protein response.* Semin Cell Dev Biol, 2007. **18**(6): p. 716-31.
67. Sidrauski, C. and P. Walter, *The transmembrane kinase Ire1p is a site-specific endonuclease that initiates mRNA splicing in the unfolded protein response.* Cell, 1997. **90**(6): p. 1031-9.
68. Sidrauski, C., J.S. Cox, and P. Walter, *tRNA ligase is required for regulated mRNA splicing in the unfolded protein response.* Cell, 1996. **87**(3): p. 405-13.
69. Patil, C.K., H. Li, and P. Walter, *Gcn4p and novel upstream activating sequences regulate targets of the unfolded protein response.* PLoS Biol, 2004. **2**(8): p. E246.

70. Cox, J.S. and P. Walter, *A novel mechanism for regulating activity of a transcription factor that controls the unfolded protein response.* Cell, 1996. **87**(3): p. 391-404.
71. Mori, K., et al., *Signalling from endoplasmic reticulum to nucleus: transcription factor with a basic-leucine zipper motif is required for the unfolded protein-response pathway.* Genes Cells, 1996. **1**(9): p. 803-17.
72. Tirasophon, W., A.A. Welihinda, and R.J. Kaufman, *A stress response pathway from the endoplasmic reticulum to the nucleus requires a novel bifunctional protein kinase/endoribonuclease (Ire1p) in mammalian cells.* Genes Dev, 1998. **12**(12): p. 1812-24.
73. Wang, X.Z., et al., *Cloning of mammalian Ire1 reveals diversity in the ER stress responses.* Embo J, 1998. **17**(19): p. 5708-17.
74. Bertolotti, A., et al., *Increased sensitivity to dextran sodium sulfate colitis in IRE1beta-deficient mice.* J Clin Invest, 2001. **107**(5): p. 585-93.
75. Shen, X., et al., *Complementary signaling pathways regulate the unfolded protein response and are required for C. elegans development.* Cell, 2001. **107**(7): p. 893-903.
76. Yoshida, H., et al., *XBP1 mRNA is induced by ATF6 and spliced by IRE1 in response to ER stress to produce a highly active transcription factor.* Cell, 2001. **107**(7): p. 881-91.
77. Lu, P.D., H.P. Harding, and D. Ron, *Translation reinitiation at alternative open reading frames regulates gene expression in an integrated stress response.* J Cell Biol, 2004. **167**(1): p. 27-33.
78. Vattem, K.M. and R.C. Wek, *Reinitiation involving upstream ORFs regulates ATF4 mRNA translation in mammalian cells.* Proc Natl Acad Sci U S A, 2004. **101**(31): p. 11269-74.
79. Hinnebusch, A.G. and K. Natarajan, *Gcn4p, a master regulator of gene expression, is controlled at multiple levels by diverse signals of starvation and stress.* Eukaryot Cell, 2002. **1**(1): p. 22-32.
80. Cyr, D.M. and D.N. Hebert, *Protein quality control--linking the unfolded protein response to disease. Conference on 'From Unfolded Proteins in the Endoplasmic Reticulum to Disease'.* EMBO Rep, 2009. **10**(11): p. 1206-10.
81. Fawcett, T.W., et al., *Complexes containing activating transcription factor (ATF)/cAMP-responsive-element-binding protein (CREB) interact with the CCAAT/enhancer-binding protein (C/EBP)-ATF composite site to regulate Gadd153 expression during the stress response.* Biochem J, 1999. **339 (Pt 1)**: p. 135-41.
82. Harding, H.P., et al., *Regulated translation initiation controls stress-induced gene expression in mammalian cells.* Mol Cell, 2000. **6**(5): p. 1099-108.
83. Ye, J., et al., *ER stress induces cleavage of membrane-bound ATF6 by the same proteases that process SREBPs.* Mol Cell, 2000. **6**(6): p. 1355-64.
84. Heath-Engel, H.M., N.C. Chang, and G.C. Shore, *The endoplasmic reticulum in apoptosis and autophagy: role of the BCL-2 protein family.* Oncogene, 2008. **27**(50): p. 6419-33.

85. Kim, I., W. Xu, and J.C. Reed, *Cell death and endoplasmic reticulum stress: disease relevance and therapeutic opportunities.* Nat Rev Drug Discov, 2008. **7**(12): p. 1013-30.
86. Kim, R., et al., *Role of the unfolded protein response in cell death.* Apoptosis, 2006. **11**(1): p. 5-13.
87. Rao, R.V., H.M. Ellerby, and D.E. Bredesen, *Coupling endoplasmic reticulum stress to the cell death program.* Cell Death Differ, 2004. **11**(4): p. 372-80.
88. Urano, F., et al., *Coupling of stress in the ER to activation of JNK protein kinases by transmembrane protein kinase IRE1.* Science, 2000. **287**(5453): p. 664-6.
89. Nishitoh, H., et al., *ASK1 is essential for endoplasmic reticulum stress-induced neuronal cell death triggered by expanded polyglutamine repeats.* Genes Dev, 2002. **16**(11): p. 1345-55.
90. Leppa, S. and D. Bohmann, *Diverse functions of JNK signaling and c-Jun in stress response and apoptosis.* Oncogene, 1999. **18**(45): p. 6158-62.
91. Nakagawa, T., et al., *Caspase-12 mediates endoplasmic-reticulum-specific apoptosis and cytotoxicity by amyloid-beta.* Nature, 2000. **403**(6765): p. 98-103.
92. Morishima, N., et al., *An endoplasmic reticulum stress-specific caspase cascade in apoptosis. Cytochrome c-independent activation of caspase-9 by caspase-12.* J Biol Chem, 2002. **277**(37): p. 34287-94.
93. Xue, Y., et al., *Spread of an inactive form of caspase-12 in humans is due to recent positive selection.* Am J Hum Genet, 2006. **78**(4): p. 659-70.
94. Hitomi, J., et al., *Involvement of caspase-4 in endoplasmic reticulum stress-induced apoptosis and Abeta-induced cell death.* J Cell Biol, 2004. **165**(3): p. 347-56.
95. Oyadomari, S. and M. Mori, *Roles of CHOP/GADD153 in endoplasmic reticulum stress.* Cell Death Differ, 2004. **11**(4): p. 381-9.
96. Scheuner, D., et al., *Translational control is required for the unfolded protein response and in vivo glucose homeostasis.* Mol Cell, 2001. **7**(6): p. 1165-76.
97. Brush, M.H., D.C. Weiser, and S. Shenolikar, *Growth arrest and DNA damage-inducible protein GADD34 targets protein phosphatase 1 alpha to the endoplasmic reticulum and promotes dephosphorylation of the alpha subunit of eukaryotic translation initiation factor 2.* Mol Cell Biol, 2003. **23**(4): p. 1292-303.
98. Kojima, E., et al., *The function of GADD34 is a recovery from a shutoff of protein synthesis induced by ER stress: elucidation by GADD34-deficient mice.* FASEB J, 2003. **17**(11): p. 1573-5.
99. Marciniak, S.J., et al., *CHOP induces death by promoting protein synthesis and oxidation in the stressed endoplasmic reticulum.* Genes Dev, 2004. **18**(24): p. 3066-77.
100. Ohoka, N., et al., *TRB3, a novel ER stress-inducible gene, is induced via ATF4-CHOP pathway and is involved in cell death.* Embo J, 2005. **24**(6): p. 1243-55.

101. McCullough, K.D., et al., *Gadd153 sensitizes cells to endoplasmic reticulum stress by down-regulating Bcl2 and perturbing the cellular redox state.* Mol Cell Biol, 2001. **21**(4): p. 1249-59.
102. Zinszner, H., et al., *CHOP is implicated in programmed cell death in response to impaired function of the endoplasmic reticulum.* Genes Dev, 1998. **12**(7): p. 982-95.
103. Han, D., et al., *IRE1alpha kinase activation modes control alternate endoribonuclease outputs to determine divergent cell fates.* Cell, 2009. **138**(3): p. 562-75.
104. Hollien, J., et al., *Regulated Ire1-dependent decay of messenger RNAs in mammalian cells.* J Cell Biol, 2009. **186**(3): p. 323-31.
105. Hollien, J. and J.S. Weissman, *Decay of endoplasmic reticulum-localized mRNAs during the unfolded protein response.* Science, 2006. **313**(5783): p. 104-7.
106. Papa, F.R., et al., *Bypassing a kinase activity with an ATP-competitive drug.* Science, 2003. **302**(5650): p. 1533-7.
107. Lin, J.H., et al., *IRE1 signaling affects cell fate during the unfolded protein response.* Science, 2007. **318**(5852): p. 944-9.
108. Lin, J.H., P. Walter, and T.S. Yen, *Endoplasmic reticulum stress in disease pathogenesis.* Annu Rev Pathol, 2008. **3**: p. 399-425.
109. Zhang, K. and R.J. Kaufman, *The unfolded protein response: a stress signaling pathway critical for health and disease.* Neurology, 2006. **66**(2 Suppl 1): p. S102-9.
110. Zhao, L. and S.L. Ackerman, *Endoplasmic reticulum stress in health and disease.* Curr Opin Cell Biol, 2006. **18**(4): p. 444-52.
111. He, B., *Viruses, endoplasmic reticulum stress, and interferon responses.* Cell Death Differ, 2006. **13**(3): p. 393-403.
112. Lindholm, D., H. Wootz, and L. Korhonen, *ER stress and neurodegenerative diseases.* Cell Death Differ, 2006. **13**(3): p. 385-92.
113. Hotamisligil, G.S., *Endoplasmic reticulum stress and the inflammatory basis of metabolic disease.* Cell, 2010. **140**(6): p. 900-17.
114. Dickhout, J.G. and J.C. Krepinsky, *Endoplasmic reticulum stress and renal disease.* Antioxid Redox Signal, 2009. **11**(9): p. 2341-52.
115. Glembotski, C.C., *Endoplasmic reticulum stress in the heart.* Circ Res, 2007. **101**(10): p. 975-84.
116. Glembotski, C.C., *The role of the unfolded protein response in the heart.* J Mol Cell Cardiol, 2008. **44**(3): p. 453-9.
117. DeGracia, D.J. and H.L. Montie, *Cerebral ischemia and the unfolded protein response.* J Neurochem, 2004. **91**(1): p. 1-8.
118. DeGracia, D.J., *Acute and persistent protein synthesis inhibition following cerebral reperfusion.* J Neurosci Res, 2004. **77**(6): p. 771-6.
119. Healy, S.J., et al., *Targeting the endoplasmic reticulum-stress response as an anticancer strategy.* Eur J Pharmacol, 2009. **625**(1-3): p. 234-46.
120. Ma, Y. and L.M. Hendershot, *The role of the unfolded protein response in tumour development: friend or foe?* Nat Rev Cancer, 2004. **4**(12): p. 966-77.

121. Moenner, M., et al., *Integrated endoplasmic reticulum stress responses in cancer.* Cancer Res, 2007. **67**(22): p. 10631-4.
122. Wang, G., Z.Q. Yang, and K. Zhang, *Endoplasmic reticulum stress response in cancer: molecular mechanism and therapeutic potential.* Am J Transl Res, 2010. **2**(1): p. 65-74.
123. Allinen, M., et al., *Molecular characterization of the tumor microenvironment in breast cancer.* Cancer Cell, 2004. **6**(1): p. 17-32.
124. Graeber, T.G., et al., *Hypoxia-mediated selection of cells with diminished apoptotic potential in solid tumours.* Nature, 1996. **379**(6560): p. 88-91.
125. Hanahan, D. and R.A. Weinberg, *The hallmarks of cancer.* Cell, 2000. **100**(1): p. 57-70.
126. Hu, M. and K. Polyak, *Molecular characterisation of the tumour microenvironment in breast cancer.* Eur J Cancer, 2008. **44**(18): p. 2760-5.
127. Polyak, K., I. Haviv, and I.G. Campbell, *Co-evolution of tumor cells and their microenvironment.* Trends Genet, 2009. **25**(1): p. 30-8.
128. Weinberg, R.A., *Coevolution in the tumor microenvironment.* Nat Genet, 2008. **40**(5): p. 494-5.
129. Chen, X., et al., *Overexpression of glucose-regulated protein 94 (Grp94) in esophageal adenocarcinomas of a rat surgical model and humans.* Carcinogenesis, 2002. **23**(1): p. 123-30.
130. Fernandez, P.M., et al., *Overexpression of the glucose-regulated stress gene GRP78 in malignant but not benign human breast lesions.* Breast Cancer Res Treat, 2000. **59**(1): p. 15-26.
131. Gazit, G., J. Lu, and A.S. Lee, *De-regulation of GRP stress protein expression in human breast cancer cell lines.* Breast Cancer Res Treat, 1999. **54**(2): p. 135-46.
132. Shuda, M., et al., *Activation of the ATF6, XBP1 and grp78 genes in human hepatocellular carcinoma: a possible involvement of the ER stress pathway in hepatocarcinogenesis.* J Hepatol, 2003. **38**(5): p. 605-14.
133. Song, M.S., et al., *Induction of glucose-regulated protein 78 by chronic hypoxia in human gastric tumor cells through a protein kinase C-epsilon/ERK/AP-1 signaling cascade.* Cancer Res, 2001. **61**(22): p. 8322-30.
134. Jamora, C., G. Dennert, and A.S. Lee, *Inhibition of tumor progression by suppression of stress protein GRP78/BiP induction in fibrosarcoma B/C10ME.* Proc Natl Acad Sci U S A, 1996. **93**(15): p. 7690-4.
135. Park, H.R., et al., *Versipelostatin, a novel GRP78/Bip molecular chaperon down-regulator of microbial origin.* Tetrahedron Letters, 2002. **43**: p. 6941-6945.
136. Park, H.R., et al., *Effect on tumor cells of blocking survival response to glucose deprivation.* J Natl Cancer Inst, 2004. **96**(17): p. 1300-10.
137. Romero-Ramirez, L., et al., *XBP1 is essential for survival under hypoxic conditions and is required for tumor growth.* Cancer Res, 2004. **64**(17): p. 5943-7.
138. Fujimoto, T., et al., *Upregulation and overexpression of human X-box binding protein 1 (hXBP-1) gene in primary breast cancers.* Breast Cancer, 2003. **10**(4): p. 301-6.

139. Fujimoto, T., et al., *Overexpression of human X-box binding protein 1 (XBP-1) in colorectal adenomas and adenocarcinomas.* Anticancer Res, 2007. **27**(1A): p. 127-31.
140. Carrasco, D.R., et al., *The differentiation and stress response factor XBP-1 drives multiple myeloma pathogenesis.* Cancer Cell, 2007. **11**(4): p. 349-60.
141. Davenport, E.L., et al., *Heat shock protein inhibition is associated with activation of the unfolded protein response pathway in myeloma plasma cells.* Blood, 2007. **110**(7): p. 2641-9.
142. Hideshima, T., et al., *The proteasome inhibitor PS-341 inhibits growth, induces apoptosis, and overcomes drug resistance in human multiple myeloma cells.* Cancer Res, 2001. **61**(7): p. 3071-6.
143. Dong, H., et al., *Dysregulation of unfolded protein response partially underlies proapoptotic activity of bortezomib in multiple myeloma cells.* Leuk Lymphoma, 2009. **50**(6): p. 974-84.
144. Bertolotti, A., et al., *Dynamic interaction of BiP and ER stress transducers in the unfolded-protein response.* Nat Cell Biol, 2000. **2**(6): p. 326-32.
145. Liu, C.Y., M. Schroder, and R.J. Kaufman, *Ligand-independent dimerization activates the stress response kinases IRE1 and PERK in the lumen of the endoplasmic reticulum.* J Biol Chem, 2000. **275**(32): p. 24881-5.
146. Credle, J.J., et al., *On the mechanism of sensing unfolded protein in the endoplasmic reticulum.* Proc Natl Acad Sci U S A, 2005. **102**(52): p. 18773-84.
147. Korennykh, A.V., et al., *The unfolded protein response signals through high-order assembly of Ire1.* Nature, 2009. **457**(7230): p. 687-93.
148. Lee, K.P., et al., *Structure of the dual enzyme Ire1 reveals the basis for catalysis and regulation in nonconventional RNA splicing.* Cell, 2008. **132**(1): p. 89-100.
149. Wiseman, R.L., et al., *Flavonol activation defines an unanticipated ligand-binding site in the kinase-RNase domain of IRE1.* Mol Cell, 2010. **38**(2): p. 291-304.
150. Zhou, J., et al., *The crystal structure of human IRE1 luminal domain reveals a conserved dimerization interface required for activation of the unfolded protein response.* Proc Natl Acad Sci U S A, 2006. **103**(39): p. 14343-8.
151. Okamura, K., et al., *Dissociation of Kar2p/BiP from an ER sensory molecule, Ire1p, triggers the unfolded protein response in yeast.* Biochem Biophys Res Commun, 2000. **279**(2): p. 445-50.
152. Kimata, Y., et al., *A role for BiP as an adjustor for the endoplasmic reticulum stress-sensing protein Ire1.* J Cell Biol, 2004. **167**(3): p. 445-56.
153. Pincus, D., et al., *BiP binding to the ER-stress sensor Ire1 tunes the homeostatic behavior of the unfolded protein response.* PLoS Biol, 2010. **8**(7): p. e1000415.
154. Kimata, Y., et al., *Two regulatory steps of ER-stress sensor Ire1 involving its cluster formation and interaction with unfolded proteins.* J Cell Biol, 2007. **179**(1): p. 75-86.

155. Shamu, C.E. and P. Walter, *Oligomerization and phosphorylation of the Ire1p kinase during intracellular signaling from the endoplasmic reticulum to the nucleus.* Embo J, 1996. **15**(12): p. 3028-39.
156. Welihinda, A.A. and R.J. Kaufman, *The unfolded protein response pathway in Saccharomyces cerevisiae. Oligomerization and trans-phosphorylation of Ire1p (Ern1p) are required for kinase activation.* J Biol Chem, 1996. **271**(30): p. 18181-7.
157. Ahluwalia, N., et al., *The p88 molecular chaperone is identical to the endoplasmic reticulum membrane protein, calnexin.* J Biol Chem, 1992. **267**(15): p. 10914-8.
158. Hammond, C., I. Braakman, and A. Helenius, *Role of N-linked oligosaccharide recognition, glucose trimming, and calnexin in glycoprotein folding and quality control.* Proc Natl Acad Sci U S A, 1994. **91**(3): p. 913-7.
159. Hochstenbach, F., et al., *Endoplasmic reticulum resident protein of 90 kilodaltons associates with the T- and B-cell antigen receptors and major histocompatibility complex antigens during their assembly.* Proc Natl Acad Sci U S A, 1992. **89**(10): p. 4734-8.
160. Le, A., et al., *Association between calnexin and a secretion-incompetent variant of human alpha 1-antitrypsin.* J Biol Chem, 1994. **269**(10): p. 7514-9.
161. Capps, G.G. and M.C. Zuniga, *Class I histocompatibility molecule association with phosphorylated calnexin. Implications for rates of intracellular transport.* J Biol Chem, 1994. **269**(15): p. 11634-9.
162. Wong, H.N., et al., *Conserved in vivo phosphorylation of calnexin at casein kinase II sites as well as a protein kinase C/proline-directed kinase site.* J Biol Chem, 1998. **273**(27): p. 17227-35.
163. Pinna, L.A., *Casein kinase 2: an 'eminence grise' in cellular regulation?* Biochim Biophys Acta, 1990. **1054**(3): p. 267-84.
164. Robinson, M.J. and M.H. Cobb, *Mitogen-activated protein kinase pathways.* Curr Opin Cell Biol, 1997. **9**(2): p. 180-6.
165. Nigg, E.A., *Cyclin-dependent protein kinases: key regulators of the eukaryotic cell cycle.* Bioessays, 1995. **17**(6): p. 471-80.
166. Cameron, P.H., et al., *Calnexin phosphorylation attenuates the release of partially misfolded alpha1-antitrypsin to the secretory pathway.* J Biol Chem, 2009. **284**(50): p. 34570-9.
167. Chevet, E., et al., *Phosphorylation by CK2 and MAPK enhances calnexin association with ribosomes.* Embo J, 1999. **18**(13): p. 3655-66.
168. Myhill, N., et al., *The subcellular distribution of calnexin is mediated by PACS-2.* Mol Biol Cell, 2008. **19**(7): p. 2777-88.
169. Jannatipour, M. and L.A. Rokeach, *The Schizosaccharomyces pombe homologue of the chaperone calnexin is essential for viability.* J Biol Chem, 1995. **270**(9): p. 4845-53.
170. Parlati, F., et al., *The calnexin homologue cnx1+ in Schizosaccharomyces pombe, is an essential gene which can be complemented by its soluble ER domain.* Embo J, 1995. **14**(13): p. 3064-72.

171. Fernandez, F.S., et al., *Purification to homogeneity of UDP-glucose:glycoprotein glucosyltransferase from Schizosaccharomyces pombe and apparent absence of the enzyme fro Saccharomyces cerevisiae.* J Biol Chem, 1994. **269**(48): p. 30701-6.
172. D'Alessio, C., et al., *Genetic evidence for the heterodimeric structure of glucosidase II. The effect of disrupting the subunit-encoding genes on glycoprotein folding.* J Biol Chem, 1999. **274**(36): p. 25899-905.
173. Abercrombie, M., J.E. Heaysman, and S.M. Pegrum, *The locomotion of fibroblasts in culture. IV. Electron microscopy of the leading lamella.* Exp Cell Res, 1971. **67**(2): p. 359-67.
174. Buckley, I.K. and K.R. Porter, *Cytoplasmic fibrils in living cultured cells. A light and electron microscope study.* Protoplasma, 1967. **64**(4): p. 349-80.
175. Lewis, W.H. and M.R. Lewis, *Behavior of cells in tissue cultures.*, in *General Cytology*, E.V. Cowdry, Editor. 1924, University of Chicago Press: Chicago. p. 63.
176. Naumanen, P., P. Lappalainen, and P. Hotulainen, *Mechanisms of actin stress fibre assembly.* J Microsc, 2008. **231**(3): p. 446-54.
177. Adams, A.E. and J.R. Pringle, *Relationship of actin and tubulin distribution to bud growth in wild-type and morphogenetic-mutant Saccharomyces cerevisiae.* J Cell Biol, 1984. **98**(3): p. 934-45.
178. Novick, P. and D. Botstein, *Phenotypic analysis of temperature-sensitive yeast actin mutants.* Cell, 1985. **40**(2): p. 405-16.
179. Pruyne, D., et al., *Mechanisms of polarized growth and organelle segregation in yeast.* Annu Rev Cell Dev Biol, 2004. **20**: p. 559-91.
180. Chowdhury, S., K.W. Smith, and M.C. Gustin, *Osmotic stress and the yeast cytoskeleton: phenotype-specific suppression of an actin mutation.* J Cell Biol, 1992. **118**(3): p. 561-71.
181. Delley, P.A. and M.N. Hall, *Cell wall stress depolarizes cell growth via hyperactivation of RHO1.* J Cell Biol, 1999. **147**(1): p. 163-74.
182. Lillie, S.H. and S.S. Brown, *Immunofluorescence localization of the unconventional myosin, Myo2p, and the putative kinesin-related protein, Smy1p, to the same regions of polarized growth in Saccharomyces cerevisiae.* J Cell Biol, 1994. **125**(4): p. 825-42.
183. Wertman, K.F., D.G. Drubin, and D. Botstein, *Systematic mutational analysis of the yeast ACT1 gene.* Genetics, 1992. **132**(2): p. 337-50.
184. Ashe, M.P., S.K. De Long, and A.B. Sachs, *Glucose depletion rapidly inhibits translation initiation in yeast.* Mol Biol Cell, 2000. **11**(3): p. 833-48.
185. Blomberg, A., C. Larsson, and L. Gustafsson, *Microcalorimetric monitoring of growth of Saccharomyces cerevisiae: osmotolerance in relation to physiological state.* J Bacteriol, 1988. **170**(10): p. 4562-8.
186. Fuge, E.K., E.L. Braun, and M. Werner-Washburne, *Protein synthesis in long-term stationary-phase cultures of Saccharomyces cerevisiae.* J Bacteriol, 1994. **176**(18): p. 5802-13.

187. McAlister, L. and D.B. Finkelstein, *Alterations in translatable ribonucleic acid after heat shock of Saccharomyces cerevisiae.* J Bacteriol, 1980. **143**(2): p. 603-12.
188. Perez, P. and S.A. Rincon, *Rho GTPases: regulation of cell polarity and growth in yeasts.* Biochem J, 2010. **426**(3): p. 243-53.
189. Pruyne, D. and A. Bretscher, *Polarization of cell growth in yeast.* J Cell Sci, 2000. **113 (Pt 4)**: p. 571-85.
190. Pruyne, D. and A. Bretscher, *Polarization of cell growth in yeast. I. Establishment and maintenance of polarity states.* J Cell Sci, 2000. **113 (Pt 3)**: p. 365-75.
191. Dohlman, H.G. and J.W. Thorner, *Regulation of G protein-initiated signal transduction in yeast: paradigms and principles.* Annu Rev Biochem, 2001. **70**: p. 703-54.
192. Elion, E.A., *Pheromone response, mating and cell biology.* Curr Opin Microbiol, 2000. **3**(6): p. 573-81.
193. Leberer, E., D.Y. Thomas, and M. Whiteway, *Pheromone signalling and polarized morphogenesis in yeast.* Curr Opin Genet Dev, 1997. **7**(1): p. 59-66.
194. Palecek, S.P., A.S. Parikh, and S.J. Kron, *Sensing, signalling and integrating physical processes during Saccharomyces cerevisiae invasive and filamentous growth.* Microbiology, 2002. **148**(Pt 4): p. 893-907.
195. Lee, B.N. and E.A. Elion, *The MAPKKK Ste11 regulates vegetative growth through a kinase cascade of shared signaling components.* Proc Natl Acad Sci U S A, 1999. **96**(22): p. 12679-84.
196. Sherman, F., *Getting started with yeast.* Methods Enzymol, 2002. **350**: p. 3-41.
197. Bidlingmaier, S. and M. Snyder, *Regulation of polarized growth initiation and termination cycles by the polarisome and Cdc42 regulators.* J Cell Biol, 2004. **164**(2): p. 207-18.
198. Benton, B.K., et al., *Cla4p, a Saccharomyces cerevisiae Cdc42p-activated kinase involved in cytokinesis, is activated at mitosis.* Mol Cell Biol, 1997. **17**(9): p. 5067-76.
199. Peter, M., et al., *Functional analysis of the interaction between the small GTP binding protein Cdc42 and the Ste20 protein kinase in yeast.* Embo J, 1996. **15**(24): p. 7046-59.
200. Simon, M.N., et al., *Role for the Rho-family GTPase Cdc42 in yeast mating-pheromone signal pathway.* Nature, 1995. **376**(6542): p. 702-5.
201. Zhao, Z.S., et al., *Pheromone signalling in Saccharomyces cerevisiae requires the small GTP-binding protein Cdc42p and its activator CDC24.* Mol Cell Biol, 1995. **15**(10): p. 5246-57.
202. Evangelista, M., et al., *Bni1p, a yeast formin linking cdc42p and the actin cytoskeleton during polarized morphogenesis.* Science, 1997. **276**(5309): p. 118-22.
203. Ozaki-Kuroda, K., et al., *Dynamic localization and function of Bni1p at the sites of directed growth in Saccharomyces cerevisiae.* Mol Cell Biol, 2001. **21**(3): p. 827-39.

204. Osman, M.A. and R.A. Cerione, *Iqg1p, a yeast homologue of the mammalian IQGAPs, mediates cdc42p effects on the actin cytoskeleton.* J Cell Biol, 1998. **142**(2): p. 443-55.
205. Brown, J.L., et al., *Novel Cdc42-binding proteins Gic1 and Gic2 control cell polarity in yeast.* Genes Dev, 1997. **11**(22): p. 2972-82.
206. Smith, G.R., et al., *GTPase-activating proteins for Cdc42.* Eukaryot Cell, 2002. **1**(3): p. 469-80.
207. Stevenson, B.J., et al., *Mutation of RGA1, which encodes a putative GTPase-activating protein for the polarity-establishment protein Cdc42p, activates the pheromone-response pathway in the yeast Saccharomyces cerevisiae.* Genes Dev, 1995. **9**(23): p. 2949-63.
208. Zheng, Y., et al., *Biochemical comparisons of the Saccharomyces cerevisiae Bem2 and Bem3 proteins. Delineation of a limit Cdc42 GTPase-activating protein domain.* J Biol Chem, 1993. **268**(33): p. 24629-34.
209. Nern, A. and R.A. Arkowitz, *A GTP-exchange factor required for cell orientation.* Nature, 1998. **391**(6663): p. 195-8.
210. Zheng, Y., A. Bender, and R.A. Cerione, *Interactions among proteins involved in bud-site selection and bud-site assembly in Saccharomyces cerevisiae.* J Biol Chem, 1995. **270**(2): p. 626-30.
211. Ziman, M. and D.I. Johnson, *Genetic evidence for a functional interaction between Saccharomyces cerevisiae CDC24 and CDC42.* Yeast, 1994. **10**(4): p. 463-74.
212. Koch, G., et al., *Association of the Rho family small GTP-binding proteins with Rho GDP dissociation inhibitor (Rho GDI) in Saccharomyces cerevisiae.* Oncogene, 1997. **15**(4): p. 417-22.
213. Masuda, T., et al., *Molecular cloning and characterization of yeast rho GDP dissociation inhibitor.* J Biol Chem, 1994. **269**(31): p. 19713-8.
214. Richman, T.J., et al., *Analysis of cell-cycle specific localization of the Rdi1p RhoGDI and the structural determinants required for Cdc42p membrane localization and clustering at sites of polarized growth.* Curr Genet, 2004. **45**(6): p. 339-49.
215. Adams, A.E., et al., *CDC42 and CDC43, two additional genes involved in budding and the establishment of cell polarity in the yeast Saccharomyces cerevisiae.* J Cell Biol, 1990. **111**(1): p. 131-42.
216. Ohya, Y., et al., *Mutational analysis of the beta-subunit of yeast geranylgeranyl transferase I.* Mol Gen Genet, 1996. **252**(1-2): p. 1-10.
217. Bose, I., et al., *Assembly of scaffold-mediated complexes containing Cdc42p, the exchange factor Cdc24p, and the effector Cla4p required for cell cycle-regulated phosphorylation of Cdc24p.* J Biol Chem, 2001. **276**(10): p. 7176-86.
218. Gulli, M.P., et al., *Phosphorylation of the Cdc42 exchange factor Cdc24 by the PAK-like kinase Cla4 may regulate polarized growth in yeast.* Mol Cell, 2000. **6**(5): p. 1155-67.
219. Irazoqui, J.E., A.S. Gladfelter, and D.J. Lew, *Scaffold-mediated symmetry breaking by Cdc42p.* Nat Cell Biol, 2003. **5**(12): p. 1062-70.

220. Bender, A. and J.R. Pringle, *Use of a screen for synthetic lethal and multicopy suppressee mutants to identify two new genes involved in morphogenesis in Saccharomyces cerevisiae.* Mol Cell Biol, 1991. **11**(3): p. 1295-305.
221. Bender, A. and J.R. Pringle, *Multicopy suppression of the cdc24 budding defect in yeast by CDC42 and three newly identified genes including the ras-related gene RSR1.* Proc Natl Acad Sci U S A, 1989. **86**(24): p. 9976-80.
222. Chant, J., et al., *Yeast BUD5, encoding a putative GDP-GTP exchange factor, is necessary for bud site selection and interacts with bud formation gene BEM1.* Cell, 1991. **65**(7): p. 1213-24.
223. Chenevert, J., et al., *A yeast gene (BEM1) necessary for cell polarization whose product contains two SH3 domains.* Nature, 1992. **356**(6364): p. 77-9.
224. Kozubowski, L., et al., *Symmetry-breaking polarization driven by a Cdc42p GEF-PAK complex.* Curr Biol, 2008. **18**(22): p. 1719-26.
225. Bender, L., et al., *Associations among PH and SH3 domain-containing proteins and Rho-type GTPases in Yeast.* J Cell Biol, 1996. **133**(4): p. 879-94.
226. Matsui, Y., et al., *Yeast src homology region 3 domain-binding proteins involved in bud formation.* J Cell Biol, 1996. **133**(4): p. 865-78.
227. Winters, M.J. and P.M. Pryciak, *Interaction with the SH3 domain protein Bem1 regulates signaling by the Saccharomyces cerevisiae p21-activated kinase Ste20.* Mol Cell Biol, 2005. **25**(6): p. 2177-90.
228. Yamaguchi, Y., K. Ota, and T. Ito, *A novel Cdc42-interacting domain of the yeast polarity establishment protein Bem1. Implications for modulation of mating pheromone signaling.* J Biol Chem, 2007. **282**(1): p. 29-38.
229. Ago, T., et al., *The PX domain as a novel phosphoinositide- binding module.* Biochem Biophys Res Commun, 2001. **287**(3): p. 733-8.
230. Stahelin, R.V., et al., *Structural and membrane binding analysis of the Phox homology domain of Bem1p: basis of phosphatidylinositol 4-phosphate specificity.* J Biol Chem, 2007. **282**(35): p. 25737-47.
231. Butty, A.C., et al., *A positive feedback loop stabilizes the guanine-nucleotide exchange factor Cdc24 at sites of polarization.* Embo J, 2002. **21**(7): p. 1565-76.
232. Ito, T., et al., *Novel modular domain PB1 recognizes PC motif to mediate functional protein-protein interactions.* Embo J, 2001. **20**(15): p. 3938-46.
233. Ogura, K., et al., *NMR structure of the heterodimer of Bem1 and Cdc24 PB1 domains from Saccharomyces cerevisiae.* J Biochem, 2009. **146**(3): p. 317-25.
234. Terasawa, H., et al., *Structure and ligand recognition of the PB1 domain: a novel protein module binding to the PC motif.* Embo J, 2001. **20**(15): p. 3947-56.
235. van Drogen-Petit, A., et al., *Insight into molecular interactions between two PB1 domains.* J Mol Biol, 2004. **336**(5): p. 1195-210.

236. Chang, F. and I. Herskowitz, *Identification of a gene necessary for cell cycle arrest by a negative growth factor of yeast: FAR1 is an inhibitor of a G1 cyclin, CLN2.* Cell, 1990. **63**(5): p. 999-1011.
237. Peter, M., et al., *FAR1 links the signal transduction pathway to the cell cycle machinery in yeast.* Cell, 1993. **73**(4): p. 747-60.
238. Peter, M. and I. Herskowitz, *Direct inhibition of the yeast cyclin-dependent kinase Cdc28-Cln by Far1.* Science, 1994. **265**(5176): p. 1228-31.
239. Butty, A.C., et al., *The role of Far1p in linking the heterotrimeric G protein to polarity establishment proteins during yeast mating.* Science, 1998. **282**(5393): p. 1511-6.
240. Nern, A. and R.A. Arkowitz, *A Cdc24p-Far1p-Gbetagamma protein complex required for yeast orientation during mating.* J Cell Biol, 1999. **144**(6): p. 1187-202.
241. Leberer, E., et al., *Genetic interactions indicate a role for Mdg1p and the SH3 domain protein Bem1p in linking the G-protein mediated yeast pheromone signalling pathway to regulators of cell polarity.* Mol Gen Genet, 1996. **252**(5): p. 608-21.
242. Lyons, D.M., et al., *The SH3-domain protein Bem1 coordinates mitogen-activated protein kinase cascade activation with cell cycle control in Saccharomyces cerevisiae.* Mol Cell Biol, 1996. **16**(8): p. 4095-106.
243. Leberer, E., et al., *Functional characterization of the Cdc42p binding domain of yeast Ste20p protein kinase.* Embo J, 1997. **16**(1): p. 83-97.
244. Loog, M. and D.O. Morgan, *Cyclin specificity in the phosphorylation of cyclin-dependent kinase substrates.* Nature, 2005. **434**(7029): p. 104-8.
245. Ubersax, J.A., et al., *Targets of the cyclin-dependent kinase Cdk1.* Nature, 2003. **425**(6960): p. 859-64.
246. Han, B.K., et al., *Bem1p, a scaffold signaling protein, mediates cyclin-dependent control of vacuolar homeostasis in Saccharomyces cerevisiae.* Genes Dev, 2005. **19**(21): p. 2606-18.
247. Xu, H. and W. Wickner, *Bem1p is a positive regulator of the homotypic fusion of yeast vacuoles.* J Biol Chem, 2006. **281**(37): p. 27158-66.
248. Klis, F.M., A. Boorsma, and P.W. De Groot, *Cell wall construction in Saccharomyces cerevisiae.* Yeast, 2006. **23**(3): p. 185-202.
249. Lesage, G. and H. Bussey, *Cell wall assembly in Saccharomyces cerevisiae.* Microbiol Mol Biol Rev, 2006. **70**(2): p. 317-43.
250. Orlean, P., *Biogenesis of yeast wall and surface components*, in *Cell Cycle and Cell Biology*, J. Pringle, Editor. 1997, Cold Spring Harbor Laboratory Press: Cold Spring Harbor. p. 229-362.
251. Cabib, E., et al., *The yeast cell wall and septum as paradigms of cell growth and morphogenesis.* J Biol Chem, 2001. **276**(23): p. 19679-82.
252. Gozalbo, D., et al., *Candida and candidiasis: the cell wall as a potential molecular target for antifungal therapy.* Curr Drug Targets Infect Disord, 2004. **4**(2): p. 117-35.
253. Sussman, A., et al., *Discovery of cercosporamide, a known antifungal natural product, as a selective Pkc1 kinase inhibitor through high-throughput screening.* Eukaryot Cell, 2004. **3**(4): p. 932-43.

254. Heinisch, J.J., *Baker's yeast as a tool for the development of antifungal kinase inhibitors--targeting protein kinase C and the cell integrity pathway.* Biochim Biophys Acta, 2005. **1754**(1-2): p. 171-82.
255. Levin, D.E., *Cell wall integrity signaling in Saccharomyces cerevisiae.* Microbiol Mol Biol Rev, 2005. **69**(2): p. 262-91.
256. Mellor, H. and P.J. Parker, *The extended protein kinase C superfamily.* Biochem J, 1998. **332 (Pt 2)**: p. 281-92.
257. Drgonova, J., et al., *Rho1p, a yeast protein at the interface between cell polarization and morphogenesis.* Science, 1996. **272**(5259): p. 277-9.
258. Mazur, P. and W. Baginsky, *In vitro activity of 1,3-beta-D-glucan synthase requires the GTP-binding protein Rho1.* J Biol Chem, 1996. **271**(24): p. 14604-9.
259. Fujiwara, T., et al., *Rho1p-Bni1p-Spa2p interactions: implication in localization of Bni1p at the bud site and regulation of the actin cytoskeleton in Saccharomyces cerevisiae.* Mol Biol Cell, 1998. **9**(5): p. 1221-33.
260. Kohno, H., et al., *Bni1p implicated in cytoskeletal control is a putative target of Rho1p small GTP binding protein in Saccharomyces cerevisiae.* Embo J, 1996. **15**(22): p. 6060-8.
261. Ozaki, K., et al., *Rom1p and Rom2p are GDP/GTP exchange proteins (GEPs) for the Rho1p small GTP binding protein in Saccharomyces cerevisiae.* Embo J, 1996. **15**(9): p. 2196-207.
262. Ketela, T., R. Green, and H. Bussey, *Saccharomyces cerevisiae mid2p is a potential cell wall stress sensor and upstream activator of the PKC1-MPK1 cell integrity pathway.* J Bacteriol, 1999. **181**(11): p. 3330-40.
263. Costanzo, M., et al., *The genetic landscape of a cell.* Science, 2010. **327**(5964): p. 425-31.
264. Drees, B.L., et al., *A protein interaction map for cell polarity development.* J Cell Biol, 2001. **154**(3): p. 549-71.
265. Fiedler, D., et al., *Functional organization of the S. cerevisiae phosphorylation network.* Cell, 2009. **136**(5): p. 952-63.
266. Gavin, A.C., et al., *Functional organization of the yeast proteome by systematic analysis of protein complexes.* Nature, 2002. **415**(6868): p. 141-7.
267. Jorgensen, P., et al., *High-resolution genetic mapping with ordered arrays of Saccharomyces cerevisiae deletion mutants.* Genetics, 2002. **162**(3): p. 1091-9.
268. Ptacek, J., et al., *Global analysis of protein phosphorylation in yeast.* Nature, 2005. **438**(7068): p. 679-84.
269. Tong, A.H., et al., *Systematic genetic analysis with ordered arrays of yeast deletion mutants.* Science, 2001. **294**(5550): p. 2364-8.
270. Tong, A.H., et al., *Global mapping of the yeast genetic interaction network.* Science, 2004. **303**(5659): p. 808-13.
271. Zhu, H., et al., *Global analysis of protein activities using proteome chips.* Science, 2001. **293**(5537): p. 2101-5.
272. Zhu, H., et al., *Analysis of yeast protein kinases using protein chips.* Nat Genet, 2000. **26**(3): p. 283-9.

273. Peterson, J., et al., *Interactions between the bud emergence proteins Bem1p and Bem2p and Rho-type GTPases in yeast.* J Cell Biol, 1994. **127**(5): p. 1395-406.
274. Denzel, A., et al., *Early postnatal death and motor disorders in mice congenitally deficient in calnexin expression.* Mol Cell Biol, 2002. **22**(21): p. 7398-404.
275. Rodan, A.R., et al., *N-linked oligosaccharides are necessary and sufficient for association of glycosylated forms of bovine RNase with calnexin and calreticulin.* Embo J, 1996. **15**(24): p. 6921-30.
276. Beaulieu, H., et al., *Interaction of mammalian neprilysin with binding protein and calnexin in Schizosaccharomyces pombe.* Biochem J, 1999. **340 (Pt 3)**: p. 813-9.
277. Collin, P., et al., *A non-chromosomal factor allows viability of Schizosaccharomyces pombe lacking the essential chaperone calnexin.* J Cell Sci, 2004. **117**(Pt 6): p. 907-18.
278. Elagoz, A., et al., *Although calnexin is essential in S. pombe, its highly conserved central domain is dispensable for viability.* J Cell Sci, 1999. **112 (Pt 23)**: p. 4449-60.
279. Marechal, A., et al., *Cell viability and secretion of active proteins in Schizosaccharomyces pombe do not require the chaperone function of calnexin.* Biochem J, 2004. **380**(Pt 2): p. 441-8.
280. Jakob, C.A., et al., *Lectins of the ER quality control machinery.* Results Probl Cell Differ, 2001. **33**: p. 1-17.
281. Fanchiotti, S., et al., *The UDP-Glc:Glycoprotein glucosyltransferase is essential for Schizosaccharomyces pombe viability under conditions of extreme endoplasmic reticulum stress.* J Cell Biol, 1998. **143**(3): p. 625-35.
282. Jannatipour, M., et al., *Calnexin and BiP interact with acid phosphatase independently of glucose trimming and reglucosylation in Schizosaccharomyces pombe.* Biochemistry, 1998. **37**(49): p. 17253-61.
283. Moreno, S., Y. Sanchez, and L. Rodriguez, *Purification and characterization of the invertase from Schizosaccharomyces pombe. A comparative analysis with the invertase from Saccharomyces cerevisiae.* Biochem J, 1990. **267**(3): p. 697-702.
284. Kalies, K.U., D. Gorlich, and T.A. Rapoport, *Binding of ribosomes to the rough endoplasmic reticulum mediated by the Sec61p-complex.* J Cell Biol, 1994. **126**(4): p. 925-34.
285. Takatsuki, A. and G. Tamura, *Effect of tunicamycin on the synthesis of macromolecules in cultures of chick embryo fibroblasts infected with Newcastle disease virus.* J Antibiot (Tokyo), 1971. **24**(11): p. 785-94.
286. Hajjar, F., P.B. Beauregard, and L.A. Rokeach, *The 160 N-terminal residues of calnexin define a novel region supporting viability in Schizosaccharomyces pombe.* Yeast, 2007. **24**(2): p. 89-103.
287. Leborgne-Castel, N., et al., *Overexpression of BiP in tobacco alleviates endoplasmic reticulum stress.* Plant Cell, 1999. **11**(3): p. 459-70.

288. Fantes, P. and P. Nurse, *Control of cell size at division in fission yeast by a growth-modulated size control over nuclear division.* Exp Cell Res, 1977. **107**(2): p. 377-86.
289. Fantes, P.A., *Control of cell size and cycle time in Schizosaccharomyces pombe.* J Cell Sci, 1977. **24**: p. 51-67.
290. Nurse, P., *Genetic control of cell size at cell division in yeast.* Nature, 1975. **256**(5518): p. 547-51.
291. Nurse, P., P. Thuriaux, and K. Nasmyth, *Genetic control of the cell division cycle in the fission yeast Schizosaccharomyces pombe.* Mol Gen Genet, 1976. **146**(2): p. 167-78.
292. Nurse, P., *Universal control mechanism regulating onset of M-phase.* Nature, 1990. **344**(6266): p. 503-8.
293. Sawin, K.E., *Cell cycle: Cell division brought down to size.* Nature, 2009. **459**(7248): p. 782-3.
294. Fantes, P., *Epistatic gene interactions in the control of division in fission yeast.* Nature, 1979. **279**(5712): p. 428-30.
295. Russell, P. and P. Nurse, *cdc25+ functions as an inducer in the mitotic control of fission yeast.* Cell, 1986. **45**(1): p. 145-53.
296. Boulton, T.G., et al., *ERKs: a family of protein-serine/threonine kinases that are activated and tyrosine phosphorylated in response to insulin and NGF.* Cell, 1991. **65**(4): p. 663-75.
297. Boulton, T.G., et al., *An insulin-stimulated protein kinase similar to yeast kinases involved in cell cycle control.* Science, 1990. **249**(4964): p. 64-7.
298. Feldman, D.E., V. Chauhan, and A.C. Koong, *The unfolded protein response: a novel component of the hypoxic stress response in tumors.* Mol Cancer Res, 2005. **3**(11): p. 597-605.
299. Koumenis, C., *ER stress, hypoxia tolerance and tumor progression.* Curr Mol Med, 2006. **6**(1): p. 55-69.
300. Saito, S., et al., *Chemical genomics identifies the unfolded protein response as a target for selective cancer cell killing during glucose deprivation.* Cancer Res, 2009. **69**(10): p. 4225-34.
301. Reimold, A.M., et al., *Transcription factor B cell lineage-specific activator protein regulates the gene for human X-box binding protein 1.* J Exp Med, 1996. **183**(2): p. 393-401.
302. Raab, M.S., et al., *Multiple myeloma.* Lancet, 2009. **374**(9686): p. 324-39.
303. Singhal, S. and J. Mehta, *Multiple myeloma.* Clin J Am Soc Nephrol, 2006. **1**(6): p. 1322-30.
304. Zhang, K., et al., *The unfolded protein response sensor IRE1alpha is required at 2 distinct steps in B cell lymphopoiesis.* J Clin Invest, 2005. **115**(2): p. 268-81.
305. Fels, D.R., et al., *Preferential cytotoxicity of bortezomib toward hypoxic tumor cells via overactivation of endoplasmic reticulum stress pathways.* Cancer Res, 2008. **68**(22): p. 9323-30.
306. Gu, H., et al., *Caspase-2 functions upstream of mitochondria in endoplasmic reticulum stress-induced apoptosis by bortezomib in human myeloma cells.* Mol Cancer Ther, 2008. **7**(8): p. 2298-307.

307. Amberg, D.C., D.J. Burke, and J.N. Strathern, *Methods in Yeast Genetics: A Cold Spring Harbor Laboratory Course Manual*. 2005, Cold Spring Harbor, New York: Cold Spring Harbor Laboratory Press.
308. Decottignies, A., et al., *ATPase and multidrug transport activities of the overexpressed yeast ABC protein Yor1p.* J Biol Chem, 1998. **273**(20): p. 12612-22.
309. Wu, C., et al., *Molecular characterization of Ste20p, a potential mitogen-activated protein or extracellular signal-regulated kinase kinase (MEK) kinase kinase from Saccharomyces cerevisiae.* J Biol Chem, 1995. **270**(27): p. 15984-92.
310. Datema, R. and R.T. Schwarz, *Formation of 2-deoxyglucose-containing lipid-linked oligosaccharides. Interference with glycosylation of glycoproteins.* Eur J Biochem, 1978. **90**(3): p. 505-16.
311. Kurtoglu, M., et al., *Under normoxia, 2-deoxy-D-glucose elicits cell death in select tumor types not by inhibition of glycolysis but by interfering with N-linked glycosylation.* Mol Cancer Ther, 2007. **6**(11): p. 3049-58.
312. Boyce, M., et al., *A selective inhibitor of eIF2alpha dephosphorylation protects cells from ER stress.* Science, 2005. **307**(5711): p. 935-9.
313. Schewe, D.M. and J.A. Aguirre-Ghiso, *Inhibition of eIF2alpha dephosphorylation maximizes bortezomib efficiency and eliminates quiescent multiple myeloma cells surviving proteasome inhibitor therapy.* Cancer Res, 2009. **69**(4): p. 1545-52.
314. Heidelberger, C., et al., *Fluorinated pyrimidines, a new class of tumour-inhibitory compounds.* Nature, 1957. **179**(4561): p. 663-6.
315. Engel, D., et al., *Novel prodrugs of tegafur that display improved anticancer activity and antiangiogenic properties.* J Med Chem, 2008. **51**(2): p. 314-23.
316. Malet-Martino, M. and R. Martino, *Clinical studies of three oral prodrugs of 5-fluorouracil (capecitabine, UFT, S-1): a review.* Oncologist, 2002. **7**(4): p. 288-323.
317. Buckheit, R.W., Jr., et al., *Comparative evaluation of the inhibitory activities of a series of pyrimidinedione congeners that inhibit human immunodeficiency virus types 1 and 2.* Antimicrob Agents Chemother, 2008. **52**(1): p. 225-36.
318. Buckheit, R.W., Jr., et al., *The structure-activity relationships of 2,4(1H,3H)-pyrimidinedione derivatives as potent HIV type 1 and type 2 inhibitors.* Antivir Chem Chemother, 2007. **18**(5): p. 259-75.
319. Talukdar, A., et al., *Discovery and development of a small molecule library with lumazine synthase inhibitory activity.* J Org Chem, 2009. **74**(15): p. 5123-34.
320. Talukdar, A., et al., *Synthesis and enzyme inhibitory activity of the s-nucleoside analogue of the ribitylaminopyrimidine substrate of lumazine synthase and product of riboflavin synthase.* J Org Chem, 2007. **72**(19): p. 7167-75.
321. Zhang, Y., et al., *A new series of 3-alkyl phosphate derivatives of 4,5,6,7-tetrahydro-1-D-ribityl-1H-pyrazolo[3,4-d]pyrimidinedione as inhibitors of*

lumazine synthase: design, synthesis, and evaluation. J Org Chem, 2007. **72**(19): p. 7176-84.
322. Eltze, M., *Affinity of the miotic drug, dapiprazole, at alpha 1-adrenoceptor subtypes A, B and D.* J Pharm Pharmacol, 1997. **49**(11): p. 1091-5.
323. Eltze, M., et al., *Failure of AH11110A to functionally discriminate between alpha(1)-adrenoceptor subtypes A, B and D or between alpha(1)- and alpha(2)-adrenoceptors.* Eur J Pharmacol, 2001. **415**(2-3): p. 265-76.
324. Berger, S.L. and C.S. Birkenmeier, *Inhibition of intractable nucleases with ribonucleoside--vanadyl complexes: isolation of messenger ribonucleic acid from resting lymphocytes.* Biochemistry, 1979. **18**(23): p. 5143-9.
325. White, M.D., S. Bauer, and Y. Lapidot, *Inhibition of pancreatic ribonuclease by 2'-5' and 3'-5' oligonucleotides.* Nucleic Acids Res, 1977. **4**(9): p. 3029-38.
326. Russo, N., R. Shapiro, and B.L. Vallee, *5'-Diphosphoadenosine 3'-phosphate is a potent inhibitor of bovine pancreatic ribonuclease A.* Biochem Biophys Res Commun, 1997. **231**(3): p. 671-4.
327. Chamberlain, J.R., et al., *Purification and characterization of the nuclear RNase P holoenzyme complex reveals extensive subunit overlap with RNase MRP.* Genes Dev, 1998. **12**(11): p. 1678-90.
328. Dichtl, B. and D. Tollervey, *Pop3p is essential for the activity of the RNase MRP and RNase P ribonucleoproteins in vivo.* Embo J, 1997. **16**(2): p. 417-29.
329. Giaever, G., et al., *Functional profiling of the Saccharomyces cerevisiae genome.* Nature, 2002. **418**(6896): p. 387-91.
330. Lygerou, Z., et al., *The POP1 gene encodes a protein component common to the RNase MRP and RNase P ribonucleoproteins.* Genes Dev, 1994. **8**(12): p. 1423-33.
331. Matsuoka, Y., et al., *Isolation and characterization of free lambda-chain of immunoglobulin produced by an established cell line of human myeloma cell origin. II. Identity of lambda-chains in cells and in medium.* J Immunol, 1969. **103**(5): p. 962-9.
332. Fostel, J.M. and P.A. Lartey, *Emerging novel antifungal agents.* Drug Discov Today, 2000. **5**(1): p. 25-32.
333. Groll, A.H. and T.J. Walsh, *Uncommon opportunistic fungi: new nosocomial threats.* Clin Microbiol Infect, 2001. **7 Suppl 2**: p. 8-24.
334. Heinisch, J.J., et al., *The protein kinase C-mediated MAP kinase pathway involved in the maintenance of cellular integrity in Saccharomyces cerevisiae.* Mol Microbiol, 1999. **32**(4): p. 671-80.
335. Kamada, Y., et al., *Activation of yeast protein kinase C by Rho1 GTPase.* J Biol Chem, 1996. **271**(16): p. 9193-6.
336. Nonaka, H., et al., *A downstream target of RHO1 small GTP-binding protein is PKC1, a homolog of protein kinase C, which leads to activation of the MAP kinase cascade in Saccharomyces cerevisiae.* Embo J, 1995. **14**(23): p. 5931-8.
337. Guo, W., F. Tamanoi, and P. Novick, *Spatial regulation of the exocyst complex by Rho1 GTPase.* Nat Cell Biol, 2001. **3**(4): p. 353-60.

338. Jung, U.S. and D.E. Levin, *Genome-wide analysis of gene expression regulated by the yeast cell wall integrity signalling pathway.* Mol Microbiol, 1999. **34**(5): p. 1049-57.
339. Madden, K., et al., *SBF cell cycle regulator as a target of the yeast PKC-MAP kinase pathway.* Science, 1997. **275**(5307): p. 1781-4.
340. Leeuw, T., et al., *Pheromone response in yeast: association of Bem1p with proteins of the MAP kinase cascade and actin.* Science, 1995. **270**(5239): p. 1210-3.
341. Labbe, S. and D.J. Thiele, *Copper ion inducible and repressible promoter systems in yeast.* Methods Enzymol, 1999. **306**: p. 145-53.
342. Nishiya, Y. and T. Imanaka, *Analysis of interaction between the Arthrobacter sarcosine oxidase and the coenzyme flavin adenine dinucleotide by site-directed mutagenesis.* Appl Environ Microbiol, 1996. **62**(7): p. 2405-10.
343. Wu, C., et al., *Functional characterization of the interaction of Ste50p with Ste11p MAPKKK in Saccharomyces cerevisiae.* Mol Biol Cell, 1999. **10**(7): p. 2425-40.
344. Martzen, M.R., et al., *A biochemical genomics approach for identifying genes by the activity of their products.* Science, 1999. **286**(5442): p. 1153-5.
345. Shevchenko, A., et al., *Mass spectrometric sequencing of proteins silver-stained polyacrylamide gels.* Anal Chem, 1996. **68**(5): p. 850-8.
346. Dejgaard, K., et al., *Organization of the Sec61 translocon, studied by high resolution native electrophoresis.* J Proteome Res, 2010. **9**(4): p. 1763-71.
347. Gelperin, D.M., et al., *Biochemical and genetic analysis of the yeast proteome with a movable ORF collection.* Genes Dev, 2005. **19**(23): p. 2816-26.
348. Ram, A.F. and F.M. Klis, *Identification of fungal cell wall mutants using susceptibility assays based on Calcofluor white and Congo red.* Nat Protoc, 2006. **1**(5): p. 2253-6.
349. France, Y.E., et al., *The polarity-establishment component Bem1p interacts with the exocyst complex through the Sec15p subunit.* J Cell Sci, 2006. **119**(Pt 5): p. 876-88.
350. Marchler-Bauer, A., et al., *CDD: a database of conserved domain alignments with links to domain three-dimensional structure.* Nucleic Acids Res, 2002. **30**(1): p. 281-3.
351. Wu, X., et al., *Structural basis for the specific interaction of lysine-containing proline-rich peptides with the N-terminal SH3 domain of c-Crk.* Structure, 1995. **3**(2): p. 215-26.
352. Longtine, M.S., et al., *Septin-dependent assembly of a cell cycle-regulatory module in Saccharomyces cerevisiae.* Mol Cell Biol, 2000. **20**(11): p. 4049-61.
353. Krogan, N.J., et al., *Global landscape of protein complexes in the yeast Saccharomyces cerevisiae.* Nature, 2006. **440**(7084): p. 637-43.
354. Leeder, A.C. and G. Turner, *Characterisation of Aspergillus nidulans polarisome component BemA.* Fungal Genet Biol, 2008. **45**(6): p. 897-911.

355. Tong, A.H., et al., *A combined experimental and computational strategy to define protein interaction networks for peptide recognition modules.* Science, 2002. **295**(5553): p. 321-4.
356. Cvrckova, F., et al., *Ste20-like protein kinases are required for normal localization of cell growth and for cytokinesis in budding yeast.* Genes Dev, 1995. **9**(15): p. 1817-30.
357. Alvarez-Tabares, I. and J. Perez-Martin, *Cdk5 kinase regulates the association between adaptor protein Bem1 and GEF Cdc24 in the fungus Ustilago maydis.* J Cell Sci, 2008. **121**(Pt 17): p. 2824-32.
358. Pramila, T., et al., *Conserved homeodomain proteins interact with MADS box protein Mcm1 to restrict ECB-dependent transcription to the M/G1 phase of the cell cycle.* Genes Dev, 2002. **16**(23): p. 3034-45.
359. Degols, G. and P. Russell, *Discrete roles of the Spc1 kinase and the Atf1 transcription factor in the UV response of Schizosaccharomyces pombe.* Mol Cell Biol, 1997. **17**(6): p. 3356-63.
360. Samejima, I., S. Mackie, and P.A. Fantes, *Multiple modes of activation of the stress-responsive MAP kinase pathway in fission yeast.* Embo J, 1997. **16**(20): p. 6162-70.
361. Shiozaki, K. and P. Russell, *Cell-cycle control linked to extracellular environment by MAP kinase pathway in fission yeast.* Nature, 1995. **378**(6558): p. 739-43.
362. Matsuyama, A., et al., *ORFeome cloning and global analysis of protein localization in the fission yeast Schizosaccharomyces pombe.* Nat Biotechnol, 2006. **24**(7): p. 841-7.
363. Nguyen, D.T., et al., *Nck-dependent activation of extracellular signal-regulated kinase-1 and regulation of cell survival during endoplasmic reticulum stress.* Mol Biol Cell, 2004. **15**(9): p. 4248-60.
364. Delom, F., et al., *Calnexin-dependent regulation of tunicamycin-induced apoptosis in breast carcinoma MCF-7 cells.* Cell Death Differ, 2007. **14**(3): p. 586-96.
365. Pecot, M.Y. and V. Malhotra, *Golgi membranes remain segregated from the endoplasmic reticulum during mitosis in mammalian cells.* Cell, 2004. **116**(1): p. 99-107.
366. Stockwell, B.R. and S.L. Schreiber, *Probing the role of homomeric and heteromeric receptor interactions in TGF-beta signaling using small molecule dimerizers.* Curr Biol, 1998. **8**(13): p. 761-70.
367. Zhu, S., H. Zhang, and M.J. Matunis, *SUMO modification through rapamycin-mediated heterodimerization reveals a dual role for Ubc9 in targeting RanGAP1 to nuclear pore complexes.* Exp Cell Res, 2006. **312**(7): p. 1042-9.
368. Avezov, E., et al., *Endoplasmic reticulum (ER) mannosidase I is compartmentalized and required for N-glycan trimming to Man5-6GlcNAc2 in glycoprotein ER-associated degradation.* Mol Biol Cell, 2008. **19**(1): p. 216-25.
369. Kamhi-Nesher, S., et al., *A novel quality control compartment derived from the endoplasmic reticulum.* Mol Biol Cell, 2001. **12**(6): p. 1711-23.

370. Milstein, M.L., T.D. Houle, and S.E. Cala, *Calsequestrin isoforms localize to different ER subcompartments: evidence for polymer and heteropolymer-dependent localization.* Exp Cell Res, 2009. **315**(3): p. 523-34.
371. Kumar, S. and S.V. Rajkumar, *Many facets of bortezomib resistance/susceptibility.* Blood, 2008. **112**(6): p. 2177-8.
372. Shah, J.J. and R.Z. Orlowski, *Proteasome inhibitors in the treatment of multiple myeloma.* Leukemia, 2009. **23**(11): p. 1964-79.
373. Lu, S., et al., *Point mutation of the proteasome beta5 subunit gene is an important mechanism of bortezomib resistance in bortezomib-selected variants of Jurkat T cell lymphoblastic lymphoma/leukemia line.* J Pharmacol Exp Ther, 2008. **326**(2): p. 423-31.
374. Oerlemans, R., et al., *Molecular basis of bortezomib resistance: proteasome subunit beta5 (PSMB5) gene mutation and overexpression of PSMB5 protein.* Blood, 2008. **112**(6): p. 2489-99.
375. Ri, M., et al., *Bortezomib-resistant myeloma cell lines: a role for mutated PSMB5 in preventing the accumulation of unfolded proteins and fatal ER stress.* Leukemia, 2010. **24**(8): p. 1506-12.
376. Ruckrich, T., et al., *Characterization of the ubiquitin-proteasome system in bortezomib-adapted cells.* Leukemia, 2009. **23**(6): p. 1098-105.
377. Chesi, M., et al., *AID-dependent activation of a MYC transgene induces multiple myeloma in a conditional mouse model of post-germinal center malignancies.* Cancer Cell, 2008. **13**(2): p. 167-80.
378. Lee, A.H., et al., *XBP-1 is required for biogenesis of cellular secretory machinery of exocrine glands.* Embo J, 2005. **24**(24): p. 4368-80.
379. Papandreou, I., et al., *Identification of an Ire1alpha endonuclease specific inhibitor with cytotoxic activity against human multiple myeloma.* Blood, 2010.
380. Scriven, P., et al., *Activation and clinical significance of the unfolded protein response in breast cancer.* Br J Cancer, 2009. **101**(10): p. 1692-8.
381. El-Benna, J., et al., *p47phox, the phagocyte NADPH oxidase/NOX2 organizer: structure, phosphorylation and implication in diseases.* Exp Mol Med, 2009. **41**(4): p. 217-25.
382. Sheppard, F.R., et al., *Structural organization of the neutrophil NADPH oxidase: phosphorylation and translocation during priming and activation.* J Leukoc Biol, 2005. **78**(5): p. 1025-42.
383. Heinemeyer, W., et al., *PRE2, highly homologous to the human major histocompatibility complex-linked RING10 gene, codes for a yeast proteasome subunit necessary for chrymotryptic activity and degradation of ubiquitinated proteins.* J Biol Chem, 1993. **268**(7): p. 5115-20.
384. Michel, S., et al., *Generation of conditional lethal Candida albicans mutants by inducible deletion of essential genes.* Mol Microbiol, 2002. **46**(1): p. 269-80.
385. Kobayashi, N. and K. McEntee, *Evidence for a heat shock transcription factor-independent mechanism for heat shock induction of transcription in Saccharomyces cerevisiae.* Proc Natl Acad Sci U S A, 1990. **87**(17): p. 6550-4.

386. Kobayashi, N. and K. McEntee, *Identification of cis and trans components of a novel heat shock stress regulatory pathway in Saccharomyces cerevisiae.* Mol Cell Biol, 1993. **13**(1): p. 248-56.
387. Marchler, G., et al., *A Saccharomyces cerevisiae UAS element controlled by protein kinase A activates transcription in response to a variety of stress conditions.* Embo J, 1993. **12**(5): p. 1997-2003.
388. Gasch, A.P., *The Environmental Stress Response: a common yeast response to environmental stresses*. Topics in Current Genetics, ed. H. S. Vol. 1. 2002, Heidelberg: Springer-Verlag.
389. Selye, H., *Confusion and controversy in the stress field.* J Human Stress, 1975. **1**(2): p. 37-44.
390. Flattery-O'Brien, J., L.P. Collinson, and I.W. Dawes, *Saccharomyces cerevisiae has an inducible response to menadione which differs from that to hydrogen peroxide.* J Gen Microbiol, 1993. **139**(3): p. 501-7.
391. Lewis, J.G., R.P. Learmonth, and K. Watson, *Induction of heat, freezing and salt tolerance by heat and salt shock in Saccharomyces cerevisiae.* Microbiology, 1995. **141 (Pt 3)**: p. 687-94.
392. Mitchel, R.E. and D.P. Morrison, *Heat-shock induction of ionizing radiation resistance in Saccharomyces cerevisiae, and correlation with stationary growth phase.* Radiat Res, 1982. **90**(2): p. 284-91.
393. Akerfelt, M., R.I. Morimoto, and L. Sistonen, *Heat shock factors: integrators of cell stress, development and lifespan.* Nat Rev Mol Cell Biol, 2010. **11**(8): p. 545-55.
394. Finkel, T. and N.J. Holbrook, *Oxidants, oxidative stress and the biology of ageing.* Nature, 2000. **408**(6809): p. 239-47.
395. Westerheide, S.D., et al., *Stress-inducible regulation of heat shock factor 1 by the deacetylase SIRT1.* Science, 2009. **323**(5917): p. 1063-6.